Yeast Cell Factory-Platform for the Screening and the Industrial Production of Flavonoids and other Phenolic Compounds

PhD thesis by Beata Joanna Lehka

Lehka, Beata Joanna

Publication date:
2017

Document Version
Publisher's PDF, also known as Version of record

Citation for published version (APA):
Lehka, B. J. (2017). *Yeast Cell Factory-Platform for the Screening and the Industrial Production of Flavonoids and other Phenolic Compounds: PhD thesis by Beata Joanna Lehka*. Roskilde Universitet.

Yeast Cell Factory-Platform for the Screening and the Industrial Production of Flavonoids and other Phenolic Compounds

PhD THESIS BY
BEATA JOANNA LEHKA
MAY 2017

Supervisors: Ernesto Simon and Assoc. Prof. Håvard Jenssen
Submission date: 31/05/2017
The thesis has been submitted to the Department of Science and Environment, Roskilde University, Denmark

PREFACE AND ACKNOWLEDGEMENTS

This thesis presents work done during my PhD study. The work was carried out at a biotech company – EVOLVA – from April 2014 to May 2017 and at Roskilde University – Department of Science and Environment – from June to December 2016.

I would like to sincerely thank my supervisors for their inspiration, encouragement and support. Ernesto Simon, thank you for your guidance throughout the whole process, for helping with experimental work and for your enormous patience. Håvard Jenssen, since my master studies you encouraged me to become a PhD student, thank you for your support and believing in me. I would also like to thank Niels Bjerg Jensen, who showed me how to be efficient in the laboratory and supported me during my last months at Evolva.

I would like to thank my colleagues from Evolva and RUC for creating an inspiring and fun working environment as well as for the constructive discussions.

A special thanks goes to Katherina Garcia Vanegas, Michael Eichenberger and Michael Naesby for collaborating with me. It was a great pleasure working with you!

I also would like to thank Bo Svensmark and Steffen Larsen for their help in the mathematical problem solving described in the current thesis.

Finally, I want to thank my husband for driving me to the laboratory during weekends and for supporting me during tough times and my parents for motivating me throughout my life.

ABSTRACT

Flavonoids are secondary plant metabolites derived from the phenylpropanoid pathway. These bioactive compounds are of great commercial interest due to their varied properties, such as anti-oxidative, anti-tumor and/or antibacterial. However, industrial production of flavonoids based on purification from plants or on their organic synthesis can be problematic. On the other hand, the so called bio-industrial production of a variety of compounds in microorganisms is gaining great popularity. The objective of this study is to produce naringenin and some of its derivatives in *Saccharomyces cerevisiae* as a model for industrial production of flavonoids.

By combining a balanced heterologous expression of (phenylpropanoid) naringenin biosynthetic pathway genes and the optimisation of yeast metabolism we developed a strain producing 430 mg/L of naringenin from glucose. In this set up naringenin was produced from phenylalanine by action of a phenylalanine ammonia lyase (PAL) in a strain overproducing phenylalanine and tyrosine. As tyrosine can also be a precursor for naringenin production via tyrosine ammonia lyase (TAL), we evaluated *in vivo* the activity of several TAL enzymes in *S. cerevisiae*. Most of the ammonia lyases have affinity to both phenylalanine and tyrosine, with a strong preference for phenylalanine. Some TALs have been described before but these either have very low overall activity on tyrosine or are also capable of using phenylalanine as substrate. Here we identified a novel TAL, an enzyme from *Aeromonas salmonicida* with relatively high activity towards tyrosine and no activity towards phenylalanine.

Production of flavonoids and stilbenoids in *S. cerevisiae* is challenging, partially due to carbon loss towards phloretic acid by the action of an unknown endogenous reductase. Through the screening of 26 putative double bond reductase knockout strains we identified Tsc13 as the enzyme responsible for the reduction of *p*-coumaroyl-CoA to phloretic acid. Since Tsc13 is an essential enzyme, a combination of homology modelling and site-saturation mutagenesis was used to identify residues that would impair its activity towards *p*-coumaroyl-CoA without compromising cell growth. Several mutations leading to lower phloretic acid production were found and discussed. As an alternative approach we complemented the deletion of the *TSC13* gene with homologues from various plants. Genes from *Arabidopsis thaliana*, *Gossypium hirsutum* and *Malus domestica* were able to sustain cell progression while not resulting in *p*-coumaroyl-CoA reduction to phloretic acid. These findings should be of great value for the industrial production of *p*-coumaric acid-derived molecules in *S. cerevisiae*.

As naringenin is a precursor for other commercially relevant flavonoids we developed a platform for the production of a library of flavonoid derivatives and screened them for antibacterial properties. Seven different yeast strains producing flavonoids (naringenin, kaempferol, dihydrokaempferol, apigenin and afzelechin), a stilbenoid (resveratrol) and a dihydrochalcone (phloretin) were used as a base for the introduction of a library of *decorating* enzymes known to be active towards some of these compounds. Cariogenic bacteria were selected as a model for the screening of the combinatorial library for antibacterial potential. Although no compounds with significant antibacterial properties were identified, the method for the construction of flavonoid libraries that is presented here could serve as a base for future screenings.

DANSK RESUME

Flavonoider er sekundære plantemetabolitter derivatiseret fra enten phenylalanin eller tyrosin. Disse bioaktive stoffer har en stor kommerciel interesse grundet deres forskellige egenskaber som fx anti-oxidative, anti-tumor og/eller antibakterielle egenskaber. Industriel produktion af flavonoider, baseret på oprensning fra planter eller organisk synthese, kan dog være problematisk. På den anden side er den såkaldte bioindustrielle produktion af en vifte stoffer vha. mikroorganismer ved at bliver mere og mere populært. Målet med dette studie er at producere naringenin samt nogle af dens derivater i *Saccharomyces cerevisiae* som model for industriel produktion af flavonoider.

Ved at kombinere et balanceret heterologt udtryk af de gener, der er involveret i de biosyntetiske reaktioner ved fremstilling af (phenylpropanoid) naringenin samt en optimering af gærmetabolismen har vi udviklet en stamme, der producerer 430 mg/L naringenin fra glukose. Under disse omstændigheder blev naringenin produceret fra phenylalanin ved hjælp af phenylalanin ammonia lyase (PAL) i en stamme, der overproducerer phenylalanin og tyrosin. Da tyrosin også kan være en forløber for naringenin-produktion via tyrosin ammonia lyase (TAL), har vi undersøgt *in vivo* aktiviteten af flere TAL enzymer i *S. cerevisiae*. De fleste ammonia lyaser har affinitet for både phenylalanin og tyrosin, med præference for phenylalanin. Nogle enzymer er tidligere beskrevet som værende TAL enzymer, men de har enten en meget lav aktivitet på tyrosin, eller også er de i stand til at bruge phenylalanin som substrat. Vi har her identificeret et nyt TAL, et enzym fra *Aeromonas salmonicida* med relativ høj aktivitet mod tyrosin og ingen aktivitet mod phenylalanin.

Produktion af flavonoider og stilbenoider i *S. cerevisiae* er udfordrende, delvist pga. kulstoftab til phloretic syre som resultat af aktiviteten af en ukendt endogen reduktase. Gennem undersøgelser af 26 formodede c-c dobbeltbindingsreduktase knockout stammer, har vi identificeret Tsc13 som det enzym, der er ansvarlig for reduktionen af *p*-coumaroyl-CoA til phloretic syre. Da Tsc13 er et essentielt enzym blev en kombination af homologi-modellering og site-mættet mutagenese brugt til at identificere aminosyrerester som kan hæmme aktiviteten på *p*-coumaroyl-CoA uden at kompromittere cellevæksten. Vi har fundet og diskuteret flere mutationer som resulterede i lavere phloretic syre produktion. Som et alternativ har vi komplementeret deletionen af *TSC13* genet med homologer fra forskellige planter. Gener fra *Arabidopsis thaliana*, *Gossypium hirsutum* og *Malus domestica* var i stand til at opretholde cellevæksten uden at resultere i *p*-coumaroyl-CoA reduktion til phloretic syre. Disse resultater kan være af stor værdi for industriel produktion af *p*-coumaric-syre-fremstillede molekyler i *S. cerevisiae*. Eftersom naringenin er en forløber for andre kommercielt relevante flavonoider, har vi udviklet en platform for produktionen af et bibliotek af flavonoid deriviater og undersøgt dem for antibakterielle egenskaber. Syv forskellige gærstammer der producerer flavonoider (naringenin, kaempferol, dihydrokaempferol, apigenin og afzelechin), et stilbenoid (resveratrol) og et dehydrochalcone (phloretin) blev brugt som base for introduktionen af et bibliotek af derivatiserende enzymer kendt for at være aktive med nogle af disse stoffer. Cariesdannende bakterier blev udvalgt som model for undersøgelsen af det kombinatoriske bibliotek af antibakteriel potentiale. Selvom ingen stoffer med signifikant antibakterielle egenskaber blev identificeret kan metoden for konstruktionen af flavonoide biblioteker fungere som base for fremtidige undersøgelser.

Table of Contents

List of publications and patents

1. Lehka BJ, Eichenberger M, Bjørn-Yoshimoto WE, Garcia Vanegas K, Buijs N, Jensen NB, Dannow Dyekjær J, Jenssen H, Simón E, Naesby M. Improving heterologous production of phenylpropanoids in *Saccharomyces cerevisiae* by tackling an unwanted side reaction of Tsc13, an endogenous double bond reductase. *FEMS Yeast Res* 2017; **17**:1–12.

2. Eichenberger M, Lehka BJ, Folly C, Fischer D, Martens S, Simón E, Naesby M. Metabolic engineering of *Saccharomyces cerevisiae* for *de novo* production of dihydrochalcones with known antioxidant, antidiabetic, and sweet tasting properties. *Metab Eng* 2017; **39**:80–89.

3. Garcia Vanegas K, Lehka BJ, Mortensen UH. SWITCH: a dynamic CRISPR tool for genome engineering and metabolic pathway control for cell factory construction in *Saccharomyces cerevisiae*. *Microb Cell Fac* 2017;**16**(25).

4. Skjoedt ML, Snoek T, Kildegaard KR, Arsovska D, Eichenberger M, Goedecke TJ, Rajkumar AS, Zhang J, Kristensen M, Lehka BJ, Siedler S, Borodina I, Jensen MK & Keasling JD. Engineering prokaryotic transcriptional activators as metabolite biosensors in yeast. *Nat Chem Biol* 2016;**12**: 951–58.

5. Simón E, Lehka BJ, Vazquez CC. Biosynthesis of phenylpropanoids and phenylpropanoid derivatives. 2016. WO 2016189121 A1.

Contribution summary

1. BJL, ME, ES, WEB and MN designed the experiment. BJL performed most of the experimental work and KGW performed parts of the experimental work. JDD performed protein modelling. BJL, ES, NB and NBJ analysed the data. BJL drafted the manuscript. MN, ES, HJ and BL edited the manuscript.

2. BJL participated in the design of the experiment, revised the manuscript.

3. BJL provided the naringenin producing pathways, assisted with the experimental work.

4. BJL provided the strains producing different levels of naringenin.

5. BJL participated in design, performed the experiments, analysed the data.

Summary and aim of the thesis

This thesis consists of a general introduction followed by three main chapters.

The general introduction gives a background overview essential for understanding the following chapters. The first part focuses on flavonoids, by describing their occurrence, biosynthesis, industrial importance, health benefits and current commercial production. The second part focuses on the production of chemicals in a microbial host, such as *Saccharomyces cerevisiae*. Also an introduction to the basic tools used in metabolic engineering of *S. cerevisiae* as well as examples of compounds commercially produced in this microbial host will be provided in the second part.

The aim of the first chapter was to establish a robust yeast production platform for naringenin, which can serve as a precursor for other flavonoids. The first strategy in the construction of a background strain was to knock out genes in competing pathways which are known to reduce the amount of the pathway precursor, phenylalanine and intermediates, cinnamic and *p*-coumaric acid. Secondly, we aimed to find which enzymatic steps were limiting the production – pathway bottlenecks. This was followed by building a robust production strain via introduction of several copies of pathway genes, with an emphasis on pathway bottlenecks and the boosting of pathway precursors, phenylalanine and tyrosine. Our naringenin producer used phenylalanine as a pathway precursor, as it is a more efficient route than when using tyrosine. The final part of chapter one described the identification of an enzyme that would allow for the efficient use of tyrosine as a pathway precursor.

The production of naringenin in *S. cerevisiae* was limited by the carbon loss towards the side product – phloretic acid. Therefore the aim of chapter two was to identify the endogenous reductase and to eliminate this enzymatic step. 26 knockout strains missing putative double-bond reductase genes were evaluated and the enzyme responsible for the formation of side product was identified. Subsequently, solutions to unwanted side product formation were developed.

The aim of chapter three was to develop a method for the production and antimicrobial testing of a combinatorial flavonoid library. Seven different yeast strains producing flavonoids (naringenin, kaempferol, dihydrokaempferol, apigenin, afzelechin), a stilbenoid (resveratrol) and a dihydrochalcone (phloretin) were used as a base for the introduction of a library of *decorating* enzymes known to be active towards some of these compounds. Based on the literature and our experiments, these molecules have moderate antibacterial activity. Therefore, the aim of this approach was to produce a library of modified compounds and screen them for increased microbial activity in several models.

GENERAL INTRODUCTION

1. Flavonoids and stilbenoids

1.1 Chemical structure of selected phenylpropanoids

Phenylpropanoids such as flavonoids, stilbenoids and dihydrochalcones are commercially interesting plant secondary metabolites, derived from the phenylpropanoid pathway (Tapas *et al*. 2008; Jiang *et al*. 2016). Flavonoids are the most ubiquitous group of plant phenolics and natural constituents of the common human diet (Yao *et al.* 2004).

The basic skeleton of flavonoids consists of 15 carbons (C6-C3-C6) with two aromatic benzene rings (A and B), connected by an oxygen-containing pyrene ring (C) (Figure 1). Depending on the oxidation and saturation status, flavonoids are divided into several subclasses (Figure 1). The main subclasses are: flavonols (quercetin, kaempferol, myricetin), flavanones (hesperetin, naringenin), flavanols (catechin, epicatechin), flavones (luteolin, apigenin, baicalein), anthocyanidins (cyanidin, delphinidin) and isoflavones (genistein, daidzein) (Jiang *et al*. 2016; Pandey and Rizvi 2009). Most of the flavonoids occur naturally in glycosylated form as *O*- or *C*-glycosides. After ingestion they are transformed into aglycones, the form lacking sugar moieties (Kim *et al.* 1998).

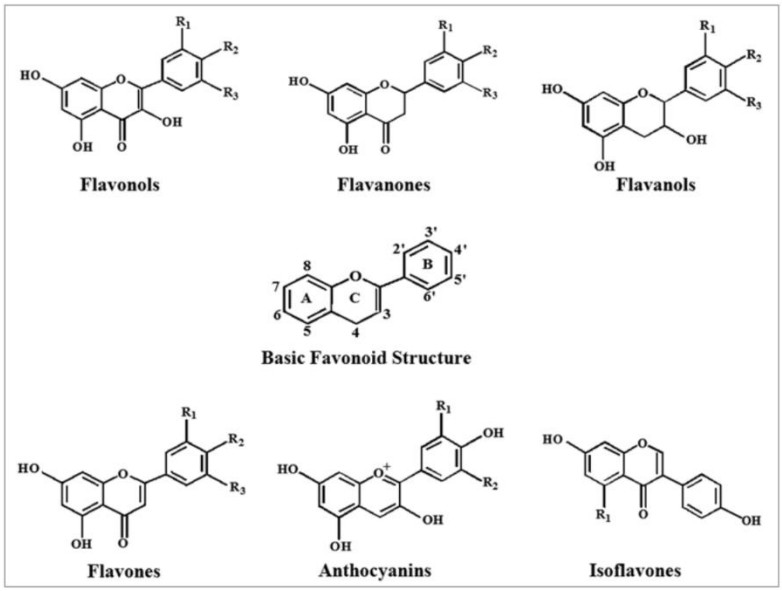

Figure 1. Basic chemical structure of 6 mayor sub-classes of flavonoids: flavonols, flavanones, flavanols, flavones, anthocyanins and isoflavones (from Pandey and Rizvi 2009).

Dihydrochalcones, e.g. phloretin, consist of 15 carbons (C6–C3–C6) and are similar in structure to their flavonoid counterparts, chalcones. The two aromatic rings are connected by a C3 chain (Figure 3).

The basic skeleton of stilbenoids, e.g. resveratrol, consists of 14 carbons (C6-C2-C6) with two aromatic rings joined by an ethylene bridge, commonly in the *trans*-configuration (Figure 3). They can occur as monomers or polymers (Rivière *et al*. 2012).

1.2 Occurrence, biosynthesis and function of flavonoids and stilbenoids in plants

1.2.1 Dietary sources

Flavonoids and stilbenoids are present in many plants and fruits and, therefore, are a natural component of the human diet. Examples of fruits rich in flavonoids and/or stilbenoids are berries, grapes, cherries, citrus fruits, apples, pears, plums, peaches and apricots. Examples of vegetables include onions, tomatoes, broccoli, kale, spinach and legumes. Herbs like tea, parsley, thyme and peppermint are also a rich source of these compounds. Coffee and Cocoa beans are also well acknowledged for their high flavonoid content (reviewed by Yao *et al.* 2004; Del Rio *et al.* 2013).

1.2.2 Biosynthesis

The general phenylpropanoid pathway leads to the formation of *p*-coumaroyl-CoA and from there it branches to give rise to a variety of compounds. Examples of the phenylpropanoid pathway products are flavonoids, stilbenoids, coumarins, curcuminoids and lignins (Figure 3) (Weisshaar & Jenkins *et al*. 1998; Vogt 2010).

Phenylalanine and tyrosine are the two aromatic amino acids that are precursors for phenylpropanoid pathway. Therefore, the shikimate pathway, in which aromatic amino acids are synthesized, is the metabolic entry point for the biosynthesis of phenylpropanoids. The shikimate pathway starts with phosphoenolpyruvate (PEP) being condensed with erythrose 4-phosphate (E4P) into 3-deoxy-D-heptulosonate 7-phosphate (DAHP) by DAHP synthase. As a next step 3-dehydroquinate synthase removes the phosphate group leading to formation of 3-dehydroquinate (DHQ) that is then dehydrated to 3-dehydroshikimate by 3-dehydroquinate dehydratase. This step is followed by a reduction of 3-dehydroshikimate into shikimate by the shikimate-5-dehydrogenase. Phosphorylation of shikimate by shikimate kinase yields the substrate for 5-enolpyruvylshikimate-3-phosphate (EPSP) synthase by which EPSP is formed. Chorismate synthase then eliminates the phosphate group from EPSP and chorismate is formed. From there the pathway branches to either tryptophan or phenylalanine and tyrosine. When chorismate is transformed to prephenate (PPA) by chorismate mutase the pathway flow is channelled towards phenylalanine and tyrosine. *Trans*-amination of prephenate by prephenate aminotransferase, yields arogenate, which is either transformed to tyrosine by arogenate dehydrogenase or phenylalanine by arogenate dehydratase (Figure 2) (Fraser and Chapple 2011).

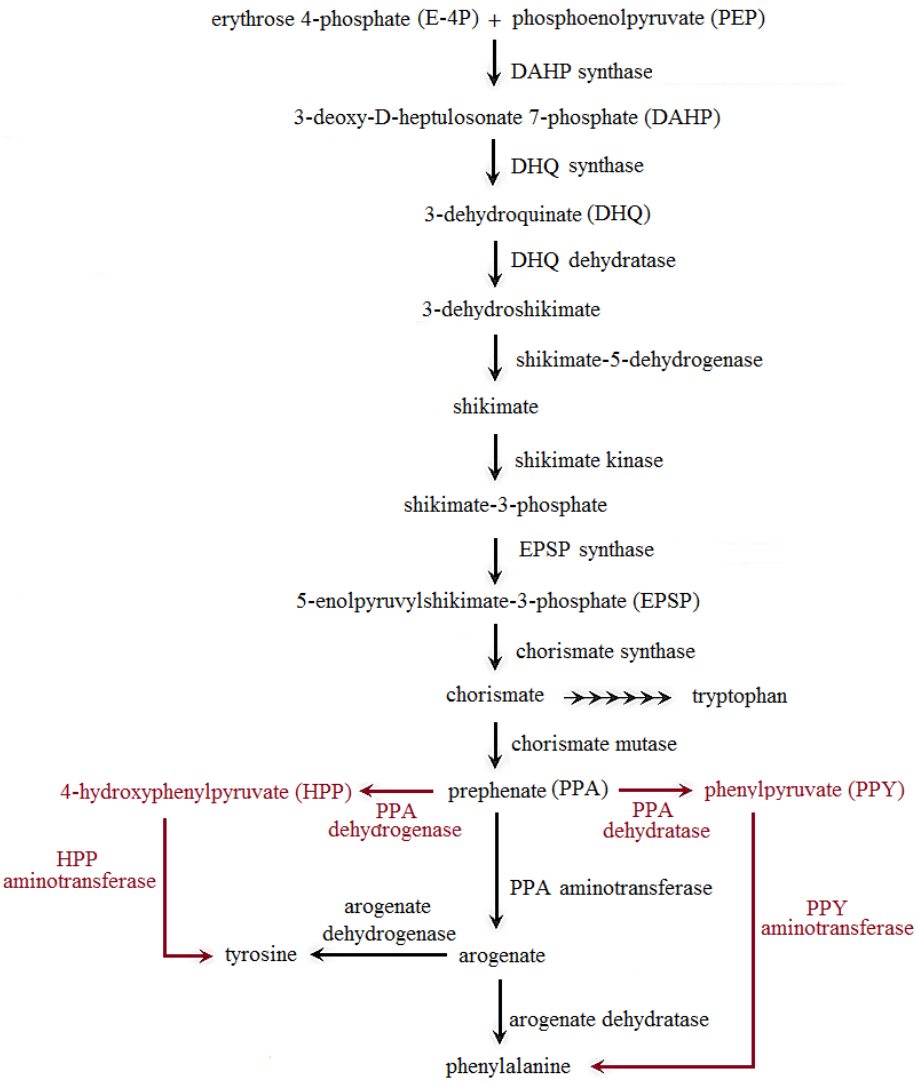

Figure 2. Model of shikimate pathway in higher plants. Black represents the classical for plants argonate pathway for synthesis of phenylalanine and tyrosine, whereas dark red represents alternative pathway for the production of these amino acids. Some reactants (ATP and PEP) and products as inorganic phosphate and water have been omitted. Figure is based on Fraser and Chapple (2011), Yoo et al. (2013) and Schenck et al. (2015) .

Recent findings of Yoo *et al.* (2013) revealed that plants also have an alternative route to the classical arogenate pathway, when entry point to the arogenate pathway becomes limiting. This alternative pathway also occurs in most microbes and is known as the phenylpyruvate pathway. In this alternative route of phenylalanine biosynthesis, prephanate (PPA) is transformed into phenylpyruvate (PPY) by prephanate dehydratase and then to phenylalanine by phenylpyruvate aminotransferase. Recently Schenck *et al.* (2015) proved that the alternative tyrosine biosynthesis model proposed by Yoo *et al.* (2013) exists in plants. In the alternative route of tyrosine biosynthesis, prephanate is transformed to 4-hydroxyphenylpyruvate (HPP) by prephenate dehydrogenase and then to tyrosine by the 4-hydroxyphenylpyruvate aminotransferase.

Malonyl-CoA is the universal building block for fatty acid biosynthesis and also a metabolic precursor for the production of flavonoids and stilbenoids. In eukaryotic cells the majority of malonyl-CoA is formed from acetyl-CoA and bicarbonate by acetyl-CoA carboxylase (ACC).

Acetyl-CoA is derived mainly from pyruvate, a product of glycolysis, via pyruvate dehydrogenase. Nevertheless, literature also reports that in eukaryotes malonyl-CoA can be made directly from malonic acid by malonyl-CoA synthetase (Chen H *et al.* 2011).

In the first step of the phenylpropanoid pathway L-phenylalanine is converted into *trans*-cinnamic acid through the non-oxidative deamination by phenylalanine ammonia lyase (PAL). In the next step, *trans*-cinnamic acid is hydroxylated at the para-position to *p*-coumaric acid (4-hydroxycinnamic acid) by cinnamate-4-hydroxylase (C4H), a cytochrome P450 monooxygenase enzyme, cooperating with a cytochrome P450 reductase (CPR). Alternatively, the amino acid L-tyrosine is converted into *p*-coumaric acid by tyrosine ammonia lyase (TAL). The *p*-coumaric acid is subsequently activated to *p*-coumaroyl-CoA by 4-coumarate-CoA ligase (4CL). Chalcone synthase (CHS) and chalcone isomerase (CHI) catalyze the condensation of a phenylpropane unit of *p*-coumaroyl-CoA with three molecules of malonyl-CoA, resulting in formation of naringenin chalcone and, finally, naringenin. If stilbene synthase (STS) is present instead of CHS, *p*-coumaroyl-CoA is condensed with three molecules of malonyl-CoA and a stilbene (i.e. resveratrol) is formed. Naringenin is a precursor for other flavonoids as well as tannins (Figure 3) (Weisshaar & Jenkins *et al*. 1998; Ferrer *et al*. 2008; Fraser and Chapple 2011).

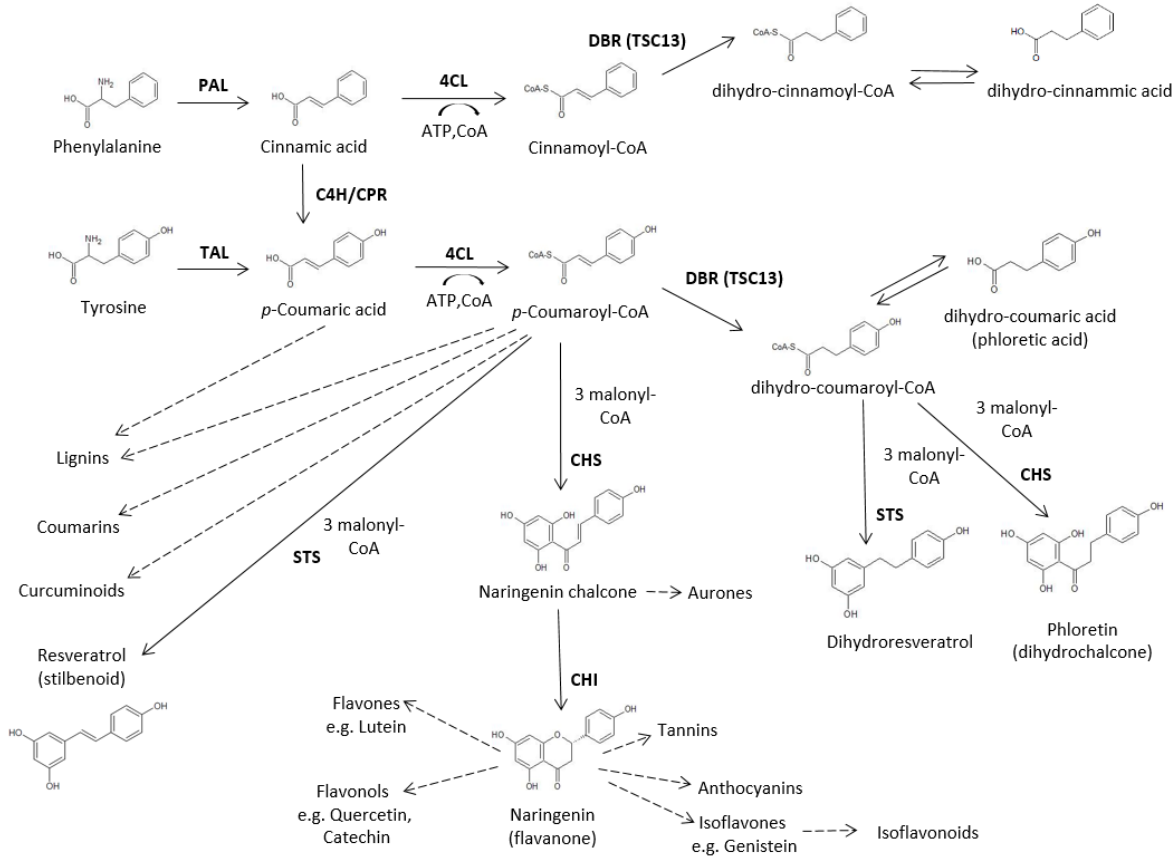

Figure 3. General phenylpropanoid pathway leading from phenylalanine or tyrosine to p-coumaroyl-CoA, from where it branches to give rise to flavonoids, stilbenoids, curcuminoids, lignins and other compounds. Solid lines represent the reaction steps, dashed lines do not represent the reaction steps but they simply indicate the products of each substrate. DBR -double bound reductase, PAL-phenylalanine ammonia lyase, C4H-cinnamate-4-hydroxylase, CPR-cytochrome P450 reductase, TAL-tyrosine ammonia lyase, 4CL-4-coumarate-CoA ligase, CHI-chalcone isomerase, CHS-chalcone synthase, STS- stilbene synthase.

1.2.3 Function in plants

In planta, phenylpropanoids serve a wide range of functions, as they are involved in the plant's response towards biotic and abiotic changes in the environment. Protection against UV radiation and microbial infections are among one of the most substantial roles of flavonoids in plants.

A wide variety of phenylpropanoid pathway derivatives have a maximum absorption spectra at 280–315 nm and, therefore, play a role in protecting DNA of plants against UV-B irradiation (Treutter 2005; Amalesh *et al.* 2011). Excess light also causes oxidative stress and flavonoids seem to be also involved in the reduction of the hazard of photo-oxidative damage (Agati *et al.* 2012). In a study by Kim *et al.* (2008) the expression of the genes involved in flavonol synthesis was induced in soybean plants upon UV-B irradiation and this led to the accumulation of kaempferol glycones (Kim *et al.* 2008). Schmitz-Hoerner and Weissenböck (2003) found that the degree of UV-B-caused damage was correlated with the phenolic contents of the barley leaves.

Several flavonoids and stilbenoids act as phytoalexins and have anti-microbial activity against plant pathogens. Production of phytoalexins in plants is induced in response to microbial stress (Ahuja *et al*. 2012). Production of stilbenoids is strongly induced upon infection with grapevine powdery mildew with the highest levels of stilbenoids accumulated in response to the pathogen observed in wild resistant cultivars of grapevine *Vitis spp.* (Schnee *et al.* 2008). Infection of citrus with *Candidatus liberibacter* – a bacteria causing the most destructive citrus disease worldwide – induces an elevated transcription of phenylpropanoid pathway genes (Aritua *et al.* 2013). Flavonoids also play a role in protecting plants from herbivores by, for example, decreasing the feeding rates of the larvae (Hoffmann-Campo *et al.* 2001; Sosa *et al.* 2004). Antioxidant effect of flavonoids and stilbenoids can also play a role in plant recovery after pathogen attack or mechanical damage by reducing the accumulated reactive oxygen species (ROS) (Agati *et al.* 2012).

Lignin, a phenylpropanoid pathway derivative, provides plants with structural integrity and a barrier against environmental stress (Lan *et al.* 2015, Bassard *et al.* 2012). Anthocyanins provide colours for flowers and fruits, contributing to the attraction of pollinators and seed dispersal (Harborne and Williams 1998, Yoshida *et al.* 2009).

Flavonoids also act as signaling molecules. For example they act as signaling molecules, during the symbiosis of legumes with nitrogen fixing bacteria, during the formation of nitrogen-fixing root nodules (Peters *et al*. 2016). Phenylpropanoids can also act as allelochemicals, disturbing the growth of associated or surrounding plants (Amalesh *et al*. 2011).

1.3. Industrial importance of flavonoids and stilbenoids

Flavonoids and stilbenoids are commercially interesting compounds for several reasons. The increasing concern of the general public about synthetic food colourants resulted in the transition towards natural dyes in the food industry. Anthocyanins are the largest group of water-soluble natural pigments and are frequently used as food colourants (reviewed by He and Giusti 2010). For the same reasons interest in natural food preservatives is increasing, so phenylpropanoid pathway derivatives display a huge potential due to their antioxidant properties (reviewed by Balasundram *et al*. 2006).

Sales of dietary supplements increased remarkably over the last decade. Factors like aging population, increased awareness of consumers for preventive healthcare and alternative medicine are the main reasons for this remarkable increase in sales (Teichner and Leskoo 2013). Derivatives of the phenylpropanoid pathway are frequently marketed and used as dietary supplements (Chun *et al*. 2007; Ríos-Hoyo and Gutiérrez-Salmeán 2016; Vidak *et al*. 2015). As an example, the stilbenoid, resveratrol is marketed as a nutraceutical as it is reported, among others, to prevent the development of metabolic syndrome (Sicińska *et al.* 2015).
Flavonoids are also an important ingredient in the cosmetic industry due to their antioxidant, anti-inflammatory and UVB absorbing properties as well as their protective effects on blood vessel walls (reviewed by Arct and Pytkowska 2008; Epstein 2009).

1.4 Health benefits of flavonoids and stilbenoids, with focus on naringenin

1.4.1 Health benefits from flavonoids and stilbenoids consumption

Plants have been used for centuries as a crucial element of folk medicine, since numerous secondary metabolites from plants possess a broad spectrum of biological activity (Petrovska 2012). Epidemiological studies report a strong association between a diet rich in flavonoids/stilbenoids and a low incidence of some common chronic diseases. The correlation between flavonoid reach foods and decreased risk of some chronic diseases might be due to the effect of single compounds as well as to combination of different molecules (Alissa and Ferns 2012; Erdogan and Vang 2016).
The raise of the *French Paradox* in the 1980s drew great attention from researchers towards flavonoids and stilbenoids, abundant in the Mediterranean diet (reviewed by Stoclet *et al*. 2004; Cordova *et al*. 2005; Del Rio *et al*. 2013). To a surprise of epidemiologists, Mediterranean populations were reported to have relatively low incidence of coronary heart disease (CHD) despite high consumption of foods rich in saturated fats. This pattern was termed as *French Paradox* and was soon attributed to the increased consumption of red wine and other antioxidant-rich foods by Mediterranean populations (Ranaud and de Lorgeril 1992). Resveratrol, a stilbene present in red wine, has been suggested to play a central role on the *French Paradox*. Nevertheless, beside resveratrol, there are other polyphenols present in red wine as flavonols (quercetin and myricetin), flavanols (catechin and epicatechin), anthocyannins, hydroxynnamates (caffeic, caftaric, and coutaric acids), and hydroxy-benzoates (Cordova *et al*. 2005).
In addition to preventing coronary heart disease, flavonoids and stilbenoids also seem to play a protective role against Type II diabetes, neurodegenerative diseases, and numerous types of cancer (reviewed by Yao *et al*. 2004; Del Rio *et al*. 2013). Abundant *in vitro* and *in vivo* studies report the mechanisms of action of these molecules and provide an explanation of the specific health promoting properties observed in the epidemiological studies (reviewed by Tapas *et al*. 2008; Lu *et al*. 2013). Therefore, flavonoids and stilbenoids can be used as nutraceuticals to prevent or treat certain disorders (reviewed by Tapas *et al*. 2008).

As discussed, flavonoids and stilbenoids are often reported to have exceptional antioxidant properties. These antioxidant activities can be based on 1) suppression of reactive oxygen species formation, 2) scavenging free radicals, and 3) upregulation of antioxidative enzymes. (Pietta 2000). The antioxidant and anti-inflammatory properties of numerous flavonoids and

stilbenoids seem to contribute to their antithrombotic, antidiabetic, anticarcinogenic, antiaging, antiallergic, hepato-, neuro- and gastro-protective properties. Many flavonoids and stilbenoids seem to prevent the occurrence of metabolic syndrome, the collection of risk factors that lead to type II diabetes and coronary heart diseases. These risk factors include hypertension, insulin resistance, obesity and elevated plasma lipids, where the last two lead to chronic low grade inflammation.

Numerous flavonoids and stilbenoids can prevent heart diseases by one or more of the following mechanisms, 1) dilate and/or protect vessels, 2) decrease blood clots formation, and 3) prevent LDLs oxidation (Stoclet *et al.* 2004). The antidiabetic activity of these molecules is often attributed to the ability to 1) decrease glucose level in the plasma, and 2) improve insulin sensitivity (Nicolle *et al.* 2011). Many flavonoids and stilbenoids are reported to inhibit cell proliferation, promote differentiation, supress angiogenesis, and/or promote apoptosis of cancer cells, are interesting for cancer research (Benavente-García and Castillo 2008; Georgiev *et al.* 2014; Singh *et al.* 2014).

Many flavonoids and stilbenoids have been identified in medical plants used for centuries against microbial infections and a variety of flavonoids and stilbenoids have been reported to have antimicrobial activity against several significant pathogens including bacteria, fungi and viruses (Cushnie and Lamb 2005).

1.4.2 Health benefits of naringenin

In nature, naringenin occurs mostly in its glucosylated form, called naringin, which contributes to the bitter taste of grapefruits. Fresh grapefruit juice contains up to 800 mg/L of naringin (Wilcox *et al.* 2006). After ingestion, naringin is deglycosylated to naringenin by intestinal microbiota (Kim *et al.* 1998). Naringenin has been reported to have antidiabetic, anti-atherosclerotic, anti-inflammatory, antioxidant, hepato-protective, anti-cancerous and neuro-protective properties (Wilcox *et al.* 2006).

One of the most well-known applications of naringenin is that the prevention of the development of metabolic syndrome and, therefore, consequent type II diabetes and coronary heart diseases (CHD). Several animal studies point towards antihyperglycemic properties of naringenin. Ortiz-Andrade *et al.* (2008) treated normoglycemic and diabetic rats with 50 mg/kg of naringenin, significantly lowering plasma glucose levels in both groups due to a decreased absorption of carbohydrates from the intestine. Kannappan and Anuradha 2010 demonstrated that administration of naringenin to Wistar rats with fructose-induced insulin resistance resulted in an improved insulin sensitivity and decreased levels of glucose, free fatty acid and triglycerides in the plasma. Annadurai *et al.* (2012) showed that diabetic Wistar rats treated with naringenin presented reduced levels of glucose and elevated levels of the insulin in the blood. Additionally, the treated animals had increased activity of pancreatic enzymatic antioxidants and in higher levels of non-enzymatic antioxidants in the plasma.

Naringenin has also been widely reported as possible anti-atherosclerosis agent when tested both *in vitro* and *in vivo*. The *in vitro* studies performed by Wu *et al.* (2009) demonstrated that LDL-bound flavonoids such as naringenin, luteolin or quercetin increased the resistance of LDL to oxidation. Assini *et al.* (2013) suggested that naringenin prevents cholesterol-induced systemic inflammation and, consequently, atherosclerosis. They showed that naringenin

supplementation to Ldlr−/− mice (metabolic syndrome model) fed with a cholesterol-rich diet, significantly attenuated the occurrence of atherosclerosis. Moreover, human trial studies have demonstrated that a daily intake of 400 mg of naringenin reduces blood low-density lipoprotein (LDL) and lowers the oxidative stress in hypercholesterolemic patients (Jung *et al.* 2003).

Another interesting health promoting property of naringenin is its role in neuroprotection. Heo *et al.* (2004) demonstrated the neuroprotective effect of naringenin *in vitro* and *in vivo*. The pretreatment of nerve cells with vitamin C and naringenin reduced hydrogen peroxide- induced neurotoxic effect. In the same study, the supplementation of naringenin (4.5 mg/kg) to mice with induced amnesia significantly improved this condition. These findings can be useful in the prevalence and treatment of neurodegenerative conditions such as Alzheimer's disease. The anti-inflammatory properties of naringenin can be useful in the case of ischemic stroke (due to lack of oxygen) as the inflammation of the brain after an ischemic stroke is the main reason for the progression of the damage. In this context, the administration of naringenin to the Sprague-Dawley rats prior to the induction of ischemic stroke reduced the degree of brain damage (Bai *et al.* 2014).

Alcohol induced liver damage was also found to be alleviated in the ethanol-fed rats, when naringenin was administrated. This effect seems attributable to its anti-inflammatory properties (Jayaraman *et al.* 2012).

Naringenin, as other flavonoids and stilbenoids, has been reported to have anti-tumor properties. Furthermore, it has been reported by Jagetia *et al.* (2003) that naringenin can have protective effect against γ-radiation. Supplementation of a relatively low dosage of naringenin to mice prior γ-radiation exposure, resulted in significantly reduced chromosome damage in the bone marrow. Moreover, naringenin showed anti-proliferative and anti-angiogenic effects when administered orally to Swiss albino mice implanted with Ehrlich ascites carcinoma cells (Anand *et al*. 2012).

1.4.3 Interactions of naringenin with drugs

Despite the variety of medical properties of naringenin, it seems that the combination of naringenin with some of the commercial drugs could interfere with their metabolism (Wilcox *et al*. 2006). In this context, it seems relatively accepted that medication should not be administrated together with grapefruit juice (Mazi-Kotwal and Madhavan 2002). The interaction of grapefruit juice with medical drugs was accidently discovered and reported in 1991, when the researchers found that the blood levels of hypertension drugs felodipine and nifedipine increased dramatically when administrated together with grapefruit juice. Later on grapefruit juice was reported to interact with numerous drugs and often lead to toxic effects (Bailey *et al*. 2012). Further studies demonstrated that naringin increases the oral bioavailability of certain compounds by competitively inhibiting their metabolism. Fuhr *et al.* (1993) demonstrated that naringenin is a competitive inhibitor of CYP1A2, an enzyme responsible for the metabolism of caffeine and other molecules. Another enzyme found to be competitively inhibited by naringenin *in vitro* was CYP3A4. This enzyme is responsible for the metabolism of the aforementioned nifedipine and is responsible for activating the dangerous aflatoxin B1 (Guengerich and Kim 1990).

1.5 Current commercial production of phenylpropanoids

The current commercial production of interesting phenylpropanoid pathway derivatives relies mainly on extraction from plants. Some phenylpropanoids can also be extracted from agro-industrial waste, e.g. peels and seed residues of citrus fruits (Balasundram *et al.* 2006). Extraction of flavonoids and stilbenoids from plants is dependent on stable supplies of good quality raw materials and requires the usage of large extensions of land. Moreover, the profile of secondary metabolites in the plant materials differs from batch to batch, so the extraction process and the resulting material are difficult to standardize. Additionally, isolation and purification of a single compound from a naturally occurring mixture of compounds might be problematic (Fowler and Koffas 2009). Furthermore, some of the interesting flavonoids are found only in rare plants that may be difficult to access, or occur only in minute amounts (Hatano *et al*. 2000; Yu *et al*. 2016). Organic synthesis of phenylpropanoids is another alternative for industrial production. However, that organic synthesis of flavonoids and stilbenoids involves the use of toxic solvents needed during the catalysis and/or purification processes, limiting their large-scale production (Fowler and Koffas 2009). Organic synthesis is often also problematic as the mix of stereoisomers produced is difficult to separate while only naturally occurring *S* configuration of flavonoids have been reported as biologically active, and therefore commercially interesting (Marston and Hostettmann 2006).

Production of a variety of compounds in microorganisms, called bio-industrial production, is gaining more and more popularity. Several hosts are reported to be used as cell factories for phenylpropanoids, such as bacteria, yeast, plant cells and tissue cultures (reviewed by Bharati and Bansal 2014; Trantas *et al.* 2015; Wang and Yu 2012; Wang *et al.* 2016).
Cost-efficient bio-industrial production requires a suitable host, a cheap carbon source, as well as an optimized production pathway and an elimination of the carbon losses towards undesired products (Hong and Nielsen 2012; Nevoigt 2008). As there is a number of advantages for using *S. cerevisiae* as a host for large scale bio-industrial production of commercially interesting compounds, this yeast has become the organism of choice in many approaches (Baerends *et al*. 2015; Hansen *et al*. 2009; Julien and Wallace 2014; Katz *et al.* 2013; Katz *et al.* 2015; Ro *et al*. 2006; Saunders *et al.* 1995; Verwaal *et al.* 2012).

2. *Saccharomyces cerevisiae* as a yeast cell factory

The baker's yeast *S. cerevisiae* has been used over five thousand years for baking and brewing due to its fermentative capabilities. According to the US Food and Drug Administration, *S. cerevisiae* is Generally Recognized As Safe (GRAS). Moreover, *S. cerevisiae* was the 1st sequenced eukaryote and is probably the best studied unicellular eukaryote model organism (Bergman 2001; Landry *et al*. 2006).
The baker's yeast is very well characterized at cellular, molecular, and genetic levels, due to the existence and continuous development of genomic, transcriptomic, proteomic and metabolomic techniques. Shortly after *S. cerevisiae* was sequenced in 1996 the online access to its genome was made available through the Saccharomyces Genome Database (SGD) (http://www.yeastgenome.org/). The SGD website is still today a first stop for thousands of scientists around the globe working with *S. cerevisiae* and provides information about the

genome, functions of the proteins, phenotypes of different mutants, protein interactions, metabolic pathways and others (Cherry *et al.* 1998).
A plethora of genetic tools for the metabolic engineering of budding yeast are available and, with the advent of CRISPR/Cas9 (Dicarlo *et al.* 2013) and other gene editing tools, the ability to easily introduce several heterologous genes at once and in a stable manner into its genome is a big advantage that has made *S. cerevisiae* a preferred host by the bio-industry (Da Silva & Srikrishnan, 2012; Jensen *et al.* 2014; Romanos *et al*. 1992).

The expression of heterologous eukaryotic genes in *S. cerevisiae* is favorable, in contrast to the expression in prokaryotes, as its gene expression machinery and intracellular compartments resemble that of other eukaryotes.
S. cerevisiae grows rapidly in rich media and has high tolerance towards ethanol, high concentrations of sugar and low pH. Being a model organism, fast growth and with a high tolerance to different conditions are desirable properties for an industrial host (Bergman 2001). *S. cerevisiae* has already been used, not only for the production of flavonoids, but for a wide spectrum of commercially-relevant products including biofuels, pharmaceuticals, food ingredients, and others (Abbott *et al.* 2009; Hong & Nielsen 2012; Keasling 2010; Li and Borodina 2015; Nielsen *et al.* 2013; Peralta-Yahya *et al.* 2012; Siddiqui *et al.* 2012). Examples of products that are currently commercially available and were produced by fermentation of engineered *S. cerevisiae* include, among others, the antimalarial drug artemisinin (Ro *et al.* 2006), the vanilla flavour vanillin (Hansen *et al.* 2009), the nutraceutical resveratrol (Baerends *et al*. 2015; Katz *et al.* 2013; Katz *et al.* 2015), the fragrance and insect repellent nootkatone (Julien and Wallace 2014; Goldblum and Warren 2014), succinic acid (Verwaal *et al.* 2012), squalene (Saunders *et al.*1995), and the sweeteners from stevia (Houghton-Larsen *et al*. 2013).

2.1 Synthetic biology tools in yeast

2.1.1 Vectors and genomic insertions of heterologous DNA

S. cerevisiae has a great DNA transformation efficiency and it can be cultivated in a defined minimal medium, which allows for the development and usage of auxotrophic markers. Integration of DNA cassettes into the yeast genome is more advantageous than expression from extrachromosomal plasmids as selection pressure does not need to be maintained and the inserts are mitotically stable (Da Silva and Srikrishnan 2012; Romanos *et al.* 1992). Moreover, the use of reusable selection markers allows for multiple rounds of gene integration (Boeke *et al.* 1987).

The degree of expression of integrated gene cassettes is dependent on the locus of the insertion site in the yeast genome. Flagfeldt *et al.* (2009) characterized 20 different loci for the integration sites in the genome of *S. cerevisiae*. They found 8.7-fold difference between the sites with lowest and highest expression of the reporter gene. Mikkelsen *et al.* (2012) also tested 14 different integration sites and got 2.5 fold difference between the lowest and highest expression sites, whereas the fitness was negatively affected in the case of 3 integration sites. Therefore, the integration sites chosen for the heterologous expression of genes need to be carefully evaluated in the context of expression and fitness of the host.

Combining traditional cloning techniques with the more flexible uracil excision reaction-based cloning (USER) has revolutionized molecular cloning by making it easier and faster. This method allows for the creation of sticky ends in any sequence containing two thymines 6-10 bp apart from each other on opposite DNA strands. DNA fragments are amplified by PCR using primers with homologous overhangs where each of the thymines is substituted by deoxyuracil (dU). The polymerase developed for this technology has proof-reading abilities but allows DNA propagation despite the presence of uracil in the DNA. The generated PCR fragments are treated with a USER enzyme mix containing both Uracil DNA glycosylase and the DNA glycosylase-lyase Endonuclease VIII activities. This enzyme mix removes the two single residues of uracil and dissociated single stranded DNA, leaving the compatible sticky ends (Nour-Eldin *et al.* 2006).

Recently a set of vectors called EasyClone were developed on the basis of the vectors described by Mikkelsen *et al.* (2012). These vectors allow for the simultaneous integration of multiple genes into the yeast genome and the recycling of the selection markers. EasyClone plasmids contain an *ori* from *E. coli*, a USER cloning cassette where a DNA of interest is inserted flanked by two terminators in opposite directions, an auxotrophic selection marker flanked by LoxP sites or DR (direct repeats), and two sequences homologous to the specific integration sites (Figure 4). These vectors are developed for the insertion of a bidirectional promoter and two genes of interest (bio-bricks) (Jensen *et al.* 2014; Mikkelsen *et al.* 2012) in each construct. The difference between Mikkelsen *et al.* (2012) and Jensen *et al.* (2014) works is that the first group integrated DNA fragments at each integration site in a stepwise manner, while the second group introduced several constructs into different integration sites simultaneously. Jensen's group used different markers flanked by LoxP sites, which were simultaneously removed at the final step, whereas Mikkelsen's group used a single *URA3* marker flanked by direct repeats that was recycled at each step.

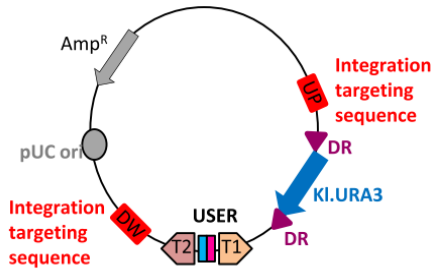

Figure 4. EasyClone vector. PUC ori- *E. coli* origin of replication*, UP and DW- sequences homologous to yeast genome, Kl.URA3-URA3 from Kluyveromyces lactis, DR- direct repeats, USER- cloning cassette (Jensen* et al. *2014).*

Shao *et al*. (2009) developed a DNA Assembler method where entire pathways can be assembled by the yeast's recombinatorial machinery into an extrachromosomal DNA construct or simply incorporated into the yeast genome. This technology is based on DNA fragments sharing homology regions between the fragments and/or yeast genome, so they can be assembled *in vivo* inside the yeast's cytosol what is called transformation-associated recombination (TAR). Kuijpers *et al.* (2013) developed a robust *in vivo* assembly method of multi-component plasmids with highly improved efficiency. This technology is based on PCR fragments flanked by 60 bp synthetic sequences with homology to other fragments but not with homology to the yeast genome (Figure 5). The number of fragments may vary but should

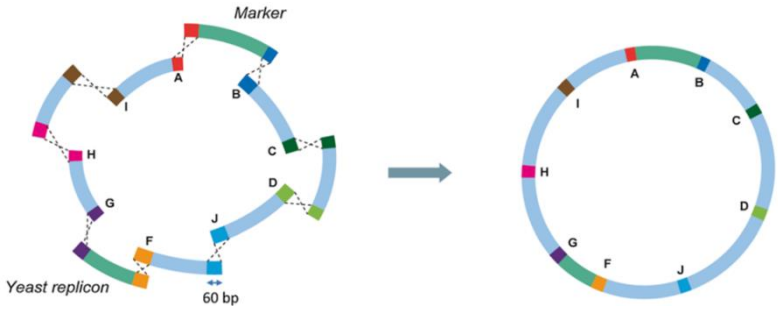

always include one coding for yeast replication sequence, one coding for a selection marker, and a variable number of fragments coding for the genes or expression cassettes of interest.

Figure 5. Model for in vivo assembly of plasmids using 60bp synthetic homologous recombination sequences (Kuijpers et al. 2013).

Yeast artificial chromosomes (YACs) are also an option for introducing and expressing multiple genes simultaneously within a cell. The YACs should contain a yeast origin of replication, a centromere and telomeres, and are able to carry large fragments of DNA. YACs can be constructed either by *in vitro* ligation or by *in vivo* TAR (Da Silva and Srikrishnan 2012; Siddiqui *et al.* 2012) and have been used for the production of small amounts of flavonoids in yeast (Naesby *et al.* 2009).

In order to achieve high expression levels of a small number of genes, 2µ plasmids or integrative Ty-plasmids can be used. Using a repetitive chromosomal DNA such as δ sequences (sequences specific to yeast Ty retrotransposon) as a recombination site allows for multiple integration of the same gene (Lee and Da Silva 1997; Sakai *et al*. 1990).

2.1.2 Promoters

There is a huge variety of *S. cerevisiae* native and foreign promoters that can be used for heterologous gene expression in this organism. These promoters can be basically divided into *constitutive* and *inducible* and have very different strength. Constitutive promoters are preferred in industrial setups as no inducers or repressors are involved and production is normally dependent on cell growth or other basic parameters.

The most common constitutive promoters are adopted from the yeast glycolytic pathway and, therefore, are normally dependent on the presence of glucose. Examples include promoters of the following genes: phosphoglycerate kinase (pPGK1), pyruvate decarboxylase (pPDC1), triosephosphate isomerase (pTPI1), alcohol dehydrogenase (pADH1), glyceraldehyde- 3-phosphate dehydrogenase (pTDH3 or pGPD), and pyruvate kinase (pPYK1). The constitutive translation elongation factor promoter pTEF1 or pTEF2 are also commonly used (Da Silva and Srikrishnan 2012).

The specific activity and strength of the promoters can be estimated in the lab by fusing them with a reporter gene such as *lacZ* or green fluorescent protein (GFP) and then measuring the end-point activity of the resulting protein. Partow *et al.* (2009) compared strength of different constitutive promoters (pTEF1, pADH1, pTPI1, pHXT7, pTDH3, pPGK1 and pPYK1) during growth on glucose. pTEF1 was one of the strongest promoters and showed no dependence on glucose. pPGK1 and pTDH3 were strongly induced in the presence of glucose and had lower activity during the absence of the sugar. By using error prone PCR, Alper *et al.* (2005) developed the library of variants of pTEF1. The different derivatives exhibited activities from

17% to 250% in relation to the original promoter. Weinhandl *et al.* (2014) investigated what promoters could be used in order to assure the expression of target genes during the ethanol growth phase (e.g. induced in the absence of glucose).

Tightly regulated inducible promoters are essential in case of e.g. production of toxic products. The most commonly used inducible promoters are the ones responsible for the galactose metabolism such as pGAL1, pGAL7, and pGAL10, which are induced by galactose and repressed by glucose. The native yeast promoters are often modified in order to reduce their strength or alter their properties e.g. dependence on glucose (Da Silva and Srikrishnan 2012). Research of entirely synthetic promoters is also emerging, both to reduce the risk of homologous recombination between genetic inserts and the native genome and to avoid the depletion of native transcription factors (Redden *et al.* 2015).

In summary, due to the intrinsic ability of *S. cerevisiae* to perform a highly efficient homologous recombination and the plethora of molecular tools available, it is possible to easily introduce and express a significant number of mitotically stable heterologous genes within the yeast genome, while tightly controlling their copy number and expression levels. Recycling selection markers and markerless genome editing techniques allow multiple transformation rounds and, consequently, the development of complex production strains in shorts periods of time (Da Silva & Srikrishnan, 2012; Jensen *et al*. 2014; Mikkelsen *et al.* 2012; Siddiqui *et al.* 2012).

2.2 Case studies

S. cerevisiae has been used as a cell factory for a wide spectrum of products ranging from bulk compounds and biofuels, to fine compounds, such as nutraceuticals or pharmaceuticals (see Figure 6).

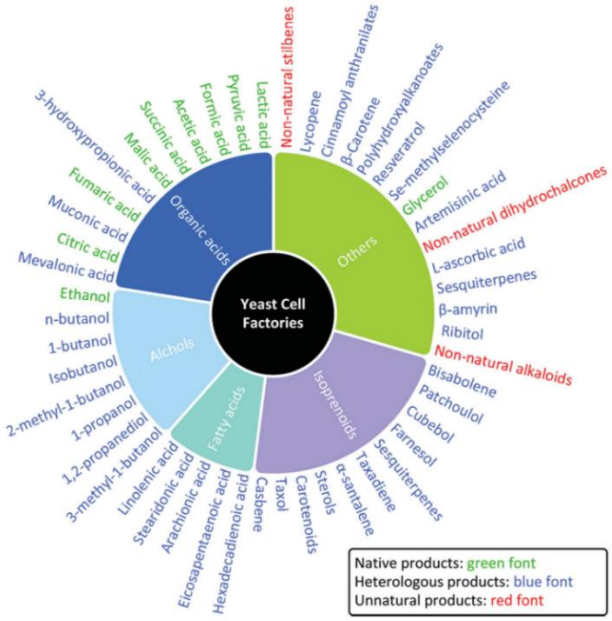

Figure 6. Examples of compounds that have been produced in yeast (Li and Borodina 2015) .

The biosynthesis of bulk chemicals and biofuels requires a very low cost production in order to be competitive with a sector that has been well established for over hundred years as is the conventional petrochemical industry. Reductions on the production costs for the biochemical industries mainly come from two angles, the economy of scale and the use of abundant and cheap carbon sources as starting material. However, the first point requires large and risky economic investments and the second is certainly not trivial from a technical perspective. The production of fine chemicals, however, allows higher prices and demands for high quality of the final products. In this context, higher unit selling prices and higher benefit margins allow the biosynthetic approaches to be already competitive with other existing production methods (Hong and Nielsen 2012; Keasling 2010; Nielsen *et al.* 2013).

2.2.1 Biofuels

Biofuels are gaining more and more popularity as they are a sustainable alternative to the finite fossil fuels. In principle, the sugars derived from biomass are converted to biofuels by microbial fermentation.

First generation bioethanol derives from the direct fermentation of glucose. The first efforts to improve production yields passed by reducing or eliminating the formation of glycerol and other side products of the fermentation process. The NADH formed during the fermentation of glucose cannot be used in the electron transport chain due to a lack of oxygen, so glycerol-3-phosphate dehydrogenases (GPD) converts it back to NAD+ leading to an accumulation of glycerol. A strain with deleted *GPD1* and *GPD2* genes does not produce glycerol but is not able to grow in anaerobic conditions. Deleting these genes combined with the introduction of other NADH sink such as NAD+-dependent acetaldehyde dehydrogenase from *Escherichia coli* and acetic acid supplementation, resulted in a strain capable of growing under anaerobic conditions without accumulating glycerol (Medina *et al.* 2010). The problem with this is approach is that glycerol has an important role in osmoregulation, which is a common problem in large scale fermentations. Therefore the efforts continue to solve this problem (Nielsen *et al.* 2013).

Obtaining biofuels from lignocellulose is a sustainable, but challenging practice. The pentose sugars xylose and arabinose are the main compounds derived from cellulose and constitute a cheap carbon source for organisms that can metabolize them. Heterologous expression of genes involved in xylose and arabinose catabolism allows *S. cerevisiae* to ferment these sugars into bioethanol (Nielsen *et al.* 2013; Peralta-Yahya *et al.* 2012). By introducing a fungal xylose and a bacterial arabinose pathway into budding yeast, Karhumaa *et al.* (2006) developed a strain that was able to co-ferment these pentose sugars. Second generation bioethanol (cellulosic ethanol), produced by *S. cerevisiae* was introduced on the market by BetaRenewables in 2013.

An example of a more advanced biofuel produced by *S. cerevisiae* is isobutanol, which is less hygroscopic, has higher energy density and mixes with gasoline better when compared to ethanol. Isobutanol is formed in yeast during valine synthesis, as a side product. Using this knowledge Chen X *et al.* (2011) developed a *S. cerevisiae* strain producing isobutanol. They overexpressed valine pathway genes *ILV2*, *ILV3* and *ILV5* and the gene coding for enzyme

involved in the first reaction of the valine catabolism in the cytosol -branched-chain amino acid aminotransferase *BAT2*. Gevo is one of the first corporations that performed isobutanol production from cellulose and they hold several patents on production of butanol and isobutanol in *S. cerevisiae* employing different strategies (Hong and Nielsen 2012).

Biofuels can also be derived from isoprenoids, plant secondary metabolites which are usually precursors for flavours and pharmaceuticals. Example of such biofuel is farnesane derived from its precursor farnesene. This advanced biofuel is produced by Amyris using a *S. cerevisiae* strain previously developed for the production of artemisinin, an antimalarial drug intermediate. Both products are derived from farnesyl pyrophosphate (FPP), therefore the yeast strain engineered to accumulate this endogenous compound can be used to manufacture both products. Introduction of heterologous farnesene synthase (FS) results in conversion of FPP to farnesene and chemical hydrogenation converts it into farnesane (Meadows *et al.* 2016; Ubersax & Platt 2010).

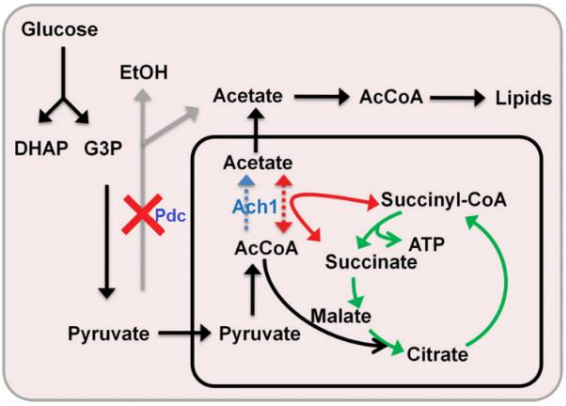

Figure 7. A strategy that can be applied in order to boost pyruvate, a precursor for e.g. carboxylic acids (modified from Chen et al. *2015).*

2.2.2 Bulk chemicals

Other than fuels, another good example of bulk or commodity chemicals can be organic acids. As budding yeast has a natural tolerance to low pH (<3), it is well fitted for the production of organic acids as, for example, carboxylic acids. A strategy to enhance the natural yeast production of a given carboxylic acid from pyruvate comprises eliminating alcoholic fermentation, directing glycolysis to the product of choice and engineering an efficient export system (Abbott *et al.* 2009). Flikweert *et al.* (1997) eliminated alcoholic fermentation by knocking out the pyruvate decarboxylase genes *PDC1, 5* and *6*. However, this resulted in a strain that had an impaired growth and required supplementation with ethanol or acetate. In another approach, van Maris *et al.* (2004) obtained a Pdc- optimised strain through adaptive evolution and reached pyruvate concentrations of up to 135 g/L. More recently, Chen *et al.* (2015) identified that a Pdc- strain is capable of restoring the levels of cytosolic acetyl-CoA when overexpressing *ACH1* (Figure 7). Ach1 is responsible for transferring acetyl molecules from the mitochondria to the cytoplasm. While pyruvate can be a final product, it can also be an intermediate on the microbial production of other carboxylic acids. Therefore the described strategy can be applied as a starting point for the production of, among others, lactic acid, malic acid and succinic acid. Succinic acid is commercially produced using budding yeast and manufactured by Reverdia (Verwaal *et al.* 2012).

2.2.3 Fine chemicals

Fine chemicals are complex, single, pure chemical substances, produced in limited quantities and with a high added value when compared to the raw material used for their production.

Among them, nutraceuticals such as flavonoids and stilbenoids can be successfully produced using engineered budding yeast. In principle, the expression of heterologous phenylpropanoid pathway genes from plants (described in section 1.2.2) is combined with the boosting of the synthesis of precursor molecules and the inhibition of competing pathways. Relevant research will be described in chapter 1 of this thesis.
The first flavonoid produced in *S. cerevisiae* was the flavanone naringenin, which is the precursor of numerous downstream flavonoids (Jiang *et al*. 2005). Ralston *et al.* (2005) identified the enzymes isoflavone synthase (IFS) and chalcone isomerase (CHI) from soybean (*Glycine max*) that, when expressed heterologously, convert naringenin chalcone into the isoflavone genisein in yeast. They also identified flavone synthase II (FSII) and the corresponding chalcone isomerase, which convert naringenin chalcone into apigenin. By expressing a whole heterologous phenylpropanoid pathway in *S. cerevisiae*, Trantas *et al*. (2009) were able to produce naringenin, resveratrol, apigenin, kaempferol and quercetin. In this work, the expression of the naringenin pathway together with the flavanone 3-hydroxylase (F3H) gene from *Glycine max* resulted in the production of kaempferol; and combined expression of F3H and F3`H from *G. max* resulted in the production of quercetin.
As shown in Figure 3, naringenin is produced by a polyketide synthase III, CHS, from *p*-coumaroyl-CoA and malonyl-CoA. If another polyketide synthase III is present instead, different derivatives can be produced. A good example of such derivatives produced commercially in *S. cerevisiae* is the stilbene resveratrol. Fermentation-produced resveratrol was introduced on the market in 2014 by Evolva (Katz *et al.* 2013; Katz *et al.* 2015; Baerends *et al*. 2015).

As mentioned before, the precursor for the antimalarial drug artemisinin, artemisinic acid, is one of the examples of isoprenoid pharmaceuticals that are produced in budding yeast. Ro *et al.* (2006) developed a strain able to produce up to 100 mg/L of artemisinic acid. The strain was developed by increasing the endogenous production of the precursor farnesyl pyrophosphate (FPP) and by the heterologous expression of genes from *Artemisia annua*. These genes included amorphadiene synthase (*ADS*) and a newly identified P450 responsible for conversion of farnesyl pyrophosphate to artemisinic acid. Increased production of farnesyl pyrophosphate was achieved by upregulating the flux through the mevalonate pathway and downregulating enzymes competing for FPP. Paddon *et al.* (2013) developed a *S. cerevisiae* strain that could reach a fermentation titer of 25 g L^{-1} of artemisinic acid. They further improved FPP production and improved the process of conversion of FPP to artemisinic acid, by heterologous expression of two additional *A. annua* genes, *ADH1* and *ALDH1*. Amyris launched commercially engineered yeast-derived artemisinin in 2013.

Taxadiene is another isoprenoid and precursor of Taxol, a chemotherapy drug, and can be produced in budding yeast. Taxadiene is produced from the yeast precursor geranylgeranyl pyrophosphate (GGPP), which is, in return, synthetized from FPP. Therefore similar FPP boosting strategies are also applied. Engels *et al.* (2008) further improved production of the taxadiene precursor by releasing the feedback inhibition from the mevalonate pathway. By introducing GGPP synthase (*GGPPS*) from *Sulfolobus acidocaldarius* and codon optimised

taxadiene synthase (*TS*) from *Taxus* species into a precursor boosted strain the authors were able to reach a titer of taxadiene of 8.7 mg/L.

CHAPTER 1: Construction of a platform strain for the production of flavonoids in *Saccharomyces cerevisiae*

1. Introduction: Production of naringenin and resveratrol in microorganisms

1.1 Heterologous expression of plant phenylpropanoid pathway genes in yeast

The phenylpropanoid pathway is described in the general introduction 1.2.2 Biosynthesis (p. 4). In this chapter the phenylpropanoid pathway from plants is described together with the relevant elements of yeast's native metabolism. Figure 8 presents the plant phenylpropanoid pathway as expressed in yeast, in relation to the host's aromatic amino acid biosynthesis machinery and in relation to the host's enzymes that lead to a formation of known side products.

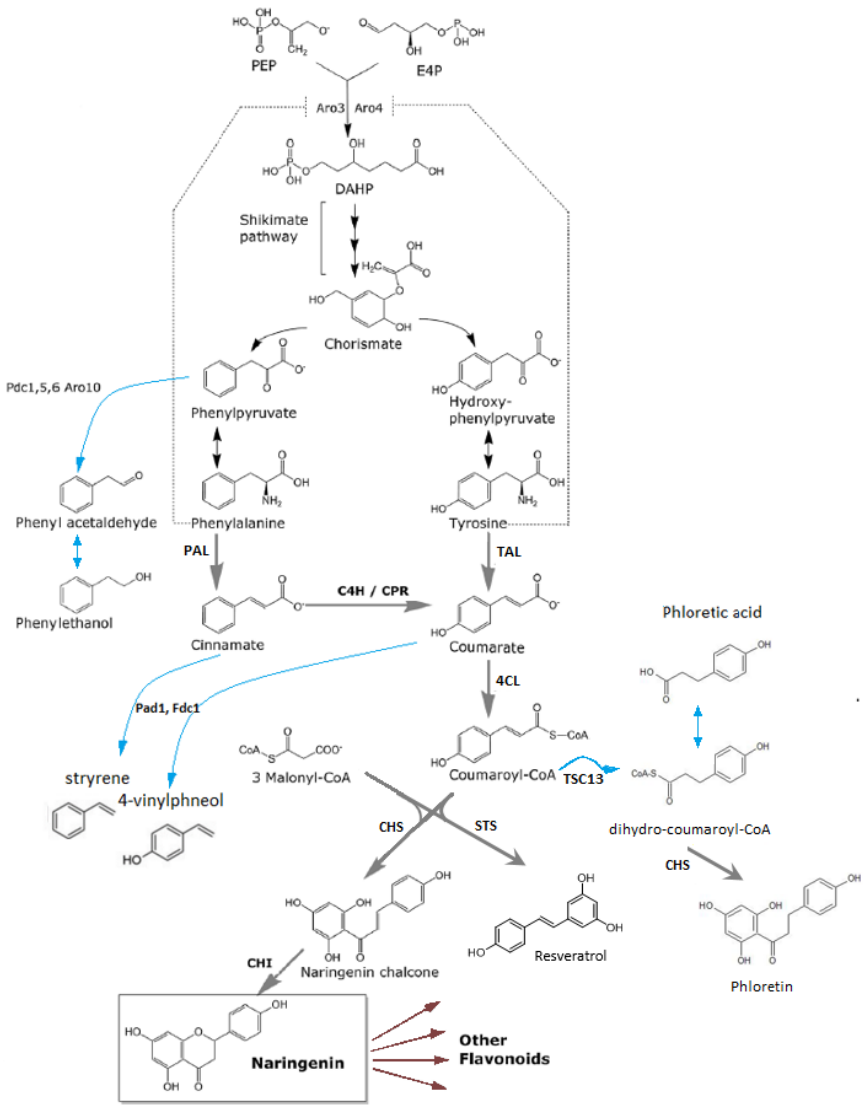

Figure 8. Model of heterologous phenylpropanoid pathway when expressed in S. cerevisiae. Black arrows indicate biosynthesis of the precursors phenylalanine and tyrosine. Dashed lines indicate feedback inhibition. Aro3 and Aro4: 3-deoxy-D-arabino-heptulosonate-7-phosphate (DAHP) synthase. Bold grey arrows indicate the flavonoid and stilbenoid production pathways as described in the general introduction 1.2.2 Biosynthesis. TAL: tyrosine ammonia lyase, PAL: phenylalanine ammonia lyase, C4H: cinnamate-4-hydroxylase, CPR - cytochrome P450 reductase, 4CL: 4-coumarate-CoA ligase, CHI:chalcone isomerase, CHS:chalcone synthase, STS: stilbene synthase. Blue arrows represent activity of endogenous yeast enzymes. Aro10: phenylpyruvate decarboxylase, Pdc1, 5, 6: pyruvate decarboxylases, Pad1: phenylacrylic acid decarboxylase, Fdc1 ferulic acid decarboxylase, Tsc13: enoyl reductase (figure adapted from Koopman et al. 2012).

In summary the precursors of the phenylpropanoid pathway phenylalanine and tyrosine are produced in yeast by the shikimate pathway. The side products phenylacetate and phenylethanol are products of the phenylalanine catabolism that is known to be catalysed by yeast endogenous enzymes Pdc1,5,6 and Aro10. Styrene and 4-vinylphenol are formed from cinnamate (cinnamic acid) by Pad1 and coumarone (*p*-coumaric acid) by Fdc1, respectively. Loss of carbon to phloretic acid is due to reduction of *p*-coumaroyl-CoA by an endogenous yeast double bound reductase, identified in this work as Tsc13 (Figure 8).

1.2 Previous relevant academic efforts

This section focuses on the previous academic efforts aiming to improve the metabolism of *S. cerevisiae* or expressing heterologous genes in this organism for the development of a suitable cell factory for phenylpropanoids. Literature focusing on boosting the levels of endogenous precursors, as well as on eliminating competitive pathways is presented in the following points.

1.2.1 Entry point of the phenylpropanoid pathway

As shown in Figure 8 phenylalanine ammonia lyase (PAL) deaminates phenylalanine into ammonia and cinnamic acid, whereas cinnamate 4-hydroxylase (C4H) converts cinnamic acid into *p*-coumaric acid. Alternatively, tyrosine ammonia lyase (TAL) enables direct conversion of tyrosine into *p*-coumaric acid.

Annotation of the ammonia lyases in the databases is complicated and often imprecise. Enzymes with affinity to both phenylalanine and tyrosine should be annotated as PAL/TAL (EC 4.3.1.25). If the enzyme is highly specific to phenylalanine, it should be annotated as PAL (EC 4.3.1.24), whereas if it's highly specific for tyrosine it should be annotated as TAL (EC 4.3.1.23). Histidine ammonia-lyases are yet a third member of the aromatic amino acid lyase family and they convert histidine into *trans*-urocanic acid (EC 4.3.1.3).

As mentioned above, the cytochrome P450 enzyme cinnamate-4-hydroxylase (C4H) together with its cognate reductase (CPR) are responsible for the formation of the central phenylpropanoid pathway intermediate *p*-coumaric acid. C4H oxidizes cinnamic acid to *p*-coumaric acid using an oxygen molecule and two electrons provided by its redox partner CPR. The CPR extracts this electrons from NADPH and places them at the P450 iron center (Schalk *et al.* 1998). Ro & Douglas (2004) were the first that functionally expressed C4H and CPR in *S. cerevisiae.* They reconstructed the entry point of the plant phenylpropanoid metabolism in *S. cerevisiae,* by co-expressing plant PAL, C4H, and a CPR enzymes.

C4H and CPR are not efficiently expressed in bacteria due to the fact that these proteins are membrane embedded and bacteria are lacking endoplasmic reticulum (Hotze *et al.* 1995). However, since some of ammonia lyases have activity towards tyrosine, it is possible to bypass C4H and express the phenylpropanoid pathway in *E. coli* without the need of the C4H/CPR combo. Hwang *et al.* (2003) were the first to produce the flavanone naringenin in *E. coli* using PAL/TAL from yeast *Rhodotorula rubra*.

In *S. cerevisiae*, the efficient expression of C4H and CPR does not pose a problem, plus the enzymes that have dominating PAL activity are generally more active than those with higher specificity for tyrosine (see figure 19 in results p. 45). Therefore, PALs are preferred for the

production of phenylpropanoids in *S. cerevisiae* (see Table 1 and Table 2). Nevertheless, co-expression of PALs and TALs may result in an increase of the carbon flux towards the phenylpropanoid pathway, making the identification of ammonia lyase with high specificity towards tyrosine and good activity in yeast an interesting area of research. Therefore, the research presented herein focuses on comparative studies as well as on studies where TALs are functionally expressed in *S. cerevisiae*.

1.2.2 Focus on tyrosine ammonia lyases

Several PAL/TAL enzymes with higher specificity towards tyrosine than towards phenylalanine have been identified in bacteria. Kyndt *et al.* (2002) identified a tyrosine-specific PAL/TAL from *Rhodobacter capsulatus*. By introducing this TAL to a *S. cerevisiae* naringenin producer, Koopman *et al*. (2012) managed to further increase the carbon flux towards the final product although the achieved titers were still in the micromolar range. Watts *et al.* (2006b) compared several PAL/TAL enzymes with a previously identified PAL/TAL from *Rhodobacter sphaeroides* (Watts *et al.* 2004), concluding that this enzyme was the most specific towards tyrosine and identifying histidine 89 as the single residue responsible for that specificity. Xue *et al.* (2007a) further confirmed that *R. capsulatus* and *R. sphaeroides* enzymes have very high specificity towards tyrosine with PAL/TAL catalytic efficiency ratios of 0.15 and 0.05 respectively. *Trans*-caffeic acid is a precursor for antibiotic saccharomicin produced by gram positive *Saccharothrix espanaensis*. Berner *et al.* (2006) identified the enzymes responsible for the production of *trans*-caffeic acid, one being tyrosine ammonia lyase encoded by *sam8*. The evaluated PAL/TAL ratio of this TAL was as low as 0.0014, when compared to TAL from R. *capsulatus* with the ratio of 0.06.

Vannelli *et al.* (2007a) evaluated several PAL/TAL from eucariotic microorganisms and bacteria, using phenylalanine and tyrosine as a substrate and determined PAL/TAL ratios. From their eight candidates, the enzyme from the yeast *Rhodotorula graminis* had the highest specificity towards tyrosine, with the PAL/TAL ratio of 1.68. The enzyme was functionally expressed in *E. coli* and in *S. cerevisiae*. Xue *et al.* (2007b) characterised PAL/TAL enzymes from *Rhodotorula glutinis* and a novel thermostable PAL/TAL from *Phanerochaete chrysosporium* (wood fungus). The PAL/TAL ratio for the newly discovered enzyme was 0.6, whereas the ratio for TAL from *R. glutinis* was 0.77. Jiang *et al.* (2005) were the first to successfully express the phenylpropanoid pathway in *S. cerevisiae* without the C4H, by introducing a PAL/TAL from the yeast *Rhodosporidium toruloides* (related to *R. graminis*). Shin *et al.* (2012) also used TAL from *R. toruloides* for resveratrol production in *S. cerevisiae* although the achieved titers were still in the micromolar range.

Another TAL enzyme from yeast *Trichosporon cutaneum* was identified by Vannelli *et al.* (2007b). This enzyme showed to be inducible by tyrosine and had the lowest PAL/TAL ratio of 0.8, when compared to PAL/TAL enzymes from *R. glutinis*, *R. graminis* and several others (not described herein). The TAL from *T. cutaneum* was described to be successfully expressed in *S. cerevisiae* (Breinig *et al.* 2005).

Hsieh *et al.* (2010) identified enzyme with TAL activity from *Bambusa oldhamii* and found that one of the enzymes, annotated as *Bo*PAL4, had the highest specificity towards tyrosine, with a PAL/TAL ratio of 1.4, due to histidine residue at its selective site - (His at position 124).

Recently Jendresen *et al.* (2015) discovered novel TALs with high specificity towards tyrosine originating from *Herpetosiphon aurantiacus* and *Flavobacterium johnsoniae*. The *E. coli*, *L. lactis* and *S. cerevisiae* strains expressing different PAL/TALs were fed with phenylalanine or tyrosine in order to measure either PAL or TAL activity. Bacterial enzymes from *H. aurantiacus* and *F. johnsoniae* expressed in *S. cerevisiae* showed an increased accumulation of *p*-coumaric acid in comparison to TAL from *S. espanaensis*, *R. sphaeroides* and *Rhodotorula rubra* (applied previously for naringenin production in *E. coli* by Hwang *et al.* 2003 and Miyahisa *et al.* 2005). Upon feeding with phenylalanine no cinnamic acid was accumulated by these strains, indicating that the enzymes are very specific for tyrosine. The kinetic analysis further confirmed very high specificity towards tyrosine of the two newly discovered TALs. These TALs were quickly applied for production of resveratrol by Li M *et al.* (2015) (*Ha*TAL) and *p*-coumaric acid by Rodriguez *et al.* (2015) (*Fj*TAL).

1.2.3 Chalcone synthase and stilbene synthase

As shown in Figure 8, *p*-coumaroyl-CoA and three molecules of malonyl-CoA can be condensed to naringenin chalcone by chalcone synthase (CHS) or to resveratrol by stilbene synthase (STS). Both of these enzymes belong to a superfamily of Type III polyketide synthases (Austin and Noel 2003). These enzymes were reported as bottlenecks when a phenylpropanoid pathway was expressed in yeast or bacteria. When Wu *et al.* (2014b) tested different combinations of gene control systems, while expressing a phenylpropanoid pathway in *E. coli*, they identified CHS as a major bottleneck. Based on the fact that a considerable amount of side products accumulated while expressing a naringenin pathway in *S. cerevisiae*, Koopman *et al.* also concluded that the CHS might control the flux through the pathway. By overexpressing the CHS on a 2 μ plasmid, they reduced side product formation to a large extent. The STS enzyme was also determined to be a bottleneck using different combinations of gene control systems in *E. coli* expressing a phenylpropanoid pathway (Wu J *et al.* 2013). By evaluating the activity of different stilbene synthases, Lim *et al.* (2011) found that the STS from *V. vinifera* had the highest turnover number amongst the tested enzymes. Also, the highest titer of resveratrol was reached when the pathway was expressed with *VvSTS* in *E. coli*.

The stilbene synthase was also expressed in close proximity with 4CL as a fusion protein or using interaction domains, under the assumption that substrate channelling will improve the titer of the final product. The STS and 4CL expressed in close proximity, improved the resveratrol titer in the studies of Zhang *et al.* (2006), Wang *et al.* (2011a), Wang *et al.* (2011b) and Wang and Yu (2012), however it was found ineffective in the studies of Li M *et al.* (2015).

1.2.4 Precursor boost

Aromatic amino acids with focus on biosynthesis of phenylalanine and tyrosine

The least abundant of all amino acids in *S. cerevisiae* are aromatic amino acids and thus are synthesised in the shikimate pathway (Braus 1991). The shikimate pathway of *S. cerevisiae* is somehow similar to the one described in plants (Figure 2 and 1.2.2 Biosynthesis, p. 3). However, the biosynthesis of phenylalanine/tyrosine in *S. cerevisiae* occurs only through the phenylpyruvate /4-Hydroxy- phenylpyruvate route of the shikimate pathway (Figure 9).
The pathway starts with the condensation of phosphoenolpyruvate (PEP) with erythrose 4-phosphate (E4P) into 3-deoxy-D-heptulosonate 7-phosphate (DAHP) by DAHP synthase (Aro3 and Aro4 in *S. cerevisiae*). In yeast, in contrast to plants and bacteria, one pentafunctional protein (Aro1) transforms DAHP to 5-enolpyruvylshikimate-3-phosphate (EPSP) in four steps. Chorismate synthase (Aro2) transforms EPSP to the chorismate. From here the pathway branches either to tryptophan or to phenylalanine and tyrosine. In the next step chorismate is transformed to prephenate (PPA) by chorismate mutase (Aro7). When prephenate dehydratase (Pha2) transforms PPA into phenylpyruvate (PPY), then aromatic aminotransferases (Aro8, Aro9) transforms PPY to phenylalanine (Phe). The prephenate (PPA) is also transformed to 4-hydroxyphenylpyruvate (HPP) by prephenate dehydrogenase (Tyr1) and then to tyrosine (Tyr) by the aromatic aminotransferases (Aro8, Aro9).

The aromatic amino acid biosynthesis in *S. cerevisiae* is controlled at the transcriptional and at the protein level. At the protein level, allosteric regulation of certain enzymes by phenylalanine, tyrosine, and tryptophan allow a balanced control of the carbon flow. In the committing step of shikimate pathway, the two isoenzymes of DAHP synthases, Aro3 and Aro4, are feedback inhibited by phenylalanine and tyrosine. At the point where Shikimate pathway is branching towards phenylalanine and tyrosine, conversion of chorismate to prephenate, Aro7 is feedback activated by tryptophan and feedback inhibited by tyrosine (Braus 1991).

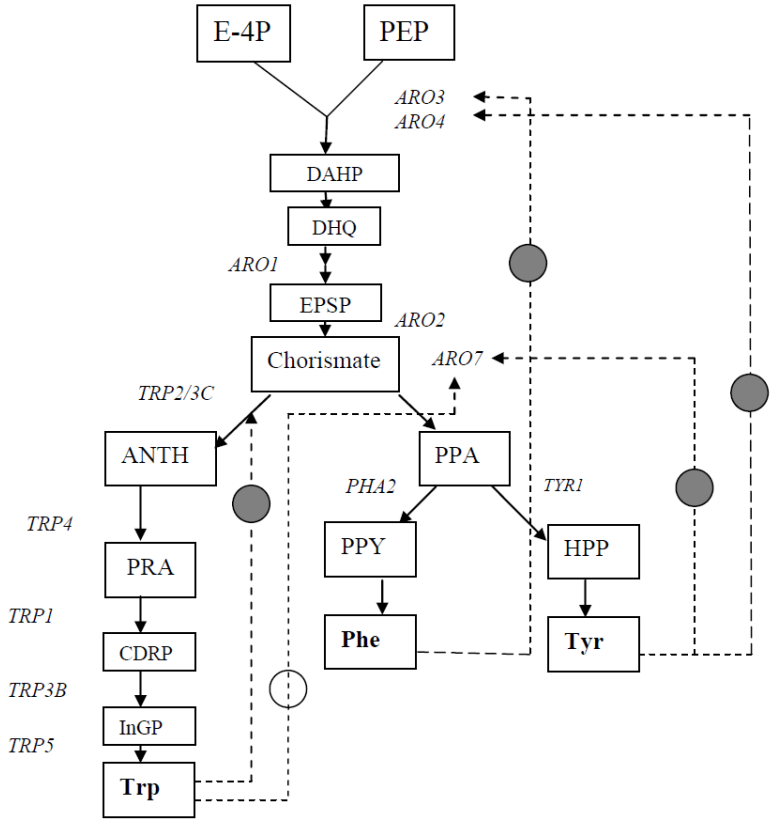

Figure 9. Diagram of shikamate pathway in S. cerevisiae. Full circles represent feed-back inhibition, whereas open circles represents activation. E-4P: erythrose 4-phosphate, PEP: phosphoenol pyruvate, DAHP: 3-deoxy-D-arabino-hetulosonate, DHQ: 3-dehydroquinate, EPSP: 5 enolpyruvoylshikimate 3-phosphate, ANTH: anthranilate, PRA - phosphoribosyl anthranilate, CDRP: 1-o-carboxyphenylamino-1-deoxyribulose 5-phosphate, InGP: indole 3-glycerol-phosphate, PPA: prephenate, PPY: phenylpyruvate, HPP: 4-hydroxyphenylpyruvate, Trp: tryptophan, Phe: phenylalanine, Tyr: tyrosine (Modified figure from Braus 1991).

Schmidheini *et al.* (1989) identified that an Aro7 mutant, where threonine is substituted with isoleucine at position 226, is insensitive to tyrosine and tryptophan regulation and has increased basal activity when compare to the wild type enzyme.

The studies of Schnappauf *et al.* (1998) identified different amino acid residues important for the feedback regulation of Aro7 by tyrosine and tryptophan. One of the best mutants they identified had a substitution of glycine by serine at position 141, which completely removed feedback inhibition by both tyrosine and tryptophan. The studies of Hartmann *et al.* (2003) identified amino acid residues important for the feedback inhibition of Aro4 by tyrosine and phenylalanine. One of the best mutant they identified had sufficient basal activity and at the same time was insensitive to tyrosine and phenylalanine, due to the substitution of lysine to leucine at position 229. Another interesting mutant they found, G226S, had the same basal activity as the WT strain and was insensitive to tyrosine, but inhibited by phenylalanine.

In order to boost production of phenylalanine and tyrosine in yeast, Luttik *et al.* (2008) tested the application of Aro4 and Aro7 feedback regulation insensitive mutants. Overexpression of tyrosine insensitive $Aro4_{K229L}$ in *S. cerevisiae* resulted in 3 to 4 fold increase in the intracellular phenylalanine and tyrosine levels, and 100 fold increase of extracellular aromatic compounds such as phenylacetate, phenylethanol and their parahydroxyl analogues. Interestingly overexpression of $Aro4_{K229L}$ together with $Aro7_{G141S}$ did not further enhance intracellular phenylalanine and tyrosine accumulation, but it did lead to a 200 fold increase in the level of extracellular aromatic compounds. All these results were achieved in the *aro3*Δ strain, however

the reason for this is not clear. One possible reason could be that a feedback resistant mutant of Aro3 has not yet been described and overexpression of Aro4 complements *aro3* deletion.

The $Aro4_{G226S}$, *aro3Δ* alterations described by Hartmann *et al.* (2003) were implemented by Koopman *et al.* (2012) and resulted in the improved production of naringenin in yeast. This effect was even stronger when the formation of side aromatic compounds was eliminated (described in more details in the 1.2.5 Aro10 paragraph).
With the aim of improving cinnamic acid production in yeast, Rodriguez *et al.* (2015) tested several scenarios, including feedback resistant DAPH synthases from *S. cerevisiae* and *E. coli* as well as feedback resistant chorismate mutases from *S. cerevisiae* , *E. coli* and *C. guilliermonii*. The overexpression of yeast $Aro4_{K229L}$ and $Aro7_{G141S}$ was the best alternative, as it resulted in enhanced cinnamic acid accumulation. All manipulations were done in the *Fj*TAL *aro10Δpdc5Δ* strain, as described in the 1.2.5 Aro10 paragraph. Interestingly, the deletion of *ARO3* was not included in this study. The alterations described by Luttik *et al.* were implicated in several other studies for production of e.g. styrene (Mckenna *et al.* 2014) or resveratrol (Li M *et al.* 2015). By overexpressing the $Aro4_{K229L}$ and $Aro7_{G141S}$ Li M *et al.* (2015) improved the resveratrol titer by 78% in batch cultures.

An interesting study on phenylalanine boost in yeast was done by Mckenna *et al.* (2014). They applied clasical metabolic evolution to the yeast overepressing *At*PAL, in order to develop a phenylalanine overproducing strain. Interestingly, they did not find feedback resistant DAPH synthases or chorismate mutase, however they found that these strains overexpressed *ARO8*, *ARO1*, *ARO2*, and *ARO3*.

Tyrosine was also boosted in a naringenin producing *E. coli* allowing increased naringenin production from glucose (Santos *et al.* 2011; Wu *et al.* 2014b). They both overexpresed bacterial feedback resistant DAHP synthase (*aroG* fbr) and feedback resistant chorismate mutase/prephenate dehydrogenase (*tyrA* fbr).

Malonyl CoA

Cytosolic malonyl-CoA is a primary precursor for the biosynthesis of fatty acids. The main route of malonyl-CoA biosynthesis is the carboxylation of acetyl-CoA into malonyl-CoA by the acetyl-CoA carboxylases (ACC) in presence of the co-factor biotin. In yeast, this cytosolic enzyme is encoded by *ACC1*. Acc1 is regulated at the transcriptional as well as at the protein level. During glucose limiting conditions, phosphorylation of *Sc*Acc1 by Snf1 protein kinase leads to degradation of Acc1 (Tehlivets *et al*. 2007). As described in the general introduction in plants malonyl-CoA is a precursor for synthesis of fatty acids as well as phytoalexins, such as flavonoids and stilbenoids. Three molecules of malonyl-CoA are required to synthetize one molecule of naringenin or resveratrol. Besides ACC, plants, animals and some microorganisms possess malonyl-CoA synthetase enzymes, which can ligate CoA to malonic acid and generate malonyl-CoA (Chen H *et al.* 2011). Several strategies aiming for an increase of the malonyl-CoA and its derivatives have been applied in microbes. Malonyl-CoA is a main limiting precursor for the production of phenylpropanoids in prokaryotic organisms and, therefore, most of the studies focusing on boosting malonyl-CoA are done in *E. coli*. Nevertheless, boost of

that precursor in the yeast's cytosol has been also explored for the efficient phenylpropanoid production.

In order to improve the heterologous production of resveratrol in *S. cerevisiae*, Shin *et al.* (2012) overexpressed the native *ACC1*, achieving a 30% improvement in the resveratrol titer. However, the growth of this strain was slightly impaired. Another strategy was the development of an Acc1 mutant resistant to Snf1 phosphorylation. Shi *et al.* (2014) investigated if a mutation in the site known to be phosphorylated by Snf1 (Serine1157) can abolish this phosphorylation. Based on phosphorylation recognition motifs they identified that serine 659 is an additional possible phosphorylation site of Acc1 and, by substituting these two serines to alanines, they obtained an Acc1 mutant insensitive to Snf1. Expression of this mutant in yeast led to an enhanced production of fatty acids, however the growth rate and final biomass was negatively affected. Li M *et al.* (2015) adopted that knowledge in the development of a resveratrol producing yeast. They introduced *Sc*Acc1$_{S659A,S1157A}$, and improved the resveratrol titer by 31%, without significant effects on final biomass. By overexpressing a malonyl-CoA synthetase from *A.thaliana* (AAE13) in *S. cerevisiae* in a resveratrol producing strain, Wang *et al.* (2014) increased the production of lipids by 1.6 fold and production of resveratrol by 2.4 fold. Nevertheless the growth was negatively affected.

Chen *et al.* (2017) attempted to boost the malonyl-CoA level in yeast by deleting transcription factors regulating fatty acid syntheis (Ino2p and Ino4p). They managed to increase the titer of the final product, 3-hydroxypropionic acid. Nevertheless, their genetic manipulation strategies negatively affected the growth of the mutant strains and only addition of inositol and choline rescued the phenotype. Interesingly in these studies the introduction of *Sc*Acc1$_{S659A,S1157A}$ did not improve the titer of the final product.

Beside boosting malonyl-CoA, Li M *et al.* (2015) also attempted to boost acetyl-CoA by applying a strategy described by Shiba *et al.* (2007) to resveratrol producer. By introducing constantly active acetyl-CoA synthetase variant (*Se*ACSL641P) from *Salmonella enterica* to *S. cerevisiae*, Shiba *et al.* (2007) managed to increase the titer of the final product, amorphadiene. Nevertheless, the resveratrol titer was not improved by this strategy in the studies of Li M *et al.* (2015).

Due to the fact that overexpression of heterologous acetyl-CoA carboxylase (ACC) from *C. glutamicum* was reported to significantly improve naringenin yield in *E. coli*, Miyahisa *et al.* 2005 concluded that malonyl-CoA must be a limiting factor when producing phenylpropanoids in *E. coli*. Since then, numerous groups have managed to significantly improve the production of phenylpropanoids in *E. coli* by boosting the malonyl-CoA pool with strategies including: heterologous expression of ACC1 (Fowler et al. 2009; Leonard *et al.* 2007; Xu *et al.* 2011), overexpression of heterologous malonyl-CoA synthetase-matB with malonate carrier protein-matC (Leonard *et al.* 2008; Wu J *et al.* 2013; Wu *et al.* 2014a; Wu *et al.* 2014b) and inhibition of fatty acid synthesis (Leonard *et al.* 2008; Lim *et al.* 2011; Santos *et al.* 2011; Wu *et al.* 2014a; Wu *et al.* 2015). The deletion of some citric acid cycle genes, based on prediction from computer models, also improved the final titer of naringenin (Fowler *et al.* 2009; Xu *et al.* 2011).

1.2.5 Efforts to eliminate side product formation

Aro10

As described before, phenylalanine and tyrosine are precursors of the phenylpropanoid pathway. Therefore, a boost of these precursors should be accompanied by an inhibition of their catabolism. When Luttik *et al.* (2008) boosted the shikimate pathway in *S. cerevisiae*, besides increased levels of phenylalanine and tyrosine, they observed an accumulation of phenylacetate and phenylethanol. When Koopman *et al.* (2012) expressed a naringenin biosynthetic pathway in *S. cerevisiae* engineered to have elevated levels of aromatic amino acids, they observed an accumulation of phenylethanol. Phenylethanol and phenylacetate are known to be products of the phenylalanine catabolism. In yeast 4 different thiamine pyrophosphate-dependent 2-oxo acid decarboxylases (Aro10, Pdc1, Pdc5, Pdc6) can catalyse phenylpyruvate decarboxylation to phenylacetaldehyde in the first step in the Ehrlich pathway. Phenylacetaldehyde can then be reduced into phenylethanol or oxidized into phenylacetate (Hazelwood *et al.* 2008), reducing the carbon flux into the phenylpropanoid pathway. Romagnoli *et al.* (2012) evaluated the activity of these enzymes towards phenylpyruvate and they rated them as following: Aro10>Pdc5> (Pdc1, Pdc6), where Aro10 exhibited superior kinetic properties. The studies of Koopman *et al.* (2012) revealed that in the strain with aromatic amino acid boost, the deletion of *ARO10* was a critical step in the reduction of phenylethanol and dramatically improved the naringenin titer while deletion of *PDC5* had no mayor effect. Nevertheless, when Rodriguez *et al.* (2015) deleted both *ARO10* and *PDC5,* in a *FjTAL* overexpressing strain (*TAL* from *F. johnsoniaeu*), it resulted in a higher level of *p*-coumaric acid when compared to the strain with *ARO10* deletion alone.

Pad1/Fdc1

Endogenous yeast enzyme, phenylacrylic acid decarboxylase (Pad1), is known to decarboxylate *trans*-cinnamic acid and *p*-coumaric acid (Goodey and Tubb 1982). As a result of this decarboxylation, toxic and volatile side products like styrene and 4-vinylphenol are formed (Figure 10).

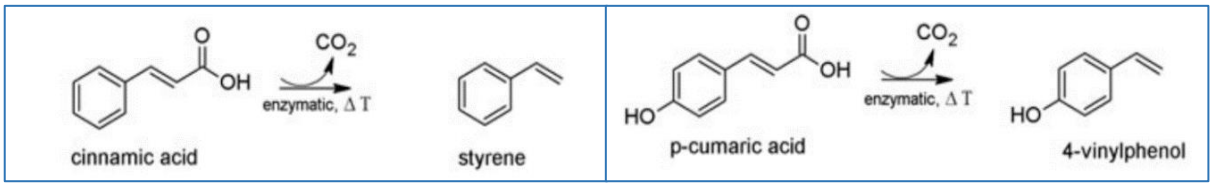

Figure 10. Decarboxylation of cinnamic acid to styrene and p-coumaric acid to 4-vinylphenol (modified version of figure from Schwarz et al. 2012).

When Ro & Douglas (2004) fed a *S. cerevisiae* expressing PAL, C4H and CPR with radiolabelled phenylalanine, they observed an accumulation of radiolabelled styrene and 4-vinylphenol. Based on that knowledge, Jiang *et al.* (2005) overexpressed PAL in a *pad1* knockout yeast strain and this resulted in an accumulation of cinnamic acid, when compared to a *PAD1* strain. Expressing a naringenin producing pathway in a *pad1* knockout strain did not result in an increased level of naringenin, but increased level of side products such as phloretin, 2`,4`,6`-trihydroxydihydrochalcone and an unknown compound (Jiang *et al.* 2005), confirming that the deletion of *pad1* must contribute to an accumulation of the *p*-coumaroyl-CoA precursor. However, contrary to what would be expected, the expression of a resveratrol

biosynthetic pathway in a *pad1* strain did not enhance the accumulation of the final product (Shin *et al.* 2011). The authors speculated that this could be due to a loss of carbon to another side product, most likely from *p*-coumaroyl-CoA. Recently Mukai *et al.* (2010) described that the enzymes coded by *PAD1* and neighbouring *FDC1* (ferulic acid decarboxylase) are both involved in the decarboxylation of cinnamic acid and *p*-coumaric acid.
Therefore, it seems a good practice to delete described genes *PAD1* and *FDC1* when expressing the phenylpropanoid pathway in *S. cerevisiae*.

Tsc13

Several studies reported a significant accumulation of phloretic acid (dihydrocoumaric acid), in *S. cerevisiae* expressing the phenylpropanoid pathway (Beekwilder *et al*. 2006; Koopman *et al.* 2012; Luque *et al.* 2014; Vos *et al.* 2015). In one case, the accumulation of phloretin, a dihydrochalcone derivative of phloretic acid was also reported (Jiang *et al.* 2005). These authors speculated that phloretic acid is derived from *p*-coumaroyl-CoA, as it requires the presence of 4CL to be formed. The reaction seems to occur in two steps, first *p*-coumaroyl-CoA is reduced to dihydro-coumaroyl-CoA by (an) unknown yeast reductase(s) and then it is hydrolysed, either spontaneously or by another unknown enzymatic reaction, to phloretic acid (Beekwilder *et al*. 2006; Koopman *et al.* 2012).
The effort to reduce this carbon loss has been, for the first time, described in the article presented as chapter 2 of this thesis. There, we identified Tsc13 as the enzyme responsible for the reduction of *p*-coumaroyl-CoA and we presented efforts aiming to solve this issue.

1.2 Summary of previous efforts on the microbial production of naringenin and resveratrol

As described before, the biosynthetic pathways of naringenin and resveratrol differs only in the last cyclization step. Due to the high similarity of both biosynthetic pathways, microbial production of both compounds is presented in Table 1 for naringenin and Table 2 for resveratrol. A higher number of studies where *S. cerevisiae* is used as a host is reported for resveratrol, whereas naringenin production is dominated by studies where *E. coli* is used.

Most of the high titers of naringenin or resveratrol reported in *E. coli* were achieved using precursor feeding strategies**.** The highest naringenin titer reported in *E. coli* (474 mg/L) was reached by Xu *et al.* (2011), with *p*-coumaric acid feeding. Lim *et al.* (2011) reached the highest resveratrol titer reported in literature in *E. coli*, 2.3 g/L, also with *p*-coumaric acid feeding. The highest titer reported in *E. coli* without precursor feeding was 100 mg/L of naringenin as reported by Wu *et al.* 2014b. This was achieved in a strain with a tyrosine and malonyl-CoA boost. These titers were achieved in shake flask.

The highest titers of naringenin and resveratrol obtained in *S. cerevisiae* were achieved without precursor feeding. Koopman *et al.* (2012) reached 54 mg/L of naringenin in shake flask culture and 108 mg/L in controlled batch reactor. The phenylpropanoid pathway genes for construction of this strain were selected only from *A. thaliana* under the hypothesis that co-expressed genes from one organism might form complexes that channel the pathway metabolites and facilitate the production of the final product. That strain included both PAL and TAL, overexpressed CHS and the aromatic amino acid boost.

The highest resveratrol titer, 4 g/L, was produced by Katz *et al.* 2013 in a feed batch fermentation, while the same strain produced only 182 mg/L in deep well plate. The pathway genes in this strain were introduced on Ty multi-integrative vectors, the resveratrol synthase was overexpressed to a higher extent than rest of the genes and *ARO10* was deleted. Malonyl-CoA was also boosted in this strain and the *SNQ2* transporter was overexpressed to facilitate export of resveratrol from the cells. Vos *et al.* (2015) performed stoichiometric analysis of the resveratrol-producing strain (obtained from Katz *et al.* 2013) when cultivated in aerobic, glucose-limited conditions. They demonstrated that resveratrol synthesis is linked to the growth rate, as production of the phenylpropanoid precursors is growth dependent. They hypothesized that production of energetically expensive compounds would likely benefit from the uncoupling of production and growth.

In summary, the reported strategies to obtain high titers when heterologously producing naringenin and resveratrol included: selection of most optimal genes, balanced expression/overexpression of different pathway genes, inhibition of side product formation and boosting pathway precursors, such as aromatic amino acids, malonyl-CoA and acetyl-CoA.

Table 1. Production of naringenin in E. coli and S. cerevisiae. S. cerevisiae (Sc), E. coli (Ec), A. thaliana (At), R. sphaeroides (Rs), R. rubra (Rr), S. coelicolor (Scoe), G. echinata (Ge), P. crispum (Pc), P. hybrid (Ph), A. majus (Am), R. toruloides (Rt), H. androsaemum (Ha), P. lobate (Pl), M. sativa (Ms), P. luminescens (Plu), C. glutamicum (Cg), R. trifolii (Rtri), P. trichocarpa (Ptr), P. deltoids (Pde), G. max (Gm). ↑ in bacteria indicates usage of strong T7 promoter, in yeast it indicates that genes were introduced on multicopy plasmids, ↑ (Ty) in yeast indicated that genes were introduced into multiple Ty sites, Phe- phenylalanine, Tyr- tyrosine, p-coum -p-coumaric acid, CO- codon optimized, fbr- feedback resistant, (B)- bioreactor, LB- lysogeny broth, TB- terrific broth, SC- synthetic complete medium, YPD- yeast extract peptone dextrose broth, SD- sabouraud dextrose broth, *MOPS- morpholinepropanesulfonic acid minimal medium.*

Microorganism	strain	Media and substrate	Production	Genes	References
E. coli	BL21(DE3)	LB, 0.36 g/L Tyr	0.452 mg/L	*RrPAL/TAL, Scoe4CL, GeCHS*	Hwang *et al.* 2003
E. coli	BW27784	TB	20.8 mg/L	*RsTAL, AtC4H, At4CL, AtCHS*	Watts *et al.* 2004
S. cerevisiae	INVSc1	SC, 0.164 g/L *p*-coum	28.3 mg/L	*AtC4H, Pc4CL, PhCHI-A, PhCHS*	Yan *et al.* 2005
S. cerevisiae	INVSc1	SC, 0.082 g/L *p*-coum	14 mg/L	*AtC4H, Pc4CL-2, PhCHS, PhCHI-A, AmAFNS2, ScCPR1*	Leonard *et al.* 2005
S. cerevisiae	AH22	YPD	7 mg/L	*pad1Δ, RtPAL/TAL, At4CL, HaCHS*	Jiang *et al.* 2005
E. coli	BLR (DE3) and	M9 modified, 0.54 g/L Tyr	57 mg/L	↑ *RrPAL/TAL , ScoeCCL ,*↑*PlCHI* ↑*GeCHS,* ↑*CgACC*	Miyahisa *et al.* 2005
E. coli	BL21	M9, 2 g/L acetate, 0.49 g/L *p*-coum	119 mg/L	↑*Pc4CL2,* ↑*PhCHS,* ↑*MsCHI,* ↑*Plu accABCD,* ↑*PluBirA,* ↑*Ec ackA,* ↑*Ec pta,* ↑*Ec acs*	Leonard *et al.* 2007
E. coli	BL21	M9, 2 g/L malonate, 0.36 g/L *p*-coum,	155 mg/L	↑*Pc4CL2,* ↑*PhCHS,* ↑*MsCHI,* ↑*RtrimatB,* ↑*RtrimatC*	Leonard *et al.* 2008
E. coli	BL21	M9 modified, 0.246 g/L *p*-coum	270 mg/L	*sdhABCD Δ, citE Δ, brnQ Δ, adhE Δ,* ↑*Plu accABCD,* ↑*Pc4CL2,* ↑*PhCHS,* ↑*MsCHI,* ↑*Ec acs,* ↑*PluBirA*	Fowler *et al.* 2009
S. cerevisiae	S288C	CM, 1.64 mg/L *p*-coum, 1.65 g/L Phe	15.6 mg/L (*p*-coum), 8.9 mg/L (phe)	*PtrPAL, PdeCPR, GmC4H, Gm4CL,GmCHS, GmCHI*	Trantas *et al.* 2009
E. coli	K12	MOPS, cerulenin	84 mg/L	CO: *RgTAL, Pc4CL, PhCHS, MsCHI,* ↑*tyrA fbr,* ↑*aroG fbr, tyrRΔ*	Santos *et al*. 2011
E. coli	BL21	LB then M9 modified, 0.427 g/L *p*-coum	474 mg/L	*Pc4CL, PhCHS, MsCHI, ΔfumC, ΔsucC,* ↑*ACC,* ↑*PGK,* ↑*GAPD,* ↑*PDH*	Xu *et al.* 2011
S. cerevisiae	CEN.PK	SC with 10 g/L (NH4)2SO4	108 mg/L (B)	*aro3Δ ScARO4 G226S, aro10Δ, pdc5Δ, pdc6Δ, AtPAL1, AtC4H, AtCHI1, At4CL3, AtCHS3,* CO: *AtCPR1,* ↑*2xAtCHS3, RcTAL1*	Koopman *et al*. 2012
E. coli	BL21(DE3)	MOPS	100.64 mg/L	CO: *RgPAL/TAL, Pc4CL,* ↑ *PhCHS,* ↑*MsCHI,* ↑*Rtri matB,* ↑*Rtri matC,* ↑*tyrA fbr,*↑ *aroG fbr*	Wu *et al.* 2014b
E. coli	BL21(DE3)	MOPS, 0.54 g/L Tyr, 2g/L malonate	391 mg/L	CO: *RgTAL, Pc4CL, PhCHS, MsCHI, Rtri matB, Rtri matC,* anti-*fabB* asRNA, anti-*fabF* asRNAs	Wu *et al.* 2014a
E. coli	BL21(DE3)	MOPS, 0.54 g/L Tyr	421.6 mg/L	*RgTAL, Pc4CL, PhCHS, MsCHI,* anti-*fabF/fumC/fabB/sucC/adhE* sgRNA	Wu *et al.* 2015

*Table 2. Production of resveratrol in E. coli and S. cerevisiae. S. cerevisiae (Sc), E. coli (Ec), A. thaliana (At), V. vinifera (Vv), N. tabacum (Nt), A. hypogaea (Ah), R. sphaeroides (Rs), R. glutinis (Rg), R. toruloides (Rt), H. androsaemum (Ha), R. trifolii (Rtri), P. trichocarpa (Ptr), P. deltoids (Pde), G. max (Gm), H. aurantiacus (Hau). ↑ in bacteria indicates usage of strong T7 promoter, in yeast it indicates that genes were introduced on multicopy plasmids, ↑ (Ty) in yeast indicated that genes were introduced into multiple Ty sites, Phe- phenylalanine, Tyr- tyrosine, p-coum -p-coumaric acid, CO- codon optimized, fbr- feedback resistant, (B)- bioreactor, LB- lysogeny broth, TB- terrific broth, SC- synthetic complete medium, YPD- yeast extract peptone dextrose broth, ,SD- sabouraud dextrose broth, YBN- yeast nitrogen base, 2*YT-, CM- auxotrophic Complete Minimal medium, FIT- feed in time medium, YP- yeast extract + peptone, MOPS- morpholinepropanesulfonic acid minimal medium.*

Microorganism	strain	Media and substrate	Production	comments	References
S. cerevisiae	FY23	SCDL , 0.01 g/L *p*-coum	1.45 µg/L	*PtrXPde 4CL, VvVST1*	Becker *et al.* 2003
S. cerevisiae	WAT11	SD, 0.012 g/L *p*-coum	0.65 mg/L	*At4CL::VvSTS*	Zhang *et al.* 2006
S. cerevisiae	CEN.PK113-3B	YBN, 0.82 g/L *p*-coum	5.8 mg/L	*Nt4CL2, VvSTS*	Beekwilder *et al.* 2006
E. coli	BL21	2xYT, 0.82 g/L *p*-coum	16 mg/L	*Nt4CL2, VvSTS*	Beekwilder *et al.* 2006
E. coli	BW27784	M9, 0.164 g/L *p*-coum	104 mg/L	*At4CL, AhSTS*	Watts *et al.* 2006a
S. cerevisiae	YPH499	CM, 1.64 g/L *p*-coum, 1.65 g/L Phe	0.31 mg/L (*p*-coum), 0.29mg/L (phe)	*PtrPAL, PdeCPR, GmC4H, Gm4CL,VvRS*	Trantas *et al.* 2009
S. cerevisiae	CEN.PK and isolated strain	YPD, 2.46 g/L *p*-coum	391 mg/L	↑*At4CL1* , ↑*VvVST1*	Sydor *et al.* 2010
S. cerevisiae	W303-1A	YPD, 15.3 mg/L *p*-coum	3.1 mg/L	*At4CL, AhSTS*	Shin *et al.* 2011
E. coli	BW27784	M9, 2.46 g/L *p*-coum, cerulenin	2300 mg/L	*At4CL, VvSTS*	Lim *et al.* 2011
S. cerevisiae	WAT11	SD	1.9 mg/L	CO: *RsTAL, At4CL::VvSTS, Ec araE*	Wang *et al.* 2011b
S. cerevisiae	CEN.PK	FIT	4000 mg/L (B)	CO: ↑(Ty) *AtPAL2,* ↑(Ty)*At4CL2,* ↑(Ty) *AtC4H::ScCYB5::AtATR2,* ↑(Ty) *VvVST1,* ↑(Ty) *VvVST1,* ↑(Ty) *Vv STS, aro10Δ, pTPI ACC1, SNQ2*	Katz *et al.* 2013
S. cerevisiae	W303-1A	YP, 2.17 g/L Tyr	5.8 mg/L (B)	*RtPAL/TAL, AtC4H, At4CL AhSTS, + ACC1*	Shin *et al.* 2012
S. cerevisiae	WAT11	SD, 64 mg/L *p*-coum	14.4 mg/L	*At4CL, VvSTS* attached to scaffolds	Wang and Yu 2012
E. coli	JM109	MOPS, 0.54 g/L Tyr	35 mg/L	*RgTAL, Pc4CL,* ↑*VvSTS,* ↑*Rtri matB,* ↑*Rtri matC*	Wu J *et al.* 2013
S. cerevisiae	WAT11	SC, 12 mg/L *p*-coum	3.5 mg/L	*At4CL::VvSTS,* ↑*AtAAE13*	Wang *et al.* 2014
S. cerevisiae	CEN.PK102-5B	FIT	415.65 mg/L on Glc, 531.41 mg /L on EtOH (B)	CO: ↑(Ty) *HauTAL,* ↑(Ty) *At4CL1,* ↑ (Ty) *VvVST1, ScARO4 K229L, ScARO7 G141S , ScACC1 S659A, S1157A*	Li M *et al.* 2015

2. Materials and methods

2.1 Yeast strains, cultivation and transformation

The *S. cerevisiae* strains used in this study are derived from NCYC 3608 (National Collection of Yeast Cultures, UK,), an S288c derivative. All yeast transformations were performed using standard Li-acetate methods according to Gietz and Schiestl (2008). The transformed yeast cells were selected on synthetic complete medium (SC) lacking uracil (SC-Ura) (MP Biomedicals, France). For phenotype analysis, typically 6 colonies of each transformant type were inoculated in 0.5 mL SC-Ura and incubated overnight at 30°C and 400 rpm in 96 well Deep Well Plates (DWP). The following day, 50 µL of each culture was transferred into 0.5 mL of fresh SC medium or, in the case of the TAL screening, into DELFT medium containing 4% glucose. Cells were then incubated for 72h at 30°C and 400 rpm in 96 well DWP.

2.2 Plasmids and strain construction

Oligonucleotides used for cloning and verification of genomic integrations/deletions are listed in Appendix 1 table 1, 2, 3. All primers were synthesized by Integrated DNA Technologies (IDT). A Kozak consensus sequence (AAAA) was introduced on the primer in front of the start codon of every cloned gene to be expressed in yeast. Constructed plasmids are listed in Appendix 1 table 4, 5 and 6. Synthetic genes were codon-optimized for *S. cerevisiae* and obtained from GeneArt (Thermo Fisher Scientific) (Appendix 1 table 7). In some cases several codon-optimised versions were ordered in order to allow for several copies of the same enzyme to be introduced in one single step, in order to avoid homologous recombination between different copies. Plasmids were constructed as integrative Easy Clone vectors according to Jensen *et al.* (2014). Integration of the flavonoid pathway was done by homologous recombination as described by Shao *et al*. (2009). Basic plasmid backbones are described by Mikkelsen *et al.* (2012). In this study three assembler plasmids were used for each integration round, allowing the simultaneous insertion and expression of up to 6 genes. Each of these plasmids have terminator and promoter sequences, and genes of interest were cloned into these plasmids by USER cloning (Nour-Eldin *et al.* 2006). The integrative vectors were digested by *Not*I HF before being transformed. The KlURA3 marker on one of the three integration vectors is flanked by direct repeats (DR), allowing for the KlURA3 marker to be looped out after each transformation round by 5-fluoroorotic acid treatment (Lee and Da Silva 1997). Plasmid pROP0768, which was constructed for yeast transposable elements (Ty)-mediated integration, was constructed as per the aforementioned technique, with some modifications (Maury *et al.* 2016). This vector contains two homology regions complementary to Ty1 elements as well as a *URA3* marker from *S. cerevisiae* under a shortened *URA3* promoter.

Cloning was performed using *E. coli* DH5α for DNA replication. Bacterial transformants were selected on Luria-Bertani (LB) agar plates containing 100 µg/mL of ampicillin. Yeast genomic DNA was extracted according to Lõoke *et al.* (2011) and genomic integration of all insertions/deletions was confirmed by PCR analysis.

Preparation of background strain for phenylpropanoid production

The background strain (EFSC4396) was prepared by deleting *ARO10,* using *AsiSI* digested EPSC3788 and *PAD1*, *FDC1,* using *AsiSI* digested EPSC2901.

TAL screening

Plasmids with PAL/TAL-coding genes (Appendix table 5) were designed so the tested genes will be part of a naringenin producing pathway. Genes were cloned on EPSC3907 assembler plasmid under control of the pTDH promoter. *PALs/TALs* were cloned together with *C4H-CPR* in order to measure their PAL+TAL activity and without C4H-CPR in order to measure TAL activity alone. Plasmids with different *PAL/TAL* variants (with or without *C4H-CPR*) were transformed into the EFSC4396 strain together with pROP266 (*CHI, CHS*) and pROP273 (*4CL*).

PAL/TAL enzymes were selected mainly based on literature (see introduction 1.2.2 p. 20-21) but also based on database searches and homology studies. The enzymes annotated as PAL/TALs and HALs in BRENDA database were also taken into consideration. Alignment of different candidates allowed us to select enzymes most likely to function as TAL's (base on substrate selectivity site). Some enzymes were also selected based on their high homology with the well-known TAL enzyme, *Rs*TAL (Watts *et al.* 2006b) using NCBI blast search. The corresponding DNA sequences were codon optimized for optimal expression in *S. cerevisiae.*

2.3 Analytical methods and sample preparation

From each culture to be analysed, samples were collected after 72h of growth and optical density was measured in MTP 96 microplates at 600 nm in an EnVision 2104 Plate Reader - 0.2 cm light path. For the analysis of the phenylpropanoids produced, 300 µL from each culture was combined with 300 µL of 96% ethanol, mixed for 30 seconds and centrifuged for 10 min. at 4000 x g. Supernatants were analysed by HPLC. Phloretic acid, *p*-coumaric acid, cinnamic acid, dihydrocinnamic acid, naringenin, resveratrol and phloretin were measured at 225 nm using an Ultimate3000 HPLC system with an Ultra C18 3µm Column (100*4.6mm) operating at 40°C, coupled to a diode array detector. Solvent A was water and solvent B was acetonitrile, both containing 50 ppm of trifluoroaceticacid (TFA). The flow rate was 1 ml/min with acetonitrile increasing from 20% at 0 min. to 60% in 9 min. Retention time of the phenylpropanoid compounds was 3 min. for phloretic acid, 3.2 min. for *p*-coumaric acid, 5.1 min. for resveratrol, 6.7 min. for cinnamic acid, 7.4 min for dihydrocinnamic acid, 7.56 min. for naringenin chalcone, 7.7 min. for phloretin, and 7.75 min. for naringenin.

Potential naringenin is calculated based on the amount of phloretic acid (or other intermediates) measured, and reflects the naringenin that would be produced if all the *p*-coumaroyl-CoA would be converted into naringenin and assuming that malonyl-CoA is not a limiting factor. The molecular mass of phloretic acid is 166.18 g/mol while naringenin is 272.26 g/mol. The ratio between these numbers is 0.61. *Potential naringenin* from phloretic acid is calculated by dividing the amount of phloretic acid produced by 0.61. *Potential naringenin* from *p*-coumaric acid (MW 164.16 g/mol) is calculated by dividing the amount of *p*-coumaric acid produced by the corresponding ratio, 0.60.

3. Results & Discussion

3.1 Production of naringenin in *S. cerevisiae*

The initial step was to construct the background strain (EFSC4396) by knocking out genes known to reduce the amount of the pathway precursor, phenylalanine and intermediates, cinnamic and *p*-coumaric acid. In order to avoid loss of phenylalanine, *ARO10,* encoding a pyrophosphate-dependent 2-oxo acid decarboxylase was deleted according to Koopman *et al.* (2012), Romagnoli *et al.* (2012) and Rodriguez *et al.* (2015). This deletion abolished production of phenylethanol in EFCS4396 strain (data not shown). In order to avoid loss of cinnamic and *p*-coumaric acid upon introduction of the phenylpropanoid pathway, *PAD1* encoding phenylacrylic acid decarboxylase and *FDC1* encoding ferulic acid decarboxylase were deleted according to Mukai *et al.* (2010).

The phenylpropanoid pathway genes used in this study were phenylalanine ammonia lyase (*At*PAL2), cinnamate-4 hydroxylase with its redox partner (*At*C4H, *At*CPR), cinnamoyl-CoA ligase (*At*4CL) from *A. thanliana,* chalcone synthase (*Ha*CHS) from *H. androsaemum* and chalcone isomerase (*Ph*CHI) from *P. hybrid*. Additionally, PALs and CHSs from other organisms were also tested. The production of phenylpropanoid precursors, phenylalanine and tyrosine, was also boosted. In order to obtain high naringenin- producer strains, the pathway genes were integrated in the genome of EFSC4396 in several iteration rounds, whereas each iteration was generated by one round of transformation. At each step the best producer was nominated as generation (GEN). The results showing the comparison of different genetic combinations in each iteration were OD-normalised in order to minimize intra and inter-experiment variability. The titers of the best producer from each generation are not normalised and are compared in Figure 18, showing the increases on production achieved by the different iterations. The genotype of the best producers is indicated in Appendix 1 table 8, whereas the number of genes in this producers is indicated in Table 3.

3.1.1. GEN0: Naringenin pathway genes, the C4H cytochrome P450 and its redox partner

At first we wanted to determine if the redox partner of *At*C4H used, *At*ATR, should be expressed separately or as a fusion protein together with C4H, and also to determine which of the two ATR genes from *A. thanliana* would be the most optimal in our set-up. The phenylpropanoid pathway genes *AtPAL2*, *At*4*CL*, *HaCHS*, and *PhCHI* were expressed in EFSC4396 with different combinations of cinnamate-4 hydroxylase (*AtC4H*) and either of two *AtATR* (*ATR1* and *ATR2*), separately and in the fused form (Figure 11). Naringenin and phloretic acid, presented herein as *potential naringenin*, were the two compounds measured. The significant accumulation of phloretic acid (result of the reduction of *p*-coumaric acid) indicates that the rate-limiting bottleneck is downstream of *p*-coumaric acid. Accumulation of phloretic acid did not affect the cellular growth or the final biomass obtained.

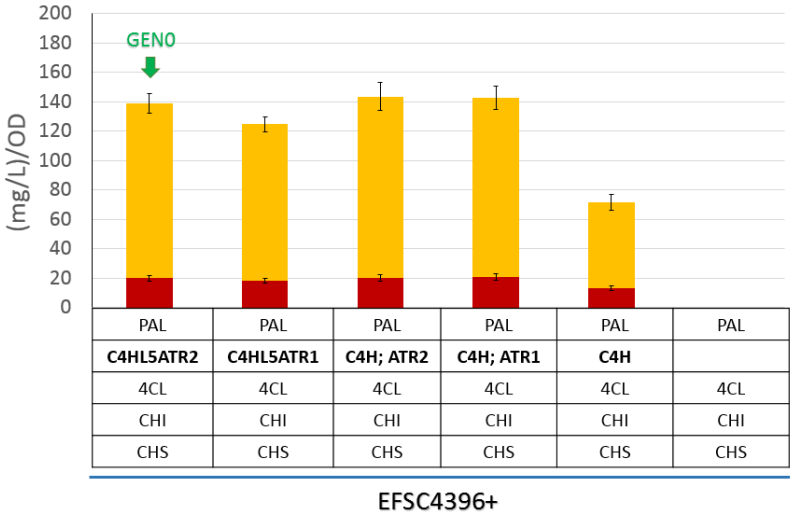

Figure 11. OD normalised production of naringenin (dark red) and potential naringenin (orange) by strains, expressing naringenin biosynthetic pathway with or without different versions of C4H redox partner from A. thaliana (ATR) (indicated in the table below chart). L5 is a linker that creates protein fusion. Error bars represent standard deviation (n=10).

The presence of either ATR1 or ATR2 significantly improved the production of naringenin and *potential naringenin*. This was expected as the activity of P450s is known to be enhanced by the presence of their reductase partners. In nature there are numerous examples of reductases linked to their redox partners. It is assumed that this is the result of evolution and a higher catalytic efficiency of these enzymes (Munro *et. al.* 2007). However, in our case, the expression of the redox partner as a protein fusion with C4H did not result in an increased production.

Even though the C4H:L5:ATR2 fusion was not more efficient than the enzymes expressed separately we chose this fusion for practical reasons as it only takes 1 spot in our expression cassettes. Therefore, a naringenin-producer strain harbouring the C4H:L5:ATR2 fusion together with the rest of the naringenin pathway genes described before, was named generation 0 (GEN0) and was used as a base for further development. It is to be noted that when Koopman *et al.* (2012) compared the different ATRs from *A. thanliana* for their naringenin producer, they found ATR1 to be functional whereas ATR2 was not, as no naringenin was produced in that strain. Based on personal communication and alignment analysis we identified that Koopman's ATR2 had only half the amino acid length when compared to the ATR2 used in our work and published in the public databases, which may explain the lack of activity of ATR2 in their studies.

The GEN0 strain, containing 1 copy of each gene (*PAL*, *C4H:L5:ATR2*, *4CL*, *CHS* and *CHI*), produced 53 mg/L of naringenin and 240 mg/L of phloretic acid (394 mg/L *potential naringenin*) in a batch culture, solely from glucose (no 4-vinylphenol was detected). This titer is higher than previously observed for a strain expressing one copy of the pathway in the batch culture. Koopman *et al*. (2012) obtained 1.55 mg/L of naringenin and 24 mg/L of phenylethanol in the strain with one integrated naringenin pathway –note that phloretic acid was not reported. A possible explanation for the higher carbon flow we observe in the phenylpropanoid pathway could be due to the fact that the background strain used by Koopman had a functional *ARO10* gene while in ours it was deleted, which may also explain the strong accumulation of phenylethanol in their producer. Jiang and colleagues (2005) reached 7 mg/L of naringenin in

shake flask culture in *pad1* knockout strain, nevertheless, *ARO10* was not deleted and they expressed TAL rather that PAL enzyme. Overall, it seems that the phenylalanine ammonia lyase used by Koopman was less efficient than the one in our strain. This was not due to the difference on the promoter as in both cases phenylalanine ammonia lyase was expressed under control of the same strong constitutive promoter, pTDH3. From our experiments we concluded that *At*PAL1 and *At*PAL2 have similar activity (Figure 19). However, in our studies genes were codon optimised for their expression in *S. cerevisiae*, allowing better expression of *AtPAL2* and funnelling more carbon through the phenylpropanoid pathway. The difference can also be attributed to different background strain used (CEN.PK vs. s288c), different genes and different growing conditions.

3.1.2 GEN1 and GEN2: Identification of bottlenecks within the naringenin pathway

As carbon is driven through a heterologous metabolic pathway, intermediates may accumulate revealing the reactions that cause bottlenecks. In order to reveal such bottlenecks in our pathway, we therefore performed an experiment where we introduced a second copy of the pathway where specific genes were absent (Figure 12).

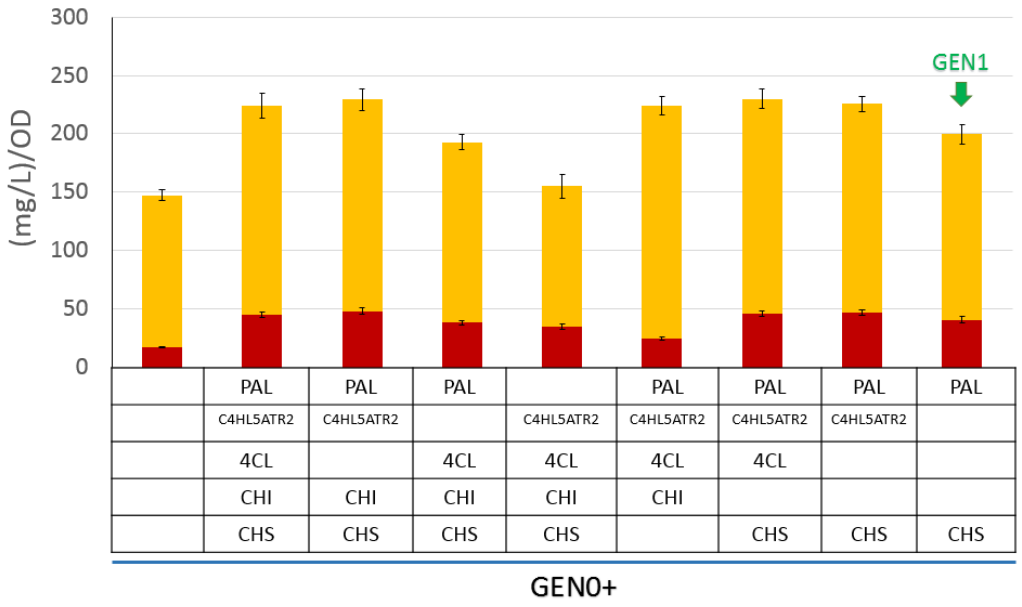

Figure 12. OD normalised production of naringenin (dark red) and potential naringenin (orange) in the strains where genes indicated in the table below chart has been introduced to GEN0 strain, the control strain (all 5 empty cells) contains p416gpd empty plasmid. Error bars represent standard deviation (n=5).

From the results above, chalcone synthase (CHS) appears to be the most limiting factor in terms of naringenin production. All strains containing an extra copy of *CHS* showed a similar, significant increase (about 100%), when compared to the parental strain or these where no extra copy of *CHS* was introduced. Phenylalanine ammonia lyase is a limiting factor in terms of phloretic acid (shown as *potential naringenin*). Likewise, the introduction of extra copie of *PAL* resulted in an increased carbon flux towards the pathway. The absence of *PAL* from the 2nd copy of the pathway resulted in approximately 32% lower *potential naringenin* and approximately 21% lower naringenin, when compared to the strain with two complete pathways. The absence of *C4H:L5:ATR2* from the 2nd copy of the pathway seems to result in

a moderate reduction in the production of naringenin and *potential naringenin* (14% and 13% respectively). The absence of *4CL* or *CHI* from the second copy of the pathway has no effects in the naringenin or *potential naringenin* titers, indicating that the activity of the resulting enzymes did not constitute a bottleneck in the parental strain.

As PAL and CHS were the main bottlenecks, the GEN0 with additional *PAL* and *CHS* was nominated as GEN1. This strain produced 113 mg/L of naringenin and 266 mg/L of phloretic acid (437 mg/L *potential naringenin*).

The same experiment was repeated in the second round of iteration where GEN1 was introduced with different gene combinations. The best clone was obtained by introducing copy of *PAL*, *CHS* and *C4H:L5:ATR2* to GEN1 strain, so CHS and PAL and C4HL5ATR2 were confirmed as a bottlenecks (data not shown). This strain, nominated as GEN2, produced 184 mg/L of naringenin (61% increase) and 405 mg/L of phloretic acid (43% increase) equivalent to 664 mg/L *potential naringenin*, and was nominated as **GEN2** strain (Figure 18).

In our work we identified phenylalanine ammonia lyase and chalcone synthase as the weaker enzymes in the heterologous pathway leading to naringenin biosynthesis in *S. cerevisiae* and, therefore, main focus for the development of strains for industrial production of flavonoids in this organism. CHS has also been identified as a bottleneck in a similar context in previous studies (Koopman *et al.* 2012; Wu *et al.* 2014b). Scheideler *et al.* (2002) also suggested that CHS may be the main regulator enzyme for the synthesis of flavonoids plants. They monitored the transcriptome of the *A. thaliana* infected with *P. syringae* and identified that *CHS* was the phenylpropanoid pathway gene induced to the highest extent upon the infection whereas *PAL* was only slightly induced. Zabala *et al.* (2006) studied the transcriptome of *Glycine max* upon similar bacterial infection and found that *CHS*, as well as genes responsible for production of isoflavonoids and located immediately downstream were also overexpressed.

3.1.3 GEN3: Comparison of CHS from different sources

As we found out that the CHS is one of the main pathway bottlenecks for the production of flavonoids in *S. cerevisiae*, we decided to compare the *in vivo* activity of different CHS available. Therefore, we cloned *CHS* from *Hypericum androsaemum*, *Petroselinum crispum*, *Petunia hybrid*, *Scutellaria baicalensis* and two *CHS*s from *Hordeum vulgare*. Expression cassettes containing the different *CHS* genes under control of the same promoter and terminator regions were integrated into the genome of GEN2 strain.

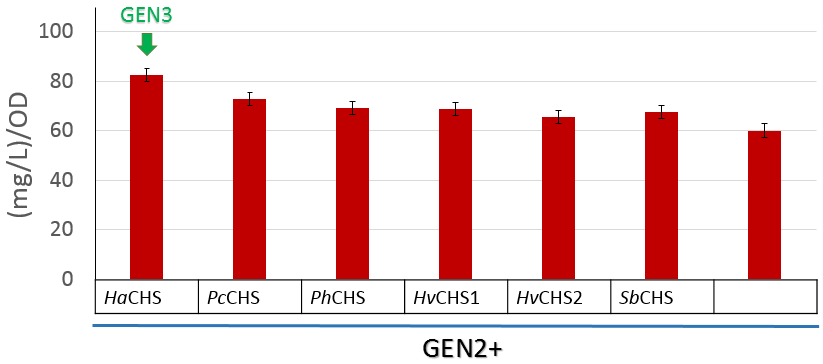

Figure 13. OD-normalised production of naringenin. GEN2 strain with CHS from H. androsaemum (Ha), the control strain GEN2 (empty cell) contains p416gpd empty plasmid. P. crispum (Pc), P. hybrid (Ph), H. vulgare (Hv), S. baicalensis (Sb). Error bars represent standard deviation (n=5).

The expression of an extra copy of the chalcone synthase from *H. androsaemum* resulted in the largest increase in naringenin production (about 36%; see Figure 13). Coincidentally, *HaCHS* was the chalcone synthase used in for the construction of GEN1 and GEN2 so the strain with an extra copy of said synthase was designed as (generation 3- GEN3) and chosen for the next iteration round for improvement of naringenin production. The markerless GEN3 strain produced 214 mg/L of naringenin and 348 mg/L of phloretic acid and 3.9 mg/L of *p*-coumaric acid (shown as 577 mg/L *potential naringenin* from phloretic and *p*-coumaric acid) (Figure 18).

Jiang *et al.* (2005) expressed *HaCHS* and other naringenin biosynthetic pathway genes from plasmids and observed a production of 7 mg/L of naringenin, 9 mg/L phloretin and 11 mg/L of 2`,4`,6`-trihydroxydihydrochalcone. The last two compounds are produced by CHS from dihydro-coumaroyl-CoA. Different CHS has been reported to have different *p*-coumaroyl-CoA/dihydro-coumaroyl-CoA specificity (Eichenberger *et al.* 2016) but, despite using the same *Ha*CHS as Jiang, our strain produced only trace amounts of phloretin. This observation is difficult to explain but could be partially justified by the higher titers achieved by our strains and a differential activity of the *Ha*CHS enzyme towards *p*-coumaroyl-CoA and its reduced counterpart.

3.1.4 GEN4: Introduction of several copies of *PAL*

Phenylalanine ammonia lyase catalyses the deamination of phenylalanine and regulates the entry of carbon into the phenylpropanoid pathway. In order to release PAL bottleneck, we introduced several copies of *PAL* into GEN3 strain (each combination was combined with one extra copy of *HaCHS*). The PAL enzymes originate from *Arabidopsis thaliana* (*At*PAL1 and *At*PAL2), *Aspergillus niger* (*An*PAL1), *Rhodosporidium toruloides* (*Rt*PAL). The strain with all PALs (Figure 14) expressed one *HaCHS* and five *PAL*s: *AtPAL1*, *AtPAL2*, *AnPAL1*, *RtPAL* plus a second codon optimised versions of *AtPAL2*.

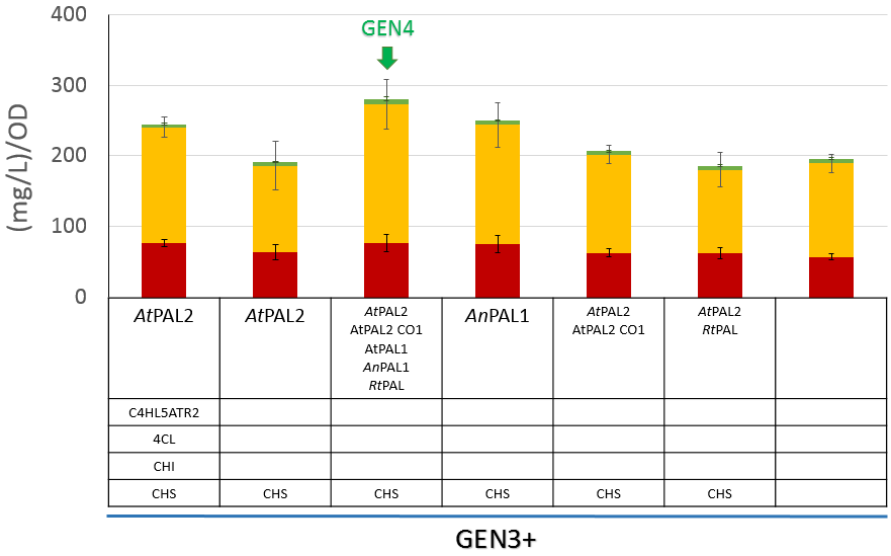

Figure 14. OD-normalised production of naringenin (dark red), potential naringenin from phloretic acid (orange) and potential naringenin from p-coumaric acid (green) in the strains where genes indicated in the table below chart were introduced to GEN3, the control strain GEN3 (empty cells) contains p416gpd empty plasmid. A. thaliana (At), A. niger (An), R. toruloides (Rt). Error bars represent standard deviation (n=5).

The introduction of extra PAL activity further increased the amount of naringenin and *potential naringenin*, but not in case when extra copy of *AtPAL2* was added. The introduction of one copy of *AnPAL* increased the total titer by approximately 27% while the introduction of whole pathway or all five *PAL*s resulted in an increase of 43% over the strain that received no extra *PAL* genes (Figure 14). The strain with all five *PAL*s produced 237 mg/L naringenin, 422 mg/L of phloretic acid and 6 mg/L *p*-coumaric acid (702 mg/L *potential naringenin* from phloretic and *p*-coumaric acid) and was defined as generation 4 (GEN4) after the URA marker was looped out. The small improvement of the 5-*PAL* strain over the one that received only the extra copy of *AnPAL* may indicate that phenylalanine has become somehow limiting and that a further increment of PAL activity may not result in further increases in titer and could even become counterproductive. To further increment the amounts of carbon being channelled towards the phenylpropanoid pathway, two possibilities have been also discussed in this work. a) the deregulation/overexpression of enzymes from the shikimate pathway to increase the levels of available aromatic amino acids, similarly to the work done by Koopman *et al.* 2012, and b) the utilization of tyrosine via the expression of enzymes with TAL activity.

3.1.5 GEN5: Introduction of several copies of *HaCHS*

In order to achieve higher flavonoid titers solving the CHS bottleneck needed to be investigated. For this reason in the fifth iteration round we chose to introduce several copies of differently codon optimized *HaCHS* at once while also comparing the activity of each version (Figure 15). The addition of one of each codon-optimised versions of *HaCHS* resulted in an increased titer of naringenin from 17% to 31%, the original version of *CHS* (*CHS* CO 0) being the one achieving slightly better numbers. The addition of two copies increased the titer on average by about 48%, whereas the addition of all 5 copies of the *HaCHS* resulted only in a 68% increase in the naringenin titer. This shows that the benefits from inserting increasing

copies of CHS are somehow capped. After the URA marker was looped out, the strain with five copies of *HaCHS* produced 272 mg/L naringenin, 321 mg/L of phloretic acid and 15 mg/L *p*-coumaric acid (552 mg/L *potential naringenin* from phloretic and *p*-coumaric acid) and it was defined as the GEN5 strain (see Figure 18).

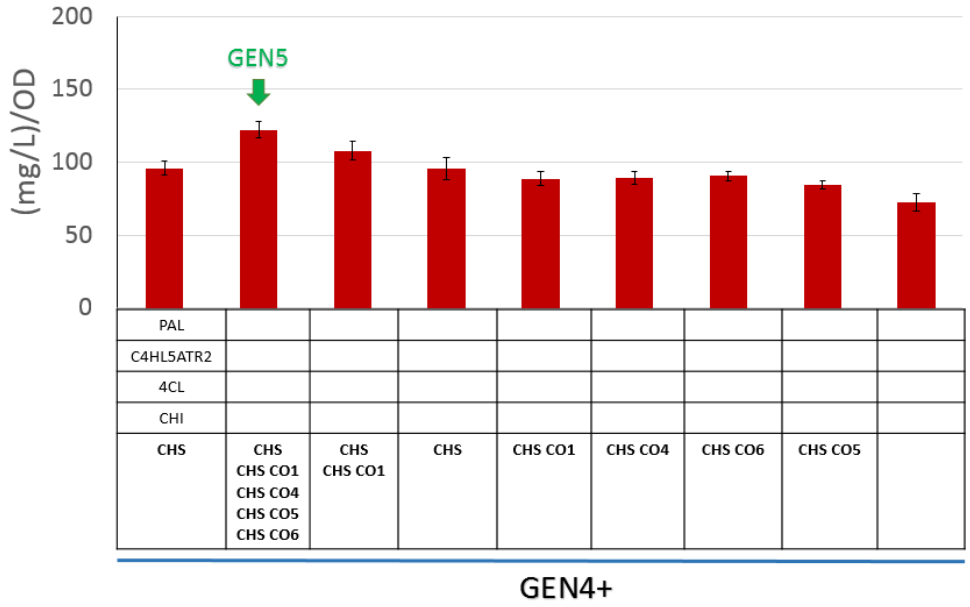

Figure 15. OD normalised production of naringenin (dark red), in GEN4 with different codon optimized versions of CHS (CO 0, 1, 4, 6 and 5), the control strain GEN4 (with 5 empty cells) contains p416gpd empty plasmid. Error bars represent standard deviation (n=5).

There are several possible reasons for the increased observed in the strains with 5 extra copies of *HaCHS* being hardly double of that of the strains with only one copy and similar to those achieved by the insertion of 2 copies. One possible reason is that due to the kinetic constants of CHS and Tsc13 a balance has been reached where extra copies of *CHS* cannot help outcompeting Tsc13. However, other explanations involving gene expression, protein localization, and others are also possible.

3.1.6 GEN6: Phenylalanine and tyrosine boost

As concluded in paragraph 3.1.4, the benefits from increasing PAL activity are limited, probably by the availability of the pathway precursor, phenylalanine. In order to boost the levels of phenylalanine available, several modifications of the shikimate pathway genes are described in literature and were tested using the GEN5 strain as background. Gene coding the feedback resistant DAHP synthase $Aro4_{K229L}$ (Hartmann *et al.* 2003) was introduced in the *ARO3* locus leading to the deletion of that gene as well as into the regular genetic integration locus XII-5 (Mikkelsen *et al.* 2012). In another setup $ARO4_{K229L}$ was combined with a $ARO7_{T226I}$ (Schmidheini *et al.* 1989) and introduced into the *ARO3* or XII-5 locus.

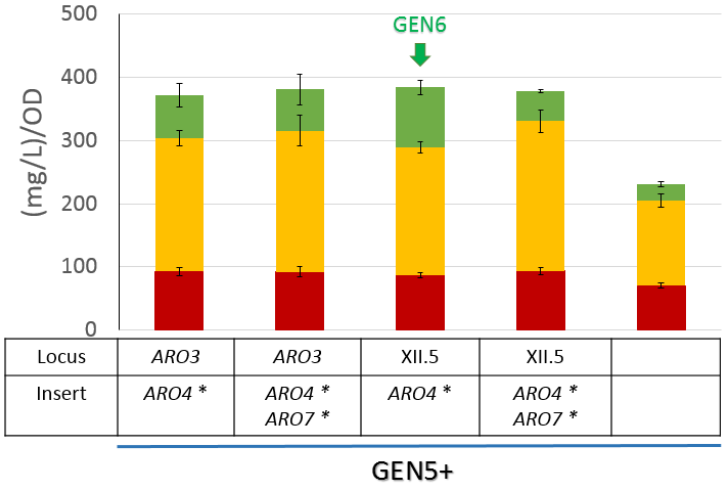

Figure 16. OD-normalised production of naringenin (dark red), potential naringenin from phloretic acid (orange) and potential naringenin from p-coumaric acid (green). Control (C) strain is GEN5 with p416gpd empty plasmid (empty cells), whereas other strains have additional copies of $ARO4_{K229L}$ or $ARO4_{K229L}$ and $ARO7_{T226I}$ in the XII-5 or strain ARO3 locus. Described mutations are marked wits asterisks. Error bars represent standard deviation (n=5).

The insertion of the expression cassettes in the *ARO3* locus did not have a positive effect on the titers achieved in both setups. The strain with $Aro4_{K229L}$ and $Aro7_{T226I}$ had a 32% higher level of naringenin and a 76% higher level of *potential naringenin* than the GEN5 control (see Figure 16). However, this strain lost productivity after the URA marker was removed and could not be used for further development. The strain with $Aro4_{K229L}$ alone showed a 24% higher level of naringenin and a 83% higher level of *potential naringenin* than the GEN5 control and was defined as GEN6. After marker removal it produced 319 mg/L of naringenin, 607 mg/L of phloretic acid and 76 mg/L of *p*-coumaric acid (showed as 649 mg/L of *potential naringenin* from phloretic and *p*-coumaric acid). By boosting the production of aromatic amino acids with overexpression of $ARO4_{K229L}$, an increased amount of carbon was incorporated into the pathway. In this conditions the strain did benefit from the extra PAL activity introduced during the 4th iteration.

Koopman *et al.* (2012) also overexpressed an Aro4 mutant in their naringenin producing strain. However they used a muation different from that in our and other studies. The variant used by Koopman ($Aro4_{G226S}$) was reported to be inhibited by phenylalanine and insensitive to tyrosine, whereas our variant ($Aro4_{K229L}$) was reported to be insensitive to feedback inhibition by both amino acids (Hartmann *et al.* 2003). Nevertheless, after introducing $ARO4_{G226S}$ and deleting *aro3*, Koopman's naringenin-producer strain accumulated a threefold higher amount of naringenin, and started accumulating phloretic acid (73% of total titer) and *p*-coumaric acid (26% of total titer). In our case, the overexpression of $ARO4_{K229L}$ only resulted in a 24% higher level of naringenin and a 83% higher level of *potential naringenin* (107% in total). This could be either the result of some undescribed feedback inhibition of $Aro4_{K229L}$ or because the background genotype used by Koopman (CEN.PK) had a low basal level of phenylalanine – and therefore were able to achieve a higher percentage of increase by relieving this bottleneck. However, Li M *et al.* (2015) were able to achieve a 78% increase in their resveratrol titers by overexpressing $ARO4_{K229L}$ and $ARO7_{G141S}$ in a CEN.PK strain.

The accumulation of *p*-coumaric acid observed in GEN6 suggests that, at this point, the ligation of CoA to *p*-coumaric acid may have become a bottleneck. This could be either because the CoA pool is limiting or, most likely, because the amount of 4CL enzyme resulting from a single copy of 4CL is no longer able to sustain the pathway flux. In that case, the addition of extra *4CL* copies would result in increased the levels of phloretic acid and naringenin. Nevertheless, when Vos *et al.* 2015 evaluated a resveratrol producing strain obtained from Katz *et al.* 2013, 13% of their total titer was *p*-coumaric acid despite the fact that they introduced 4CL on a Ty plasmid, designed for multiple integration.

Another possible explanation for the accumulation of *p*-coumaric acid is an eventual feedback inhibition of 4CL by its product or other products of the phenylpropanoid pathway. Alberstein *et al.* (2012) reported that the 4CL from *Populus tomentosa* was inhibited by naringenin *in vitro.* It would be interesting to test the performance of our producer with an additional copy of a feedback resistant 4CL.

3.1.7 Approach to alleviate the CHS bottleneck

GEN5 and GEN6 contain 10 copies of the *HaCHS* gene but still produce plenty of *potential naringenin* in form of phloretic and *p*-coumaric acid. For that reason, the aim of the last iteration discussed here was to release the CHS bottleneck by introducing multiple copies of this gene. This was done by the Ty1 element-mediated multiple integration of two codon optimized versions of *HaCHS* into GEN5 and GEN6. This method uses similar integration site and allows insertion of approximately 12 genetic inserts in a single step (Maury *et al.* 2016). Twenty transformants from each GEN5 and GEN6 were grown and analyzed for production, showing a high variability that possibly indicate that the number of copies inserted was also variable. Therefore only the best variants of producers are presented in Figure 17.

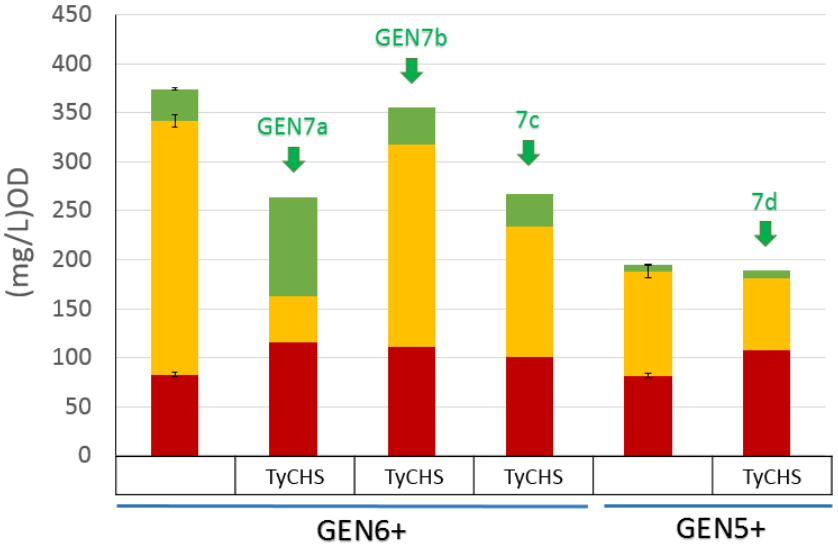

Figure 17. OD-normalised production of naringenin (dark red), potential naringenin from phloretic acid (orange) and potential naringenin from p-coumaric acid (green), by the GEN7 isolates. GEN5 and GEN6 have CHS introduced on Ty elements, control strains (empty cells) carry a p416gpd empty plasmid. Error bars in control strains represent standard deviation (n=4).

The best clone in terms of naringenin production was selected from the GEN6 pool (see Figure 17, clone GEN7a) and produced 430 mg/L of naringenin (40% increase), 107 mg/L phloretic acid and 227 mg/L *p*-coumaric acid (556 mg/L *potential naringenin* from phloretic and *p*-coumaric acid). This was the only clone with a tendency to accumulate less phloretic acid. The second best producing clone isolated from the GEN6 pool (see Figure 17, clone GEN7b) produced 396 mg/L of naringenin (35% increase), 448 mg/L of phloretic acid and 80 mg/L *p*-coumaric acid (867 mg/L *potential naringenin* from phloretic and *p*-coumaric acid). There was one more clone from this pool where naringenin increased by 21% at the expense of *p*-coumaric acid (see Figure 17, clone 7c). The introduction of *CHS* on the Ty1 plasmid on GEN5 also resulted in a 31% increase in the naringenin levels of one of the clones (see Figure 17, clone 7d). This isolate produced 384 mg/L of naringenin, 159 mg/L of phloretic acid and 17 mg/L *p*-coumaric acid (289 mg/L *potential naringenin* from phloretic and *p*-coumaric acid).

Unfortunately the bottleneck at the level of the chalcone synthase was not fully released by this approach. The deletion of *TSC13* discussed in chapter two may help by eliminating the accumulation of phloretic acid but the poor activity of the chalcone synthase enzyme would still limit the production of flavonoids. To solve this bottleneck it may be possible to engineer better versions of CHS but there are other factors that may be limiting the CHS activity. There are several studies showing that CHS may be inhibited noncompetitively by phenylpropanoid pathway products such as naringenin, naringenin chalcone and the others (Dao *et al.* 2011), so this may offer an alternative explanation to the aggravation of CHS bottleneck as higher naringenin titers are achieved. Kreuzaler and Hahlbrock (1975) described in an *in vitro* experiment that 27.2 µg/mL of naringenin chalcone (product of CHS, substrate of CHI) inhibited the activity of CHS from *Petroselinum hortense* by 50%. Hinderer and Seitz (1985) demonstrated that the same concentration of naringenin inhibited CHS from *Daucus carota.* Sydor *et al.* (2010) suspected that resveratrol synthesis in yeast might be feedback inhibited by the product as feeding extra *p*-coumaric acid after 120h did not result in an increase in the resveratrol levels. However, by growing the producer strain with and without addition of 500 mg/L of resveratrol they concluded that resveratrol does not have an inhibitory effect on its synthesis as the strain with 500 mg/L resveratrol accumulated the same amount of resveratrol as the control strain, plus an additional 500 mg/L. As 3 molecules of malonyl-CoA are used to make a molecule of naringenin, another possibility is that the levels of available malonyl-CoA are not sufficient to support the full activity of CHS. If this was the case, boosting the levels of available cytosolic malonyl-CoA could help further increasing the production of flavonoids and its derivatives.

3.1.8 Summary

Relatively high titers of naringenin have been achieved through precursor feeding, as described in the literature. Xu *et al.* (2011) and Wu *et al.* (2015) managed to produce 474 mg/L and 421 mg/L in *E. coli* through supplementation with *p*-coumaric acid and tyrosine respectively. However, for large scale, industrial fermentation processes, the supplementation of expensive phenylpropanoic precursors is not optimal. Herein we provide a platform for the production of naringenin from glucose in *S. cerevisiae*, reaching a titer of 430 mg/L (Figure 18, GEN7a) and

opening the door for further improvements. This is, to our knowledge, the highest reported titer of naringenin produced in microorganism from glucose as sole carbon source.

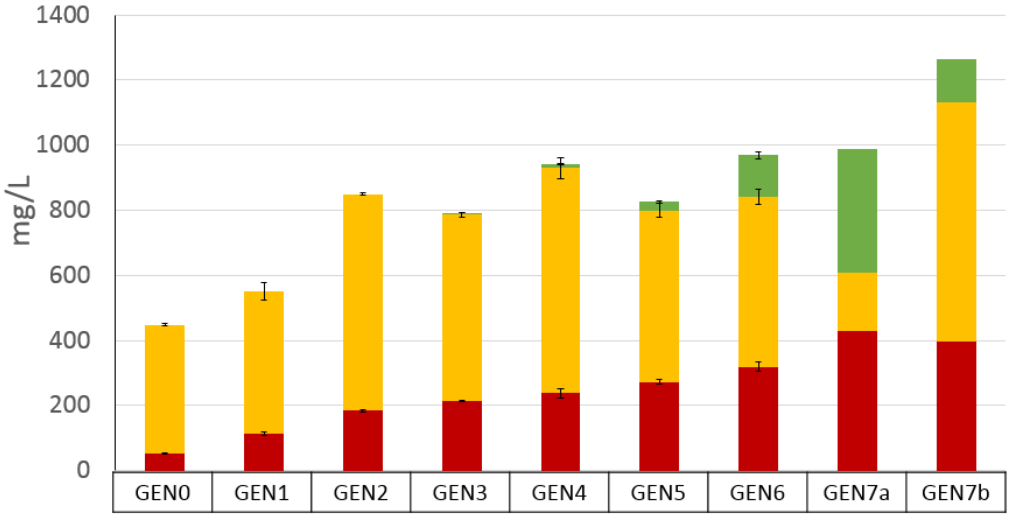

Figure 18. Production of naringenin (dark red), potential naringenin from phloretic acid (orange) and potential naringenin from p-coumaric acid (green) in different generations (GEN). Error bars represent standard deviation (n=5) whereas for two variants presented for the last generation (7a, 7b), n=1.

Table 3. Number of genes present in strain from every generation (GEN).

Gene /generation	*PAL*	*C4HL5ATR2*	*4CL*	*CHS*	*CHI*	Other genes
GEN0	1	1	1	1	1	
GEN1	2	1	1	2	1	
GEN2	3	2	1	3	1	
GEN3	3	2	1	4	1	
GEN4	8	2	1	5	1	
GEN5	8	2	1	10	1	
GEN6	8	2	1	10	1	1 *ARO4* K229L
GEN7	8	2	1	10 +~24	1	1 *ARO4* K229L

After an initial evaluation PAL and CHS were identified as the main bottlenecks in the heterologous pathway leading to the biosynthesis of naringenin in *S. cerevisiae* that we used. The PAL bottleneck was released at GEN4 as extra copies of PAL did not improve the production of *potential naringenin* as strongly as it would correspond to the number of genes inserted. Therefore we assumed that the carbon flow going into the pathway was limited by the levels of phenylalanine available. By boosting the production of aromatic amino acids through the overexpression of $ARO4_{K229L}$ higher titers of *potential naringenin* were observed (Figure 18).

Regarding the cyclization step leading to naringenin, the addition of one extra copy of *HaCHS* to GEN2 and GEN4 lead to an increase in titers of 36% and 31% respectively. However the addition of two or five extra copies resulted only in a further 48% and 68% increase. Moreover, when multiple copies of *HaCHS* were introduced through Ty insertion the titer of naringenin was only improved by 40%. Therefore, further strategies beyond the simple overexpression of

CHS would have to be implemented for the successful development of industrial strain. Several possible strategies have been discussed as possible alternatives. Even though naringenin chalcone is known to spontaneously isomerise into naringenin (Mol *et al.* 1985), it is also possible that this isomerization (supposedly facilitated by CHI) could be a limiting factor. Alternatively, naringenin chalcone might also inhibit the activity of CHS (Hinderer and Seitz 1985). Therefore, a possible approach could be the introduction of several copies of CHI into GEN5 and/or GEN6. Another approach could be to boost the production of cytosolic malonyl-CoA. Despite most of the strategies where researchers boosted the malonyl-CoA in *S. cerevisiae* resulted in a negative effect on growth, some strategies seem to have achieved significant increases without significantly affecting the cell's viability. Shin *et al.* (2012) overexpresed the endogenous gene coding for acetyl-CoA carboxylase (*ACC1*) by replacing its native promoter with the stronger GAL promoter. This strategy improved resveratrol titers by 30%. Interestingly, when Li M *et al.* (2015) introduced *Sc*Acc1$_{S659A,S1157A}$ to the CEN.PK strain they did not observe any negative effect on the final biomass in contrast to Shi *et al.* (2014). As Li M *et al.* improved their resveratrol production by a 31%, this strategy could be another option to try in future efforts on the development of a naringenin producer. If these strategies do not release the CHS bottleneck, it would be interesting to investigate if the activity of *Ha*CHS is inhibited by naringenin. If it's the case that CHS is inhibited by naringenin, accelerating the naringenin export through the introduction/overexpression of a relevant transporter or the development of a feedback insensitive CHS variant would be possible solutions.

3.2 Screening for enzymes with PAL and TAL activity for expression in *S. cerevisiae*

In addition to the importance of TAL enzymes in prokaryotic phenylpropanoid producers, co-expressing *TAL* with *PAL* in the phenylpropanoid yeast producer would likely increase the carbon flux towards the pathway. Additionally, expressing *TAL* in a yeast strain where both tyrosine and phenylalanine are boosted would likely balance the metabolism of that strain as both substrates, and not only phenylalanine, would be used. For these reasons we tested the activity of different TAL enzymes in yeast. As *in vitro* kinetic analysis do not always reflect the *in vivo* activity of heterologous enzymes, we evaluated the *in vivo* performance of several previously reported PAL/TAL enzymes, together with several novel TAL enzymes identified by homology and database searching, by expressing the corresponding codon optimized genes in *S. cerevisiae*.

The enzyme activity of PAL is reported to be reduced by its product, cinnamic acid (Blount *et al.* 2000). Therefore, to avoid the accumulation of cinnamic acid, we introduced the chosen PAL/TALs in *S. cerevisiae* as a part of a whole naringenin pathway and measured the amounts of the final product and the pathway intermediates.

In order to discriminate between the PAL (from phenylalanine → cinnamic acid → *p*-coumaric acid) and the TAL (from tyrosine → *p*-coumaric acid) activities, all PALs/TALs were introduced together with the genes required for the production of naringenin from cinnamic acid (with C4H-CPR) or from *p*-coumaric acid (without C4H-CPR). The TAL activity was determined based on measurements of the pathway intermediates from the strains encoding the

naringenin pathway without C4H-CPR. The PAL activity was determined by subtracting the values obtained for TAL activity from the values obtained from strains encoding naringenin pathway where C4H-CPR was included (representing the PAL and TAL activity together) (Figure 19).

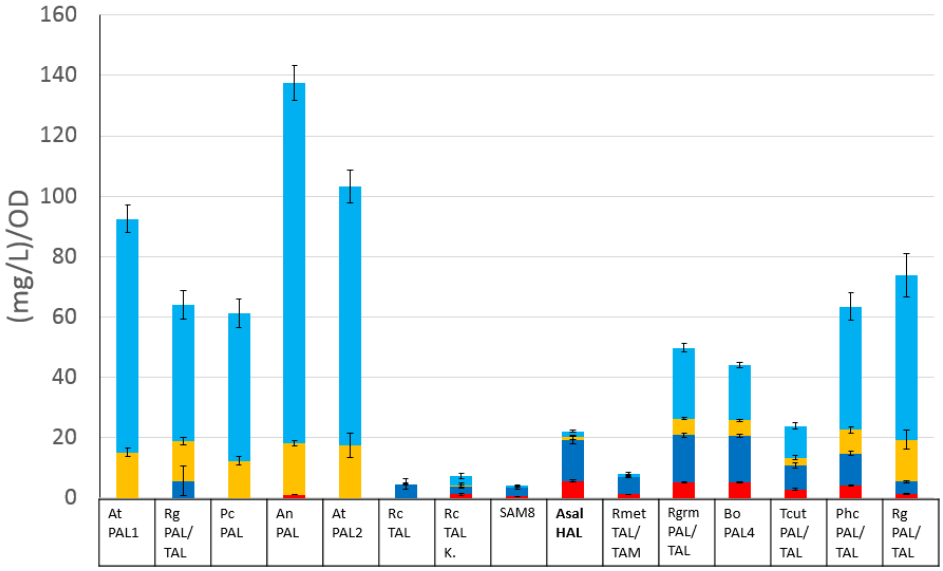

Figure 19. PAL+TAL and TAL activity of different enzymes. Naringenin derived from TAL activity (red), potential naringenin derived from TAL activity (dark blue), naringenin derived from PAL activity (orange), potential naringenin derived from PAL activity (light blue). Error bars represent standard deviation (n=6). The results do not include non-active enzymes evaluated in this study.

The enzymes that showed TAL activity in *S. cerevisiae* (Figure 19) were enzymes from fungi: *R. toruloides* (*Rt*PAL/TAL), *R. graminis* (*Rgram*PAL/TAL), *T. cutaneum* (*Tcut*PAL/TAL), *P. chrysosporium* (*Phc*PAL/TAL), *R. glutinis* (*Rg*PAL/TAL); or bacteria: *R. capsulatus* (*Rc*TAL), *S. espanaensis* (SAM8), *A. salmonicida* (*Asal*HAL), *R. metallidurans* (RmetTAL/TAM); or plant *B. oldhamii* (*Bo*PAL4). Most of the active enzymes identified as TALs in the present work were previously described to have activity towards tyrosine. Nevertheless, the enzyme from *Aeromonas salmonicida* annotated as HAL in the databases, was identified by us as a novel, highly active and very specific TAL when expressed in *S. cerevisiae*. Our results show that the TAL activity of *Asal*HAL is comparable with the best previously known TALs from *R. graminis* (Vanneli *et al.* 2007) and *B. oldhamii* (Hseih *et al.* 2010), while showing a much higher specificity towards tyrosine. The newly identified TAL from *A. salmonicida* showed a much higher activity than previously reported specific TALs as *Rc*TAL from *R. capsulatus* and SAM8 from *S. espanaensis* (Berner *et al.* 2006). Surprisingly, *Rt*PAL/TAL had very strong PAL activity and minor TAL activity when tested in our setup. These findings somewhat agree with those reported in Jiang *et al.* (2005) as when they expressed the phenylpropanoid pathway in *S. cerevisiae* without the C4H-CPR and using *Rt*PAL/TAL obtained a very a low titer –that can be explained by the low activity of *Rt*PAL/TAL on tyrosine.

Xue *et al.* (2007b) reported a higher activity of the TAL from *R. glutinis* towards tyrosine than towards phenylalanine, whereas Vannelli *et al.* (2007a) showed nearly two-fold higher activity towards phenylalanine than towards tyrosine. In our system, *Rg*PAL/TAL appears to have a 12-fold higher activity for phenylalanine than tyrosine (Figure 19). In contrast,

*Rgram*PAL/TAL had similar activity towards the both substrates whereas, in kinetic studies, Vannelli *et al.* (2007a) and Vannelli *et al.* (2007b) described a four and two times higher activity towards phenylalanine respectively. In agreement with our findings, when Vannelli *et al.* (2007b) evaluated the kinetic parameters of *Phc*PAL/TAL they concluded that this enzyme has almost the same activity towards phenylalanine as to tyrosine. The disagreements between our experiments and some enzyme kinetic studies further emphasize the need of *in vivo* activity analysis when selecting the most suitable genes for heterologous expression.

Our screening for the novel TALs was done in parallel with Jendresen *et al.* (2015) who identified two novel specific TALs from *H. aurantiacus* and *F. johnsoniae* by expression of the heterologous genes in *S. cerevisiae* and growth in presence of tyrosine. However, as discussed above and as their reporter molecule was *p*-coumaric acid, it is possible that some of the enzymes tested suffered from product feedback-inhibition. Additionally, they found a TAL that was very active in *E. coli*, *T. cutaneum* XAL, but it was not tested in *S. cerevisiae.* Jendresen *et al.* (2015) provided us with TALs from *H. aurantiacus* and *F. johnsoniae* and XAL from *T. cutaneum*, so we tested these enzymes in our system and compared them to our best candidates. The results are presented in Figure 20.

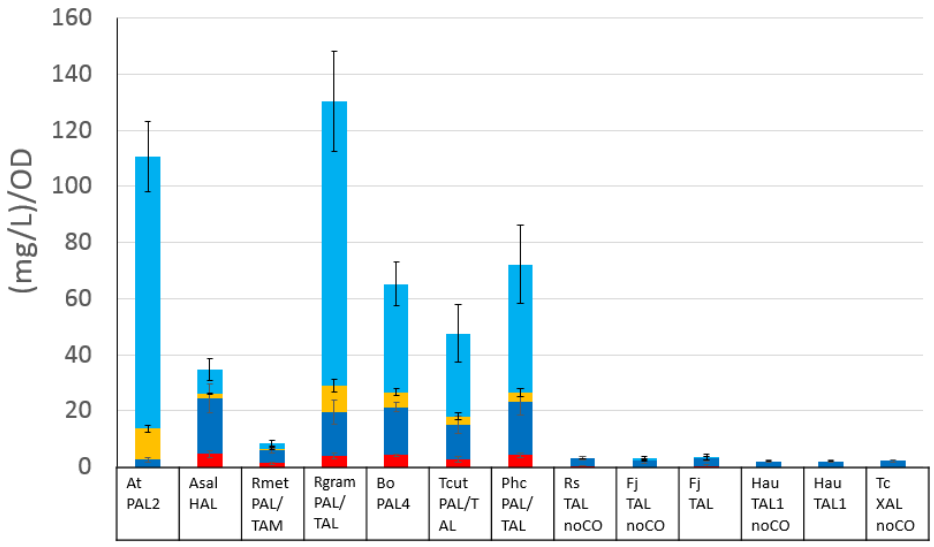

Figure 20. PAL+TAL and TAL activity of chosen enzymes from current study in comparison to TALs identified by Jendresen et al. (2015). Naringenin derived from TAL activity (red), potential naringenin derived from TAL activity (dark blue), naringenin derived from PAL activity (orange), potential naringenin derived from PAL activity (light blue). RsTAL and TcXAL are the only enzymes for which the DNA sequence was not codon optimized for S. cerevisiae (noCO). Error bars represent standard deviation (n=6).

The TAL enzymes identified by Jendresen *et al.* (2015) showed a quite specific TAL activity, however they were not able to match *Asal*HAL and other TAL enzymes in our setup. This could be due to the fact that in the Jendresen *et al.* (2015) study the strains were fed with tyrosine while in our setup the tyrosine was produced from glucose, so the enzyme's activity may be limited by the availability of the substrate.

Louie *et al.* (2006) describes that the His 89 in the *R. sphaeroides* TAL is conserved in enzymes with activity towards tyrosine while it is replaced by other amino acids in PALs and HALs. In

PALs this residue is described to usually be phenylalanine (see Figure 21). Interestingly, this rule seems to apply to most of the enzymes previously described in literature but not to the newly discovered TALs such as *Asal*HAL, *Fj*TAL, *Hau*TAL, *Rmet*TAL/TAM and *An*PAL. Based on our experiments, *Asal*HAL is a very specific TAL but we find phenylalanine instead of histidine at the selectivity switch region. Interestingly, *Hau*TAL, which also has TAL activity, has leucine at that region. However, *An*PAL, with strong PAL activity, also has leucine at that region. These findings would suggest that, while possibly generally valid, using Louie's description of the selectivity switch to circumscribe database searches when looking for TAL or PAL enzymes may limit the success of such efforts.
Interestingly, *Rt*PAL/TAL had very strong PAL activity and minor TAL activity while having a histidine at the putative substrate selective site –which would normally qualify this enzyme as TAL. As *Asal*HAL, *Fj*TAL, *Rmet*TAL/TAM have a histidine in the position following the putative selectivity switch amino acid one could hypothesize that this is the site has some role on determining the specificity for tyrosine in these enzymes.

```
BoPAL4          RPRVKASSEWILNCLAHGGDIYGVTTGFGGTSHRRTK--DGPALQVELLRHLNAGIFGTG  132
PcPAL           RAGVKASSDWVMDSMNKGTDSYGVTTGFGATSHRRTK--QGGALQKELIRFLNAGIFGNG  146
AtPAL1          RAGVNASSDWVMESMNKGTDSYGVTTGFGATSHRRTK--NGVALQKELIRFLNAGIFGST  153
AtPAL2          RAGVKASSDWVMESMNKGTDSYGVTTGFGATSHRRTK--NGTALQTELIRFLNAGIFGNT  145
AnPAL           IDAINGSVIALAECLRDGHHIYGVNTGFGGSADSRTN--QTTTLQSSLLQLLQSGILTAS  118
PhcPAL/TAL      HERVLQSRRVIVDKVSTQRSVYGVSTGFGGSADTRTS--DPLQLGHALLQHQHVGVLPTQ  152
TcXAL           AGPVRASVDF--KESKKHTSIYGVTTGFGGSADTRTS--DTEALQISLLEHQLCGFLPTD  125
TcutPAL/TAL     AGPVRASVDF--KESKKHTSIYGVTTGFGGSADTRTS--DTEALQISLLEHQLCGFLPTD  125
RgramPAL/TAL    RARVDKSVDF--LKAQLQNSVYGVTTGFGGSADTRTE--DAVSLQKALIEHQLCGVTPTS  152
RtPAL/TAL       RSKIDKSVEF--LRSQLSMSVYGVTTGFGGSADTRTE--DAISLQKALLEHQLCGVLPSS  146
RgPAL/TAL       REKIDASVEF--LRTQLDNSVYGVTTGFGGSADTRTE--DAISLQKALLEHQLCGVLPTS  152
SAM8            IVRMGASARTIEEYLKSDKPIYGLTQGFGPLVLFDAD--SELEQGGSLISHLGTGQ----  92
FjTAL           VNRVNESFNFLK-EFSGNKVIYGVNTGFGPMAQYRIKESDQIQLQYNLIRSHSSGT----  84
AsalHAL         MARIQRGADFLDRLLAEEGVIYGVTTGYGDSVTRPVPAELVPELPLHLTRFHGCGL----  95
RmetTAL/TAM     LGKVADARARFEQVAAANVPIYGVSTGFGELVHNWVDIEHGRALQENLLRSHCAGV----  91
HauTAL          LAQIEASCAYINQAVKEHQPVYGVTTGFGGMANVIIS--PEEA-----AELQNNAIWYHK  88
RcTAL           RERCARAHARLEHAIAEQRHIYGITTGFGPLANRLIGADQGAELQQNLIYHLATGV----  95
RsTAL           RDRCRASEARLGAVIREARHVYGLTTGFGPLANRLVSGENVRTLQANLVHHLASGV----  94
```

Figure 21. Partial amino acid sequence alignment of RsTAL with PAL, TAL and PAL/TAL enzymes tested in this study. The residue marked in red is described (Watts et al. 2006b) as responsible for substrate selectivity. Clustal Omega was used for the alignment.

The HAL enzyme from *Aeromonas salmonicida subsp. salmonicida A449* has been described for the first time as a TAL, being as active on tyrosine as the best of the previously reported PAL/TALs while being more than 5 times more active than the previously reported specific TALs.

Appendix 1

Appendix 1 table 1. Primers used in this study to amplify pathway genes. The name of each primer corresponds to bio-brick name indicated in Appendix Table 4.

Primers for pathway genes	Primer sequence, 5´ to 3´
#162 AtPAL2 F	ATCAACGGGUAAAATGGACCAAATTGAAGCAATGC
#162 AtPAL2 R	CGTGCGAUTTAGCAGATTGGAATAGGTGCAC
#100 At4CL2 F	AGCGATACGUAAAATGACGACACAAGATGTGATAGTC
#100 At4CL2 R	CACGCGAUCTAGTTCATTAATCCATTTGCTAG
#221 PhCHI F	AGCGATACGUAAAATGTCTCCACCAGTTTCTGTTAC
#221 PhCHI R	CACGCGAUCTACACACCGATAACAGGTATTG
#222HaCHS F	CGTGCGAUTAATTAATTGCGACTGAATGAAG
#222HaCHS R	ATCAACGGGUAAAATGGTTACTGTTGAAGAAGTTAG
#223 C4H L5 F	AGCGATACGUAAAATGGATTTGTTATTGCTGGAAAAG
#223 C4H L5 R	AGCTGCAGCUTCTTTTGCTGCAGCTTCAGCGCTACAATTTCTGGGTTTCATG
#226 C4H F	AGCGATACGUAAAATGGATTTGTTATTGCTGGAAAAG
#226 C4H R	CACGCGAUTTAACAATTTCTGGGTTTCATG
#231 L5 ATR2 F	AGCTGCAGCUAAAGAAGCTGCAGCAAAAGCTGGTAGGAGGAGCGGTTCG
#231 L5 ATR2 R	CACGCGAUTTACCATACATCTCTCAGATATCTAC
#232 L5 ATR1 F	AGCTGCAGCUAAAGAAGCTGCAGCAAAAGCTACTTCTGCACTTTATGCCTCCG
#232 L5 ATR1 R	CACGCGAUTTACCACACATCTCTCAAGTATCTTCCC
#227 AtATR2 F	CGTGCGAUTTACCATACATCTCTCAGATATCTACC
#227 AtATR2 R	ATCAACGGGUAAAATGTCCAGTAGCTCTTCCTC
#228At ATR1 F	CGTGCGAUTTACCACACATCTCTCAAGTATC
#228At ATR1 R	ATCAACGGGUAAAATGACTTCTGCACTTTATGCC
#304 HaCHS F	AGCGATACGUAAAATGGTTACTGTTGAAGAAGTTAG
#304 HaCHS R	CACGCGAUTAATTAATTGCGACTGAATGAAG
#290 PcCHS F	AGCGATACGUAAAATGGCTAATCATCATAATGCTG
#290 PcCHS R	CACGCGAUTCAGTGAGTGAATGTAGCAGGCACAC
#291 PhCHS F	AGCGATACGUAAAATGGTTACTGTTGAAGAATATAG
#291 PhCHS R	CACGCGAUTTATGTGGCTACAGAGTGTAAAACC
#292 HvCHS1 F	AGCGATACGUAAAATGGCTGCTACAATGACCGTTG
#292 HvCHS1 R	CACGCGAUGCGGTCAAGCAGTGGCACCGGCGG
#293 HvCHS2 F	AGCGATACGUAAAGCGGTCATGCAGAAGCTGCAGTAG
#293 HvCHS2 R	CACGCGAUATGGCTGCAGTAAGATTGAAAGAAG
#294 SbCHS F	AGCGATACGUAAATTAGTTTAAAGGAACGCTGTGC
#294 SbCHS R	CACGCGAUATGGTTACTGTCGAAGAATTCC
#317 AtPAL1 F	AGCGATACGUAAAATGGAGATTAACGGGGCACACAAG
#317 AtPAL1 R	CACGCGAUTTAACATATTGGAATGGGAGCTC
#319 AnPAL1 F	AGCGATACGUAAAATGTTGGACAAGCACATCCCAGACG
#319 AnPAL1 R	CACGCGAUTTATTGTTGGAAGGAGTTCAAAATAG
#314 AtPAL2 (CO2) F	CGTGCGAUTTAGCAGATAGGAATAGGAGCACC
#314 AtPAL2 (CO2) R	ATCAACGGGUAAAAATGGATCAAATCGAAGCTATGTTG
#318 RtPAL F	AGCGATACGUAAAATGGCTCCATCATTGGATTCTATT
#318 RtPAL R	CACGCGAUTTATGCTAACATCTTCAACAAAACG
#328 HaCHS (CO4) F	AGCGATACGUAAAATGGTTACCGTAGAAGAGGTACGTAAAG
#328 HaCHS (CO4) R	CACGCGAUTCAATTAATAGCAACACTATGCAAC
#327 HaCHS (CO1)F	AGCGATACGUAAAATGGTTACAGTCGAAGAAGTGAG
#327 HaCHS (CO1)R	CACGCGAUTTAATTTATGGCAACGGAGTGC
#329 HaCHS (CO5) F	CGTGCGAUTTAGTTTATAGCAACGCTATGCAAAAC
#329 HaCHS (CO5) R	ATCAACGGGUAAAATGGTAACGGTTGAAGAAGTAAGG
#330 HaCHS (CO6) F	AGCGATACGUAAAATGGTGACTGTTGAAGAAGTAAG
#330 HaCHS (CO6) R	CACGCGAUTTAATTAATAGCTACTGAGTGAAG
#148 ARO4 K229L F	AGCGATACGUAAAATGAGTGAATCTCCAATGTTCGC
#148 ARO4 K229L R	CACGCGAUCTATTTCTTGTTAACTTCTCTTCTTTGTC
#218 ARO7 T226I F	CGTGCGAUTTACTCTTCCAACCTTCTTAGCAAG
#218 ARO7 T226I R	ATCAACGGGUAAAATGGATTTCACAAAACCAGAAACTG

Appendix 1 table 2. Primers used in this study to amplify promoters and primers used for verification of genomic integrations/deletions.

Primers for promoters	**Primer sequence, 5´ to 3´**
pPGK1 R	ACCCGTTGAUGCCGCTTGTTTTATATTTGTTGTAAAAAG
pPGK1 F	CACGCGAUGGCCTGGAAGTACCTTCAAAGAATG
pTEF1 F	ATTAAGTCCUGGATCCTAGGTCTAGAGATCTGTTTAGCTTG
pTEF1 R	ACCGCCCCTUGGTTGTTTATGTTCGGATGTGATGTG
pPDC1 F	CGTGCGAUGCCGATCTATGCGACTGGGTGAG
pPDC1 R	ACGTATCGCUTTTTGATAGATTTGACTGTGTTATTTTGCG
pTDH3 F	CGTGCGAUGCCGATCTCAGTTCGAGTTTATCATTATC
pTDH3 R	ACGTATCGCUTTTTGTTTGTTTATGTGTGTTTATTC
pTEF2 F	CGTGCGAUGCCGATCTGGGCCGTATACTTACA
pTEF2 R	ACGTATCGCUTGTTTAGTTAATTATAGTTCGTTGACC
pTPI1 F	ACCCGTTGAUTTTTAGTTTATGTATGTG
pTPI1 R	CACGCGAUGAGTTATAATAATCCTACGTTAG
Genotyping primers	**Primer sequence, 5´ to 3´**
RES629 *ARO10*KO conf F	GTGTAATGAACTGAACGCCG
RES630 *ARO10*KO conf R	TATCAGTCAGTACGTCTCCAAGG
RES295 *PAD1*KO conf F	ATATCAAAAACAGGGCAAGGGAC
RES297 *FDC1*KO conf R	ACTGTTGATCATCTGCCTATTAGTC
RES417 UP R	TCTCAGGTATAGCATGAGGTCGCTCAT
RES418 DW F	CCTGCAGGACTAGTGCTGAGGCATTAAT
RES658 X-2-UP F	TGCGACAGAAGAAAGGGAAG
RES659 X-2 DW R	GAGAACGAGAGGACCCAACAT
RES395 XI-2 UP F	GTTTGTAGTTGGCGGTGGAG
RES396 XI-2 DW	GAGACAAGATGGGGCAAGAC
RES511 XVI-20 UP F	GGCTTGTGGTCACCTGTCAT
RES512 XVI-20 DW R	GAATTATGGTAATTTTGATTATC
RES377 X-4 UP	CTCACAAAGGGACGAATCCT
RES378 X-4 DW	GACGGTACGTTGACCAGAG
RES375 X-3 UP F	TGACGAATCGTTAGGCACAG
RES376 X-3 DW	CCGTGCAATACCAAAATCGAG
RES397 XI-5 UP	CAAATCCGAGTTAGGAATCGTCC
RES398 XI-5 DW	TTCGAATGCGAATCCGCATGTG
ARO3 UP	TGCTTTGTTCAAGAAGGTACG
ARO3 DW	TGTATCTCAGTTGACATCTATCAC
RES458 XII-5 UP	CCACCGAAGTTGATTTGCTT
RES459 XII-5 DW	GTGGGAGTAAGGGATCCTGT

Appendix 1 table 3. Primers used in this study to amplify PAL/TAL genes. The name of each primer corresponds to bio-brick name indicated in appedndix 1 table 5.

Primers for PAL/TAL genes	**Primer sequence, 5´ to 3´**
#269AtPAL1 F	ATCAACGGGU AAAATGGAGATTAACGGGGCACACAAG
#269AtPAL1 R	CGTGCGAU TTAACATATTGGAATGGGAGCTC
#271RtPAL/TAL F	ATCAACGGGU AAAATGGCTCCATCATTGGATTCTATTTCTC
#271RtPAL/TAL R	CGTGCGAU TTATGCTAACATCTTCAACAAAACG
#273RcTAL F	ATCAACGGGU AAAATGACCCTGCAATCTCAAACAGC
#273RcTAL R	CGTGCGAU TTAAGCAGGTGGATCGGCAGCTGC
#274RcTAL K F	ATCAACGGGU AAAATGACCTTACAATCCCAAACTGC
#274RcTAL K R	CGTGCGAU TTAGGCTGGAGGGTCTGCTGCGG
#275SAM8 F	ATCAACGGGU AAAATGACACAGGTAGTTGAAAGGCAG
#275SAM8 R	CGTGCGAU TCATTATCCGAAGTCTTTTCCATCAGC
#276PcPAL F	ATCAACGGGU AAAATGGAAAATGGTAATGGTGCTAC
#276PcPAL R	CGTGCGAU TTAGCAAATAGGTAGTGGTGCAC
#278AnPAL F	CGTGCGAUTTATTGTTGGAAGGAGTTCAAAATAG
#278AnPAL R	ATCAACGGGUAAAATGTTGGACAAGCACATCCC
#279PgramPAL/TAL F	CGTGCGAUTTAAAACATTCTGTTCATAAACTTG
#279PgramPAL/TAL R	ATCAACGGGUAAAATGGCTCATGCTGATTTGTGC
#Asal HAL F	CGTGCGAUTCACAAAGAGGATTCTTGGTACAAAG
#Asal HAL R	ATCAACGGGUAAAAATGAACAAGTCCGAAATGAAGTACG
#281Rmet TAL/TAM F	CGTGCGAUTTAGGCCAATTCAATACCAGCAC
#281Rmet TAL/TAM R	ATCAACGGGUAAAAATGCCACATGCTCATCCAGCTG
#282Sg TAL/TAM F	CGTGCGAUTTATCTCAATTGGATGTCGGTTTC
#282Sg TAL/TAM R	ATCAACGGGUAAAAATGGCCTTGACTCAAGTCGAAAC
#283Rgram PAL F	CGTGCGAUTTAAGCCAACATCTTAACCAAAACG
#283Rgram PAL R	ATCAACGGGUAAAAATGGCCCCATCTTTGGATTCTTTG
#284BoPAL4 F	CGTGCGAUTCAGTTGATTGGCAATGGTTCACC
#284BoPAL4 R	ATCAACGGGUAAAAATGGCTGGTAATGGTCCAATCGTTAAG
#285Nflsh HAL/PAL F	CGTGCGAUTCAGTCCAAACCTGAAGAAGAACAC
#285Nflsh HAL/PAL R	ATCAACGGGUAAAAATGCCAGCTTCTTGGGTTAGAGGTAC
#287Tcut PAL/TAL F	CGTGCGAUTCAGAACATCTTACCAACAGCACC
#287Tcut PAL/TAL R	ATCAACGGGUAAAAATGTTCATCGAAACTAACGTTGCTAAG
#288PhcPAL/TAL F	CGTGCGAUTTAAGCCTTAATGGACTTGACCAATTG
#288PhcPAL/TAL R	ATCAACGGGUAAAAATGCCATCCAGAATCGACTACTAC
#289Rg PAL/TAL2 F	CGTGCGAUTCAGGCCATCATCTTAACCAAAAC
#289Rg PAL/TAL2 R	ATCAACGGGUAAAAATGGCCCCATCCGTTGATTCTATTG
#606 RsTALnotCO F	CGTGCGAUAACCGGACTCTGTTGCAGCAGATGG
#606 RsTALnotCO R	ATCAACGGGUAAAATGCTGGCAATGAGCCCTCCGAAAC
#607 FjTALnotCO F	CGTGCGAUATTGTTAATCAGGTGGTCTTTTAC
#607 FjTALnotCO R	ATCAACGGGUAAAATGAACACCATCAACGAATATCTG
#608 FjTAL F	CGTGCGAUGTTGTTAATCAAGTGATCCTTAAC
#608 FjTAL R	ATCAACGGGUAAAATGAACACCATCAACGAATACTTG
#609 HaTAL1notCO F	CGTGCGAUGCGAAACAGAATAATACTACGCAGAC
#609 HaTAL1notCO R	ATCAACGGGUAAAATGAGCACCACCCTGATTCTGACCGG
#610 HaTAL1 F	CGTGCGAUTCTGAACAAGATGATGGATCTCAAAC
#610 HaTAL1 R	ATCAACGGGUAAAATGTCCACCACCTTGATTTTGACTG
#611 TcXALnotCO F	CGTGCGAUAAACATTTTACCAACTGCACCCATC
#611 TcXALnotCO R	ATCAACGGGUAAAAATGGCAAAAGCAGCACCGGTTGAAC

Appendix 1 table 4. Plasmids used for construction of strains used in this study (indicated in appendix1 table7). Int. site means "insertion site", int. stands for integration, p stands for "promoter" and CO1-5 stands for different codon optimised versions of the same gene. The relative orientation of genes (biobricks) is either forward (F) or reverse (R) as indicated.

Name	Type	Int. site	Backbone	Biobrick R	P	Biobrick F	Biobrick F
pROP266	assembler2	-	EPSC2651	#222 HaCHS	pPGK1-pTEF1	#221 PhCHI	
pROP273	assembler3	X.2	EPSC3908		pPDC1	#100 At4CL2	
pROP280	assembler1	X.2	EPSC3907	#162 AtPAL2	pTDH3-pTEF2	#223 C4H L5	#231 L5 ATR2
pROP281	assembler1	X.2	EPSC3907	#162 AtPAL2	pTDH3-pTEF2	#223 C4H L5	#232 L5 ATR1
pROP0270	assembler1	X.2	EPSC3907	#162 AtPAL2	pTDH3-pTEF2	#226 C4H	
pROP0322	assembler1	X.2	EPSC3907	#162 AtPAL2	pTDH3		
pROP0271	assembler3	X.2	EPSC3908	#227 AtATR2	pTPI1-pPDC1	#100 At4CL2	
pROP0272	assembler3	X.2	EPSC3908	#228 AtATR1	pTPI1-pPDC1	#100 At4CL2	
pROP0336	assembler1	XI-2	EPSC3915	#162 AtPAL2	pTDH3-pTEF2	#223 C4H L5	#231 L5 ATR2
pROP0337	assembler3	XI-2	EPSC3916		pPDC1	#100 At4CL2	
pROP0338	assembler1	XI-2	EPSC3915	#162 AtPAL2	pTDH3		
pROP0339	assembler2	-	EPSC2651	#222HaCHS	pPGK1		
pROP0340	assembler1	XI-2	EPSC3915		pTEF2	#223 C4H L5	#231 L5 ATR2
pROP0341	assembler2	-	EPSC2651		pTEF1	#221 PhCHI	
pROP0423	assembler1	XVI-20	EPSC2856	#162 AtPAL2	pTDH3-pTEF2	#223 C4H L5	#231 L5 ATR2
pROP0424	assembler3	XVI-20	EPSC2857		pPDC1	#100 At4CL2	
pROP0425	assembler1	XVI-20	EPSC2856	#162 AtPAL2	pTDH3		
pROP0465	single int.	X.4	pX-4		pTEF2	#304 HaCHS	
pROP0466	single int.	X.4	pX-4		pTEF2	#290 PcCHS	
pROP0467	single int.	X.4	pX-4		pTEF2	#291 PhCHS	
pROP0468	single int.	X.4	pX-4		pTEF2	#292 HvCHS1	
pROP0469	single int.	X.4	pX-4		pTEF2	#293 HvCHS2	
pROP0470	single int.	X.4	pX-4		pTEF2	#294 SbCHS	
pROP0496	assembler1	X.3	EPSC3913	#162 AtPAL2	pTDH3-pTEF2	#223 C4H L5	#231 L5 ATR2
pROP0497	assembler3	X.3	EPSC3914		pPDC1	#100 At4CL2	
pROP0498	assembler1	X.3	EPSC3913	#162 AtPAL2	pTDH3		
pROP0499	assembler1	X.3	EPSC3913	#162 AtPAL2	pTDH3-pTEF2	#317 At PAL1	
pROP0501	assembler2	-	EPSC2651	#222 HaCHS	pPGK1-pTEF1	#319 An PAL1	
pROP0502	assembler3	X.3	EPSC3914	#314 AtPAL2 (CO2)	pTPI1-pPDC1	#318 RtPAL	
pROP0528	assembler1	XI-5	EPSC3921	#162 AtPAL2	pTDH3-pTEF2	#223 C4H L5	#231 L5 ATR2
pROP0530	assembler2	-	EPSC2651	-	pTEF1	#327 HaCHS (CO1)	
pROP531	assembler1	XI-5	EPSC3921		pTEF2	#328 HaCHS (CO4)	
pROP532	assembler2	-	EPSC2651	#222 HaCHS	pPGK1-pTEF1	#327 HaCHS (CO1)	
pROP533	assembler3	XI-5	EPSC3922	#329HaCHS (CO5)	pTPI1-pPDC1	#330 HaCHS (CO6)	
pROP0534	assembler3	XI-5	EPSC3922	#329HaCHS (CO5)	pTPI1		
pROP0535	assembler3	XI-5	EPSC3922		pPDC1	#330 HaCHS (CO6)	
pROP0167	single int.	ARO3	EPSC3754		pTEF1	#148 ARO4 K229L	
pROP0263	single int.	ARO3	EPSC3754	#218_ARO7T226I	pPGK1-pTEF1	#148 ARO4 K229L	
pROP540	single int.	XII-5	pXII-5		pTEF1	#148 ARO4 K229L	
pROP0542	single int.	XII-5	pXII-5	#218_ARO7T226I	pPGK1-pTEF1	#148 ARO4 K229L	
pROP0768	multiple int.	Ty1C	EPSC23886	#329HaCHS (CO5)	pTDH3-pTEF2	#327 HaCHS (CO1)	

Appendix 1 table 5. Plasmids used for construction of strains with different PAL/TAL enzymes. Int. site means "insertion site" and p stands for "promoter". The relative orientation of genes (biobricks) is either forward (F) or reverse (R) as indicated.

Name	Type	Int. site	Backbone	Biobrick R	P	Biobrick F	Biobrick F
pROP0381	assembler1	X.2	EPSC3907	#269AtPAL1	pTDH3-pTEF2	#223 C4H L5	#231 L5 ATR2
pROP0383				#271RtPAL/TAL			
pROP0385				#273RcTAL			
pROP0386				#274RcTAL K			
pROP0387				#275SAM8			
pROP0388				#276PcPAL			
pROP0390				#278AnPAL			
pROP0391				#279PgramPAL/TAL			
pROP0392				#Asal HAL			
pROP0393				#281Rmet			
pROP0394				#282Sg TAL/TAM			
pROP0395				#283Rgram PAL			
pROP0396				#284BoPAL4			
pROP0397				#285Nflsh HAL/PAL			
pROP0399				#287Tcut PAL/TAL			
pROP0400				#288PhcPAL/TAL			
pROP0401				#289Rg PAL/TAL2			
pROP0770				#606RsTALnoCO			
pROP0771				#607FjTALnoCO			
pROP0772				#608FjTAL			
pROP0773				#609 HaTAL1noCO			
pROP0774				#610HaTAL1			
pROP0775				#611TcXALnoCO			
pROP0402				#269AtPAL1	pTDH3		
pROP0404				#271RtPAL/TAL			
pROP0406				#273RcTAL			
pROP0407				#274RcTAL K			
pROP0408				#275SAM8			
pROP0409				#276PcPAL			
pROP0411				#278AnPAL			
pROP0412				#279PgramPAL/TAL			
pROP0413				#Asal HAL			
pROP0414				#281Rmet			
pROP0415				#282Sg TAL/TAM			
pROP0416				#283Rgram PAL			
pROP0417				#284BoPAL4			
pROP0418				#285Nflsh HAL/PAL			
pROP0420				#287Tcut PAL/TAL			
pROP0421				#288PhcPAL/TAL			
pROP0422				#289Rg PAL/TAL2			
pROP0776				#606RsTALnoCO			
pROP0777				#607FjTALnoCO			
pROP0778				#608FjTAL			
pROP0779				#609HaTAL1noCO			
pROP0780				#610HaTAL1			
pROP0781				#611TcXALnoCO			

Appendix 1 table 6. Backbones of the plasmids (indicated in Appendix 1 table 4, 5 and appendix2 table 12). EPSC are plasmids constructed for this study, whereas the plasmids annotated differently are obtained from Mikkelsen et al. (2012).

Name	Backbone	Type	Int. site	Insert info
pU0002			-	Amp^r, ORI
pX-4	pYU-URA3-3	single integration	X-4	522bp X.4 Up, 451bp X.4 Down, tADH1, tCYC1, URA3
EPSC3907	pYU-URA3-3	assembler1	X.2	490bp X.2 Down, tFBA, tPGI, tCYC1, URA3
EPSC2651	pU0002	assembler2	-	tFBA, tPGI, tTDH2, tENO2
EPSC3908	pU0002	assembler3	X.2	531bp X.2 Up, tTDH2, tENO2
EPSC3915	pYU-URA3-3	assembler1	XI.2	563bp XI.2 Down, tFBA, tPGI, URA3
EPSC3916	pU0002	assembler3	XI.2	569bp XI.2 Up, tTDH2, tENO2
EPSC2856	pYU-URA3-3	assembler1	XVI.20	651bp XVI.20 Down, tFBA, tPGI, URA3
EPSC2857	pU0002	assembler3	XVI.20	690bp XVI.20 Up, tTDH2, tENO2
EPSC3913	pYU-URA3-3	assembler1	X.3	560bp X.2 Down, tFBA, tPGI
EPSC3914	pU0002	assembler3	X.3	564bp X.2 Up, tTDH2, tENO2
EPSC3921	pYU-URA3-3	assembler1	XI.5	521bp XI.5 Down, tFBA, tPGI, URA3
EPSC3922	pU0002	assembler3	XI.5	663bp XI.5 Up, tTDH2, tENO2
pXII-5	pYU-URA3-3	single integration	XII.5	500bp XII.5 Up, 500bp XII.5 Down, URA3
EPSC3754	pYU-URA3-3	single integration	*ARO3*	500bp *ARO3* Up, 500bp *ARO3* Down, URA3
EPSC3788	pYU-URA3-3	single integration	*ARO10*	500bp *ARO10* Up, 500bp *ARO10* Down, Amp^r.URA3
EPSC2901	pYU-URA3-3	single integration	*PAD1FDC1*	500bp *PAD1* Up, 500bp *FDC1* Down, Amp^r.URA3
EPSC23886	pYU-URA3-3	multiple integration	Ty1C	Ty1C Up, Ty1C Down, ura3d-60

Appendix 1 table 7. Genes, accession numbers and source organism.

Gene	Accession no	Organism
*At*PAL2	NP_190894	*Arabidopsis thaliana*
*At*C4H	NM_128601	*Arabidopsis thaliana*
*At*ATR2	NP_849472	*Arabidopsis thaliana*
*Ph*CHI	P11650	*Petunia hybrid*
*Ha*CHS	Q9FUB7	*Hypericum androsaemum*
*At*4CL2	NP_188761	*Arabidopsis thaliana*
*Ms*CHI	P28012.1	*Medicago sativa*
*At*PAL1	L33677.1	*Arabidopsis thaliana*
*An*PAL1	A2QIQ7	*Aspergillus niger*
*Rt*PAL	P11544	*Rhodosporidium toruloides*
PcCHS	P16107	*Petroselinum crispum*
PhCHS	P08894	*Petunia hybrid*
HvCHS1	*P26018*	*Hordeum vulgare*
HvCHS2	Q96562	*Hordeum vulgare*
SbCHS	Q9LRB2	*Scutellaria baicalensis*
AtPAL1	AY303128.1	*Arabidopsis thaliana*
RtPAL/TAL	P11544	*Rhodosporidium toruloides*
RcTAL	YP_003577239.1	*Rhodobacter capsulatus*
RcTAL K.	WP_013066811.1	*Rhodobacter capsulatus*
SAM8	WP_015103237.1	*SacchAROthrix espanaensis*
PcPAL	1W27_A	*Petroselinum crispum*
AnPAL	A2QIQ7	*Aspergillus niger*
Pgram PAL/TAL	XP_003330746	*Puccinia graminis*
Asal HAL	ABO89050	*Aeromonas salmonicida subsp. salmonicida A449*
Rmet TAL/TAM	Q1LRV9	*Ralstonia metallidurans*
Sg TAL/TAM	Q8GMG0	*Streptomyces globisporus*
Rgram PAL	ABC14780	*Rhodotorula graminis*
BoPAL4	GU592807	*Bambusa oldhamii*
Nflsh HAL/PAL	XP_001260409	*Neosartorya fischeri*
Tcut PAL/TAL	ABA69898	*Trichosporon cutaneum*
PhcPAL/TAL	ACW34079	*Phanerochaete chrysosporium*
Rg PAL/TAL2	AHB63479.1	*Rhodotorula glutinis*
RsTAL	WP_011842214.1	*Rhodobacter sphaeroides*
FjTAL	WP_012023194.1	*Flavobacterium johnsoniae*
HaTAL1	ABX04526.1	*Herpetosiphon aurantiacus*
TcXAL	AKE50834.1	*Trichosporon cutaneum*

Appendix 1 table 8. Genotype of strains produced in the present study, all based on S. cerevisiae S288C.

Strain	Genotype
EFSC4396	MATalpha, hoΔ , ura3::KanMX, pad1-fdc1::LoxP-NATMX-LoxP, ARO10Δ
GEN0	MATalpha, hoΔ , ura3::KanMX, pad1-fdc1::LoxP-NATMX-LoxP, ARO10Δ, X.2::DR/pTDH3-AtPAL2-tPGI1/TEF2-C4H L5 ATR2-tCYC1/pPGK1-HaCHS-tENO2/pTEF1-PhCHI-tFBA1/pPDC1-At4CL2-tADH2
GEN1	MATalpha, hoΔ , ura3::KanMX, pad1-fdc1::LoxP-NATMX-LoxP, ARO10Δ, X.2::DR/pTDH3-AtPAL2-tPGI1/TEF2-C4H L5 ATR2-tCYC1/pPGK1-HaCHS-tENO2/pTEF1-PhCHI-tFBA1/pPDC1-At4CL2-tADH2, XI.2::DR/pTDH3-AtPAL2-tPGI1/pPGK1-HaCHS-tENO2
GEN2	MATalpha, hoΔ , ura3::KanMX, pad1-fdc1::LoxP-NATMX-LoxP, ARO10Δ, X.2::DR/pTDH3-AtPAL2-tPGI1/TEF2-C4H L5 ATR2-tCYC1/pPGK1-HaCHS-tENO2/pTEF1-PhCHI-tFBA1/pPDC1-At4CL2-tADH2, XI.2::DR /pTDH3-AtPAL2-tPGI1/pPGK1-HaCHS-tENO2, XVI-20: DR/pTDH3-AtPAL2-tPGI1/TEF2-C4H L5 ATR2-tCYC1/pPGK1-HaCHS-tENO2
GEN3	MATalpha, hoΔ , ura3::KanMX, pad1-fdc1::LoxP-NATMX-LoxP, ARO10Δ, X.2::DR/pTDH3-AtPAL2-tPGI1/TEF2-C4H L5 ATR2-tCYC1/pPGK1-HaCHS-tENO2/pTEF1-PhCHI-tFBA1/pPDC1-At4CL2-tADH2, XI.2::DR /pTDH3-AtPAL2-tPGI1/pPGK1-HaCHS-tENO2, XVI-20: DR /pTDH3-AtPAL2-tPGI1/TEF2-C4H L5 ATR2-tCYC1/pPGK1-HaCHS-tENO2, X-4: DR /pTEF1-HaCHS-tADH1
GEN4	MATalpha, hoΔ , ura3::KanMX, pad1-fdc1::LoxP-NATMX-LoxP, ARO10Δ, X.2::DR/pTDH3-AtPAL2-tPGI1/TEF2-C4H L5 ATR2-tCYC1/pPGK1-HaCHS-tENO2/pTEF1-PhCHI-tFBA1/pPDC1-At4CL2-tADH2, XI.2::DR /pTDH3-AtPAL2-tPGI1/pPGK1-HaCHS-tENO2, XVI-20: DR /pTDH3-AtPAL2-tPGI1/TEF2-C4H L5 ATR2-tCYC1/pPGK1-HaCHS-tENO2, X-4: DR /pTEF1-HaCHS-tADH1, X.3::DR/pTDH3-AtPAL2-tPGI1/pTEF2-AtPAL1-tCYC1/ pPGK1-HaCHS-tENO2/pTEF1-AnPAL1-tFBA1/pTPI1 AtPAL2 (CO2)-tADH1/pPDC1-RtPALl -tTDH2
GEN5	MATalpha, hoΔ , ura3::KanMX, pad1-fdc1::LoxP-NATMX-LoxP, ARO10Δ, X.2::DR/pTDH3-AtPAL2-tPGI1/TEF2-C4H L5 ATR2-tCYC1/pPGK1-HaCHS-tENO2/pTEF1-PhCHI-tFBA1/pPDC1-At4CL2-tADH2, XI.2::DR /pTDH3-AtPAL2-tPGI1/pPGK1-HaCHS-tENO2, XVI-20: DR /pTDH3-AtPAL2-tPGI1/TEF2-C4H L5 ATR2-tCYC1/pPGK1-HaCHS-tENO2, X-4: DR /pTEF1-HaCHS-tADH1, , X.3::DR/pTDH3-AtPAL2-tPGI1/pTEF2-AtPAL1-tCYC1/ pPGK1-HaCHS-tENO2/pTEF1-AnPAL1-tFBA1/pTPI1 AtPAL2(CO2)-tADH1/pPDC1-RtPAL -tTDH2, XI-5::DR/ pTEF2-Ha CHS(CO4) -tCYC1/pPGK1-Ha CHS-tENO2/pTEF1-HaCHS(CO1) -tFBA1/pTPI1-HaCHS(CO5) -tADH1/pPDC1-HaCHS(CO6)-tTDH2
GEN6	MATalpha, hoΔ , ura3::KanMX, pad1-fdc1::LoxP-NATMX-LoxP, ARO10Δ, X.2::DR/pTDH3-AtPAL2-tPGI1/TEF2-C4H L5 ATR2-tCYC1/pPGK1-HaCHS-tENO2/pTEF1-PhCHI-tFBA1/pPDC1-At4CL2-tADH2, XI.2::DR /pTDH3-AtPAL2-tPGI1/pPGK1-HaCHS-tENO2, XVI-20: DR /pTDH3-AtPAL2-tPGI1/TEF2-C4H L5 ATR2-tCYC1/pPGK1-HaCHS-tENO2, X-4: DR /pTEF1-HaCHS-tADH1, X.3::DR/pTDH3-AtPAL2-tPGI1/pTEF2-AtPAL1-tCYC1/ pPGK1-HaCHS-tENO2/pTEF1-AnPAL1-tFBA1/pTPI1 AtPAL2(CO2)-tADH1/pPDC1-RtPAL -tTDH2, XI-5::DR/ pTEF2-Ha CHS(CO4) -tCYC1/pPGK1-Ha CHS-tENO2/pTEF1-HaCHS(CO1) -tFBA1/pTPI1-HaCHS(CO5) -tADH1/pPDC1-HaCHS(CO6)-tTDH2, XII.5::DR pTEF1-ARO4 K229L-tCYC1
GEN7	MATalpha, hoΔ , ura3::KanMX, pad1-fdc1::LoxP-NATMX-LoxP, ARO10Δ, X.2::DR/pTDH3-AtPAL2-tPGI1/TEF2-C4H L5 ATR2-tCYC1/pPGK1-HaCHS-tENO2/pTEF1-PhCHI-tFBA1/pPDC1-At4CL2-tADH2, XI.2::DR /pTDH3-AtPAL2-tPGI1/pPGK1-HaCHS-tENO2, XVI-20: DR /pTDH3-AtPAL2-tPGI1/TEF2-C4H L5 ATR2-tCYC1/pPGK1-HaCHS-tENO2, X-4: DR /pTEF1-HaCHS-tADH1, X.3::DR/pTDH3-AtPAL2-tPGI1/pTEF2-AtPAL1-tCYC1/ pPGK1-HaCHS-tENO2/pTEF1-AnPAL1-tFBA1/pTPI1 AtPAL2(CO2)-tADH1/pPDC1-RtPAL -tTDH2, XI-5::DR/ pTEF2-Ha CHS(CO4) -tCYC1/pPGK1-Ha CHS-tENO2/pTEF1-HaCHS(CO1) -tFBA1/pTPI1-HaCHS(CO5) -tADH1/pPDC1-HaCHS(CO6)-tTDH2, XII.5::DR pTEF1-ARO4 K229L-tCYC1, Ty1C::-pura3d 60-URA3-tURA3/pTEF2-HaCHS(CO1)--tCYC1/pTDH3-HaCHS(CO5)-tADH1

CHAPTER 2: Improving heterologous production of phenylpropanoids in *Saccharomyces cerevisiae* by tackling an unwanted side reaction of Tsc13, an endogenous double-bond reductase.

As mentioned several times in current thesis, the production of phenylpropanoids and their derivatives in yeast is known to be affected by a *p*-coumaroyl-CoA reductase, resulting in an the unwanted accumulation of phloretic acid. The following article combines classical functional screening of gene deletions with metabolic engineering approaches in order to find this reductase and to improve the usefulness of yeast as production platform for of phenylpropanoids and other cinnamic acid- and *p*-coumaric acid-derived products for industrial applications.

We identified an endogenous yeast enzyme, Tsc13, as the responsible for the reduction of *p*-coumaroyl-CoA and thus the formation of phloretic acid. This enzyme clearly seems to outcompetes CHS for their common substrate, *p*-coumaroyl-CoA, reducing the amount of carbon that is directed to product formation.

The aim of the work described in the article and the following chapter was to eliminate this source of carbon loss. Tsc13 is an essential enzyme involved in fatty acid synthesis and cannot simply be deleted. Instead, we evaluated two different approaches to solve this problem, of which one clearly offers a feasible working solution.

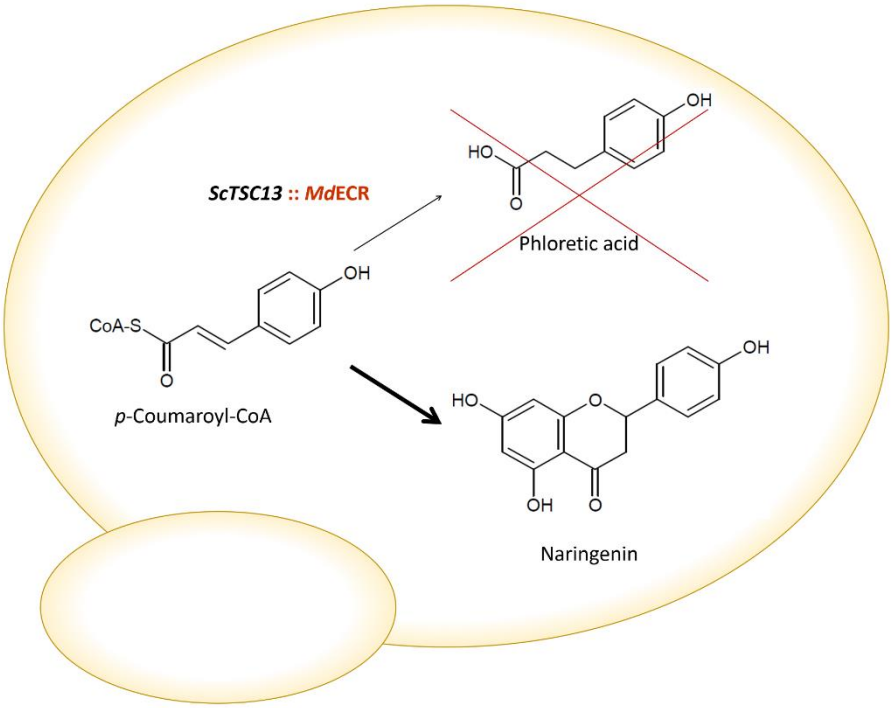

FEMS Yeast Research, 17, 2017, fox004

doi: 10.1093/femsyr/fox004
Advance Access Publication Date: 10 October 2016
Research Article

RESEARCH ARTICLE

Improving heterologous production of phenylpropanoids in *Saccharomyces cerevisiae* by tackling an unwanted side reaction of Tsc13, an endogenous double-bond reductase

Beata Joanna Lehka[1,2], Michael Eichenberger[3,4], Walden Emil Bjørn-Yoshimoto[5], Katherina Garcia Vanegas[1,6], Nicolaas Buijs[1], Niels Bjerg Jensen[1], Jane Dannow Dyekjær[1], Håvard Jenssen[2], Ernesto Simon[1,3] and Michael Naesby[3,*]

[1]Evolva Biotech A/S, Lersø Parkallé 42, DK-2100, Copenhagen Ø, Denmark, [2]Department of Science and Environment, Roskilde University, Universitetsvej 1, DK-4000, Roskilde, Denmark, [3]Evolva SA, Duggingerstrasse 23, CH-4153, Reinach, Switzerland, [4]Department of Biology, Technical University Darmstadt, Schnittspahnstrasse 10, DE-64287, Darmstadt, Germany, [5]Department of Drug Design and Pharmacology, University of Copenhagen, Jagtvej 162, DK-2100, Copenhagen Ø, Denmark and [6]Department of systems Biology, Technical University of Denmark, Kemitorvet Building 208, DK-2800, Kgs. Lyngby, Denmark

*Corresponding author: Evolva SA, Duggingerstrasse 23, CH-4153, Reinach, Switzerland. Tel: +41 61 485 20 16; E-mail: michaeln@evolva.com
One sentence summary: Replacement of essential yeast reductase with corresponding gene from apple allows more efficient production of flavonoids by eliminating formation of side products.
Editor: Pascale Daran-Lapujade

ABSTRACT

Phenylpropanoids, such as flavonoids and stilbenoids, are of great commercial interest, and their production in *Saccharomyces cerevisiae* is a very promising strategy. However, to achieve commercially viable production, each step of the process must be optimised. We looked at carbon loss, known to occur in the heterologous flavonoid pathway in yeast, and identified an endogenous enzyme, the enoyl reductase Tsc13, which turned out to be responsible for the accumulation of phloretic acid via reduction of *p*-coumaroyl-CoA. Tsc13 is an essential enzyme involved in fatty acid synthesis and cannot be deleted. Hence, two approaches were adopted in an attempt to reduce the side activity without disrupting the natural function: site saturation mutagenesis identified a number of amino acid changes which slightly increased flavonoid production but without reducing the formation of the side product. Conversely, the complementation of *TSC13* by a plant gene homologue essentially eliminated the unwanted side reaction, while retaining the productivity of phenylpropanoids in a simulated fed batch fermentation.

Keywords: *Saccharomyces cerevisiae*; flavonoids; phloretic acid; *TSC13*

Received: 7 October 2016; **Accepted:** 8 January 2017

INTRODUCTION

Phenylpropanoids and their flavonoid derivatives are natural constituents of the common human diet (Yao *et al.* 2004). They are also commercially interesting and frequently marketed and used as dietary supplements (Chun, Chung and Song 2007; Vidak, Rozman and Komel. 2015), food colourants (He and Giusti 2010), and preservatives (Balasundram, Sundram and Samman 2006). Flavonoids are present in most plants, including berries, fruits and vegetables used for human consumption. *In planta*, these compounds serve several functions such as signalling, pigmentation, UV and pathogen protection, as well as providing plants with structural integrity (Ferrer *et al.* 2008; Falcone Ferreyra, Rius and Casati 2012). In humans, numerous reports have linked them to health benefits due to various biological activities (recently reviewed by Yao *et al.* 2004; Tapas, Sakarkar and Kakde 2008; Lu, Xiao and Zhang 2013).

Current commercial production of flavonoids relies almost exclusively on extraction from plants, which makes the process dependent on stable supplies of good quality raw materials. Furthermore, a number of interesting flavonoids are found only in rare plants, which may be difficult to access, or occur only in minute concentrations or in mixtures with similar compounds, making their isolation and purification difficult (Hatano *et al.* 2000; Yu *et al.* 2016). As an alternative, organic synthesis is also challenging since in many cases a mix of stereoisomers is produced and, hence, toxic solvents may be needed during the catalysis or purification processes (Fowler and Koffas 2009). As a response to these obstacles, the use of microorganisms as cell factories for industrial production is gaining popularity, and as such the yeast *Saccharomyces cerevisiae* has already been used, not only for production of flavonoids but also for a wide spectrum of products including e.g. fuels, pharmaceuticals, food ingredients and other chemicals (Abbott *et al.* 2009; Keasling 2010; Hong and Nielsen 2012; Peralta-Yahya *et al.* 2012; Nielsen *et al.* 2013). Hence, the use of yeast for commercial production of flavonoids would seem to offer an excellent opportunity, being well suited for large-scale fermentation (Wang *et al.* 2011; Baerends *et al.* 2015; Katz *et al.* 2015; Trantas *et al.* 2015).

The flavonoid biosynthetic pathway in plants starts with the conversion of L-phenylalanine into *trans*-cinnamic acid through the non-oxidative deamination by phenylalanine ammonia lyase (PAL). Next, *trans*-cinnamic acid is hydroxylated at the para position to *p*-coumaric acid (4-hydroxycinnamic acid) by cinnamate-4-hydroxylase (C4H). C4H is a cytochrome P450 monooxygenase, needing regeneration by a cytochrome P450 reductase (CPR). Alternatively, the amino acid L-tyrosine can be converted into *p*-coumaric acid by tyrosine ammonia lyase (TAL). *P*-Coumaric acid is subsequently activated to *p*-coumaroyl-CoA by the 4-coumarate-CoA ligase (4CL). From here it branches out to give rise to flavonoids, stilbenoids, curcuminoids, lignins, etc. (Weisshaar and Jenkins 1998). In the case of most flavonoids, a chalcone synthase (CHS) and a chalcone isomerase (CHI) catalyse the condensation of *p*-coumaroyl-CoA with three molecules of malonyl-CoA, resulting in the formation of naringenin chalcone and finally naringenin (Fig. 1) (Weisshaar and Jenkins 1998; Ferrer *et al.* 2008). Naringenin represents a key branch point, from which a large array of different flavonoids are synthesised.

Several studies have reported the production of naringenin in *Escherichia coli* (Hwang *et al.* 2003; Leonard *et al.* 2007; Santos, Koffas and Stephanopoulos 2011; Wu *et al.* 2014). However, since cytochrome P450 monooxygenases and their cognate reductases are not well expressed in bacteria (Hotze, Schröder and Schröder 1995), a bacterial host may not be optimal depending on the desired end product. In yeast, Ro and Douglas (2004) were the first to reconstruct the entry point of the plant phenylpropanoid pathway, by co-expressing PAL, C4H and a CPR. Building on these results, the naringenin biosynthetic pathway has subsequently been efficiently expressed in yeast, showing production titres close to those obtained in *E. coli* (Jiang, Wood and Morgan 2005; Yan, Kohli and Koffas 2005; Trantas, Panopoulos and Ververidis 2009; Koopman *et al.* 2012), thus making *S. cerevisiae* a promising host for the production of phenylpropanoids and flavonoids. Another important consideration regarding the choice of production host is the ability to efficiently use cheap carbon sources, and the ability to funnel the carbon into the desired product. Thus, in addition to an optimised biosynthetic pathway, it is essential that the host metabolism can be adapted to the heterologous production during fermentation, and that undesired by-product formation, resulting in carbon loss, can be eliminated (Nevoigt 2008; Hong and Nielsen 2012). Previous reports using *S. cerevisiae* for expression of flavonoid pathways have described accumulation of such undesired by-products. In particular, several studies reported a significant accumulation of phloretic acid (dihydrocoumaric acid) (Beekwilder *et al.* 2006; Koopman *et al.* 2012; Luque *et al.* 2014; Vos *et al.* 2015) and in one case also phloretin (dihydrochalcone, DHC), a direct derivative of phloretic acid (Jiang, Wood and Morgan 2005). These authors speculated that phloretic acid is derived from *p*-coumaroyl-CoA in two steps: *p*-coumaroyl-CoA is first reduced to dihydro-coumaroyl-CoA by an unknown yeast reductase(s) and then dihydro-coumaroyl-CoA is hydrolysed, either spontaneously or by another unknown enzymatic reaction (Beekwilder *et al.* 2006; Koopman *et al.* 2012).

This hypothesis fits well with what is known from plants, in particular apples (*Malus domestica*), where phlorizin, the 2′-glucoside of phloretin, is the major phenolic compound. The biosynthetic pathways of these compounds have been studied in some detail. Formation of phloretin depends on CoA-activated phloretic acid which in turn is the result of a *p*-coumaroyl-CoA double-bond reduction. Gosch *et al.* (2009) determined that incubation of *p*-coumaroyl-CoA with NADPH and an enzyme preparation from young apple leaves resulted in the formation of dihydro-coumaroyl-CoA. They proposed that dihydro-coumaroyl-CoA is synthesised from *p*-coumaroyl-CoA by an unknown NADPH-dependent double-bond reductase (DBR) (Fig. 1). Based on similarities to the enoyl reduction steps in fatty acid biosynthesis, they suggested a side activity of a fatty acid dehydrogenase to be involved. Based on these previous studies, in both yeast and plants, we decided to screen the Yeast Knock Out (YKO) collection for NAD(P)H-dependent reductases, with the aim of identifying the enzymatic activity responsible for phloretic acid formation in yeast. We identified Tsc13 as the main contributor to this activity, and then tested two different approaches aimed at reducing or eliminating the loss of carbon in this side reaction of the flavonoid pathway.

MATERIALS AND METHODS

Chemicals

Trans-cinnamic acid (CAS nr.: 140-10-3), *p*-coumaric acid (CAS nr.: 501-98-4), phloretic acid (CAS nr.: 501-97-3), naringenin (CAS nr.: 67604-48-2) and dihydro-cinnamic acid (CAS nr.: 501-52-0) were obtained from Sigma Aldrich, Copenhagen, Denmark. Phloretin (CAS nr.: 60-82-2) was obtained from Extrasynthese, Genay Cedex, France.

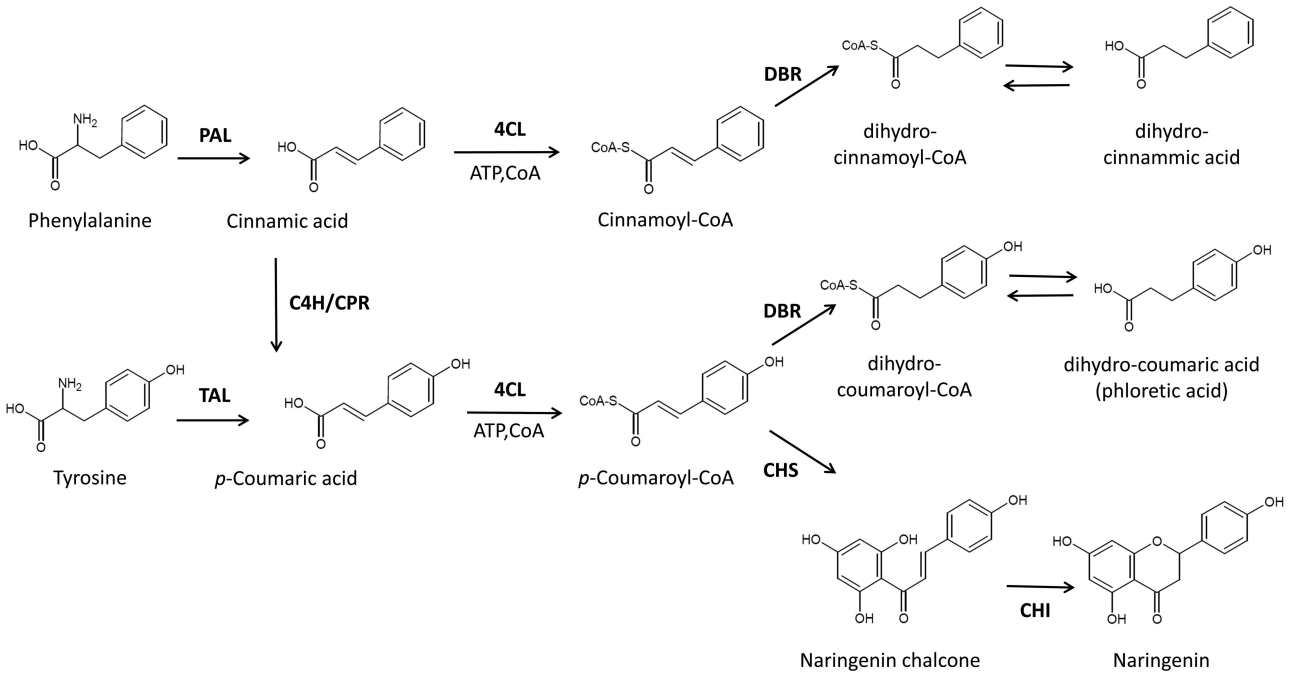

Figure 1. General phenylpropanoid pathway from phenylalanine to p-coumaroyl-CoA, where it branches out to flavonoids, stilbenoids, etc. The pathway to the key intermediate naringenin is shown. The DBR activity instead gives rise to DHCs. DBR, double-bound reductase; PAL, phenylalanine ammonia lyase; C4H, cinnamate-4-hydroxylase; CPR, cytochrome P450 reductase; TAL, tyrosine ammonia lyase; 4CL, 4-coumarate-CoA ligase; CHI, chalcone isomerase; CHS, chalcone synthase.

Yeast strains, transformation and cultivation

Strains constructed for the expression of flavonoids were derived from a *Saccharomyces cerevisiae* derivative of S288c (National Collection of Yeast Cultures, Norwich, UK, NCYC 3608). The YKO strains (Winzeler *et al.* 1999) were selected from the YKO collections YSC1056 and YSC1057 obtained from Open Biosystems, (Huntsville, Madison, Alabama, USA) now part of Dharmacon (GE Health), http://dharmacon.gelifesciences.com/non-mammalian-cdna-and-orf/yeast-knockout-collection.
From the YKO library, all NAD(P)H-dependent reductases and oxidoreductases with known substrate specificity were evaluated, and a total of 26 enzymes were selected based on structural similarity of their substrates to *p*-coumaroyl-CoA, e.g. the presence of enoyl double bonds. Most of the YKOs were homozygous diploids; however, for essential genes YKOs were obtained as heterozygous diploids (Table 1). Since an original wt is not provided with the YKO collection, the experiment was run without a genuine control strain, and strains were instead compared to each other based on relative production levels.

All yeast transformations were done using standard Li-acetate methods according to Gietz and Schiestl (2008). Transformed yeast cells were selected on synthetic complete (SC) medium lacking uracil (SC-Ura) (Illkirch Cedex, France, MP Biomedicals).

For each strain tested, six colonies were inoculated in 0.5 mL SC-Ura and incubated overnight at 30°C and 400 rpm in 96 well deep well plates (DWP). The following day, 50 μL of each culture was transferred into 0.5 mL of fresh SC medium or, for YKO library screening, into SC medium containing 5 μL of 100 mg mL^{-1} *p*-coumaric acid in 96% ethanol. The transformants were then incubated for 96 h at 30°C and 400 rpm in 96 well DWP.

To test the production of phenylpropanoids in strains where *TSC13* had been substituted by homologous genes, the cells were cultivated in synthetic feed-in-time (FIT) fed-batch medium (Baesweiler, Germany, m2p-labs) for 72 h at 30°C and 200 rpm in 24 well DWP. FIT medium was prepared according to the manufacturer's instructions and then supplemented with the supplied vitamin solution (final concentration 1% v/v), and the

Table 1. Selected NAD(P)H-dependent yeast oxidoreductases screened in this study (Winzeler *et al.* 1999).

Genotype	Systematic name
oye2/oye2	YHR179W
ylr460c/ylr460c	YLR460C
adh7/adh7	YCR105W
ydr541c/ydr541c	YDR541C
gre2/gre2	YOL151W
adh6/adh6	YMR318C
yml131w/yml131w	YML131W
ymr226c/ymr226c	YMR226C
oye3/oye3	YPL171C
ypl088w/ypl088w	YPL088W
aad4/aad4	YDL243C
aad6/aad6	YFL056C
dfg10/dfg10	YIL049W
zta1/zta1	YBR046C
ari1/ari1	YGL157W
aad3/aad3	YCR107W
frd1/frd1	YEL047C
shh3/shh3	YMR118C
osm1/osm1	YJR051W
lot6/lot6	YLR011W
ayr1/ayr1	YIL124W
yjr096w/yjr096w	YJR096W
ydl124w/ydl124w	YDL124W
TSC13/tsc13	YDL015C
SDH3/sdh3	YKL141W
ERG27/erg27	YLR100W

Table 2. Genes, accession numbers, EC numbers and source organism.

Gene	Accession no	EC number	Organism
*At*PAL2	NP_190894	4.3.1.24.	*Arabidopsis thaliana*
*At*C4H	NM_128601	1.14.13.11.	*Arabidopsis thaliana*
*At*ATR2	NP_849472	1.6.2.4.	*Arabidopsis thaliana*
*Ph*CHI	P11650	5.5.1.6.	*Petunia hybrida*
*Ha*CHS	Q9FUB7	2.3.1.74.	*Hypericum androsaemum*
*At*4Cl	NP_188761	6.2.1.12.	*Arabidopsis thaliana*
*Ms*CHI	P28012	5.5.1.6.	*Medicago sativa*
*At*ECR	NP_191096	1.3.1.93.	*Arabidopsis thaliana*
*Gh*ECR2	ABV60089	1.3.1.38.	*Gossypium hirsutum*
*Md*ECR	XP_008382818	1.3.1.93.	*Malus domestica*
*At*PAL1	L33677	4.3.1.24.	*Arabidopsis thaliana*
*An*PAL1	A2QIQ7	4.3.1.24.	*Aspergillus niger*
*Rt*PAL	P11544	4.3.1.25.	*Rhodosporidium toruloides*

enzyme mix (final concentration 0.8% v/v) prior to use. Control strain used was BLY2 with an empty pRS416-GPD plasmid (described in Mumberg, Mailer and Funk 1995).

To test the growth of strains, they were cultivated in SC medium (2% glucose) for 72 h at 30°C and 200 rpm in 24 DWP. To confirm the results from the FIT batch experiment, a strain with *Md*ECR and a control strain (BLY2 with pRS416-GPD) were cultivated in the synthetic fed-batch medium the (Baesweiler, Germany, m2p-labs) is already provided above for 72 h at 30°C and 180 rpm in 100 mL shake flasks (total volume 25 mL). For this experiment, FIT medium was prepared as described above but 0.4% v/v of the enzyme mix was added at three time points: immediately prior to use, at 22 h and at 46 h.

Plasmids and strains construction

Oligonucleotide primers used for cloning and verification of genomic integrations/deletions are listed in Tables S1–S3 (Supporting Information). All primers were synthesised by Integrated DNA Technologies, Leuven, Belgium. Constructed plasmids are listed in Tables S4–S6 (Supporting Information). Synthetic genes were codon optimised for *S. cerevisiae* and obtained from GeneArt (Naerum, Denmark, Thermo Fisher Scientific) (Table 2). Classic and USER cloning techniques (Nour-Eldin *et al.* 2006) were used. Cloning was performed using *E. coli* DH5α competent cells, and transformants were selected on Luria-Bertani (LB) agar plates containing 100 mg mL^{1} of ampicillin.

Strains used for the reductase screening

For the YKO reductase screening, a plasmid coding for an incomplete naringenin pathway (At4CL, MsCHI and HaCHS) was assembled *in vivo* in the YKO strains using homologous recombination tags, essentially as described by Kuijpers *et al.* (2013). The fragments for the plasmid assembly were obtained by AscI digestion of the plasmids indicated in Table S4 (Supporting Information).

For the construction of BLY2 and BLY3 (Table 3), and strains with partial flavonoid pathways, the plasmids (Table S5, Supporting Information) were constructed as integrative Easy Clone vectors according to Jensen *et al.* (2014). Integration of the flavonoid pathway was done by homologous recombination as described by Shao, Zhao and Zhao (2009). Basic backbones are described by Mikkelsen *et al.* (2012), who also describes the techniques used for plasmid construction. Three assembler plasmids were used for each integration, each having homology either to each other or to a specific region of the yeast genome. Each of these plasmids already has terminator sequences, and promoters and gene coding sequences were pre-cloned into these plasmids by USER cloning (Nour-Eldin *et al.* 2006). The KlURA3 marker on some of the integration vectors is flanked by direct repeats (DR). The KlURA3 marker was looped out after each transformation round, by recombination between the DRs and growing cells with 5-fluoroorotic acid (Lee and Da Silva 1997). Yeast genomic DNA was extracted according to Lõoke, Kristjuhan and Kristjuhan (2011), and genomic integration of all insertions/deletions was confirmed by PCR analysis.

Table 3. Strains used in the present study, all based on S. cerevisiae S288C.

BLY1	MATalpha, hoΔ0, ura3Δ0::KanMX, pad1-fdc1Δ0::LoxP-NatMX-LoxP, aro10::DR
BLY2	MATalpha, hoΔ0, ura3Δ0::KanMX, pad1-fdc1Δ0::LoxP-NatMX-LoxP, aro10::DR, X.2::DR pTDH3-AtPAL2-tPGI1/TEF2-C4H L5 ATR2-tCYC1/pPGK1-HaCHS-tENO2/pTEF1-PhCHI-tFBA1/pPDC1-At4Cl-tTDH2
BLY3	MATalpha, hoΔ0, ura3Δ0::KanMX, pad1-fdc1Δ0::LoxP-NatMX-LoxP, aro10::DR, X.2::DR/pTDH3-AtPAL2-tPGI1/TEF2-C4H L5 ATR2-tCYC1/pPGK1-HaCHS-tENO2/pTEF1-PhCHI-tFBA1/pPDC1-At4Cl-tTDH2, XI.2::DR pTDH3-AtPAL2-tPGI1/pPGK1-HaCHS-tENO2, XVI-20::DR pTDH3-AtPAL2-tPGI1/TEF2-C4H L5 ATR2-tCYC1/pPGK1-HaCHS-tENO2, X-4::DR pTEF1-HaCHS-tCYC1, X.3::DR/pTDH3-AtPAL2-tPGI1/pTEF2-AtPAL1-tCYC1/pPGK1-HaCHS-tENO2/pTEF1-AnPAL1-tFBA1/pTPI1 AtPAL2 CO2-tADH1/pPDC1-RtPal -tTDH2, XI-5::DR/pTEF2-Ha CHS_co4-tCYC1/pPGK1-Ha CHS-tENO2/pTEF1-HaCHS_co1-tFBA1/pTPI1-HaCHS_co5-tADH1/pPDC1-HaCHS_co6-tTDH2, XII.5::DR pTEF1-Aro4 K229L-tCYC1

The reductases Tsc13 and Dfg10 were overexpressed on the multicopy plasmid pRS426-GPD (described in Mumberg, Mailer and Funk 1995) in strain BLY3. Strain BLY3, accumulating *p*-coumaric acid, was obtained by increasing the copy number of PAL genes and by boosting the supply of endogenous aromatic amino acids via the introduction of Aro4 K229L as described by Mckenna *et al.* (2014). Control strain used was BLY3 with an empty pRS426-GPD plasmid.

Strain for testing the *TSC13* SSM library

Knockout of *TSC13* results in non-viable cells due to its essential role as described by Kohlwein *et al.* (2001). In order to test *tsc13* mutants, these were therefore introduced prior to deleting *TSC13*. The collection of *tsc13* mutants (site saturation mutagenesis (SSM) library), plus a wild-type (wt) control, was initially introduced episomally on the pRS416-GPD plasmid (Mumberg, Mailer and Funk (1995)), before deleting the native *TSC13*. The *TSC13* deletion cassette was constructed to contain the bleomycin resistance gene (*ble*), flanked by 500 bp regions both upstream and downstream of *TSC13* (cloned in pROP671). A naringenin producer strain comprising either the wt *TSC13* (control) or the SSM library plasmid mix was transformed with 300 ng of the *TSC13* deletion cassette.

Tsc13 homology modelling

The homology model of Tsc13 was built based on the structure of a *trans*-2-enoyl reductase from *Homo sapiens* (Protein Data Bank

ID 1YXM; Jansson *et al.* submitted). An initial sequence alignment was completed using EMBOSS Water Pairwise Sequence Alignment tool (Smith and Waterman 1981) using the standard alignment settings and the Pearson FASTA output. The homology model was constructed using the Homology Model tool in MOE (MOE 2013) using default settings, including the Protonate3D tool for placement of hydrogens and minimisation refinement of the final model with AMBER10:EHT force field. To mimic the natural cofactor NADP+, the crystal structure template 1YXM has an adenine molecule bound in the cofactor site. However, there is no substrate bound (apo state). Therefore, a hexanoyl-CoA substrate was modelled into the active site by superimposing the Tsc13 homology model on the active sites of 1YXM and 1W6U (Alphey *et al.* 2005) using PyMol [PyMol]. Based on the resulting model, residues predicted to be within 4.5 Å from the putative active site were selected for mutagenesis.

SSM library screening

A total of 25 amino acids were predicted to be in the region of the Tsc13 active site: Arg8, Lys30, Phe62, Phe89, Cys90, Glu91, Tyr92, Leu93, Leu97, Val98, His99, Ser100, Leu101, Phe102, Leu105, Tyr138, Glu144, Gln150, Phe151, Thr155, Tyr182, Tyr219, Cys220, His221 and Ile222. The total *TSC13* SSM library, produced by MAX randomisation (Nov 2012), was ordered from GeneArt (Thermo Fischer Scientific) and cloned into a pRS416-GPD plasmid. Approximately 30 000 primary transformants from the SSM library were collected and subjected to *TSC13* deletion. Approximately 10 000 colonies, selected for deletion of wt *TSC13*, were obtained of which 3786 were finally tested. This number was derived from a calculation including a couple of assumptions and based on the work of Nov (2012). Briefly, we aimed to have a theoretical chance of 99.99% of finding one of the two best (K = 2) amino acids for each position that was mutated. Using the MAX randomisation, in which all amino acids are equally represented, the number of clones to screen was calculated according to Nov (2012) as 88 clones for each of the 25 mutations (http://stat.haifa.ac.il/~yuval/toplib/). This number was further adjusted for an estimated knock-in efficiency of 70% (the ratio of clones with correct exchange of the *TSC13* wt gene with a mutant) and a ratio of 83% correct mutant genes obtained from gene synthesis (as reported by the supplier). Hence the number of clones to screen was calculated as 25*88/(0.70*0.83) = 3786.

All clones were analysed by HPLC for production of *p*-coumaric acid, phloretic acid and naringenin. Two controls with wt *TSC13* and two controls with only empty pRS416-GPD plasmids were included in each of the test units (96 well DWP). Mutants that displayed alterations in production patterns relative to the wt (average phloretic acid at least 20% lower or average naringenin at least 20% higher), were re-tested for production of phenylpropanoids, confirmed for *TSC13* deletion, and finally the plasmid harbouring the mutated *tsc13* was isolated and sequenced.

Introduction of *TSC13* plant homologues

The native open reading frame (ORF) of *TSC13* was replaced by gene homologues from *Arabidopsis thaliana* (*At*ECR), *Gossypium hirsutum* (*Gh*ECR2) and *Malus domestica* (*Md*ECR), according to the method described by Fairhead *et al.* (1996) using a split URA3 cassette. The homologues were under the control of the native *TSC13* promoter. The split URA3 cassettes were amplified by PCR using the primers listed in Table S3 (Supporting Information). The PCR fragments used to create the split URA3 cassettes were stitched together by the USER enzyme (Kildegaard *et al.* 2016), further ligated and finally PCR amplified. After transformation, correct insertion of the homologues was verified by PCR (using primers RES1056 TSC13 UP and RES1061 TSC13 DW) and further confirmed by sequencing of the PCR fragment.

Sample preparation and analytical methods

The optical density (OD) was measured at 600 nm in cuvettes using classical spectrophotometer or in MTP 96 microplates using an EnVision 2104 Plate Reader. For compound quantification, 100 μL from each culture was combined with 100 μL 96% ethanol, whirl mixed for 30 s at 1500 rpm and centrifuged for 10 min at 4000 × *g*. Supernatants were analysed by HPLC.

Phloretic acid, *p*-coumaric acid, cinnamic acid, dihydrocinnamic acid, naringenin and phloretin were measured at 225 nm using an Ultimate3000 HPLC with an Ultra C18 3μm Column (100 × 4.6 mm) operating at 40°C, coupled to a diode array detector. Solvent A was water and solvent B was acetonitrile, both containing 50 ppm trifluoroacetic acid. The flow rate was 1 mL/min with acetonitrile increasing from 20% at 0 min to 60% in 9 min.

RESULTS

Confirming the phenylpropanoid substrate of the endogenous reductase

The aim of this study was to identify the reductase responsible for the formation of phloretic acid in *Saccharomyces cerevisiae* and to obtain a strain capable of producing naringenin without accumulating phloretic acid. Hence, we first wanted to confirm *p*-coumaroyl-CoA as the intermediate being converted into phloretic acid. We constructed a small collection of yeast strains which expressed various enzymes of the phenylpropanoid pathway. We observed phloretic acid formation in a strain expressing *At*PAL, *At*C4H, *At*CPR and *At*4CL, but not in strains expressing either *At*PAL alone or *At*PAL together with *At*C4H and *At*CPR (Fig. S1, Supporting Information). This indicated that *p*-coumaroyl-CoA, and not *p*-coumaric acid, is the actual substrate of the unknown yeast endogenous reductase, in agreement with what was suggested by Beekwilder *et al.* (2006) and Koopman *et al.* (2012). In a strain expressing only *At*PAL and *At*4CL, we observed formation of dihydro-cinnamic acid, in addition to the presumed precursor cinnamic acid. In contrast, a strain expressing only *At*PAL produced only cinnamic acid. This demonstrated that also cinnamoyl-CoA is a substrate for the endogenous reductase (Fig. S1).

Screening for an endogenous *p*-coumaroyl-CoA DBR

To narrow in on the endogenous activity responsible for phloretic acid formation, we looked at publicly available information about yeast enzymes. We assumed that the enzyme would be an NAD(P)H-dependent reductase, based on previous *in vitro* results with plant extracts (Gosch *et al.* 2009), and we then further looked for enzymes of which the reported substrate showed some structural similarity to *p*-coumaroyl-CoA. From previous work in our labs, we also knew that overexpression of *FAS1/FAS2* does not change the level of phloretic acid in strains expressing *At*PAL and *At*4CL, so we excluded these enzymes. Hence, based on the above criteria, a collection of 26 genes were selected and the corresponding strains from the YKO collection were transformed with a plasmid carrying 4-coumarate-CoA ligase (*At*4CL) and cultivated for 96 h in medium supplemented

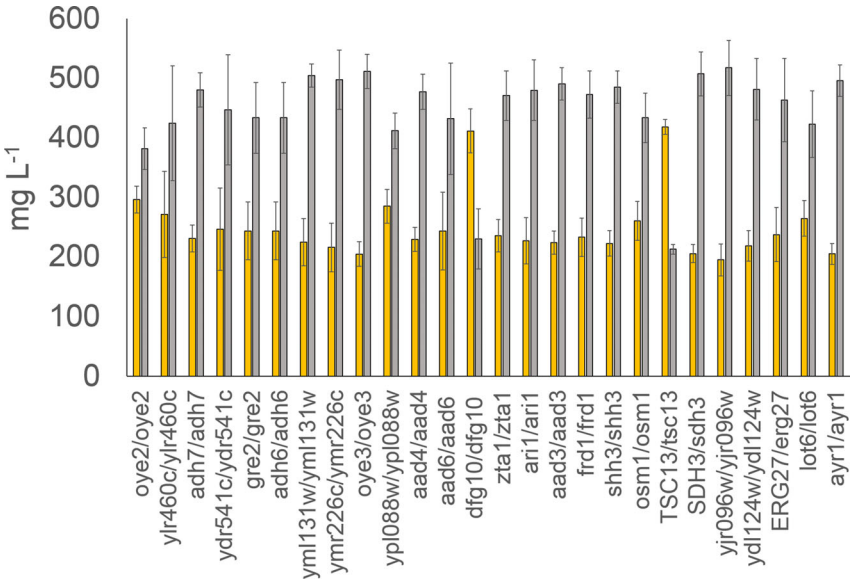

Figure 2. Concentrations of p-coumaric acid remaining (orange) and phloretic acid produced (gray) by different YKO strains after 96 h of growth in SC media containing p-coumaric acid. Most knockouts were homozygous diploids with only TSC13/tsc13, SDH3/sdh3 and ERG27/erg27 tested as heterozygous diploids. Error bars represent standard deviation (n = 6).

with *p*-coumaric acid. We assumed that any loss of endogenous reductase activity on the *p*-coumaroyl-CoA would lead to lower production of phloretic acid. Therefore, instead of measuring *p*-coumaroyl-CoA product formation, which requires special analytical setup, we analysed the samples for consumption of *p*-coumaric acid and for production of phloretic acid. Out of the 26 strains tested, two YKO strains, *TSC13/tsc13* and *dfg10/dfg10*, both consumed less *p*-coumaric acid and produced less phloretic acid (Fig. 2).

Overexpression of TSC13 and DFG10 in a naringenin-producing strain

As a next step, we overexpressed *TSC13* or *DFG10* in a yeast strain which accumulates *p*-coumaroyl-CoA as an intermediate of the naringenin pathway. This strain, BLY3, had been engineered to improve the endogenous supply of aromatic amino acids, which had inadvertently resulted in an unbalanced naringenin pathway and, thus, in the accumulation of pathway intermediates. In this strain, *TSC13* or *DFG10* was overexpressed on a multicopy 2μ plasmid and analysed for any increase in the production of phloretic acid. The strain overexpressing *DFG10* showed no change in the level of phloretic acid, *p*-coumaric acid or naringenin. In contrast, the strong overexpression of *TSC13* resulted in a clear increase in the level of phloretic acid and the appearance of the derivative phloretin. Interestingly, this was mirrored by a sharp decrease in the naringenin concentration (Fig. 3). This was somewhat surprising since the level of *p*-coumaric acid, a direct precursor of naringenin chalcone/naringenin, remained unchanged. However, the observed compound levels might be explained by 4CL and/or CHS being rate limiting in the current strain. Thus, a constant level of *p*-coumaric acid may simply reflect a limitation in 4CL activity, with both Tsc13 and CHS being active only on the CoA activated compound. With these two enzymes competing for *p*-coumaroyl-CoA, the overexpression of Tsc13 would therefore leave less substrate for naringenin production. The increased pool of CoA activated dihydro-coumaric acid (phloretic acid) either dissociates to give rise to the observed

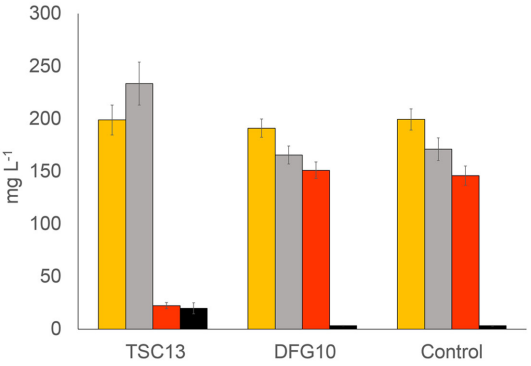

Figure 3. Phenylpropanoid production profile (p-coumaric acid (orange), phloretic acid (grey) naringenin (red) and phloretin (black)) in BLY3, overexpressing TSC13 or DFG10 on multicopy plasmid pRS426-GPD. Control strain is BLY3 with pRS426-GPD empty plasmid. Error bars represent standard deviation (n = 6).

increase in phloretic acid or is used by CHS to produce phloretin. With CHS being limiting that would further decrease the production of naringenin. In any case, the results clearly showed that Tsc13 is the main enzyme responsible for reduction of *p*-coumaroyl-CoA while Dfg10 plays only a minor role.

Modelling the active site of Tsc13 for SSM screening

TSC13 is an essential gene, but we speculated whether it would be possible to engineer the corresponding enzyme, and thereby eliminate the non-specific activity on *p*-coumaroyl-CoA while maintaining its native activity. While a six-membrane-spanning topology, embedded in the ER membrane, has been proposed for yeast Tsc13 (Paul, Gable and Dunn 2007), there is, to our knowledge, no crystal structure or three-dimensional homology model of the enzyme available. Hence, we decided to create such a homology model in order to predict the active site of Tsc13. As Tsc13 contains a C-terminal 3-oxo-5α-steroid 4-dehydrogenase domain, the crystal structure of a similar protein, the 1YXM *trans*-2-enoyl CoA reductase, was selected as a

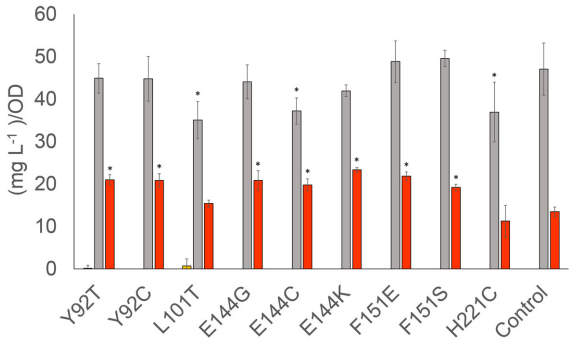

Figure 4. Phenylpropanoid production profile (p-coumaric acid (orange), phloretic acid (grey), naringenin (red)) in the naringenin-producing strain, where native TSC13 was replaced by different tsc13 mutants. Control strain is BLY2 with pRS416-GPD empty plasmid. Error bars represent standard deviation (n = 5). For statistical analysis, one-way ANOVA was used and the threshold of significance for the p value was 0.05. For all values significantly different than the control the bar are marked with asterisk.

basis for the model. For validation, the resulting Tsc13 homology model was submitted to the DALI server (http://ekhidna.biocenter.helsinki.fi/dali_server, Holm and Rosenström, Nucleic Acids Research, 2010, W545-W549) to search for known proteins with similar structures. The top 12 hits included chains A-D from 1YXM, but also 4FC6 and 4FC7 which have known *trans*-2-enoyl CoA reductase activity.

Based on the model, 25 residues predicted to be within 4.5 Å from the putative active site were selected for mutagenesis: Arg8*, Lys30*, Phe62*, Phe89, Cys90*, Glu91, Tyr92, Leu93, Leu97, Val98, His99, Ser100, Leu101, Phe102, Leu105, Tyr138*, Glu144, Gln150, Phe151*, Thr155*, Tyr182*, Tyr219, Cys220*, His221* and Ile222. Residues marked with an asterisk are predicted to be involved in binding of both the substrate and the co-factor NAD(P)H. These residues were then subjected to SSM and the library of mutants was cloned into a single copy yeast expression vector. The mutant library was introduced into the naringenin-producing strain, BLY2, before mass deletion of the native *TSC13* gene.

To ensure a reasonable coverage of the SSM library, a total of 3786 clones were analysed for growth and metabolite production. This resulted in 18 clones which were confirmed both in terms of their altered phenylpropanoid production profile and for deletion of wt *TSC13*. Each specific *tsc13* mutation was identified by sequencing. This narrowed down the number of specific mutations to nine different substitutions, involving five different positions. The level of phloretic acid was slightly lowered in case of L101 T, E 144C and H221C, whereas the level of naringenin was elevated in all mutants except L101 T and H221C (Fig. 4). We speculate that this increase might in fact be due to a reduced activity of the *tsc13* mutants on *p*-coumaroyl-CoA, thus leaving more substrate available for naringenin formation.

Complementation of Tsc13 by plant homologues

An alternative way to circumvent unwanted phloretic acid formation would be the substitution of Tsc13 with an enzyme which is able to complement its normal function, but does not show activity on *p*-coumaroyl-CoA. Complementation of a non-functional Tsc13 with plant homologues from *Arabidospis thaliana* (AtECR) and *Gossypium hirsutum* (*Gh*ECR2) has been described previously (Gable *et al.* 2004; Paul, Gable and Dunn 2007; Song *et al.* 2009). In addition, a collection of *TSC13* gene homologues from plants which were overexpressed in yeast did not exhibit any noticeable effect on phloretin production, suggesting a lack of DBR activity on *p*-coumaroyl-CoA (Eichenberger *et al.* 2017). Based on these complementation and overexpression studies, we selected three homologues—*A. thaliana* AtECR, *G. hirsutum* *Gh*ECR2 and *Malus domestica* *Md*ECR—in order to evaluate their ability to complement *TSC13* in yeast, without interfering with the heterologous naringenin pathway. DNA sequences encoding each of the three homologues were inserted in place of the *TSC13* ORF into the yeast genome by homologous recombination, thus placing these homologues under the control of the native regulatory sequences. The production of phloretic acid, *p*-coumaric acid and naringenin was evaluated in small-scale (DWP), fed-batch fermentation and, in addition, the growth of these strains was tested during batch growth on glucose.

Replacement of *TSC13* with any of the three plant homologues AtECR, *Gh*ECR2 and *Md*ECR resulted in viable cells, demonstrating the ability to, at least partially, complement the loss of Tsc13 cellular function. However, the growth in batch fermentation was clearly affected, and final OD600 after 72 h was substantially lower, reaching approximately 48%–55% compared to the wt control for the *Gh*ECR2 and *Md*ECR, and just a bit more than 11% for the AtECR. The reduced biomass formation appeared to depend on whether glucose or ethanol was used as carbon source (Fig. S2, Supporting Information). Both GhECR and MdECR resulted in only slightly reduced growth rates on glucose (0.316 and 0.321 h^{-1}, respectively, compared to 0.383 for the wt) whereas after the diauxic shift, the growth on ethanol was seriously impaired. In contrast, the AtECR strain grew poorly on both substrates (growth rate on glucose 0.096 h^{-1}), and the formation of crystals could be observed in the medium (Fig. S3, Supporting Information). We did not investigate further the nature and composition of these crystals. The observed growth patterns are likely a result of suboptimal production, in the complemented strains, of the very long chain fatty acids (VLCFAs) which are important for structure and function of membranes (Tehlivets, Scheuringer and Kohlwein 2007). In the study of Song *et al.* (2009), the production of C26 fatty acids was shown to be reduced in a yeast strain complemented by the GhECR2, associated with a slight reduction in growth rate. A key point, demonstrated here by the batch fermentation results, was the poor complementation during growth on ethanol.

In order to evaluate phloretic acid formation, the complemented strains were regrown in DWP and, with the aim of preventing formation and growth on ethanol, using a simulated fed batch protocol based on the FIT enzymatic glucose release. Strains were grown for 72 h and finally cultures were analysed for production of flavonoid intermediates. In this fed batch setup, the final ODs of the complemented strains, as compared to the wt control, reached a relatively higher level than what was seen for the batch cultures (Fig. S4, Supporting Information). More interestingly, no phloretic acid was detected in the three strains complemented with plants homologues, whereas the control strain (BLY2) accumulated large amounts of this by-product (Fig. 5). Instead, the complemented strains accumulated *p*-coumaric acid, part of which was further metabolised to naringenin. Accumulation of *p*-coumaric acid, as opposed to naringenin, was expected due to the limited CHS activity in the background BLY2 strain. In addition, the supply of malonyl-CoA might have been negatively affected by an impaired synthesis of VLCFAs, for example, via the resulting accumulation of palmitoyl-CoA. This has previously been suggested to cause feedback inhibition of malonyl-CoA formation (Tehlivets, Scheuringer and Kohlwein 2007), which would then

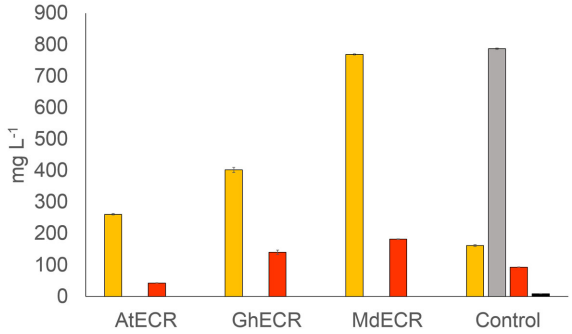

Figure 5. Production of flavonoid pathway intermediates (p-coumaric acid (orange), phloretic acid (gray), naringenin (red) and phloretin (black)) in BLY2 where TSC13 was replaced by homologous genes from three different organisms: A. thaliana, AtECR; G. hirsutum, GhECR2; and M. domestica, MdECR. Control strain is BLY2 with pRS416-GPD empty plasmid. Error bars represent standard deviation (n = 3).

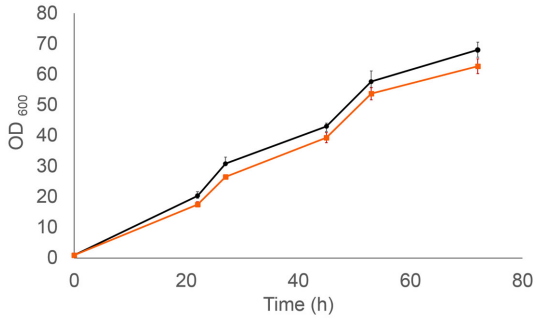

Figure 7. Growth of control strain BLY2 (black line with square marks) and the strain where *TSC13* was replaced by the homologous gene *Md*ECR from *M. domestica* (orange line with circle marks). The experiment was designed as described in Figure 6. Error bars represent standard deviation (n = 3).

further reduce the production of naringenin. However, regarding the final level of *p*-coumaric acid and the observed differences between the three complemented strains, it is difficult to point to a single obvious explanation. Since it is only partially correlated to final OD, the reason(s) for this variation is unclear, but could be a result of various stress reactions of the cell.

As the most promising candidate, the MdECR strain was grown in 100 mL shake flask culture, in which the glucose release rate was further reduced, aiming to reach a final OD close to the wt control. This resulted in the gradual accumulation of *p*-coumaric acid and naringenin during 72 h (Fig. 6) in the *Md*ECR-expressing strain, while growth was only marginally effected, as compared to the control (Fig. 7). In contrast to the wt control, which accumulated large amounts of phloretic acid, no by-product formation was seen in the MdECR strain, similar to our observation in the DWP experiment. Obviously, the rate of converting *p*-coumaric acid to naringenin is still limiting and far from optimal in this strain background. Nonetheless, the results demonstrate the feasibility of using plant homologues for complementing the Tsc13 in a controlled fermentation with slow glucose release, thereby eliminating the unwanted side activity of the native enzyme. The optimal growth rate for a commercial production would of course need to be determined for a strain with a fully optimised flavonoid pathway.

DISCUSSION

Production of small biochemical molecules by fermentation, using genetically engineered host strains such as yeasts and bacteria, has emerged as one of the most promising trends in the recent quest for sustainable production methods. A major factor for achieving a commercially viable and successful fermentation process is the stable supply of cheap and renewable raw materials. An equally important factor is the efficient use of the raw material, which in terms of fermentation means a highly optimised production strain as well as a downstream process for recovery of the product. In the current work, we focused on optimising a yeast host strain for production of phenylpropanoid-derived compounds, with the specific goal of eliminating one of the major side products, phloretic acid, associated with this production.

Metabolic side reactions, such as the reduction of *p*-coumaroyl-CoA, drain carbon from the compound of interest. Hence, this enzymatic activity interferes with the industrial production of relevant flavonoids and stilbenoids. That *p*-coumaroyl-CoA is in fact the target for reduction had previously been suggested (Beekwilder *et al.* 2006; Koopman *et al.* 2012), and we confirmed this by showing that phloretic acid formation depends on the expression of 4CL, the CoA ligase.

An initial screen of host reductases identified the enzymes Tsc13 and Dfg10 as possible candidates, involved in the phloretic acid formation. *TSC13* encodes an essential enzyme annotated

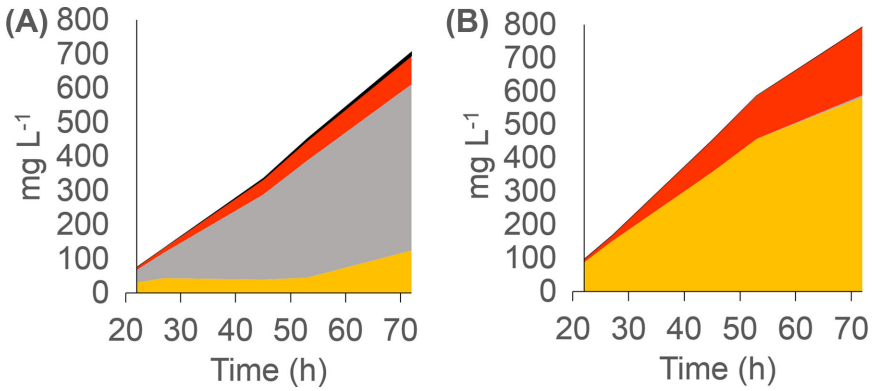

Figure 6. Production of flavonoid pathway intermediates (*p*-coumaric acid (orange), phloretic acid (gray), naringenin (red) and phloretin (black)) in BLY2 (**A**) and in the strain where *TSC13* was replaced by the homologous gene *Md*ECR from *M. domestica* (**B**). The experiment was performed in shake flasks containing FIT media. Control strain is BLY2 with pRS416-GPD empty plasmid. Standard deviation varied between 1.4% and 8% of the total value for each point (n = 3).

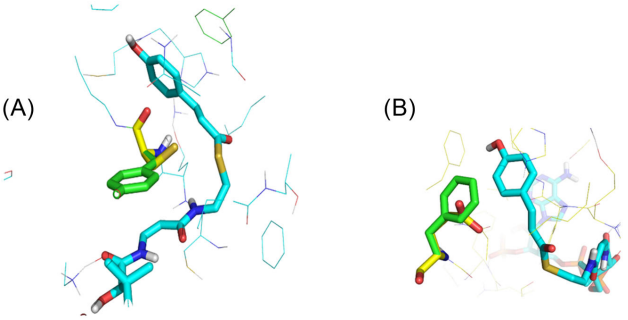

Figure 8. Overlay model of the T92C mutation, affecting the interaction of *p*-coumaroyl-CoA (cyan) with tyrosine (green) or cysteine (yellow) (**A**). Overlay model of the P151G mutation, affecting the interaction of *p*-coumaroyl-CoA (cyan) with phenylalanine (green) or glutamine (yellow) (**B**).

as a *trans*-2-enoyl-CoA reductase. It catalyses the reduction of *trans*-2,3-enoyl-CoA intermediates in the elongation cycle of VLCFAs (Kohlwein *et al.* 2001; Paul, Gable and Dunn 2007; Wakashima, Abe and Kihara 2014). *DFG10* encodes a putative polyprenol reductase (Mösch and Fink 1997). In a naringenin-producing strain, overexpression of Tsc13, but not Dfg10, lead to increased phloretic acid production, and a concomitant decrease in naringenin, which strongly suggested that Tsc13 is the main enzyme responsible for the *p*-coumaroyl-CoA reductase activity in yeast, and we therefore decided to focus on this enzyme in an attempt to reduce by-product formation.

As a first approach, we used SSM (Chronopoulou and Labrou, 2011) to engineer the native Tsc13 by mutagenesis. Based on *in silico* modelling of the putative catalytic site, 25 amino acids were mutated. Unfortunately, the SSM library did not turn up any mutations which abolished phloretic acid production. This may be a natural consequence of the fact that *TSC13* is an essential gene, and that major changes to the active site would be potentially lethal. Thus, mutations conferring smaller changes with less impact were selected by this approach.

Most interesting was the increase of naringenin production in several strains, while levels of phloretic and *p*-coumaric acids showed only minor changes. As shown in Fig. 8A, the aromatic ring of wt Y92 interacts with the carbonylic double bonds of CoA, stabilising the *p*-coumaroyl-CoA conformation in the active site, and this interaction is lost by mutation to C92 or T92. Also, in our model, wt F151 interacts with the conjugated electron system of *p*-coumaroyl-CoA, including the double bond to be reduced. Mutation of this residue to E151 or S151 would disrupt this stabilising interaction (Fig. 8B). These mutations may therefore reduce the affinity for *p*-coumaroyl-CoA, which in turn would make more substrate available for CHS, leading to the observed increase in naringenin. Regarding E144, it is not clear how mutations at this residue would affect the structural environment of the active site. Interestingly, all three residues are conserved between Tsc13 and the three plant homologues (Fig. S5, Supporting Information). We suspect that they are all essential for function at the active site, but that certain substitutions, which do not disrupt the native function in fatty acid synthesis, are tolerated. This corresponds well with the findings of Paul, Gable and Dunn (2007), who mutated several conserved residues to alanine, without Tsc13 loss of function.

We believe the approach of using SSM to improve enzyme activity is viable, but in our case a better model or the crystal structure of the active site would be needed. Alternatively, a random mutagenesis approach could be combined with a more efficient screening assay. However, in the current study, we chose to not continue this line of work.

As an alternative to mutagenesis, we tested the feasibility of replacing the *TSC13* gene with a plant homologue. One rationale for this approach was the fact that many plants are not known to produce DHCs despite having a continuous supply of *p*-coumaroyl-CoA. Thus, in these plants the enzymes involved in fatty acid synthesis may be less promiscuous. Alternatively, apples and other plant species known to produce DHCs might have specific enzymes dedicated to the reduction of *p*-coumaroyl-CoA, with other enoyl-reductases specific for fatty acid synthesis. This would of course not, *a priori*, exclude the possibility that the specificity for phenylpropanoids may have evolved from an enoyl-reductase of the fatty acid synthesis system. In the current study, we were interested in reductases that would not reduce *p*-coumaroyl-CoA while still being able to complement the natural activity of Tsc13 in the synthesis of VLCFAs. We therefore focused on reductases with functional similarity to Tsc13 (categorised as an EC 1.3.1.93), and selected three plant homologues from *Arabidopsis thaliana*, *Gossypium hirsutum* and *Malus domestica*.

Complementation of Tsc13 has been demonstrated previously by two of those enzymes: Gable *et al.* (2004) reported that the *At*ECR homologue from *A. thaliana* (NP_191096) was able to complement a temperature-sensitive yeast Tsc13 mutant, and that it interacts with yeast Elo2 or Elo3, members of the VLCFA synthase complex. Paul, Gable and Dunn (2007) determined that *At*ECR has a membrane topology similar to Tsc13. We were able to confirm the ability of *At*ECR to complement Tsc13, although it did not seem to fully reconstitute function, as indicated by a decrease in specific growth rate in batch fermentation. Chemical analysis of a yeast strain expressing this homologue showed no phloretic acid production.

Another study has demonstrated complementation of Tsc13 in yeast by two homologues from cotton: *Gh*ECR1 (ABV60088) and *Gh*ECR2 (ABV60089) (Song *et al.* 2009). This study showed that *Gh*ECR1/2 were both present in the ER fraction, indicating a cellular localisation similar to Tsc13. Both enzymes complemented the Tsc13 KO strain when expressed on plasmids, but whereas *GhECR1* impaired growth substantially, *Gh*ECR2 did not affect growth to any larger extent. In the current study, we confirmed the ability of *Gh*ECR2 to complement Tsc13, although with more pronounced growth inhibition in batch fermentation than what was reported earlier (Song *et al.* 2009). Also with this homologue we detected no production of phloretic acid.

Finally, the apple enzyme *Md*ECR (XP_008382818) was tested in the current study. This enzyme was selected based on homology to *At*ECR and *Gh*ECR2 described above. Furthermore, it had very high similarity to the ENRL-1, which was previously found not to be involved in the production of DHCs (Dare *et al.* 2013). In the current study, the strain expressing the *Md*ECR homologue showed the best performance in terms of naringenin and *p*-coumaric acid production, and produced no phloretic acid. Growth of the complemented strain was somewhat inhibited when grown in batch cultivation. However, cultivating this strain in a fed-batch fermentation clearly improved the growth, most of all by preventing growth on ethanol.

In summary, all three plant homologues completely abolished phloretic acid formation, albeit with different abilities to complement native Tsc13. The growth inhibition we observed is likely linked to the synthesis of VLCFAs. In yeast, a large fraction of VLCFAs is used for the biosynthesis of sphingolipids and phosphatidylinositol, important components of the cell membrane, and disruption of Tsc13 is known to result in accumulation of fatty acids shorter than 26 carbons (Kohlwein *et al.* 2001). Hence, incomplete complementation would lead to a deficiency in these long fatty acids. In a study on cotton ECRs (Song

et al. 2009), the strain complemented with *Gh*ECR2 showed a reduced level of VLCFAs compared to the wt strain, supporting the notion that this could be the reason for the growth inhibition. Preliminary results from our labs, where we overexpressed *Md*ECR from a multicopy plasmid, indicated that further overexpression alone may not help. However, this could be due to the fact that Tsc13 normally functions as part of a larger complex, and that other components would also have to be overexpressed, or that interaction between these components, when including a non-native enzyme, is not optimal. Alternatively, the growth rate of a production strain might be adjusted to match the turnover rate of the heterologous reductase, e.g. by an appropriate fermentation process, which restores the balance of VLCFA synthesis and the overall fatty acid profile. The results from our shake flask fermentation (Fig. 7) appear to support this idea.

CONCLUSION

The native yeast Tsc13 VLCFA enoyl-reductase was identified as the main enzyme responsible for reducing heterologously produced *p*-coumaroyl-CoA. This side activity resulted in phloretic acid accumulation and thereby, serious carbon loss in the flavonoid biosynthetic pathway expressed in yeast.

Two different approaches to reduce this carbon loss were examined: mutation of native Tsc13 and replacement with a plant homologue. In the first approach, we obtained small improvements in the production of naringenin but were not able to eliminate the production of phloretic acid. In the second approach, we demonstrated that complementation of Tsc13 by plant homologues can completely eliminate the side product formation.

The possible effects of this Tsc13 complementation on the VLCFA synthesis machinery and the ensuing consequences of altering the composition of fatty acid derived were not investigated in this study, but would be an interesting subject for further studies. Here we achieved at least partial restoration of VLCFA acid synthesis, since loss of C26 fatty acids is lethal to yeast, and consequently we were able to do a fed-batch cultivation in which the complemented strain exhibited growth rates comparable to the wt Tsc13 strain. Obviously, for a final production strain, the optimal feed rate, and thus the maximum achievable growth rate, would have to be determined with an optimised heterologous pathway. The goal would be to avoid growth on ethanol, as is common in most fed-batch protocols, but also to prevent any accumulation of fatty acid intermediates that could disrupt the membrane structure and homeostasis, as well as preventing feedback inhibition of precursors like malonyl-CoA needed for flavonoid biosynthesis.

In short, we believe that, in particular, the latter approach is a viable route toward reducing carbon loss to undesired phloretic acid and, hence, for further optimisation of phenylpropanoid production in yeast. In combination with an otherwise balanced biosynthetic pathway, this should allow construction of flavonoid-producing cell factories with no side product formation and, consequently, a more efficient and economic industrial process.

SUPPLEMENTARY DATA

Supplementary data are available at FEMSYR online.

ACKNOWLEDGEMENTS

The authors wish to thank Carlos Casado Vázquez and Richard J. S. Baerends for helpful discussions, Jørgen Hansen for reviewing this manuscript and Nicholas Milne for improving the language. Plasmids in Supplementary Table S5 and S6 were based on vectors kindly provided by Esben H. Hansen.

FUNDING

The research of ME and MN is partially financed by the European Union Seventh Framework Programme under Grant agreements no. 613745, Promys and no. 613793, Bachberry.

Conflict of interest. Håvard Jenssen declares no competing interest. All other authors were supported by, or are directly employed by Evolva.

REFERENCES

Abbott DA, Zelle RM, Pronk JT *et al*. Metabolic engineering of Saccharomyces cerevisiae for production of carboxylic acids: current status and challenges. *FEMS Yeast Res* 2009;**9**:1123–36.

Alphey MS, Yu W, Byres E *et al*. Structure and reactivity of human mitochondrial 2,4-dienoyl-CoA reductase. *J Biol Chem* 2005;**280**:3068–77.

Baerends RJS, Simon E, Meyer JP *et al*. *A Method For Producing Modified Resveratrol*. 2015. WO 2015028324 A2. http://www.google.com/patents/WO2015028324A2?cl=tr (11 January 2016, date last accessed).

Balasundram N, Sundram K, Samman S. Phenolic compounds in plants and agri-industrial by-products: antioxidant activity, occurrence, and potential uses. *Food Chem* 2006;**99**:191–203.

Beekwilder J, Wolswinkel R, Jonker H *et al*. Production of resveratrol in recombinant microorganisms. *Appl Environ Microb* 2006;**72**:5670–2.

Chronopoulou EG, Labrou NE. Site-saturation mutagenesis: a powerful tool for structure-based design of combinatorial mutation libraries. *Curr Protoc Protein Sci* 2011.

Chun OK, Chung SJ, Song WO. Estimated dietary flavonoid intake and major food sources of U.S. adults. *J Nutr* 2007;**137**:1244–52.

Dare AP, Tomes S, Cooney JM *et al*. The role of enoyl reductase genes in phloridzin biosynthesis in apple. *Plant Physiol Biochem* 2013;**72**:54–61.

Eichenberger M, Lehka B, Folly C *et al*. Metabolic engineering of *Saccharomyces cerevisiae* for de novo production of dihydrochalcones with known antioxidant, antidiabetic, and sweet tasting properties. *Metabolic Engineering* 2017;**39**:80–9.

Fairhead C, Llorente B, Denis F *et al*. New vectors for combinatorial deletions in yeast chromosomes and for gap-repair cloning using "split-marker" recombination. *Yeast* 1996;**12**:1439–57.

Falcone Ferreyra ML, Rius SP, Casati P. Flavonoids: biosynthesis, biological functions, and biotechnological applications. *Front Plant Sci* 2012;**3**:1–15.

Ferrer JL, Austin MB, Stewart C *et al*. Structure and function of enzymes involved in the biosynthesis of phenylpropanoids. *Plant Physiol Biochem* 2008;**46**:356–70.

Fowler ZL, Koffas MAG. Biosynthesis and biotechnological production of flavanones: Current state and perspectives. *Appl Microbiol Biot* 2009;**83**:799–808.

Gable K, Garton S, Napier JA *et al*. Functional characterization of the Arabidopsis thaliana orthologue of Tsc13p, the enoyl reductase of the yeast microsomal fatty acid elongating system. *J Exp Bot* 2004;**55**:543–5.

Gietz RD, Schiestl RH. High-efficiency yeast transformation using the LiAc/SS carrier DNA/PEG method. *Nat Protoc* 2008;**2**:31–4.

Gosch C, Halbwirth H, Kuhn J *et al*. Biosynthesis of phloridzin in apple (Malus domestica Borkh.). *Plant Sci* 2009;**176**:223–31.

Hatano T, Aga Y, Shintani Y *et al*. Minor flavonoids from licorice. *Phytochemistry*. 2000;**55**:9–13.

He J, Giusti MM. Anthocyanins: natural colorants with health-promoting properties. *Annu Rev Food Sci Technol* 2010;**1**:163–87.

Hong KK, Nielsen J. Metabolic engineering of Saccharomyces cerevisiae: a key cell factory platform for future biorefineries. *Cell Mol Life Sci* 2012;**69**:2671–90.

Hotze M, Schröder G, Schröder J. Cinnamate 4-hydroxylse from Catharanthus roseus, and a strategy for the functional expression of plant cytochrome P450 proteins as translational fusion with P450 reductase in Escherichia coli. *FEBS Lett* 1995;**374**:345–50.

Hwang E, Il, Kaneko M, Ohnishi Y *et al*. Production of plant-specific flavanones by Escherichia coli containing an artificial gene cluster. *Appl Environ Microb* 2003;**69**:2699–706.

Jansson A, Ng S, Arrowsmith C *et al*. Crystal structure of perixomal trans 2-enoyl CoA reductase (PECRA), Submitted (MAY-2005) to the PDB data bank.

Jensen NB, Strucko T, Kildegaard KR *et al*. EasyClone: method for iterative chromosomal integration of multiple genes in Saccharomyces cerevisiae. *FEMS Yeast Res* 2014;**14**:238–48.

Jiang H, Wood KV, Morgan JA. Metabolic engineering of the phenylpropanoid pathway in Saccharomyces cerevisiae metabolic engineering of the phenylpropanoid pathway in Saccharomyces cerevisiae. *Appl Environ Microb* 2005;**71**:2962–9.

Katz M, Smits HP, Förster J *et al*. *Metabolically Engineered Cells for the Production of Resveratrol or an Oligomeric or Glycosidically-Bound Derivative Thereof*. 2015. US 9040269 B2. http://www.google.com/patents/US9040269 (11 January 2017, date last accessed).

Keasling JD. Manufacturing molecules through metabolic engineering. *Science (80-)* 2010;**330**:1355–8.

Kildegaard KR, Jensen NB, Schneider K *et al*. Engineering and systems-level analysis of Saccharomyces cerevisiae for production of 3-hydroxypropionic acid via malonyl-CoA reductase-dependent pathway. *Microb Cell Fact* 2016;**15**:13.

Kohlwein SD, Eder S, Oh CS *et al*. Tsc13p is required for fatty acid elongation and localizes to a novel structure at the nuclear-vacuolar interface in *Saccharomyces cerevisiae*. *Mol Cell Biol* 2001;**21**:109–25.

Koopman F, Beekwilder J, Crimi B *et al*. De novo production of the flavonoid naringenin in engineered Saccharomyces cerevisiae. *Microb Cell Fact* 2012;**11**:155.

Kuijpers NG, Solis-Escalante D, Bosman L *et al*. A versatile, efficient strategy for assembly of multi-fragment expression vectors in *Saccharomyces cerevisiae* using 60 bp synthetic recombination sequences. *Microb Cell Fact* 2013;**12**:47.

Lee FW, Da Silva NA. Sequential delta-integration for the regulated insertion of cloned genes in Saccharomyces cerevisiae. *Biotechnol Prog* 1997;**13**:368–73.

Leonard E, Lim KH, Saw PN *et al*. Engineering central metabolic pathways for high-level flavonoid production in Escherichia coli. *Appl Environ Microb* 2007;**73**:3877–86.

Lõoke M, Kristjuhan K, Kristjuhan A. Extraction of genomic DNA from yeasts for pcr- based applications. *Biotechniques* 2011;**50**:325–8.

Lu MF, Xiao ZT, Zhang HY. Where do health benefits of flavonoids come from? Insights from flavonoid targets and their evolutionary history. *Biochem Bioph Res Co* 2013;**434**:701–4.

Luque A, Sebai SC, Santiago-Schübel B *et al*. In vivo evolution of metabolic pathways by homeologous recombination in mitotic cells. *Metab Eng* 2014;**23**:123–35.

Mckenna R, Thompson B, Pugh S *et al*. Rational and combinatorial approaches to engineering styrene production by Saccharomyces cerevisiae. *Microb Cell Fact* 2014;**13**:123.

Mikkelsen MD, Buron LD, Salomonsen B *et al*. Microbial production of indolylglucosinolate through engineering of a multigene pathway in a versatile yeast expression platform. *Metab Eng* 2012;**14**:104–11.

Molecular Operating Environment (MOE). Chemical Computing Group Inc., 1010 Sherbooke St. West, Suite #910, Montreal, QC, Canada, H3A 2R7, 2013. 08, 2016.

Mösch HU, Fink GR. Dissection of filamentous growth by transposon mutagenesis in Saccharomyces cerevisiae. *Genetics* 1997;**145**:671–84.

Mumberg D, Mailer R, Funk M. Yeast vectors for the controlled expression of heterologous proteins in different genetic backgrounds. 1995;**156**:119–22.

Nevoigt E. Progress in metabolic engineering of Saccharomyces cerevisiae. *Microbiol Mol Biol R* 2008;**72**:379–412.

Nielsen J, Larsson C, van Maris A *et al*. Metabolic engineering of yeast for production of fuels and chemicals. *Curr Opin Biotechnol* 2013;**24**:398–404.

Nour-Eldin HH, Hansen BG, Nørholm MHH *et al*. Advancing uracil-excision based cloning towards an ideal technique for cloning PCR fragments. *Nucleic Acids Res* 2006;**34**:e122.

Nov Y. When second best is good enough: Another probabilistic look at saturation mutagenesis. *Appl Environ Microb* 2012;**78**:258–62.

Paul S, Gable K, Dunn TM. A six-membrane-spanning topology for yeast and Arabidopsis Tsc13p, the enoyl reductases of the microsomal fatty acid elongating system. *J Biol Chem* 2007;**282**:19237–46.

Peralta-Yahya PP, Zhang F, del Cardayre SB *et al*. Microbial engineering for the production of advanced biofuels. *Nature* 2012;**488**:320–8.

Ro D, Douglas CJ. Reconstitution of the entry point of plant phenylpropanoid metabolism in yeast (Saccharomyces cerevisiae): implications for control of metabolic flux into the phenylpropanoid pathway. *J Biol Chem* 2004;**279**:2600–7.

Santos CNS, Koffas M, Stephanopoulos G. Optimization of a heterologous pathway for the production of flavonoids from glucose. *Metab Eng* 2011;**13**:392–400.

Shao Z, Zhao H, Zhao H. DNA assembler, an in vivo genetic method for rapid construction of biochemical pathways. *Nucleic Acids Res* 2009;**37**:1–10.

Smith TF, Waterman MS. Identification of common molecular subsequences. *J Mol Biol* 1981;**147**:195–7.

Song WQ, Qin YM, Saito M *et al*. Characterization of two cotton cDNAs encoding trans-2-enoyl-CoA reductase reveals a putative novel NADPH-binding motif. *J Exp Bot* 2009;**60**:1839–48.

Tapas A, Sakarkar D, Kakde R. Flavonoids as nutraceuticals: a review. *Trop J Pharm Res* 2008;**7**:1089–99.

Tehlivets O, Scheuringer K, Kohlwein SD. Fatty acid synthesis and elongation in yeast. *Biochim Biophys Acta* 2007;**1771**:255–70.

Trantas EA, Koffas MA, Xu P *et al*. When plants produce not enough or at all: metabolic engineering of flavonoids in microbial hosts. *Front Plant Sci* 2015;**6**:1–16.

Trantas E, Panopoulos N, Ververidis F. Metabolic engineering of the complete pathway leading to heterologous biosynthesis of various flavonoids and stilbenoids in Saccharomyces cerevisiae. *Metab Eng* 2009;**11**:355–66.

Vidak M, Rozman D, Komel R. Effects of flavonoids from food and dietary supplements on glial and glioblastoma multiforme cells. *Molecules* 2015;**20**:19406–32.

Vos T, de la Torre Cortés P, van Gulik WM *et al*. Growth-rate dependency of de novo resveratrol production in chemostat cultures of an engineered Saccharomyces cerevisiae strain. *Microb Cell Fact* 2015;**14**:133.

Wakashima T, Abe K, Kihara A. Dual functions of the trans -2-enoyl-CoA reductase TER in the sphingosine 1-phosphate metabolic pathway and in fatty acid elongation. *J Biol Chem* 2014;**289**:24736–48.

Wang Y, Halls C, Zhang J *et al*. Stepwise increase of resveratrol biosynthesis in yeast Saccharomyces cerevisiae by metabolic engineering. *Metab Eng* 2011;**13**:455–63.

Weisshaar B, Jenkins G. Phenylpropanoid biosynthesis and its regulation. *Curr Opin Plant Biol* 1998;**1**:251–7.

Winzeler EA, Shoemaker DD, Astromoff A *et al*. Functional characterization of the S. cerevisiae genome by gene deletion and parallel analysis. *Science* 1999;**285**:901–6.

Wu J, Yu O, Du G *et al*. Fine-tuning of the fatty acid pathway by synthetic antisense RNA for enhanced (2S)-naringenin production from L-tyrosine in Escherichia coli. *Appl Environ Microb* 2014;**80**:7283–92.

Yan Y, Kohli A, Koffas MAG. Biosynthesis of natural flavanones in Saccharomyces cerevisiae. *Appl Environ Microb* 2005;**71**:5610–3.

Yao LH, Jiang YM, Shi J *et al*. Flavonoids in food and their health benefits. *Plant Foods Hum Nutr* 2004;**59**:113–22.

Yu JS, Moon E, Choi SU *et al*. Asarotonide, a new phenylpropanoid with a rare natural acetonide group from the rhizomes of Acorus gramineus. *Tetrahedron Lett* 2016;**57**:1699–701.

Supplementary Material

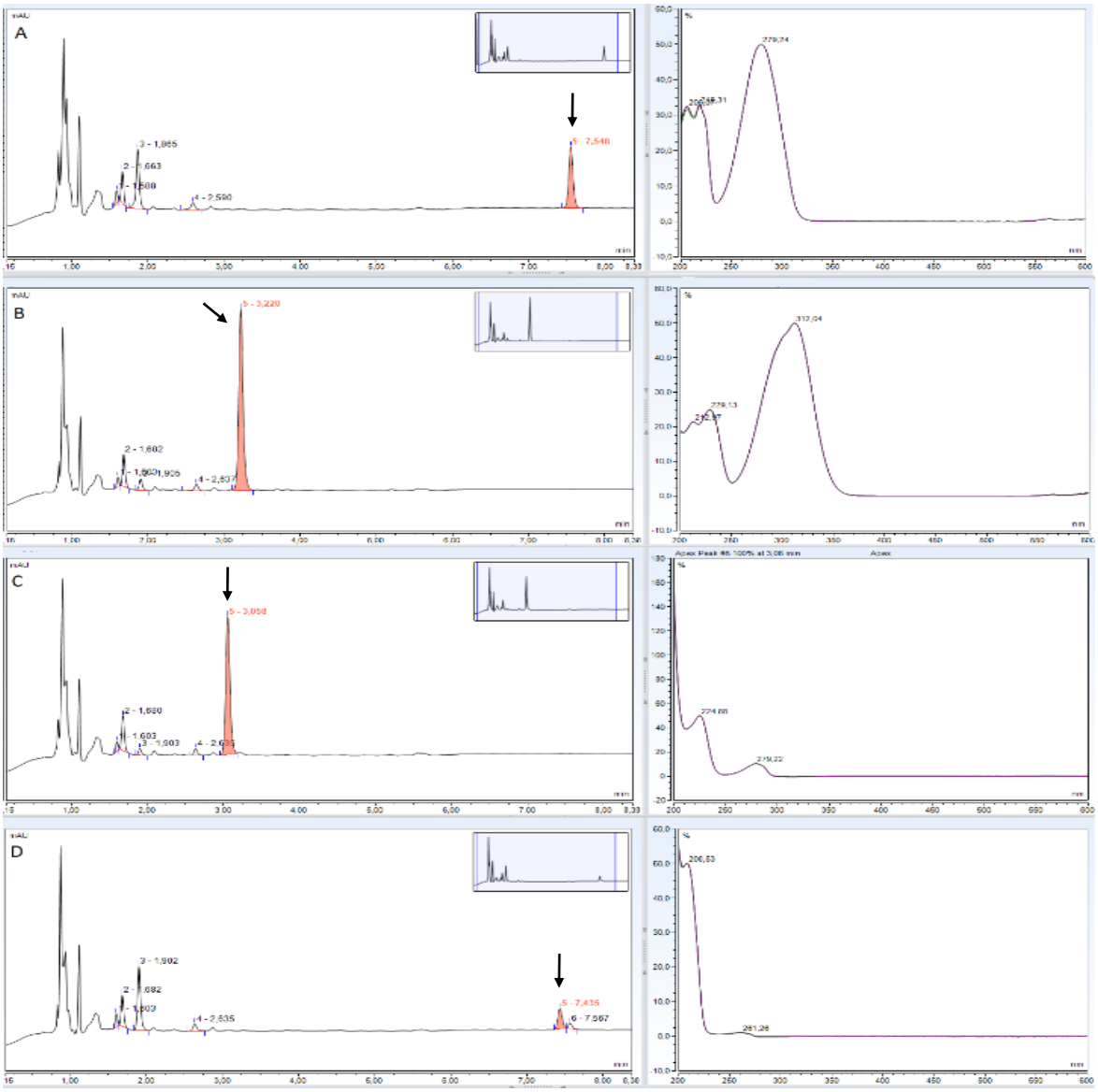

Supplementary Figure 1. Chromatograms (left) and UV absorption profiles of the indicated peaks (right) of the strains with: (A) PAL alone, resulting in production of cinnamic acid, (B) PAL together with C4H and CPR, resulting in production of p-coumaric acid, (C) PAL together with C4H, CPR, and 4CL, resulting in production of phloretic acid, and (D) PAL together with 4CL, resulting in production of dihydrocinnamic acid.

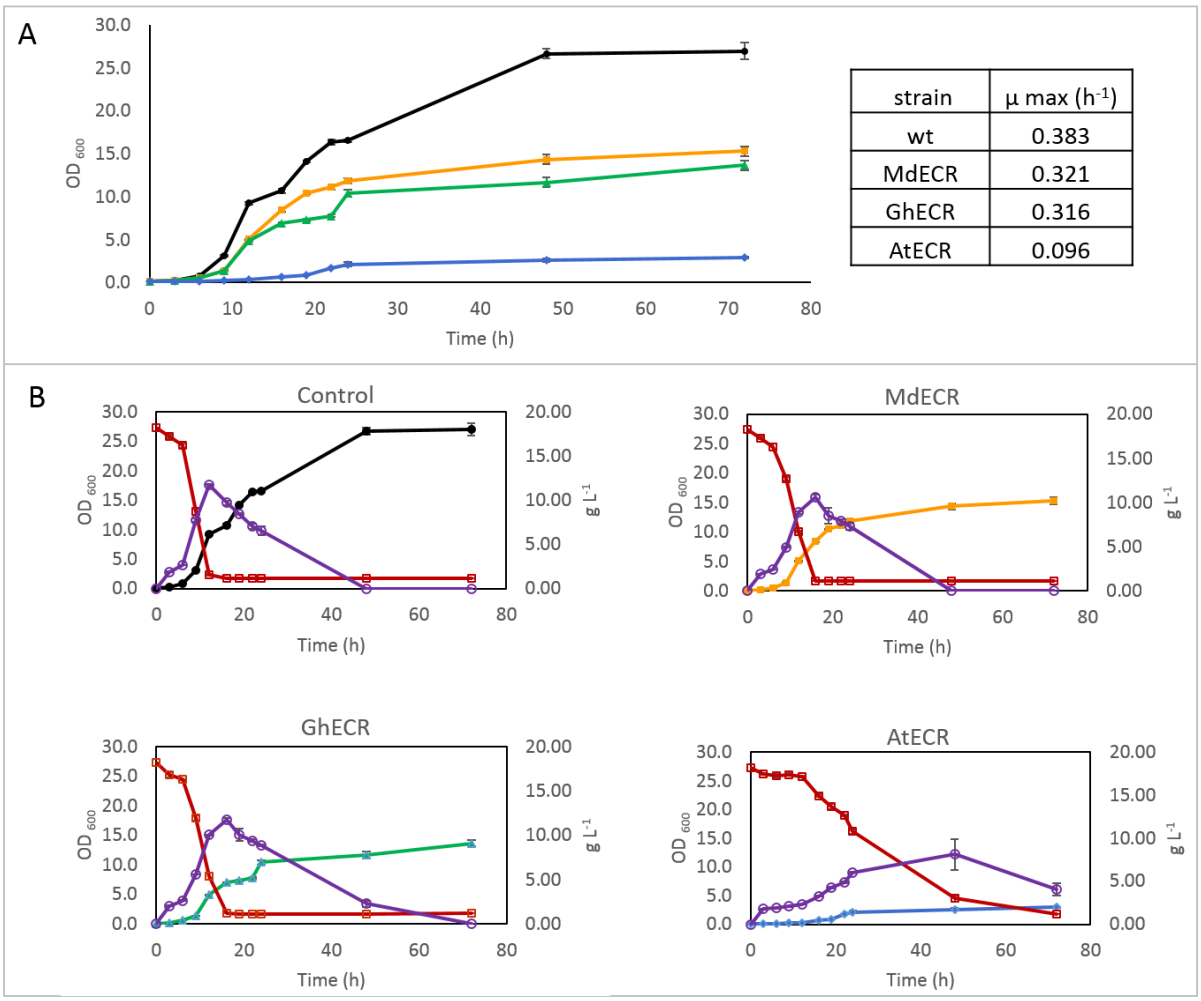

strain	μ max (h^{-1})
wt	0.383
MdECR	0.321
GhECR	0.316
AtECR	0.096

Supplementary Figure 2. Batch fermentation of strains complemented with TSC13 homologues. Growth of strains compared to (A), and growth of individual strains in relation to measured concentrations of glucose and ethanol (B). Table inserted in panel A shows maximum growth rates (μmax h^{-1}) calculated according to Jakubowska and Korona (2012) and based on time points up to 12h. The control strain was BLY2 with a pRS416-GPD empty plasmid (black line with square marks). The homologues of the other strains were MdECR (orange line with circle marks), GhECR (green line with triangle marks), and AtECR (blue line with rhombus marks), respectively. In panel B the level of glucose (dark red line with hollow square marks) and ethanol (purple line with hollow circle marks) is shown. Error bars represent standard deviation (n=3).

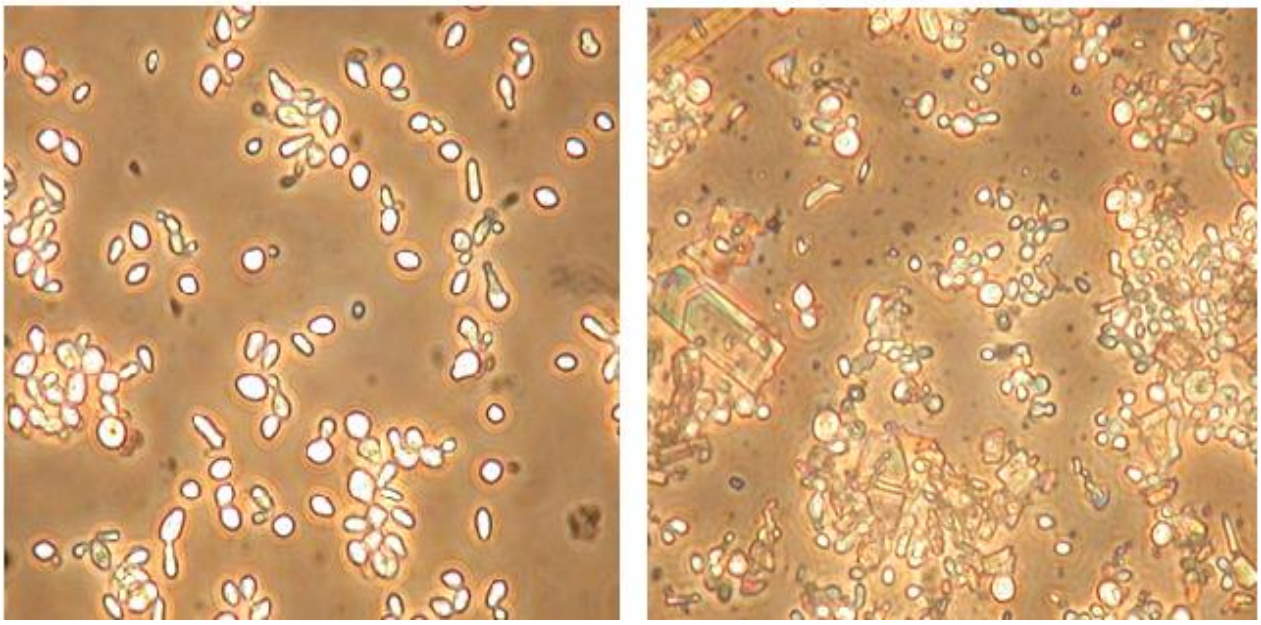

Supplementary Figure 3. Morphology of the yeast cells grown for 72h. Control on the left (BLY2 with pRS416-GPD empty plasmid, and BLY2 strain complemented with AtECR on the right. The growth of this strain resulted in formation of visible crystals in the broth medium. Images were taken at x400 magnification, using a Nikon camera with ELWD condenser: N.A. 0.3 (O.D. 75mm) coupled to an Eclipse TS100 microscope.

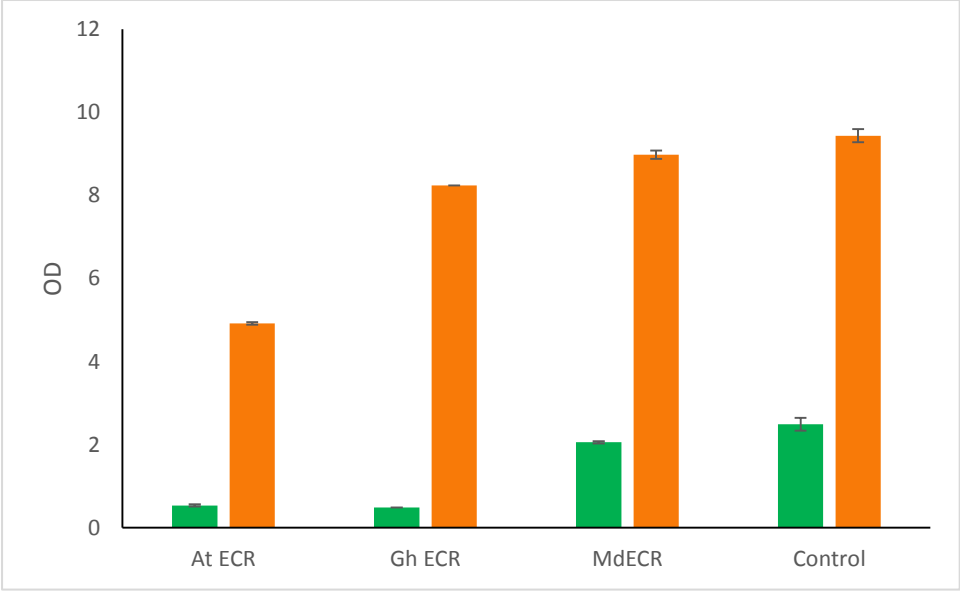

Supplementary Figure 4. The final biomass reached after 24h (green) and 72h (orange) when strains were cultivated under simulated fed batch conditions. The TSC13 in strain BLY2 was replaced by homologous genes from three different plants: A. thaliana, AtECR; G. hirsutum, GhECR2; and M. domestica, MdECR; Control strain is BLY2 with a pRS416-GPD empty plasmid. Error bars represent standard deviation (n=3). The OD was measured in MTP 96 microplates and should be taken as a relative OD.

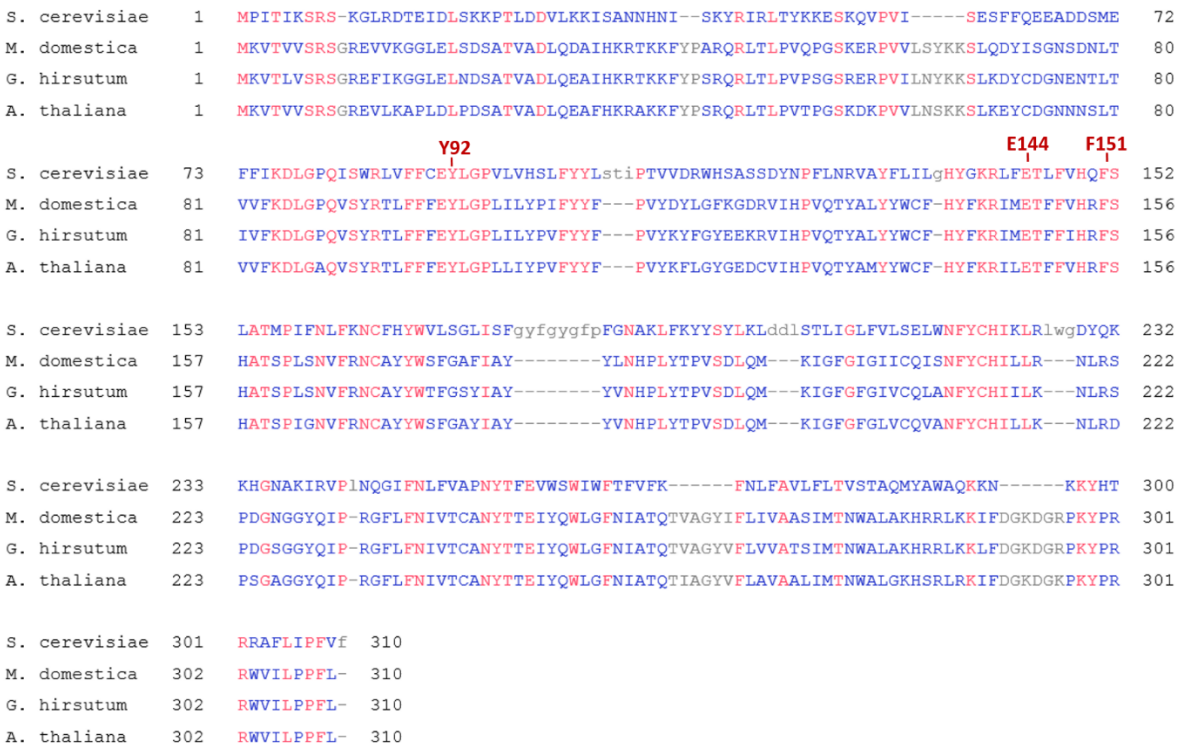

Supplementary Figure 5. The residues Y92, E144 and F151 are conserved between Tsc13 and the three plant homologues. Shown are the sequences of Tsc13 (NP_010269) and the three ECRs from Malus domestica (NP_191096), Gossypium hirsutum), and Arabidopsis thaliana (XP_008382818).

Supplementary Table 1. Primers used in this study to amplify pathway genes. The name of each primer corresponds to bio-brick name indicated in supplementary Table 6.

Primer name	Primer sequence, 5´ to 3´
#162 AtPAL2 F	ATCAACGGGUAAAATGGACCAAATTGAAGCAATGC
#162 AtPAL2 R	CGTGCGAUTTAGCAGATTGGAATAGGTGCAC
#100 At4CL2 F	AGCGATACGUAAAATGACGACACAAGATGTGATAGTC
#100 At4CL2 R	CACGCGAUCTAGTTCATTAATCCATTTGCTAG
#221 PhCHI F	AGCGATACGUAAAATGTCTCCACCAGTTTCTGTTAC
#221 PhCHI R	CACGCGAUCTACACACCGATAACAGGTATTG
#222HaCHS F	CGTGCGAUTAATTAATTGCGACTGAATGAAG
#222HaCHS R	ATCAACGGGUAAAATGGTTACTGTTGAAGAAGTTAG
#223 C4H L5 F	AGCGATACGUAAAATGGATTTGTTATTGCTGGAAAAG
#223 C4H L5 R	AGCTGCAGCUTCTTTTGCTGCAGCTTCAGCGCTACAATTTCTGGGTTTCATG
#231 L5 ATR2 F	AGCTGCAGCUAAAGAAGCTGCAGCAAAAGCTGGTAGGAGGAGCGGTTCG
#231 L5 ATR2 R	CACGCGAUTTACCATACATCTCTCAGATATCTAC
#304 HaCHS F	AGCGATACGUAAAATGGTTACTGTTGAAGAAGTTAG
#304 HaCHS R	CACGCGAUTAATTAATTGCGACTGAATGAAG
#317 AtPAL1 F	AGCGATACGUAAAATGGAGATTAACGGGGCACACAAG
#317 AtPAL1 R	CACGCGAUTTAACATATTGGAATGGGAGCTC
#319 AnPAL1 F	AGCGATACGUAAAATGTTGGACAAGCACATCCCAGACG
#319 AnPAL1 R	CACGCGAUTTATTGTTGGAAGGAGTTCAAAATAG
#314 AtPAL2 (OPT2) F	CGTGCGAUTTAGCAGATAGGAATAGGAGCACC
#314 AtPAL2 (OPT2) R	ATCAACGGGUAAAAATGGATCAAATCGAAGCTATGTTG
#318 RtPAL F	AGCGATACGUAAAATGGCTCCATCATTGGATTCTATT
#318 RtPAL R	CACGCGAUTTATGCTAACATCTTCAACAAAACG
#328 HaCHS (OPT4) F	AGCGATACGUAAAATGGTTACCGTAGAAGAGGTACGTAAAG
#328 HaCHS (OPT4) R	CACGCGAUTCAATTAATAGCAACACTATGCAAC
#327 HaCHS (OPT1)F	AGCGATACGUAAAATGGTTACAGTCGAAGAAGTGAG
#327 HaCHS (OPT1)R	CACGCGAUTTAATTTATGGCAACGGAGTGC
#329HaCHS (OPT5) F	CGTGCGAUTTAGTTTATAGCAACGCTATGCAAAAC
#329HaCHS (OPT5) R	ATCAACGGGUAAAATGGTAACGGTTGAAGAAGTAAGG
#330HaCHS (OPT6) F	AGCGATACGUAAAATGGTGACTGTTGAAGAAGTAAG
#330HaCHS (OPT6) R	CACGCGAUTTAATTAATAGCTACTGAGTGAAG
#148 ARO4 K229L F	AGCGATACGUAAAATGAGTGAATCTCCAATGTTCGC
#148 ARO4 K229L R	CACGCGAUCTATTTCTTGTTAACTTCTCTTCTTTGTC
#451 TSC13 up F	AGGGTTTAAUTACTGTTTTAGTTGATTTGAGTTAATTTG
#451 TSC13 up R	AGGACTTAAUTTTCTAGATAGCTAAATAGAATATAATC
#452 TSC13 Down F	AGGCATTAAUATGCAAGGTAAAGAGATATTAGC
#452 TSC13 Down R	AGGTCTTAAUAAATTTGGTCCGATCATTATTGGTGCTTC
#382 Sh ble F	AAGGGGCGGUGTTGACAATTAATCATCGGCATAG
#382 Sh ble R	ATTAATGCCUTTGCTGGCCTTTTGCTCACATGTTG

Supplementary Table 2. Primers used in this study to amplify promoters (a) and primers used for verification of genomic integrations/deletions (b).

	Primer name	Primer sequence, 5´ to 3´
a	**pTEF1 F**	ATTAAGTCCUGGATCCTAGGTCTAGAGATCTGTTTAGCTTG
	pTEF1 R	ACCGCCCCTUGGTTGTTTATGTTCGGATGTGATGTG
	pTEF2 F	CGTGCGAUGCCGATCTGGGCCGTATACTTACA
	pTEF2 R	ACGTATCGCUTGTTTAGTTAATTATAGTTCGTTGACC
	pPGK1 R	ACCCGTTGAUGCCGCTTGTTTTATATTTGTTGTAAAAAG
	pPGK1 F	CACGCGAUGGCCTGGAAGTACCTTCAAAGAATG
	pTEF1 F	CGTGCGAUGCCGCACACACCATAGCTTCAAAATG
	pTEF1 R	ACGTATCGCUGTGAGTCGTATTACGGATCC
	pPDC1 F	CGTGCGAUGCCGATCTATGCGACTGGGTGAG
	pPDC1 R	ACGTATCGCUTTTTGATAGATTTGACTGTGTTATTTTGCG
	pTEF2 R	ACCCGTTGAUTTTTGTTTGTTTATGTGTG
	pTDH3 F	ACGTATCGCUTGTTTAGTTAATTATAGTTC
	pTPI1 F	ACCCGTTGAUTTTTAGTTTATGTATGTG
b	**RES417 UP R**	TCTCAGGTATAGCATGAGGTCGCTCAT
	RES418 DW F	CCTGCAGGACTAGTGCTGAGGCATTAAT
	RES395 XI-2 UP F	GTTTGTAGTTGGCGGTGGAG
	RES396 XI-2 DW	GAGACAAGATGGGGCAAGAC
	RES511 XVI-20 UP F	GGCTTGTGGTCACCTGTCAT
	RES512 XVI-20 DW R	GAATTATGGTAATTTTGATTATC
	RES658 X-2-UP F	TGCGACAGAAGAAAGGGAAG
	RES659 X-2 DW R	GAGAACGAGAGGACCCAACAT
	RES375 X-3 UP F	TGACGAATCGTTAGGCACAG
	RES376 X-3 DW	CCGTGCAATACCAAAATCGAG
	RES377 X-4 UP	CTCACAAAGGGACGAATCCT
	RES378 X-4 DW	GACGGTACGTTGACCAGAG
	RES397 XI-5 UP	CAAATCCGAGTTAGGAATCGTCC
	RES398 XI-5 DW	TTCGAATGCGAATCCGCATGTG
	RES458 XII-5 UP	CCACCGAAGTTGATTTGCTT
	RES459 XII-5 DW	GTGGGAGTAAGGGATCCTGT
	RES1056 TSC13 UP	ACCGAAGCCACCTCTGGAACCACC
	RES1061 TSC13 DW	ACATGACAGGATGTCCATTGAACCTC

Supplementary Table 3. Primers used in this study to amplify split URA cassettes.

Primer name	Primer sequence, 5´ to 3´
RES1057_TSC13upFWD	TCCACGGGAACCACCTCTGCTACC
RES1058_TSC13UpupREV	ATTTTCAAATUAAATTCAAAATATGTATCTCTC
RES1059_TSC13dwFWD	ATAGTGTCCUCCTGTTTGCAACATGCC
RES1060_TSC13Dw R	TCCGATCATTATTGGTGCTTCCAGG
RES1062_KlURA3upFWD	ACCTTCGGCTUCATGGCAATTCC
RES1063_KlURA3upREV	TCAAACCCTTCTTCTCTTCCTCC
RES1064_KlURA3dwFWD	CAGTTATGAGGGTACTGTCGTTCC
RES1065_KlURA3dwREV	AGGACACTAUAGGGCGAATTGGGTACC
RES1066_AtFARfwdU	AATTTGAAAAUGAAGGTCACCGTCGTTTCTAG
RES1067_AtFARrevU	AAGCCGAAGGUTACAAGAATGGTGGCAAAATAACC
RES1068_GhFARfwdU	AATTTGAAAAUGAAGGTCACCTTGGTCAG
RES1069_GhFARrevU	AAGCCGAAGGUTACAAGAATGGTGGCAAAATAACCC
RES1070_MdFARfwdU	AATTTGAAAAUGAAGGTCACCGTCGTTTCTAG
RES1071_MdFARrevU	AAGCCGAAGGUTACAAGAATGGTGGCAAAATAACCC

Supplementary Table 4. Plasmids for HRT plasmid assembly.

Name	Insert info	Promoter	Biobrick
pEVE4730	Z-tag, A-tag		
pEVE1968	A-tag, ARS/CEN, CmR, B-tag		
pEVE3852	B-tag pGPD1->HaCHS, C-tag	pGPD1	HaCHS
pEVE3996	C-tag pPGK1-> MsCHI, D-tag	pPGK1	MsCHI
pEVE4957	D-tag pTEF1->At4CL, E-tag	pTEF1	At4CL
pEVE1916	E-tag, Z-tag		

Supplementary Table 5. Plasmids used for construction of strains used in this study (indicated in Table 3). Int. site means "insertion site" and p is "promoter". The relative orientation of genes (biobricks) is either forward (F) or reverse (R) as indicated.

Name	Type	Int. site	Backbone	Insert info	Biobrick R	P	Biobrick F	Biobrick F
pROP280	assembler 1	X.2	EPSC3907	AtPAL2 <-pTDH3-pTEF2-> C4H-L5-ATR2	#162 AtPAL2	pTDH3-pTEF2	#223 C4H L5	#231 L5 ATR2
pROP266	assembler 2	-	EPSC2651	HaCHS <-pPGK1-pTEF1->PhCHI	#222 HaCHS	pPGK1-pTEF1	#221 PhCHI	
pROP273	assembler 3	X.2	EPSC3908	pPDC1->At4CL2		pPDC1	#100 At4CL2	
pROP336	assembler 1	XI.2	EPSC3915	AtPAL2 <-pTDH3-pTEF2-> C4H-L5-ATR2	#162 AtPAL2	pTDH3-pTEF2	#223 C4H L5	#231 L5 ATR2
pROP337	assembler 3	XI.2	EPSC3916	pPDC1->At4CL2		pPDC1	#100 At4CL2	
pROP338	assembler 1	XI.2	EPSC3915	AtPAL2 <-pTDH3	#162 AtPAL2	pTDH3		
pROP339	assembler 2	-	EPSC2651	pPGK1->HaCHS	#222 HaCHS	pPGK1		
pROP423	assembler 1	XVI.20	EPSC2856	AtPAL2 <-pTDH3-pTEF2-> C4H-L5-ATR2	#162 AtPAL2	pTDH3-pTEF2	#223 C4H L5	#231 L5 ATR2
pROP465	single integration	X-4	pX-4	pTEF1->Ha CHS		pTEF2	#304 HaCHS	
pROP499	assembler 1	X.3	EPSC3913	AtPAL2 <-pTDH3-pTEF2->At PAL1	#162 AtPAL2	pTDH3-pTEF2	#317 AtPAL1	
pROP501	assembler 2	-	EPSC2651	HaCHS <-pPGK1-pTEF1->AnPal1	#222 HaCHS	pPGK1-pTEF1	#319 AnPAL1	
pROP502	assembler 3	X.3	EPSC3914	AtPAL2 (OPT2) <-pTPI1-pPDC1->RtPAL	#314 AtPAL2 (OPT2)	pTPI1-pPDC1	#318 RtPAL	
pROP531	assembler 1	XI-5	EPSC3921	pTEF2->HaCHS (OPT4)		pTEF2	#328 HaCHS (OPT4)	
pROP532	assembler 2	-	EPSC2651	HaCHS <-pPGK1-pTEF1->HaCHS (OPT1)	#222 HaCHS	pPGK1-pTEF1	#327 HaCHS (OPT1)	
pROP533	assembler 3	XI-5	EPSC3922	HaCHS (OPT5)<-pTPI1-pPDC1->HaCHS (OPT6)	#329HaCHS (OPT5)	pTPI1-pPDC1	#330 HaCHS (OPT6)	
pROP540	single int.	XII-5	pXII-5	pTEF1->ARO4 K229L		pTEF1	#148 ARO4 K229L	
pROP671	single int.	*TSC13*	pU0002	500bp TSC13 Up, pTEF1-> Sh ble , 500bp TSC13 Down	#451 TSC13 up	pTEF1	#382 Sh ble	#452 TSC13 Down

Supplementary Table 6. Backbones of the plasmids (indicated in Supplementary Table 5). EPSC are plasmids constructed for this study, whereas the plasmids annotated differently are obtained from Mikkelsen et al. (2012).

Name	Backbone	Type	Int. site	Insert info
pU0002			-	Amp^r, ORI
pX-4	pYU-URA3-3	single integration	X-4	522bp X.4 Up, 451bp X.4 Down, tADH1, tCYC1, URA3
EPSC3907	pYU-URA3-3	assembler1	X.2	490bp X.2 Down, tFBA, tPGI, tCYC1, URA3
EPSC2651	pU0002	assembler2	-	tFBA, tPGI, tTDH2, tENO2
EPSC3908	pU0002	assembler3	X.2	531bp X.2 Up, tTDH2, tENO2
EPSC3915	pYU-URA3-3	assembler1	XI.2	563bp XI.2 Down, tFBA, tPGI, URA3
EPSC3916	pU0002	assembler3	XI.2	569bp XI.2 Up, tTDH2, tENO2
EPSC2856	pYU-URA3-3	assembler1	XVI.20	651bp XVI.20 Down, tFBA, tPGI, URA3
EPSC2857	pU0002	assembler3	XVI.20	690bp XVI.20 Up, tTDH2, tENO2
EPSC3913	pYU-URA3-3	assembler1	X.3	560bp X.2 Down, tFBA, tPGI
EPSC3914	pU0002	assembler3	X.3	564bp X.2 Up, tTDH2, tENO2
EPSC3921	pYU-URA3-3	assembler1	XI.5	521bp XI.5 Down, tFBA, tPGI, URA3
EPSC3922	pU0002	assembler3	XI.5	663bp XI.5 Up, tTDH2, tENO2
pXII-5	pYU-URA3-3	single integration	XII.5	500bp XII.5 Up, 500bp XII.5 Down, URA3

CHAPTER 3: Platform for heterologous production and antimicrobial screening of flavonoid derivatives

1. Introduction: Genetic engineering in drug discovery and antibacterial properties of flavonoids

1.1 Genetic engineering and drug discovery

In the early stages of random drug discovery, an extremely large number of compounds need to be evaluated in order to find the best candidates that may, after going through a thorough evaluation process, finally reach the shelves (Figure 1). Natural products have been used for centuries as a crucial element of traditional medicine (Petrovska 2012) and are still important in current drug development –more than 60% of modern drugs have a natural origin (Cragg 1997). The highly differentiated assortment of a secondary metabolites of plants provide a great source of chemical diversity. Novel drug discovery from plant has traditionally involved the use of extracts that are, at first, tested for the chosen medical properties and then fractionated to separate the individual compounds that are finally screened for their medical properties (Savoia 2012). However, creating very large libraries of new drug candidates through this methodology is very time-consuming and labour-intensive. In recent times, modern organic chemistry as well as genetic engineering have been proven to be valid alternatives to produce diverse and large libraries of molecules.

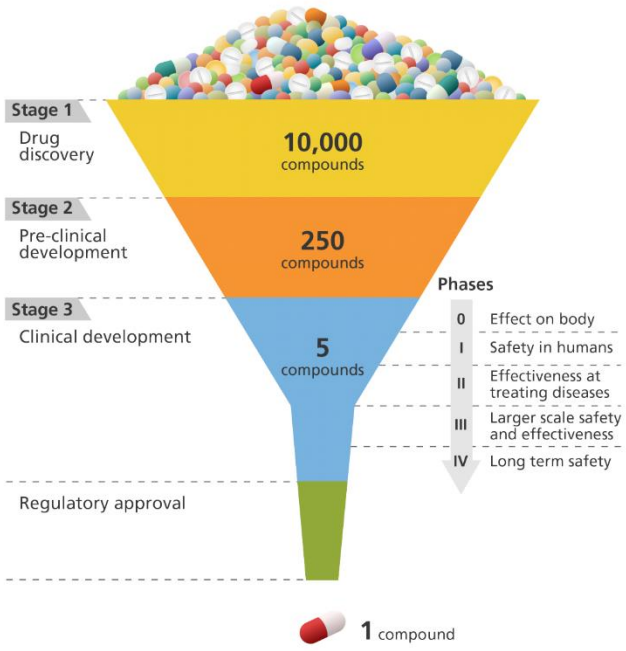

Figure 1. An illustration showing the different stages involved in developing a drug.
Image credit: Genome Research Limited.
http://www.yourgenome.org/facts/how-are-drugs-designed-and-developed

Moreover, genetic and metabolic engineering often enable the microbial production of the newly discovered drug candidates from inexpensive materials such as glucose. This is achieved through the heterologous expression of chosen genes in a known microbial host as well as by the optimization of the host's metabolism. To increase the molecular diversity, a given compound can be further decorated with a variety of functional groups by expressing in the microbial host the genes coding for the relevant enzymes. Such modifications could enhance the activity of known drugs and facilitate the development of novel compounds with interesting properties. Plant or other organism's

cDNA libraries representing the transcriptome of a given tissue/organism are a great source of genetic diversity that can be useful on this molecular decoration (Khosla and Keasling 2003).

As described in the general introduction, yeast artificial chromosomes (YACs) are a great tool for introducing and co-expressing a large number of genes into *S. cerevisiae*. Using this technology Naesby *et al.* (2009) developed a platform to generate structurally diverse flavonoids. They were able to assemble approximately 50 random gene-encoding DNA cassettes in a single step and to express diverse flavonoid biosynthetic pathways. Using the same technology Klein *et al.* (2014) developed a platform for the production of a variety of small molecules to be used in drug discovery. As a source of genetic diversity they used cDNA derived from different organisms and known biochemical pathways including: alkaloid, benzoxazinoid, flavonoid, flavanol, lignin, polyunsaturated fatty acid, tetra- and diterpenoid and included different Type III polyketide synthases. From the resulting combinatorial library they identified 74 different active compounds in an antiviral screening, including number of completely novel molecules never described before. Inspired by this study we developeloped a semi-random approach to crate a more targeted and rich library of flavonoid derivatives and aimed to screen it for antimicrobial properties (Figure 2). As a model we used a cariogenic bacteria known to cause dental cariers (Beighton 2005; Paes Leme *et al.* 2006).

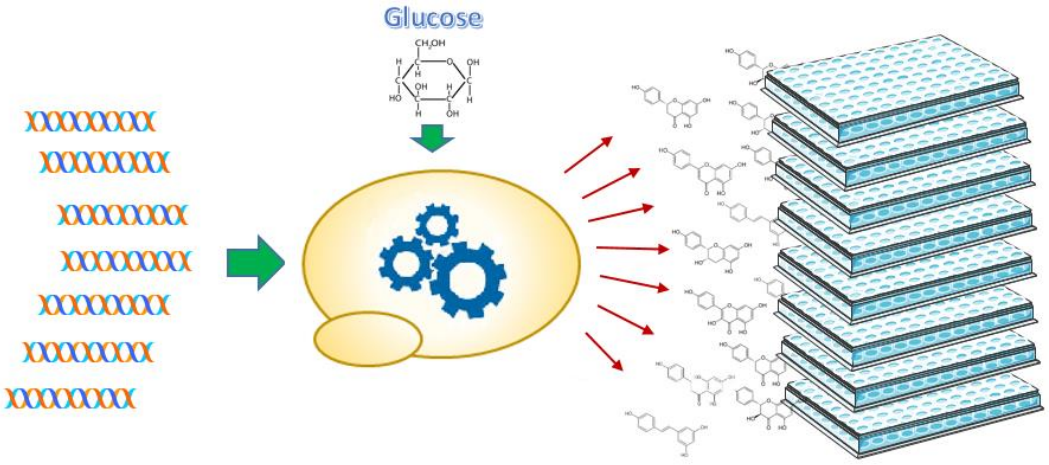

Figure 2. Model for production of flavonoid library in yeast.

1.2 Need for antimicrobial alternatives

Due to the current increase in the number of infections by antibiotic-resistant bacteria, the research on new antimicrobial compounds is critical. As bacteria are fast at evolving under selection pressure, resistance to a specific antibiotic usually develops a few years after the antibiotic has been introduced to the general population. Then, horizontal gene transfer between different species of bacteria allows spread of resistance among the same and different bacterial species (Davies and Davies 2010). Unfortunately, in the past decades the use of antimicrobials in general hygiene products has been abused. Triclosan, for example, can be found in toothpaste, soaps, house cleaning products, and in surgical cleaning solutions. Regrettably, triclosan has been reported to induce the expression of an efflux pump that

makes bacteria less susceptible to a number of antibiotics and helps the selection process for new resistant variants (Davison *et al.* 2010). Therefore, in addition to the need for development of new antibiotics, problematic antibacterial agents present in every day hygiene products should be replaced with new, safer antimicrobial alternatives. As flavonoids have been widely reported to show antimicrobial potential (Cushnie and Lamb 2005; Cushnie and Lamb 2011; Daglia 2012), they could be a possible alternative to the currently used antimicrobial products. For instance, some natural extracts rich in flavonoids as well as individual flavonoids have been reported to prevent dental caries *in vivo* (described in subsection 1.4), which can likely be attributed to their antibacterial properties (described in subsection 1.5).

1.3 Caries lesions and cariogenic bacteria

Caries lesions, known as cavities, are a public health problem around the globe. They result from the interaction of oral microorganisms, including cariogenic bacteria, and diet elements such as sucrose (Figure 24). The acidic environment caused by the fermentation of sugars by acidogenic microorganisms favours the progression of acid tolerant bacteria as well as leads to demineralization of the tooth. The cariogenic bacteria form a biofilm on the surface of the tooth (Beighton 2005; Bowen 2016; Paes Leme *et al.* 2006). In principle, the biofilm is a community of different bacterial species growing in extracellular matrix, attached to hard surface (Lopez *et al*. 2010). Sucrose serves as a substrate for the cariogenic bacteria to synthetize carbohydrate coated adhesion molecules, enabling them to colonize an oral cavity. Bacterial glycosyltransferases are essential for producing various glycoconjugates between bacteria and saliva coated tooth surface, leading to the formation of the dental biofilm known as plaque (Paes Leme *et al.* 2006). Prevention strategies for dental caries include: elimination of the cariogenic bacteria, inhibition of plaque formation and increasing the tooth resistance to demineralization (Bowen 2016). Dental plaque which occurs on the surface of the tooth is dominated by gram-positive bacteria, such as *Streptococcus mutans*, *Streptococcus sobrinus*, *Streptococcus sanguinis*, *Streptococcus mitis*, *Streptococcus salivarius*, and lactobacilli. *S. mutans* is the principal etiological agent related to dental caries, though other acidogenic/aciduric microorganisms are also involved (Beighton 2005; Kuramitsu *et al.* 2007; Salman and Senthikumar 2015). The strain closely related to *S. mutans*, *S. sobrinus*, is also strongly associated with the dental lesions. Both *S. mutans* and *S. sobrinus* belonging to the group of *mutans* streptococci (Hirose *et al.* 1993; Salman and Senthikumar 2015). *S. sanguinis* is an opportunistic bacteria that, by secreting the natural antimicrobial agent hydrogen peroxide, modifies the environment so it becomes less hospitable for cariogenic strains (Kuramitsu *et al.* 2007). Antibiotic resistance has been reported for *S. mutans* strains isolated from the urban population of India. Out of 100 patients, 38 harbored *S. mutans*, and 26 of the isolates were resistant to penicillin, amoxicillin and ampicillin (Dhamodhar *et al.* 2014).

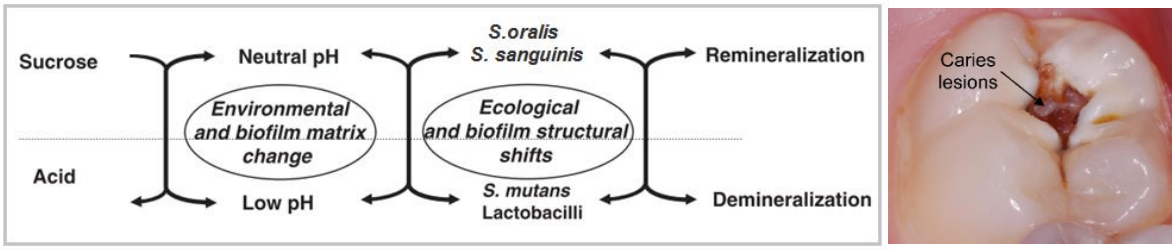

Figure 3. Scheme of cariogenic biofilm formation in the presence of sucrose (adapted from Paes Leme et al. 2006), (left). Caries lesions (Goršeta 2015) (right).

1.4 Effect of flavonoids on caries lesions *in vivo*

Ammar *et al.* (1990) and Wood (2007) demonstrated that naringenin and quercetin can inhibit caries lesions *in vivo.* Ammar *et al.* (1990) conducted a human trail where individuals used a toothpaste containing 0.1% of either naringenin or quercetin and found that, after one week of treatment with either formulation, the number of pathogenic bacteria from dental plaque samples was significantly reduced. After three weeks, the treatments also resulted in a reduction of the dental plaque formation. In the studies of Wood (2007), a sucrose rich diet on experimental rats was supplemented with 0.09%, 0.18%, 0.36% or 0.72% of naringenin for 42 days. As a result, the plaque formation as well as the development of dental caries were significantly reduced by all doses of naringenin, with the highest dosage reduced the dental caries by up to a 71%. Arslan *et al.* (2012) evaluated the anti-cariogenic properties of propolis in rats preinfected with *S. sobrinus* and fed with a cariogenic diet. Propolis is well-known natural antimicrobial element, a mixture of wax and resins, collected from various plants by the honey bees. The flavonoid-rich propolis extract, when applied toppically for 5 weeks, resulted in a significant reduction of the caries lesions. Prabhakar *et al.* (2015) tested the potency of propolis and *aloe vera* extracts to disinfect the tooth after excavation of dental caries in humans. Their results showed that the treatment with both extracts significantly reduced the bacterial counts. The caries-preventive effect of the flavonoid-rich extracts and the individual flavonoids can likely be attributed to their antibacterial properties. *In vitro* antibacterial studies of natural extracts and individual flavonoids will be presented in the next subsection, first for a wide spectrum of bacteria and then specifically for the cariogenic bacteria.

1.5 Flavonoids as alternative antibacterial agents

A large number of researchers have tested the antimicrobial properties of plant extracts known from folk medicine to have the antimicrobial properties. The fractionation of plant extracts followed by an antimicrobial assay and compound identification has allowed the identification of many compounds related to the plant's medical properties. Many of the studies revealed that phenylpropanoids, including flavonoids, often contribute to the antimicrobial properties of plants (Cushnie and Lamb 2005; Daglia 2012). This section will present the antimicrobial properties of natural extracts, as well as individual flavonoids and their derivatives, against different pathogenic bacteria as well as discuss the correlation between the molecular structure and the antibacterial activity. Emphasis will be put on the compounds used in the current study (Figure 4) and the antimicrobial effects of flavonoids and other polyphenols on cariogenic bacteria.

1.5.1 Inspiration from nature- antibacterial effects of natural extracts *in vitro*

The plant *Parashorea lucida* occurs in the Andean Mountains of South America and has been known by the locals for its antimicrobial properties for centuries. D`Almeida *et al.* (2012) tested a fractionated extract of this plant against several human antibiotic-resistant gram positive and gram-negative pathogenic bacteria. Fractions containing mixtures of phenylpropanoids such as prenyl- and phenethyl-esters of cinnamic and caffeic acids showed antimicrobial effects on antibiotic-resistant clinical isolates of *E. faecalis.* For this strain the minimum inhibitory concentration (MIC) of ampicillin was 64 µg/mL whereas the MIC of some plant fractions was as low as 25 µg/mL.

Patra *et al.* (2014) evaluated the antimicrobial properties of *Phytolacca Americana*, an herbal medicine from South and Central America, against two microorganisms causing oral disease. The crude extract of this plant completely inhibited the growth of *P. gingivalis* and partially inhibited the growth of *S. mutans* at 0.2 mg/mL and 1.8 mg/mL respectively. They further concluded that several flavonoids isolated from this plant were responsible for its antimicrobial activity. In another study, the extract of the tropical plant *Swartzia polyphylla* was found to be effective against the cariogenic gram-positive *S. mutans* and *S. sobrinus*. This extract was fractionated and tested, being a fraction containing flavonoids the one with the strongest antimicrobial activity (Osawa *et al.* 1992). Extracts from the tropical plants *A. heterophyllus*, *R. graveolens* and *M. japonieus* were reported by Sato *et al.* (1996) to show antibacterial activity against various cariogenic bacteria at a concentration of 100 µg/mL. Again, when the extracts were fractionated, the fractions containing flavonoids had the strongest antimicrobial properties.

Uzel *et al.* (2005) tested four different Anatolian propolis ethanol extracts for their antimiocrobial properties. The MIC for the best propolis extract was as low as 2 µg/mL for *S. sobrinus* and *E. faecalis*, 4 µg/mL for two *Candida* species, 8 µg/mL for the gram-positive *S. mutans*, *S. aureus* and *S. epidermidis* and the gram-negative *E. aerogenes*. This extract was also effective against *E. coli* and the yeast *C. tropicalis* with an MIC of 16 µg/ml as well as against *S. typhimurium* and *P. aeruginosa* with an MIC of 32 µg/ml. Arslan *et al.* (2012) also tested a propolis extract on the growth of some cariogenic bacteria *in vitro*. The MIC of the propolis extract varied between 50 µg/ml and 100 µg/ml for *S. mutans* and *S. sobrinus*. The main active compounds found in propolis samples are flavonoids such as pinocembrin, pinostropin, naringenin, isalpinin, pinobanksin and quercetin, as well as the cinnamic acid derivative -cinnamyl cinnamate (Uzel *et al.* 2005).

As the antibacterial potential of numerous plants can often be atributed to individual phenylpropanoids such as flavonoids and stilbenoids, the focus of the next subsection is on antibacterial properties of individual compounds with emphasis on the compounds used in the current study (Figure 4).

1.5.2 Antibacterial activity of phenylpropanoids *in vitro*

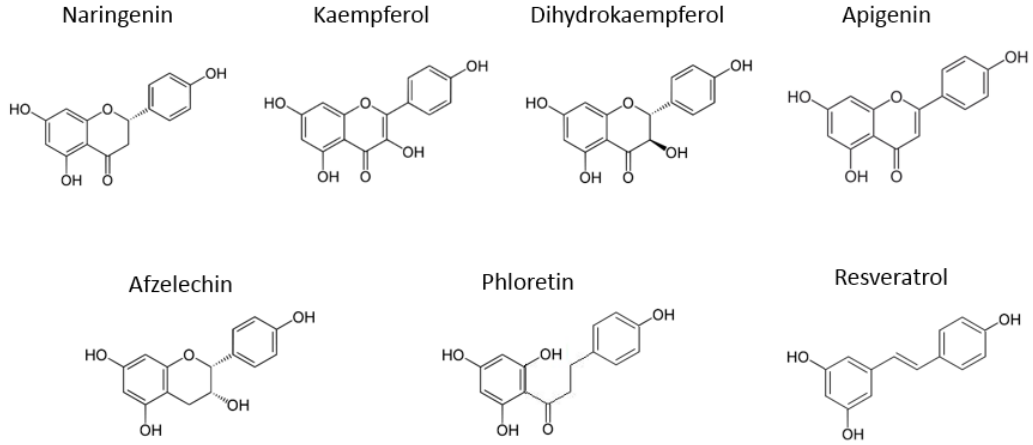

Figure 4. Structure of the flavonoids (naringenin, kaempferol, dihydrokaempferol, apigenin, afzelechin), chalcone (phloretin) and stilbenoid (resveratrol) used in this study.

Numerous research has evaluated the activity of various flavonoids against several pathogens (Cushnie and Lamb 2005). The minimum inhibitory concentration (MIC) values for some of these compounds are indicated in Appendix 2 table 9 and table 10.
In general, naringenin has a comparatively high MIC value (Lee *et al.* 2013; Mandalari *et al.* 2007; Tsuchiya *et al.* 1996; Sato *et al.*1996), with the exception of a study by Alvarez *et al.* (2008). A naringenin derivative- 7-O-butyl naringenin (Figure 5) was reported to have antibacterial activity against several strains of methicillin-resistant *Staphylococcus aureus* (MRSA) and *Helicobacter pylori* (Moon *et al.* 2013) with 26 times lower MIC than naringenin (Lee *et al.* 2013). Cells treated with this compound showed severe membrane damage when examined by Scanning Electron Microscopy. 7-*O*-butyl naringenin was found to strongly inhibit urease, an enzyme that enables *H. pylori* to survive the acidic environment of the host stomach (Moon *et al.* 2013).

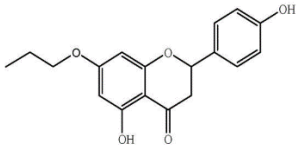

Figure 5. Structure of 7-O-butyl naringenin (Moon et al. 2013).

Kaempferol was reported to be effective against vancomycin-resistant enterococci (VRE), *S. aureus*, *S. pneumonia, E. coli,* two candida species (Tajuddeen *et al.* 2014), clindamycin resistant and sensitive strains of *P. acnes* (Lim *et al*.2007) and MRSA (Tsuchiya *et al.*1996). Dihydrokaempferol was reported to be effective against *S. aureus*, MRSA, VRE, *E. coli* and two candida species (Tajuddeen *et al.* 2014). In the studies of Wu T *et al.* (2013) in addition to kaempferol, quercetin and chrysin also inhibited the growth of *E. coli* and the compounds showed a rigidifying effect when tested on model membranes, which was positively correlated with their antibacterial effect. Quercetin was also found to have an inhibitory effect on the growth of *S. aureus* (Alvarez *et al.*2008).

Apigenin showed antibacterial activity against gram negative *E. aerogenes*, *E. cloacae*, *P. aeruginosa*, *P. mirabilis*, *S. typhi*, *E. coli* (Basile *et al.* 1999) and gram positive *S. pyogenes* (Lucarini *et al.* 2015). Scutellarein was also reported by Lucarini *et al.* (2015) as a potent antibacterial compound.

The dihydrochalcone phloretin was found to be effective against several MRSA strains, as well as against *L. monocytogenes* and *S. typhimurium*. This compound partially inhibited lactate dehydrogenase and isocitrate dehydrogenase isolated from *S. aureus*, interfering with the utilization of biological fuels (Barreca *et al.*2014).

Resveratrol was also reported to inhibit the growth of *B. cereus*, and moderately inhibit the growth of *E. faecalis*, *S. aureus*, MRSA (Paulo *et al.* 2010), as well as *E. faecalis* and *P. aeruginosa* (Chan 2002).

Flavonoids and cariogenic bacteria *in vitro*

The only MIC reported for naringenin and cariogenic bacteria was determined using the disc diffusion method, being 250 µg/disc for *S. mutans* and 500 µg/disc for *S. sobrinus*, whereas the MIC of several isoflavonoids was much only 64 µg/disc (Osawa *et al.* 1992). Patra *et al.* (2014) demonstrated that kaempferol extracted from *P. americana*, strongly inhibited the growth of *S. mutans* (with an MIC of 8 µg/mL). Quercetin, isolated from the same plant, strongly inhibited the growth of *S. mutans* (with an MIC of 8 µg/mL). In the hands of Iwaki *et al.* (2006) kaempferol extracted from *Polygonum tinctorium* showed antimicrobial activity against several different strains of *S. mutans*, with an MIC between 25-50 µg/mL, and on *S. sobrinus* with an MIC of 200 µg/mL. Koo *et al.* (2002) demonstrated that pinocembrin derived from propolis samples were effective against *S. mutans* and *S. sobrinus* with an MIC of 64 µg/mL.

Sato *et al.* (1996) reported that prenylated flavonoids, artocarpin and artocarpesin (Figure 6), strongly inhibited the growth of plaque-forming streptococci, with an MIC varying from 6.25 to 12.5 µg/mL.

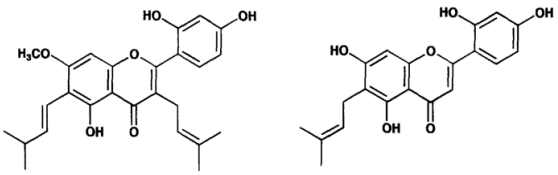

Figure 6. Structure of artocarpin (left) and artocarpesin (right) (Sato et al. 1996).

Other prenylated flavonoids isolated from Leguminosae showed strong antimicrobial potential against a wide range of cariogenic bacteria. Flavanone derivatives such as sophoraflavanone G (5,7,2',4'-tetrahydroxy-8-1avandulylflavanone) and 5,7,2',6'-tetrahydroxy-8-1avandulylflavanone (Figure 7) inhibited the growth of several strains of cariogenic *S. mutans*, *S. sobrinus*, *S. rattus* with an MIC between 1.56 µg/mL-2.5 µg/mL (Tsuchiya *et al.* 1994).

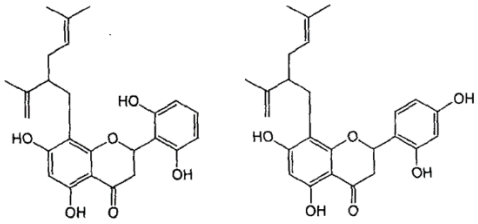

Figure 7. Sophoraflavanone G (5,7,2',4'-tetrahydroxy-8-1avandulylflavanone) (right) and 5,7,2',6'-tetrahydroxy-8-lavandulylflavanone (left), (Tsuchiya et al. 1994).

Sophoraflavanone G was found to reduce membrane fluidity when tested in artificial membranes. Again, naringenin, the basic flavonoid backbone, showed a similar effect but at higher concentrations (Tsuchiya and Iinuma 2000).

The preventive effect of flavonoids against dental caries (described in point 1.4) can also be attributed to their ability to reduce biofilm formation. Badria and Zidan (2004) found that naringenin and apigenin inhibited the adhesive properties of some *S. mutans* strains at 12.5 µg/mL. Koo *et al.* (2002) demonstrated that apigenin inhibited the activity of various glucosyltransferases and, in further studies, treated early-formed biofilms with 359 µg/mL of apigenin twice a day for 1 min. With such a treatment, further accumulation of biofilm formed by *S. mutans* was reduced by 43% (Koo *et al.* 2003).

Structure vs antibacterial properties

A number of studies have analysed which functional groups and at which positions are important for the antibacterial activity of flavonoids (Figure 8) and chalcones (Figure 9). This subsection will focus on the structure of these molecules in relation to their antibacterial effect on gram positive bacteria.

Flavonoids

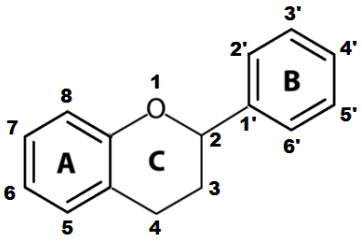

Figure 8. Basic structure of flavonoids.

Tsuchiya *et al.* (1996) evaluated the antimicrobial properties of various flavanones isolated from leguminosae against MRSA, aiming to deduce their structure activity-relationship. They observed that the B ring of the active flavanones is dihydroxylated at the 2′ and 4′ or 2′ and 6′ positions. They also deduced that hydroxyl groups at positions 5 and 7 of the A ring contribute to the antibacterial activity of flavanones. The presence of an aliphatic group (lavandulyl, geranyl or prenyl) at the 6 or 8 positions of the A ring strongly enhanced the anti-MRSA activity (MIC 3-12 µg/mL) in relation to flavanones lacking the aliphatic group, most likely due to increased lipophilic properties. Compounds active against a wide range of cariogenic bacteria identified by Tsuchiya *et al.* (1994) also fulfill the anti-MRSA structural properties described in Tsuchiya *et al.* (1996). The addition of aliphatic chains at position 3 to the epicatechin molecule was also reported to enhance its anti-MRSA activity (Stapleton *et*

al. 2004). The antibacterial relevance of aliphatic chains in flavonoid derivatives was further reported by Céliz *et al.* (2011). They showed that naringenin derivatives with aliphatic chains (>6 carbons) in the position 7 of the A ring presented antimicrobial activity against gram positive strains of *E. faecium*, *S. aureus*, *L. monocytogenes* and *B. subtilis*. The activity increased gradually with the length of the aliphatic chain, whereas the fatty acids alone did not have any antibacterial properties. In agreement with Tsuchiya *et al.* (1996), Osawa *et al.* (1992) concluded that the hydroxyl groups at positions 5, 7, 2′ and 4′ were important for the antibacterial properties of the tested flavonoids. Sato *et al.* (1996) likewise reported the antibacterial importance of hydroxyl groups at positions 5, 2′ and 4′or 5, 7, 2′ and 4′ of flavonoids, when tested on cariogenic bacteria. The hydrophobic prenyl group at the A or C ring of flavonoids further enhanced the antimicrobial properties of a variety of oral pathogens, including *mutans* streptococci. The importance of a hydroxyl group at position 5 and 7 was also reported by Alcaráz *et al.* (2000). Additionally, Wu T *et al.* (2013) revealed that a hydroxyl group at position 3 in the C ring of flavonoids is important for decreasing the fluidity of the artificial membranes. Acylated flavonol glucosides extracted from *S. palustris* were identified by Liu *et al.* (1999) as compounds with antimicrobial activity against gram positive *B. cereus*, *S. epidermidis*, *S. aureus*, and *M. luteus* (MIC 4-64 μg/mL). The presence of one or two *cis*-*p*-coumaroyl groups in the flavonol molecule was found to be important for their antibacterial activity. The presence of a single sugar moiety in the flavonoid molecule has been generally reported to reduce the antibacterial activity. By glycosylating flavonoids, Céliz *et al.* (2011) did not enhance their antimicrobial activity. Basile *et al.* (1999) reported that the glycosylated form of apigenin had strongly reduced antibacterial potential when compared to the aglycone. The same was reported for phloretin, where glycosylation reduced the antibacterial activity of this compound (Barreca *et al.* 2014). Mandalari *et al.* (2007) also reported that enzymatic deglycosylation of flavonoids increased their antimicrobial potency. However, luteolin-7-*O*-glucoside, was reported to inhibit growth of two bacterial strains (Chiruvella *et al.* 2007), but these were gram negative strains and the activity of this molecule was not compared to its aglycone form. The presence of methoxy groups at positions 5 and 7 was also reported to strongly reduce the activity of flavonoids (Alcaráz *et al.* 2000).

Chalcones

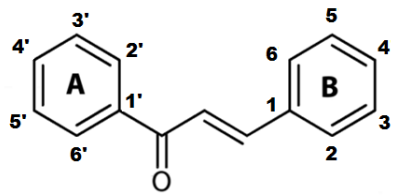

Figure 9. Basic structure of chalcones.

By evaluating different chalcones, Alcaráz *et al.* (2000) concluded that the presence of a hydroxyl group at position 2′ of these molecules was related to their anti-MRSA activity. Similarly, the antibacterial significance of a hydroxyl group at position 2′ of chalcones was also reported by Avila *et al.* (2008). They additionally found that a hydroxyl group at position 4 and a hydrophobic group (prenyl or geranyl) in position 3’ were important for the

antibacterial activity of chalcones when tested against *S. aureus* and *B. cereus.* The MIC of compounds with such characteristics varied between 3.9 and 31.2 μg/mL for gram positive bacteria, whereas they had no significant activity against gram negative. Barreca *et al.* (2014) also showed that the presence of a hydroxyl group at position 2′ and the absence of sugar moieties were important for the antibacterial activity of chalcones.

Knowledge of the structure-antibacterial activity relationship of flavonoids allows us to apply a semi-random, rather than random approaches when aiming to develop potential antibacterial compounds. Inspired by Klein *et al.* (2014) who, using the random approach, produced potential antiviral drugs in yeast, we aimed to develop a platform to screen phenylpropanoids produced in yeast for antibacterial properties using a semi-random approach. Based on literature, cariogenic bacteria were selected as a suitable model for screening flavonoids, chalcones and stilbenoids and their derivatives for antibacterial potential.

2. Materials and methods

2.1 Chemicals

Naringenin (CAS no: 67604-48-2), apigenin (CAS no: 520-36-5), kaempferol (CAS no: 520-18-3), dihydrokaempferol (CAS no: 480-20-6), phloretin (CAS no: 60-82-2), dimethyl sulfoxide (DMSO) (CAS no: 67-68-5) and tetracycline (CAS no: 60-54-8) were purchased from Sigma-Aldrich, St. Louis, USA. No commercial standard of afzelechin was available. Resveratrol was obtained from Evolva, Reinach, Switzerland.

2.2 Microbial strains and maintenance

Strains of gram-positive *S. mutans* (Clinical strain 237/03 SSI), *S. sobrinus* (NTCC 10921 SSI) and *S. sangunis* (Clinical strain 337199 SSI) were obtained from Statens Serum Institut, Copenhagen, Denmark. The strains were routinely cultivated in brain-heart infusion (BHI) broth (Sigma-Aldrich) at 37°C for 12 h. The *S. cerevisiae* strain AM1, derived from S288c, was obtained from Klein *et al.* (2014). The strain was routinely cultivated in Yeast Extract Peptone Dextrose (YPD) broth (Scharlab Microbiology, Sentmenat, Spain) at 30°C for 12 h. Stock cultures were stored at -80°C in BHI (for bacteria) or YPD (for yeast), containing 20% (v/v) glycerol.

2.3 Antimicrobial library construction

Oligonucleotide primers were used for DNA cloning and are listed in Appendix 2, table 11. All primers were synthesized by Integrated DNA Technologies (IDT), Coralville, USA. Constructed plasmids are listed in Appendix 2 table 12 and 13. Synthetic genes were codon optimized for *S. cerevisiae* and obtained from GeneArt (Thermo Fisher Scientific, Waltham, USA) (Appendix 2 table 14). Classic and USER cloning techniques (Nour-Eldin *et al.* 2006) were used for DNA cloning. Cloning was performed using *E. coli* DH5α competent cells and transformants were selected on Luria-Bertani (LB) agar plates containing 100 µg/mL of ampicillin. The genotype of yeast strains used in this study is described in Appendix 2 table 15. Plasmids for construction of strains AM2, AM7 and AM8 were constructed using plasmids listed in Appendix 2 table 12. The plasmids were constructed as described in Chapter 1, materials and methods, point 2.2 p. 31. Strains AM2-AM6 were constructed by Michael Eichenberger from AM2. Plasmids for the construction of strains AM2-AM6 (Appendix 2 table 13a) and plasmids with the *decorating* enzymes (Appendix 2 table 13b) were assembled *in vivo* in the producer strains using homologous recombination tags as described by Kuijpers *et al.* (2013). Fragments for *in vivo* assembly were obtained by *AscI* digestion of the plasmids indicated in Appendix 2 table 13a and b. The strains AM2-AM8 were transformed with the mix of *decorating* enzymes.

All yeast transformations were done using standard Li-acetate methods according to Gietz and Schiestl (2008). The transformed yeast cells were selected on synthetic complete medium (SC) (MP Biomedicals, Santa Ana, USA) lacking lysine (SC-Lys), histidine (SC-His) or leucine (SC-Leu), according to requirements.

2.4 Preparation of extracts from flavonoid and flavonoid derivative producers

Extracts from basic flavonoids producers (AM1-AM8) was prepared as follows. Each strain was inoculated in 30 mL of SC media and incubated for 96 h at 30°C and 180 rpm in shake flasks. Non inoculated SC media was used as a control. The cultures were transferred in sterile conditions to 50 mL falcon tubes, whirl mixed for 30 sec. at 1500 rpm and centrifuged for 10 min. at 4000 x g. For each strain, 25.5 mL of supernatant was transferred into sterile 50 mL falcon tubes and 0.5 mL was sampled for analytical purposes. The remaining 25 mL was freeze-dried. Freeze-dried extracts were dissolved in 2.5 mL of sterile MilliQ water and 1.8mL was transferred into sterile 2 mL Eppendorf tubes. In that way, the extracts were 10 times up-concentrated.

The yeast library producing flavonoid derivatives was prepared and screened for antimicrobial properties as follows. The number of clones to be evaluated was set up so we would assure a coverage of 95% (95% chance that each combination of *decorating* enzymes will be represented when picking individual colonies). This was evaluated using a binominal distribution equation and a Bonferroni correction equation (Sham and Purcell 2014).

The mix of *decorating* enzymes were introduced into different producers according to Kuijpers *et al.* (2013) technology–see figure 5 and subsection 2.1.1 in general introduction. The number of possible HR plasmid combinations resulting from the cloning of the different *decorating* enzymes used was calculated as follows. Fragment BC contained either the *Gm*F6H gene or a non-coding sequence (NCS) –meaning 2 possibilities for this fragment. Fragment CD encoded either *Ph*F3'H, *Sl*F3'5'H or NCS1 (3 possibilities). Fragment DE encoded either *Ss*3AT, *At*3AT or NCS2 (3 possibilities). Finally fragment EF encoded either *At*A3GTor NCS3, which gives 2 possibilities for this fragment. The fragments ZA, AB, FG, GH and HZ were unique (1 possibility) so are not included in the calculation. The fragments are assembled randomly but one fragment of each type is needed for the correct assembly of the plasmids. Therefore, the number of possible combinations is 2 x 3 x 3 x 2 = 36.

Then, the following equation for binominal distribution was used to calculate the number of independent clones to be analysed to achieve a 95 % coverage:

$$B(n,k)=\binom{n}{k}p^k q^{n-k}$$

Where B *(n,k)* is the probability of getting *k* successes in *n* trials, *p* is the probability of obtaining one specific plasmid (1/36) and *q* is the probability of obtaining a different plasmid (35/36). In order for *n* to be the only unknown in the equation we need to set the success rate (*k*) to be 0. The probability of obtaining zero of a specific plasmid (*k* = 0) would be:

$$B(n,0)=\binom{n}{0}p^0 q^n = q^n = \left(\frac{35}{36}\right)^n$$

Now we want to calculate how many samples we need to pick (*n*) to have 5% probability of getting 0 plasmid (and 95% probability of getting at least 1 plasmids) of interest, therefore *n* = log(0.05)/log(35/36) =107.

Since we want to calculate the probability of selecting 36 specific plasmids (and not just one) we used the *Bonferroni correction*. *Bonferroni correction* allows to correct the individual significance level to α/m, so that the family-wise error is α.

$$\alpha' = \frac{\alpha}{m} = \frac{0.05}{36} = 0.001388889$$

So instead of 5%, for each plasmid we need 0.05/36 = 0.001388889 (0.138%).
If we solve the equation for the binomial distribution with *Bonferroni correction*
n = log(0.00138)/ log(35/36) = 234

From every producer (AM2-AM8) transformed with the mix of *decorating* enzymes, 234 colonies were inoculated in 0.7 mL SC media in 96 DWP. In each 96 DWP three wells were inoculated with the AM1 control strain and three with the parental producer strain, three wells contained SC media only. The plates were incubated for 96h at 30°C and 400 rpm. As a backup, aliquots from each plate were frozen in 96 well microtiter plates in 20% (v/v) glycerol.
For harvesting, the plates were whirl-mixed for 30 sec. and centrifuged for 10 min. at 4000 x g. 0.6 mL of supernatant was transferred in sterile conditions into a fresh 96-DWP and sealed with an adhesive PCR foil seal (4titude). Prior freeze drying the foil was perforated by sterile needle. In sterile conditions, the dried extracts were dissolved in 120ul sterile MilliQ water. In that way, the extracts were 5x up-concentrated.

2.5 Antimicrobial assay

For all antimicrobial tests sterile 96-well microtiter plates (flat base) were used. In each experiment the bacteria concentration was 2 x 10^8 /mL colony forming units (CFU) for *S. mutans*, 2 x 10^6 /mL CFU for *S. sobrinus* and 2 x 10^6 /mL CFU for *S. sangunis*, in Tryptic Soy Broth (TSB) (Sigma-Aldrich) supplemented with 1% glucose. Due to the fact that the bacteria formed non uniform biofilm in case of *S. mutans* and clumps in case of *S. sobrinus*, direct OD measurements did not reflect cell counts. Therefore, OD_{530} was instead determined using cells homogenized with 5µL of 25% tween 80 as described by (Brandl and Huynh 2014). Bacterial growth was then determined by measuring the optical density OD_{530} using an ELISA multi-detection microplate reader Synegry HT. The percentage of inhibition was calculated as follows:

$$Inhibition\ (\%) = \left(1 - \left(\frac{\text{Absorbance of the sample}}{\text{Absorbance of the control}}\right)\right) \times\ 100\%$$

Antimicrobial properties of individual, purified compounds

In order to test the antimicrobial potential of our chosen compounds, the broth microdilution method was used according to CLSI (Clinical and Laboratory Standards Institute, 2009) guidelines. The purified commercial compounds (naringenin, kaempferol, dihydrokaempferol, apigenin, phloretin and resveratrol) were tested in different concentration ranges due to their different solubility in DMSO/water. The final concentration of DMSO used was 4% in every case as described by (Patra *et al.* 2014). The highest concentrations where no visible precipitate was formed were: 900 µg/mL for naringenin, resveratrol and phloretin, 80 µg/mL for kaempferol, 600 µg/mL for dihydrokaempferol and 100 µg/mL for apigenin. The tested concentration ranges were 28 - 900 µg/mL for naringenin, resveratrol and phloretin, 5 - 80 µg/mL for kaempferol, 18.75 - 600 µg/mL for dihydrokaempferol and

3.125 - 100 µg/mL for apigenin. The DMSO concentration was then adjusted to 4% in all wells.

Antimicrobial test of yeast extracts

First, the extract from the producers listed in Supplementary table 15, including controls (SC media and tetracycline), was evaluated for antimicrobial properties. Each 10x up-concentrated supernatant was diluted 2, 4 and 10 times in Eppendorf tubes, then 100 µL of each type was transferred into a well of a 96 sterile microtiter plate, creating "master plate". From each master plate, 10 µL was transferred into a well of a new 96 sterile microtiter plate; then 90 µL of bacterial solution in TSB was added. Next, the combinatorial antimicrobial library was evaluated. From each producer, 5 x up-concentrated supernatant (extract) was transferred from 96-DWP into 96 sterile microtiter plate, creating "master plates". From each master plate 5 µL of extract was transferred to the 96 microtiter plate, then combined with 5 µL of water and the 90 µL of bacterial solution. Each plate contained three water controls, three controls for the AM1 non-producing strain, three controls for the corresponding phenylpropanoid producer strain, and three controls for SC media only extracts. Each plate was inoculated with only one type of bacteria and control wells with media only were included. The plates were incubated at 37 °C for 24 h.

3. Results and discussion

3.1 Antimicrobial properties of individual compounds

The antimicrobial properties of individual, purified flavonoids (naringenin, kaempferol, dihydrokaempferol, phloretin and apigenin) and one stilbenoid (resveratrol) against cariogenic *S. mutans* and *S. sobrinus* and commensal *S. sanguinis* are presented in Table 4.

In general, after 24h incubation the compounds were more effective against cariogenic strains of *S. mutans* and *S. sobrinus* than against the commensal strain of *S. sanguinis.* At a concentration of 250 µg/mL, phloretin inhibited the growth of *S. mutans* and *S. sobrinus* by 93% and 87% respectively, whereas 900 µg/mL was required to inhibit the growth of *S. sanguinis* by 90%. Resveratrol at a concentration of 250 µg/mL inhibited the growth of *S. mutans* and *S. sobrinus* by 88% and 86% respectively, whereas 450 µg/mL inhibited the growth of *S. sanguinis* by 95%. At the maximum tested concentration of 80 µg/mL, kaempferol precipitated after 24h incubation, and 40 µg/mL inhibited the growth of *S. mutans* and *S. sobrinus* by 25% and 50% respectively, whereas growth of *S. sanguinis* was not affected. At a concentration 600 µg/mL, dihydrokaempferol inhibited the growth of *S. mutans* and *S. sobrinus* by 73% and 76% respectively, whereas growth of *S. sanguinis* was, again, not affected. Naringenin, at a concentration of 450 µg/mL, inhibited the growth of *S. mutans* and *S. sobrinus* by 85% and 90% respectively, whereas 900 µg/mL inhibited the growth of *S. sanguinis* by 30%. At the maximum tested concentration, 100 µg/mL apigenin only inhibited the growth of *S. sobrinus* but just by a 20%.

Table 4. Percentage of inhibition of S. mutans, S. sobrinus and S. sanguinis by different phenylpropanoids. The minimum concentration of compound which inhibited the growth of bacteria by ≥80% is presented in the table. For compounds that did not reach an 80% inhibition, the maximum percentage of inhibition is still presented. Kaempferol at the highest tested concentration of 80 µg/mL precipitated after 24h incubation, therefore only results from 40 µg/mL is presented. Percentage of inhibition (%inh.), standard deviation (sd), n=6.

Strain	***S. mutans***			***S. sobrinus***			***S. sanguinis***		
Compound	**µg/mL**	**%inh.**	**sd**	**µg/mL**	**%inh.**	**sd**	**µg/mL**	**%inh.**	**sd**
Naringenin	450	85	0.7	450	90.5	6.3	900	30.5	3.9
Kaempferol	40	25.2	5	40	50.2	5.6	40	-	-
Dihydrokaempferol	600	73.5	3.1	600	76.5	2.3	600	-	-
Apigenin	100	-	-	100	20.5	1.1	100	-	-
Resveratrol	225	88.6	1.6	225	86.6	5.2	450	95.3	4
Phloretin	225	93.9	1.3	225	87.7	1.9	900	90.1	2.7

Despite the fact that naringenin was evaluated *in vivo* to act against dental caries (Ammar *et al.* 1990; Wood 2007), minimal literature concerning the effect of naringenin on cariogenic bacteria is available. In our assay 450 µg/mL of naringenin inhibited *S. mutans* and *S. sobrinus* by 85% and 90% respectively. Using the disc diffusion method, Osawa *et al.* (1992) reported the MIC of naringenin was 250 µg/disc when tested on *S. mutans* and 500 µg/disc when tested on *S. sobrinus.* These numbers however cannot be directly compared as different methods were used, microdilution and disc diffusion assay. In the disc diffusion assay, the compound is diluted in agar and the actual concentration at which this compound inhibits the bacterial growth cannot be directly determined. The disc diffusion method is generally used

as a preliminary antimicrobial screen and the microdilution assay is often performed afterwards.

At a concentration of 40 µg/mL, kaempferol inhibited the growth of *S. mutans* by only 25%, considerably lower than that reported by Patra *et al.* (2014) where kaempferol extracted from *P. Americana,* inhibited the growth of *S. mutans* by 97% at a concentration 8 µg/mL, using the same method. When Iwaki *et al.* (2006) tested kaempferol extracted from a natural source using the agar dilution method, the MIC value determined for different strains of *S. mutans* was in the range of 25-50 µg/mL. The lower potency of the kaempferol in our hands might be due to the fact that a clinical strain was used, in contrast to a commercial strain used by Patra *et al.* (2014) and Iwaki *et al.* (2006). The fact that we used a synthetic compound rather than a compound extracted from a natural source could also influence the results. The growth of *S. sobrinus* was inhibited 50% by 40 µg/mL of kaempferol, whereas in the studies of Iwaki *et al.* (2006) the MIC of kaempferol was 200 µg/mL. Different strains were used in both studies. The natural origin of kaempferol and increased temperature could be the reason why 200 µg/mL was dissolved in BHI agar in the Iwaki *et al.* (2006) studies. Apigenin was only reported to affect the biofilm formation by cariogenic bacteria (Badria and Zidan 2004; Koo *et al.* 2002; Koo *et al.* 2003; Koo and Jeon *et al.* 2009). It is very likely that, due to its low solubility, the MIC was not defined in ours and in other studies.

There is no literature reporting inhibition of the cariogenic bacteria growth by dihydrokaempferol, phloretin and resveratrol. Despite the high MIC reported here, naringenin, dihydrokaempferol, phloretin and resveratrol might still be interesting as they inhibit cariogenic bacteria to a higher extent than the growth of commensal strains of *S. sanguinis*.

As several flavonoids have been reported to affect the membranes (Tsuchiya and Iinuma 2000; Moon *et al.* 2013; Wu T *et al.* 2013) it would be interesting to evaluate the morphology of flavonoid treated bacteria using electron or confocal microscopy.

3.2 Amounts of phenylpropanoids produced by the parental strains

The identity and the concentrations of different phenylpropanoids in the supernatant of the phenylpropanoid yeast producers were confirmed using commercial standards and are presented in Table 5. Due to a lack of commercial standard for afzelechin, the amount of this compound was not possible to determine for (strain AM6). However, the molecule dominating in the supernatant of that producer had approximately the same mass as afzelechin, indicating that the identity of the molecule was correct.

Table 5. The concentration of the produced compounds by strains in current study.

Producer	Compound	Type	[C] µg/mL
AM2	Naringenin	flavanone	30
AM3	Kaempferol	flavonol	13
AM4	Dihydrokaempferol	dihydroflavonol	30
AM5	Apigenin	flavone	15
AM6	afzelechin	flavan-3-ol	-
AM7	Resveratrol	stilbenoid	80
AM8	Phloretin	dihydrochalcone	10

Relatively low concentrations of phenylpropanoids were produced by the AM2-AM8 yeast strains (Table 5) in relation to the antimicrobial potential of the corresponding compounds (Table 4).

3.3 Effects of yeast extracts on microbial growth

Initially, the effect of the non-diluted and diluted extracts, on the bacterial growth, was examined. This was investigated in order to obtain optimal conditions for the final screening where the extract activity would have the lowest impact on the microbial growth.

Various extract concentrations (1x, 2.5x, 5x and 10x) were combined with the bacterial solution (1:9), resulting in final concentrations of 10%, 25%, 50% and 100% (100% corresponds to the original concentration in the supernatant of the producers etc…). Due to the formation of non-uniform biofilm or cell aggregates, the bacteria were re-suspended with tween 80 prior optical density measurement.

As expected, the non-diluted extract of the control strain AM1 strongly inhibited the growth of *S. mutans* and *S. sobrinus* (Figure 10). However, the non-diluted SC media extract also inhibited the growth of *S. mutans*, indicating that there is something in the SC medium that, when up-concentrated enough, has antimicrobial effects on its own. The maximal concentration of the SC medium extract that had minimal effect on the growth of the bacterial strains was 25%. The 25% extract of the control strain AM1 slightly affected the growth of the *S. mutans*, *S. sobrinus* (Figure 11a) and *S. sanguinis* (Figure 11b) when compared to SC alone and a water control. The inhibitory effect of the WT yeast supernatant extracts is likely due to the fact that yeast can secrete antimicrobial compounds e.g. bacteriocins, lysozyme and sulphur dioxide (Buyuksirit and Kuleasan 2014; Roostita *et al.* 2011).

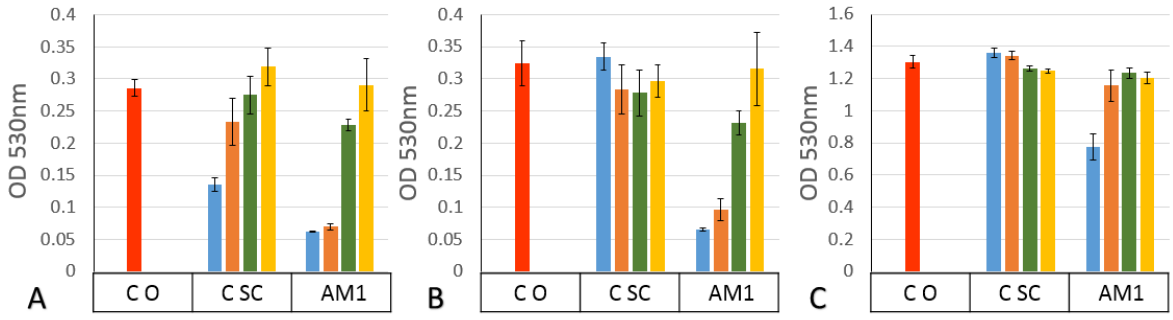

Figure 10. Effect of SC media extract (C SC), yeast extracts of control strain not producing any phenylpropanoids (AM1) and water control (C 0) on growth of A: S. mutans B: S. sobrinus and C: S. sanguinis. 100% (blue), 50% (orange), 25% (green) and 10% (yellow) (% of concentration corresponding to original supernatant). Error bars represent standard deviation (n=6).

The supernatant extracts from basic phenylpropanoid producers were also tested in order to determine if the 25% extracts would be suitable for the final screening of the antimicrobial library (to assure that the effect would be due to a derivative produced and not due to a parental compound). The 25% extracts from different producers affected the growth of bacteria to a similar extent as the control strain AM1 or higher (Figure 11). Therefore this concentration was chosen for the screening of the library clones producing flavonoid derivatives.

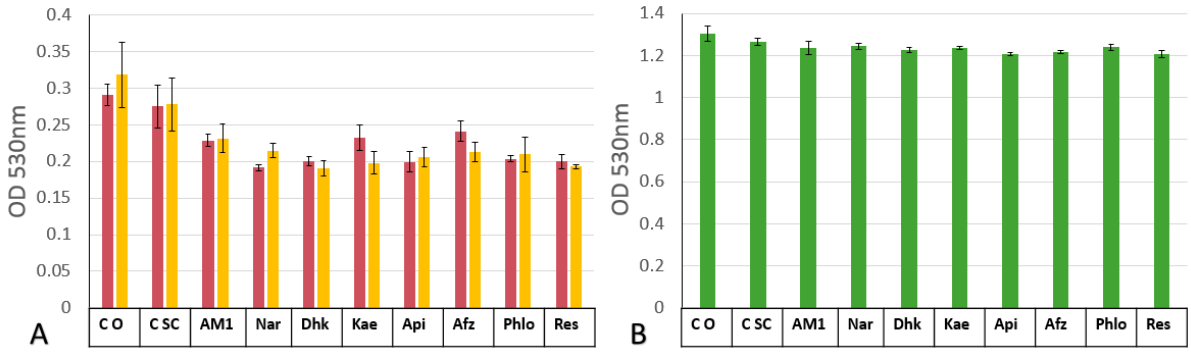

Figure 11. Effects of the 25% yeast extracts on growth of A: S. mutans (red) and S. sobrinus (yellow) and B: S. sanguinis (green). C 0: water control, C SC: media extract, AM1: control yeast strain extract , Nar: naringenin producing strain extract, Dhk: dihyrrokaempferol producing strain extract, Kae: kaempferol producing strain extract, Api: apigenin producing strain extract, Afz: afzelechin producing strain extract, Phlo: phloretin producing strain extract, Res: resveratrol producing strain extract. Error bars represent standard deviation (n=6).

Assuming a concentration of extract used of 25%, the concentration of the produced basic compounds (Table 5) and under the assumption that the *decorating* enzymes would convert the 100% of the substrates (Figure 4) into the *decorated* molecules the generated antimicrobial compounds would have to show antimicrobial effects at a concentration range from 2.5 to 20 µg/mL, a good range for molecules with a good antimicrobial potential. However, considering the effective range of the individual pure compounds (Table 4), molecules with a minor increase in antimicrobial effectiveness would not be detected as positive hits in the screening.

3.3.1 Selection of the *decorating* enzymes

As mentioned in the introduction, the design of the combinatorial library of *decorating* enzymes was performed by a semi-random approach. Therefore, in order to select the optimal *decorating* enzymes for our combinatorial library we evaluated the literature-reported flavonoid structure-antibacterial activity relationship. As some of the modifications of flavonoids described in the literature were quite challenging to achieve in our lab, it could only inspire our research to a certain extent. The *decorating* enzymes were not shown to work on all produced basic parental molecules (Figure 25) when tested in our lab. The *decorating* enzymes were pretested on flavonoids but not on dihydrochalcone, phloretin or stilbenoid resveratrol. For this reason, the application of the chosen *decorating* enzymes to phloretin and resveratrol producers are part of the random approach. The summary of the combinatorial library plan is presented in Figure 34c.

Hydroxyl groups at positions 3, 5, 7, 4′, 2′ and 6′ have been reported in literature to be important for the antimicrobial activity of flavonoids (Alcaráz *et al.* 2000; Osawa *et al.* 1992; Sato *et al.* 1996; Tsuchiya *et al.* 1996; Wu T *et al.* 2013). As flavonoids from our collection have hydroxyl groups at 5, 7, and 4′ positions (Figure 34b), our strategy was to avoid modifications at thus sites. The ideal *decorating* enzyme which could contribute to antimicrobial activity of flavonoids would be flavonoid 2′ –hydroxylase, as the hydroxyl group at this position was reported to be essential for the antibacterial activity (Osawa *et al.* 1992; Sato *et al.* 1996; Tsuchiya *et al.* 1996). Nevertheless, the enzyme that would

hydroxylate simple flavonoid molecules at 2′ position has not yet been reported. Another ideal modification according to literature would be enzymes *decorating* the flavonoid molecule with the aliphatic chain e.g. prenyltransferases (Avila *et al.* 2008; Céliz *et al.* 2011; Sato *et al.* 1996; Stapleton *et al.* 2004; Tsuchiya *et al.* 1996). However, flavonoid prenyltransferases from our collection were not active in yeast.

The available flavonoid hydroxylases active in yeast were flavonoid 3'-hydroxylase (F3'H) from *Petunia hybrid* and flavonoid 3',5'-hydroxylase and flavonoid 6-hydroxylase (F3'5'H) from *Solanum lycopersicum*. The first two enzymes were proven to be active on flavanone (naringenin) and flavonol (kaempferol). Based on the literature F3'H from *P. hybrid* can also hydroxylate dihydrokaempferol, the dihydroflavonol. F3'H can convert naringenin to eriodictyol, kaempferol to quercetin and dihydrokaempferol to dihydroquercetin (Seitz *et al.* 2007). According to literature F3'5'H from *S. lycopersicum* can hydroxylate either at 3'5' or only at 3'. Beside flavanones and flavonols this enzyme also accepts dihydroflavonols (dihydrokaempferol) as substrates. F3'5'H can convert naringenin to 5,7,3′,4′,5′-pentahydroxyflavanone, kaempferol to myricetin and dihydrokaempferol to dihydromyricetin (Olsen *et al.* 2010; Seitz *et al.* 2007). The flavonoid 6-hydroxylase (F6H) from *Glycine max* was proven to work in our lab on flavanones (naringenin) and flavone (apigenin). It was also reported in the literature to be active on and eriodictyol (flavanone) (Latunde-dada *et al.* 2001). This enzyme can for example convert apigenin to scutellarein. Enzymatic steps leading from naringenin to its different derivatives are presented in Figure 33.

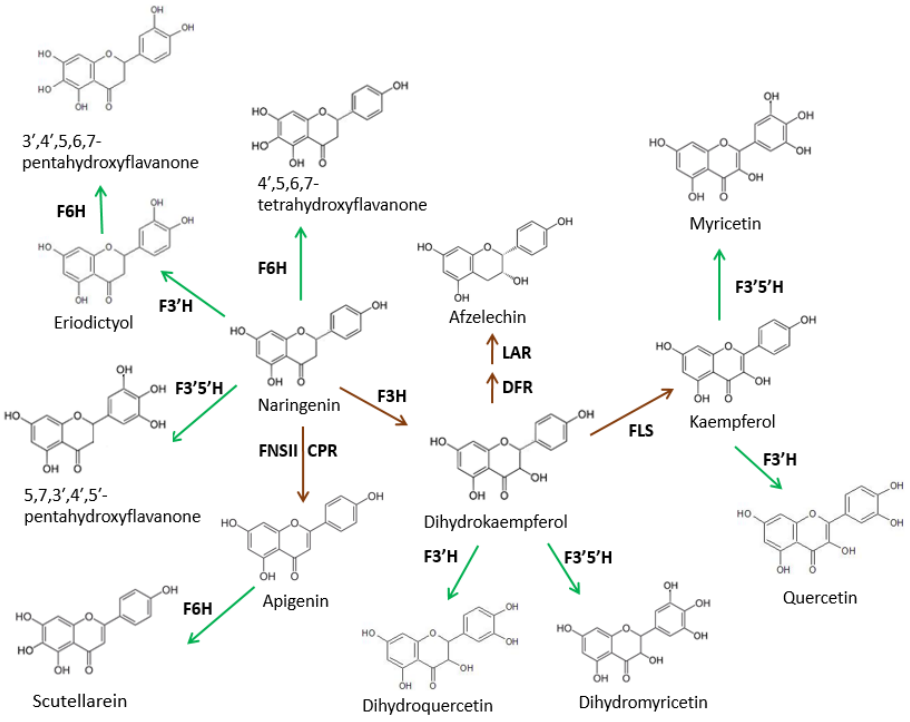

Figure 33. Enzymatic steps leading from naringenin to its derivatives. Brown arrows indicate enzymatic steps leading to formation parental flavonoids (produced by AM3-AM6). Green arrows indicate enzymatic steps leading to formation of derivatives of parental molecules (base on kinetic experiments described in the literature). The origin of the genes is indicated in Appendix 2 table 14. FNSII- flavone synthase; F3H-flavanone 3 hydroxylase; FLS- flavonol synthase; DFR-dihydroflavonol reductase; LAR- leucoanthocyanidin reductase, F3',5' H- flavonoid 3',5'-hydroxylase; F3' H- flavonoid 3'-hydroxylase; F6H- flavonoid 6'-hydroxylase.

In current study F3'H, F3'5'H and F6H were used as *decorating* enzymes, even though the modifications they perform were not reported to enhance or reduce antimicrobial activity (Figure 34b), however they allow us to produce derivatives of our molecules. To design an alteration in flavonoids that could enhance the antimicrobial activity of our compounds, we selected anthocyanin 3-O-UGT and two anthocyanin 3-O-glucoside:6'-*O*-*p*-coumaroyltransferase base on Liu *et al.* (1999). This enzyme was only tested previously on anthocyanins, however these compounds are similar to flavonoids. The possible modifications of flavonoids when using our *decorating* enzymes are presented in Figure 34c.

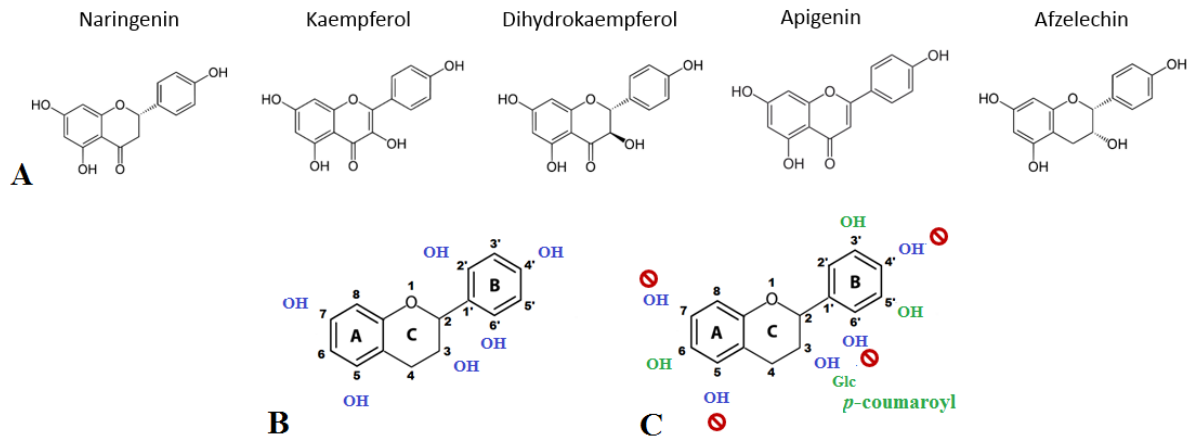

Figure 34. (A) Flavonoids used in this study. (B and C) General structure of flavonoids and hydroxyl groups reported in the literature to be related to antibacterial properties of flavonoids (blue).(C) Modification that are expected to take place by using our decorating enzyme combinations (green).

3.3.2 Final screening of the antimicrobial library

As described in subsection 3.2, prior to the final experiment, a 25% extract from the parental yeast strains as well as from the different basic phenylpropanoid producer strains were determined to be most suitable for the final experiment (Figure 11). Extracts from each producer with *decorating* enzymes was distributed on three 96 well plates.

We initially aimed to screen the combinatorial library on *S. mutans* and *S. sobrinus*, and, if any of the extracts would significantly inhibit the cariogenic bacteria, planned to also test on the *S. sanguinis*. Unfortunately, none of the extracts from the library significantly inhibited the growth of the cariogenic bacteria. Since only a slight increase on inhibition was observed in some clones over the control and the basic naringenin producer the experiment was terminated. As an example, the results of the experiment where extracts of a naringenin producer with a combinatorial library were tested are presented in Figure 35 for *S. mutans* and Figure 36 for *S. sobrinus*. For samples where a slight inhibition was observed, the experiment was repeated and the samples where inhibition was reproduced are indicated by light orange data points (Figure 36). Despite the low increase in inhibition observed, some of the extracts could have been fractionated and further investigated if time permitted. The results for AM3-AM8 producers are described in Supplementary figures 1 and 2.

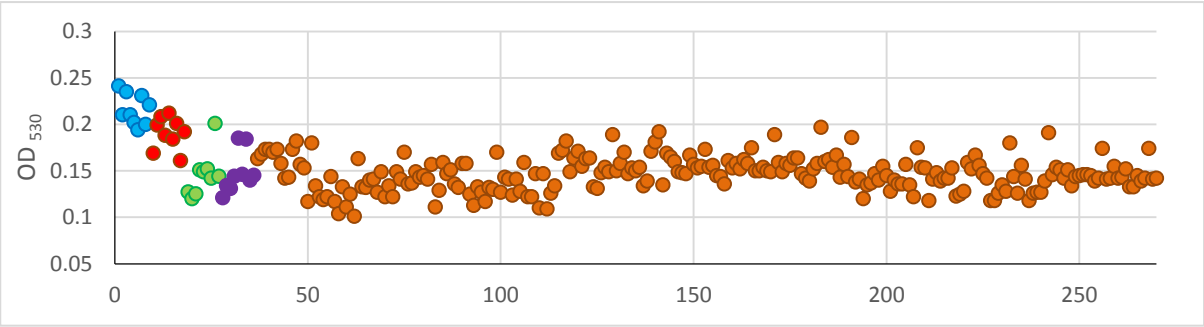

Figure 35. Effect of 25% yeast extracts of the naringenin producer transformed with mix of decorating enzymes on S. mutans. X-axis are individual samples. Water control (blue), SC media control (red), control yeast strain extract AM1 (green), naringenin producer yeast strain extract AM2 (purple), and AM2 with combinatorial library yeast extract (orange).

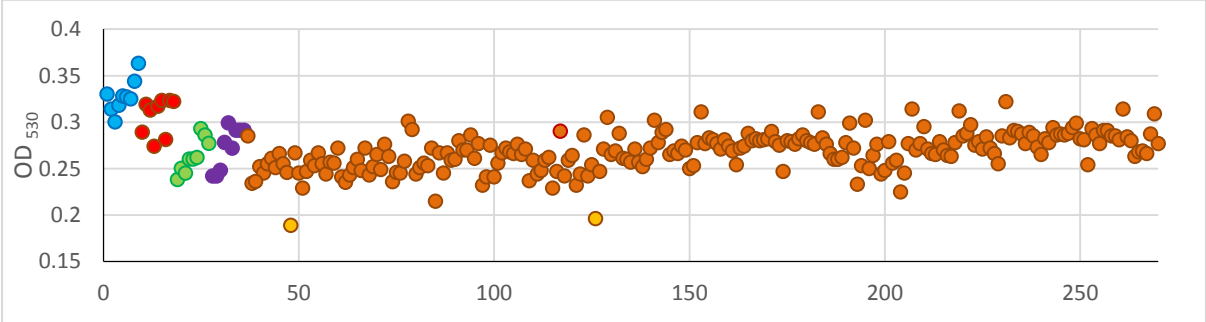

Figure 36. Effect of 25% yeast extracts of the naringenin producer transformed with mix of decorating enzymes on S. sobrinus. X-axis are individual samples. Water control (blue), SC media control (red), control yeast strain extract AM1 (green), naringenin producer yeast strain extract AM2 (purple), and AM2 with combinatorial library yeast extract (orange).The samples where inhibition was confirmed in a second experiment are marked in light orange.

As mentioned before, flavonoids with aliphatic chains and 2′ hydroxyl group were frequently reported to have enhanced antibacterial properties. Therefore, and on the light of the results, the current experiment may have been more successful if the combinatorial library would have included enzymes such as prenyltransferases and flavonoid 2′ –hydroxylase.

The lack of activity of prenyltransferases on naringenin in our lab may have been due to levels of the prenyl donor, dimethylallyl pyrophosphate (DMAPP). The problem of prenylation of naringenin in yeast was previously reported by Li H *et al.* (2015). In order to functionally express prenyl transferases in yeast dimethylallyl pyrophosphate (DMAPP), would have to be boosted in our producers. The well-studied prenyltransferase naringenin 8-dimethylallyltransferase would be a great candidate to use in our combinatorial library, if combined with DMAPP boost. The resulting molecule, 8-Dimethylallylnaringenin could be also decorated by flavonoid 2′ –hydroxylase, as the only known flavonoid 2′ –hydroxylase is described to use 8-Dimethylallylnaringenin as a substrate (Yamamoto *et al.* 2001).

However, there is still a risk that prenylated flavonoids could also inhibit the growth of *S. cerevisiae* and, therefore, couldn't be produced by the yeast. Sohn (2004) has previously shown that some of the prenylated flavonoids might have an inhibitory effect on the growth of *S. cerevisiae* but had a significantly higher inhibitory effect against bacteria.

As the combinatorial library was constructed in the strain obtained from Klein *et al.* (2014), developed previously for antiviral screening, the natural step forward would be to screen the library generated in this work for antiviral properties. This strain has incorporated the Brome Mosaic Virus (BMV) replication system under an inducible promoter, where one of the viral

components is fused with a *URA3* marker and one is fused with the Renilla luciferase reporter gene. The yeast variants producing compounds that inhibit the viral replication system would then be resistant to 5-Fluoroorotic acid (5-FOA) as they would not transcribe the *URA3* gene. As Renilla luciferase is also incorporated into the viral replication system the strains preselected on 5-FOA can be filtered again based on a lack of luciferase activity. Inducing the BMV replication system and screening the combinatorial library on 5-FOA would give us a preliminary idea if any of the produced compounds have antiviral properties. Subsequent elimination of the strains showing luciferase activity would be the next step of selection. As anti-cariogenic properties of flavonoids have also been attributed to their anti-biofilm properties, it could also be interesting to evaluate the combinatorial library in this regard. Nevertheless, due to the timeframe of this PhD project, we could not continue with any of these strategies.

The extracts of the combinatorial library did not bring significant positive results. This could be due to the fact that insufficient concentration was tested, as the experiment was limited by the inhibitory effects of the yeast extract. However, it also could be due to the fact that the chosen modifications did not show any antibacterial activity.
Despite the fact that we did not isolate any flavonoid derivative with good inhibitory properties against cariogenic bacteria, the platform for flavonoid production and the antimicrobial screening described in the thesis could be applied in different, future studies.

Contributions

Michael Eichenberger provided the *decorating* enzymes and strains AM2-AM6. Bo Svensmark and Steffen Larsen helped with the calculations regarding library coverage.

Overall conclusions and perspectives

The first objective of this study was to develop an efficient *S. cerevisiae* factory for the production of naringenin. The metabolism of *S. cerevisiae* was successfully optimised for the production of phenylpropanoids by deleting the genes of known competing pathways, blocking the production of side products from phenylalanine, cinnamic and *p*-coumaric acid in a naringenin producer strain.

The expression of the naringenin biosynthetic pathway resulted in the production of naringenin as well as in the production of the side product phloretic acid. Phenylalanine ammonia lyase (PAL) and chalcone synthase (CHS) were then identified as pathway bottlenecks. The PAL bottleneck was easily released by introducing several versions of this gene derived from different organisms. As chalcone synthase turned out to be the main pathway bottleneck we evaluated the activity of several CHS enzymes and determined that the CHS from *H. androsaemum* resulted in the highest activity when expressed in *S. cerevisiae*. Regrettably, the contribution to the improvement in the naringenin titer by subsequent addition of further copies of the CHS gene was lower for each copy introduced. To overcome the CHS limitation, two copies of the gene were introduced using a Ty1 element-mediated multiple integration strategy. Even though this strategy was expected to pull the pathway intermediates towards naringenin to a large extent, the strain still accumulated substantial amounts of *potential naringenin* in the form of phloretic acid and *p*-coumaric acid.

The strategy of introducing genes allowing the boost of the production of aromatic amino acids ($ARO4_{K229L}$ and $ARO7_{T226I}$) was successful as it resulted in higher naringenin and *potential naringenin* levels. Tyrosine was also expected to accumulate in the resulting strain. Therefore, co-expression of *PAL* and *TAL* could likely be a good future strategy as it would balance metabolism due to both substrates being used. For that reason, we decided to test different enzymes for tyrosine ammonia lyase activity in *S. cerevisiae*. A novel TAL enzyme from *A. salmonicida* was identified. The TAL activity of this enzyme was comparable with the previously described best performer TALs and showed a much higher specificity towards tyrosine, when compared to these enzymes.

As the production of naringenin in the best producer strains was most likely limited by the activity of CHS and not by the amount of carbon entering the pathway, the newly identified *Asa*lHAL/TAL was not combined with an optimized naringenin producing strain. However, a highly active, substrate specific TAL enzyme like *Asa*lHAL could be an interesting addition once the CHS bottleneck is relieved.

Overall, by applying different strategies we managed to develop a strain producing 430 mg/L of naringenin, 107 mg/L phloretic acid and 227 mg/L *p*-coumaric acid from glucose in batch growth conditions. If there were no time limits to this thesis, the boost of the other pathway precursor, malonyl-CoA, would be the next strategy to be tested. The development of a novel robust CHS would also be an extremely interesting step forward.

Naringenin is a precursor and the starting point for the synthesis of other, more complex flavonoids. By introducing *decorating* enzymes that hydroxylate, glucosylate, methylate or modify in other ways the naringenin backbone, the strains and findings presented in this work

can be used in the development of strains to produce a plethora of commercially relevant compounds.

Although the findings presented in chapter one were not published in a peer reviewed journal as an independent work, they led to the publication of a patent (Simón *et al.* 2016) and contributed to the publication of an academic article. Strains GEN0, GEN1 and GEN2 were used in Skjoedt *et al.* 2016, as they produced different levels of naringenin and constituted a suitable model for testing a naringenin biosensor.

A precursor for the synthesis of naringenin as well as many interesting derivatives, *p*-coumaroyl-CoA, is reduced in yeast to phloretic acid by a mechanism that was previously unknown. The accumulation of phloretic acid in *S. cerevisiae* expressing the phenylpropanoid pathway is described in the literature, making it difficult to use this organism for the commercial production of flavonoids. Solving this problem was the aim of chapter two. The work was recently published in the journal FEMS Yeast Research: Lehka *et al.* 2017. By evaluating the activity of 26 reductases *in vivo*, we identified that Tsc13 is responsible for reduction of *p*-coumaroyl-CoA to phloretic acid. A full knockout of this gene results in lethality so, in order to eliminate this side reaction while preserving the cellular functions of the enzyme, we attempted two alternative approaches: 1) a site saturation mutagenesis and screening for gene mutants, and 2) the replacement of the gene by plant homologues. Using the site saturation mutagenesis approach, we identified a couple of mutants which resulted in slightly increased naringenin production but had no effects on the accumulation of phloretic acid. Using the second strategy, we identified a *TSC13* homologue from *M. domestica* that was able to complement a native *TSC13* deletion and resulted in a strain that did not accumulate phloretic acid, and when cultivated in feed-bath conditions, exhibited comparable growth rates to the WT strain. Due to time constraints this strategy was not implemented in the best naringenin producer but, since the phenylpropanoid pathway branches towards different products at the point where *p*-coumaroyl-CoA is formed, the substitution of the *TSC13* gene by its homolog from the apple tree would be of high importance for the production of various phenylpropanoids with potential commercial relevance.
Besides the publication of Lehka *et al.* 2017, the work presented here resulted in contributions to two other scientific publications. Garcia Vanegas *et al.* 2017 describes another approach to improve the production of naringenin in *S. cerevisiae* through the downregulation of the expression of *TSC13* in different degrees. Eichenberger *et al.* (2016) describes how the identification of Tsc13 and its overexpression allowed the boost of the levels of phloretic acid and the *de novo* production of the dihydrochalcone phloretin.

As naringenin can be a precursor and a starting point for the synthesis of other, more complex flavonoids, the aim of chapter three was to develop a method to produce a combinatorial flavonoid library and to test it for antibacterial properties, using cariogenic bacteria as a model. As the parental backbone molecules (naringenin, kaempferol, dihydrokaempferol, apigenin, resveratrol and phloretin) exhibited a moderate antibacterial activity and the concentration of the yeast extract was limited, a considerable increase in the activity of the flavonoid derivatives would be needed in order to detect the antibacterial effects with the

developed screening methods. Assuming that the enzymes were active on the chosen flavonoid backbones, the addition of a hydroxyl group at position 3', 5' or 6 and the addition of a glucoside or acyl glucoside group at position 3 did not enhance substantially the antimicrobial activity of these compounds. Based on literature search one could think that that this semi-combinatorial approach may be more successful with if active prenyltransferases were included in the list of used as *decorating* enzymes, so we would suggest this as an eventual follow-up work. As the pathogenicity of cariogenic bacteria is largely due to their ability to form biofilms, the library could also be tested against a model of biofilm formation. However, due to the time constraints and the lack of a high throughput screening method, this was not possible. The antimicrobial library could also be evaluated for antiviral properties, as the assay was previously incorporated in to the parental strain as described in Klein *et al.* (2014). While under the conditions and concentrations tested no active molecules were identified, we have constructed a combinatorial flavonoid library and generated a proof of concept for the screening method of this and similar libraries for active molecules.

Appendix 2

*Appendix 2 table 9. The minimum inhibitory concentration, MIC values reported in the literature for flavonoids. *Not MIC but significant growth inhibition.*

Compound	Method	Species	MIC	References
Naringenin	Spot on method	MRSA	5.44 mg/mL	Lee *et al.* 2013
	Agar diffusion	MRSA	200-400 µg/mL	Tsuchiya *et al.* 1996
	Broth dilution	*E. coli*	800 µg/mL	Mandalari *et al.* 2007
		S. aureus	1000 µg/mL	
	Broth dilution	*S. aureus*	107 µg/mL	Alvarez *et al.* 2008
		E. coli	67.3 µg/mL	
	Paper disc diffusion	*S. mutans*	250 µg/disc (8mm disc)	Osawa *et al.* 1992
		S. sobrinus	500 µg/disc (8mm disc)	
7-*O*-butyl naringenin	Spot on method	MRSA	205 µg/mL	Lee *et al.* 2013
	Broth dilution	*H. pylori*	65.8 µg/mL *	Moon *et al.* 2013
Hesperetin	Broth dilution	*H. pylori*	60.4 µg/mL *	Moon *et al.* 2013
Kaempferol	Broth dilution	VRE	6.25 µg/mL	Tajuddeen *et al.* 2014
		S. aureus	6.25 µg/mL	
		S. pneumonia	12.5 µg/mL	
		E. coli	12.5 µg/mL	
	Broth dilution	*E. coli*	25 µg/mL (MIC_{50})	Wu T *et al.* 2013
	Broth dilution	*P. acnes*	32 µg/mL- 64 µg/mL	Lim *et al.* 2007
	Agar diffusion	MRSA	25 µg/mL	Tsuchiya *et al.* 1996
	Broth dilution	*S. mutans*	8 µg/mL	Patra *et al.* 2014
	Agar diffusion	*S. mutans*	25-50 µg/mL	Iwaki *et al.* 2006
		S. sobrinus	200 µg/mL	
Dihydrokaempferol	Broth dilution	MRSA	12.5 µg/mL	Tajuddeen *et al.* 2014
		VRE	6.25 µg/mL	
		S. aureus	6.25 µg/mL	
		E. coli	6.25 µg/mL	
Quercetin	Broth dilution	*S. aureus*	33.8 µg/mL	Alvarez *et al.* 2008
	Broth dilution	*E. coli*	36 µg/mL (MIC_{50})	Wu T *et al.* 2013
	Broth dilution	*S. mutans*	8 µg/mL	Patra *et al.* 2014
Chrysin	Broth dilution	*E. coli*	37 µg/mL	Wu T *et al.* 2013
Apigenin	Broth dilution	*E. aerogenes*	4 µg/mL	Basile *et al.* 1999
		E. cloacae	4 µg/mL	
		P. aeruginosa	8 µg/mL	
		P. mirabilis	16 µg/mL	
		S. typhi	128 µg/mL	
		E. coli	128 µg/mL	
	Broth dilution	*S. pyogenes*	50 µg/mL	Lucarini *et al.* 2015
Scutellarein	Broth dilution	*S. pyogenes*	25 µg/mL	Lucarini *et al.* 2015
Eriodictyol	Broth dilution	*E. coli*	250 µg/mL	Mandalari *et al.* 2007
		B. subtilis	250 µg/mL	
		S. aureus	800 µg/mL	
Luteolin-7-*O*-glucoside	Paper disc diffusion	*S. typhimurium*	50 µg/disc (6mm disc)	Chiruvella *et al.* 2007
		P. vulgaris	50 µg/disc (6mm disc)	
Pinocembrin	Broth dilution	*S. mutans*	64 µg/mL	Koo *et al.* 2002
		S. sobrinus	64 µg/mL	

Appendix 2 table 10. The minimum inhibitory concentration, MIC values reported in the literature for phloretin and resveratrol.

Compound	Method	Species	MIC	References
Phloretin	Broth dilution	MRSA	7.81 - 31.25 µg/mL	Barreca *et al.* 2014
		L. monocytogenes	65.5 µg/mL	
		S. typhimurium	125 µg/mL	
Resveratrol	Broth dilution	*B. cereus*	50 µg/mL	Paulo *et al.* 2010
		E. faecalis	100 µg/mL	
		S. aureus	100 µg/mL	
		MRSA	200 µg/mL	
	Broth dilution	*E. faecalis*	171 µg/mL	Chan 2002
		P. aeruginosa	342 µg/mL	

Appendix 2 table 11. Primers used in this stud y to amplify pathway genes. The name of each primer corresponds to bio-brick name indicated in Appendix 2 Table 12.

Primer name	Primer sequence, 5´ to 3´
#162 AtPAL2 F	ATCAACGGGUAAAATGGACCAAATTGAAGCAATGC
#162 AtPAL2 R	CGTGCGAUTTAGCAGATTGGAATAGGTGCAC
#100 At4CL2 F	AGCGATACGUAAAATGACGACACAAGATGTGATAGTC
#100 At4CL2 R	CACGCGAUCTAGTTCATTAATCCATTTGCTAG
#221 CHI F	AGCGATACGUAAAATGTCTCCACCAGTTTCTGTTAC
#221 CHI R	CACGCGAUCTACACACCGATAACAGGTATTG
#222 CHS F	CGTGCGAUTAATTAATTGCGACTGAATGAAG
#222 CHS R	ATCAACGGGUAAAATGGTTACTGTTGAAGAAGTTAG
#231 ATR2 L5 F	CGTGCGAUTTACCATACATCTCTCAGATATCTACC
#231 ATR2 L5 R	ATCAACGGGUAAAATGTCCAGTAGCTCTTCCTC
#223 L5 C4H F	AGCGATACGUAAAATGGATTTGTTATTGCTGGAAAAG
#223 L5 C4H R	AGCTGCAGCUTCTTTTGCTGCAGCTTCAGCGCTACAATTTCTGGGTTTCATG
#415 TSC13 F	AGCGATACGUCCCGGGAAAATGCCTATCACCATAAAAAGC
#415 TSC13 R	CACGCGAUGGTCGACGTCAAAATACAAATGGAATCAAG
#419 AmpOri F	ACAGGAAACUTAATAGAACAAATCACATATTTAATC
#419 AmpOri R	ATAAATGCTUCAATAATATTGAAAAAGGAAGAATATG
#676 p+lys F	ACACTCCCGUAATTCCACTTGCAATTACATAAAAAATTC
#676 p+lys R	AGTTTCCTGUAGCTTCGCAAGTATTCATTTTAGACCC
#418 tFBAtPGI,Cm F	AAGCATTTAUCAGGGTTATTGTCTCATGAGCGG
#418 tFBAtPGI,Cm R	ACGGGAGTGUATTGACGCTGGCGTACTGGCTTTC
Primer name	**Primer sequence, 5´ to 3´**
pPGK1 R	ACCCGTTGAUGCCGCTTGTTTTATATTTGTTGTAAAAAG
pPGK1 F	CACGCGAUGGCCTGGAAGTACCTTCAAAGAATG
pTEF1 F	ATTAAGTCCUGGATCCTAGGTCTAGAGATCTGTTTAGCTTG
pTEF1 R	ACCGCCCCTUGGTTGTTTATGTTCGGATGTGATGTG
pPDC1 F	CGTGCGAUGCCGATCTATGCGACTGGGTGAG
pPDC1 R	ACGTATCGCUTTTTGATAGATTTGACTGTGTTATTTTGCG
pTDH3 F	CGTGCGAUGCCGATCTCAGTTCGAGTTTATCATTATC
pTDH3 R	ACGTATCGCUTTTTGTTTGTTTATGTGTGTTTATTC
pTEF2 F	CGTGCGAUGCCGATCTGGGCCGTATACTTACA
pTEF2 R	ACGTATCGCUTGTTTAGTTAATTATAGTTCGTTGACC
Genotyping primers	**Primer sequence, 5´ to 3´**
Res417 R	TCTCAGGTATAGCATGAGGTCGCTCAT
Res418 F	CCTGCAGGACTAGTGCTGAGGCATTAAT
RES395 XI-2 UP F	GTTTGTAGTTGGCGGTGGAG
RES396 XI-2 DW	GAGACAAGATGGGGCAAGAC

Appendix 2 table12. Plasmids used for construction of strains AM2, AM7 and AM8 (see Appendix 2 table 15). Int. site means "insertion site", int. stands for integration, p stands for "promoter" The relative orientation of genes (biobricks) is either forward (F) or reverse (R) as indicated.

Plasmid name	Type	Int. site	Backbone	Insert info	Biobrick R	P	Biobrick F	Biobrick F
pROP854	assembler1	XI.2	pROP805	AtPAL2 <-pTDH3-pTEF2-> C4H-L5-ATR2	#162 AtPAL2	pPGK1-pTEF1	#223 C4H L5	#231 L5 ATR2
pROP669	assembler2	-	EPSC2651	HaCHS <-pPGK1-pTEF1->PhCHI	#222 HaCHS	pTDH3-pTEF2	#221 PhCHI	
pROP337	assembler3	XI.2	EPSC3916	pPDC1->At4CL2		pPDC1	#100 At4CL2	
pROP670	assembler2	-	EPSC2651	HaCHS <-pPGK1-pTEF1-> TSC13	#222 HaCHS	pTDH3-pTEF2	#415 TSC13	
pROP805	assembler1	XI.2	EPSC3915	563bp XI.2 Down, tFBA, tPGI, LYS2	#419 Amp ORI		#676 pLys2t	#418 tFBA, tPGI, Cm

Appendix 2 table 13. (a) Plasmids used for construction of strains AM3, AM4, AM5 and AM6 (see Appendix 2 table 15), (b) plasmids encoding different decorative enzymes.

	Name	Description
a	pEVE4745	pEVE4745:: Z-tag, 500bpUp XI-3, 500bpDown XI-3, A-tag, Amp^r
	pEVE3168	pEVE3168:: A-tag, Kl_His5 , B-tag, Amp^r
	pEVE22290	pEVE22290::B-tag, 600bpNCS1, D-tag, Amp^r
	pEVE4015	pEVE4015::D-tag, pTEF1->MdF3H, E-tag, Ampr
	pEVE1916	pEVE1916::E-tag, 600bpNCS2, Z-tag, Amp^r
	pEVE2177	pEVE2177::C-tag, 600bpNCS2 , D-tag, Amp^r
	pEVE4135	pEVE4135::B-tag, pGPD1->CuFLS, C-tag, Amp^r
	pEVE23312	pEVE23312::B-tag, pGPD1->AjFNSII, C-tag, Amp^r
	pEVE4012	pEVE4012::D-tag, pTEF1->AtCPR-1, E-tag, Amp^r
	pEVE4015	pEVE23320::D-tag, pTEF1->MdF3H-1, E-tag, Amp^r
	pEVE4024	pEVE4024::E-tag, pPDC1->AaDFR, F-tag, Amp^r
	pEVE1918	pEVE1918::G-tag, 600bpNCS2, Z-tag, Amp^r
b	pEVE4728	pEVE4728:: Z-tag, pSC101 LEU2 A-tag, Amp^r
	pEVE1968	pEVE1968::A-tag, ARS/CEN CmR B-tag, Amp^r
	pEVE24765	pEVE46765::**B**-tag, pGPD1->GmF6H, **C**-tag, Amp^r
	pEVE2176	pEVE2176::**B**-tag, 600bpNCS1, **C**-tag, Amp^r
	pEVE3999	pEVE3999::**C**-tag, pPGK1-> PhF3'H , **D**-tag, Amp^r
	pEVE24070	pEVE24070::**C**-tag, pPGK1-> Sl F3'5'H , **D**-tag, Amp^r
	pEVE27453	pEVE27453::**C**-tag, 1kbNCS1 , **D**-tag, Amp^r
	pEVE27305	pEVE27305::**D**-tag, pTEF1->Ss3AT, **E**-tag, Amp^r
	pEVE27306	pEVE27306::**D**-tag, pTEF1->At3AT, **E**-tag, Amp^r
	pEVE27454	pEVE27454::**D**-tag, 1kbNCS2, **E**-tag, Amp^r
	pEVE4401	pEVE4401::**E**-tag, pPDC1->AtA3GT, **F**-tag, Amp^r
	pEVE27455	pEVE27455::**E**-tag, 1kbNCS3, **F**-tag, Amp^r
	pEVE27534	pEVE27534::F-tag, pTEF2->AtCPR1, G-tag, Amp^r
	pEVE4062	pEVE4062::G-tag, pTEF2->ScCPR, H-tag, Amp^r
	pEVE4062	pEVE4062::H-tag, 600bpNCS2, Z-tag, Amp^r

Appendix 2 table 14. Genes, accession numbers and source organism.

Gene	Accession nr	Organism
AtPAL2	NP_190894	*Arabidopsis thaliana*
AtC4H	NM_128601	*Arabidopsis thaliana*
AtATR2	NP_849472	*Arabidopsis thaliana*
PhCHI	P11650	*Petunia hybrid*
HaCHS	Q9FUB7	*Hypericum androsaemum*
At4CL2	NP_188761	*Arabidopsis thaliana*
AtTSC13	GL348717.1	*Arabidopsis thaliana*
VvSTS	DQ459351	*Vitis vinifera*
AtCPR-1	Q9SB48	*Arabidopsis thaliana*
MdF3H	Q06942	*Malus domestica*
CuFLS	Q9ZWQ9	*Citrus unshiu*
AjFNSII	Q9SSX5	*Antirrhinum majus*
AaDFR	Q84L22	*Anthurium andraeanum*
VvLAR	Q4W2K4	*Vitis vinifera*
GmF6H	CYP71D9	*Glycine max*
PhF3'H	AF155332	*Petunia hybrid*
Sl F3'5'H	EU626067	*Solanum lycopersicum*
Ss3AT	AY395719	*Salvia splendens*
At3AT	NM_100275	*Arabidopsis thaliana*
AtA3GT	AY072325	*Arabidopsis thaliana*

Appendix 2 table 15. Genotype of phenylpropanoid producers used in this study.

Strain name	compound produced	genotype
AM1	Control	MATalpha trp1 lys2 leu2 his3 ura3 arg4 KIN1::GAL1-NewRNA1 ECM3::GAL1-NewRNA2 MGA1::GAL1-RNA3(pA22)URA3 MPT5::GAL1-RNA3(pA22)yRenillaLuc PRP5::ADH1-yFireflyLuc
AM2	Naringenin	EYS1244, XI.2::DR LYS2 DR/pPGK1-AtPAL2-tPGI1/TEF1-C4H L5 ATR2-tCYC1/pTDH3-HaCHS-tENO2/pTEF2-PhCHI-tFBA1/pPDC1-At4CL2-tADH2
AM3	Kaempferol	EYS1244, XI.2::DR LYS2 DR/pPGK1-AtPAL2-tPGI1/TEF1-C4H L5 ATR2-tCYC1/pTDH3-HaCHS-tENO2/pTEF2-PhCHI-tFBA1/pPDC1-At4CL2-tADH2 XI-3::loxP-HIS3-loxP/pGPD1-CuFLS_co-tCYC1/pPGK1-stuffer-tADH2/pTEF1-MdF3H-1_co-tENO2
AM4	Dihydrokaempferol	EYS1244, XI.2::DR LYS2 DR/pPGK1-AtPAL2-tPGI1/TEF1-C4H L5 ATR2-tCYC1/pTDH3-HaCHS-tENO2/pTEF2-PhCHI-tFBA1/pPDC1-At4CL2-tADH2 XI-3::loxP-HIS3-loxP/pPGK1-stuffer-tCYC1/pTEF1-MdF3H-1_co-tENO2
AM5	Apigenin	EYS1244, XI.2::DR LYS2 DR/pPGK1-AtPAL2-tPGI1/TEF1-C4H L5 ATR2-tCYC1/pTDH3-HaCHS-tENO2/pTEF2-PhCHI-tFBA1/pPDC1-At4CL2-tADH2 XI-3::loxP-HIS3-loxP/pGPD1-AjFNSII_co-tCYC1/pPGK1-stuffer-tADH2/pTEF1-AtCPR-1_co-tENO2
AM6	Afzelechin	EYS1244, XI.2::DR LYS2 DR/pPGK1-AtPAL2-tPGI1/TEF1-C4H L5 ATR2-tCYC1/pTDH3-HaCHS-tENO2/pTEF2-PhCHI-tFBA1/pPDC1-At4CL2-tADH2 XI-3::loxP-HIS3-loxP/pPGK1-stuffer-tCYC1/pTEF1-MdF3H-1_co-tENO2/pPDC1-AaDFR_co-tFBA1/pTEF2-VvLAR_co-tPGI1
AM7	Phloretin	EYS1244, XI.2::DR LYS2 DR/pPGK1-AtPAL2-tPGI1/TEF1-C4H L5 ATR2-tCYC1/pTDH3-HaCHS-tENO2/pTEF2-TSC13-tFBA1/pPDC1-At4CL2-tADH2
AM8	Resveratrol	EYS1244, XI.2::DR LYS2 DR/pPGK1-AtPAL2-tPGI1/TEF1-C4H L5 ATR2-tCYC1/pTDH3-VvSTS-tENO2/pPDC1-At4CL2-tADH2

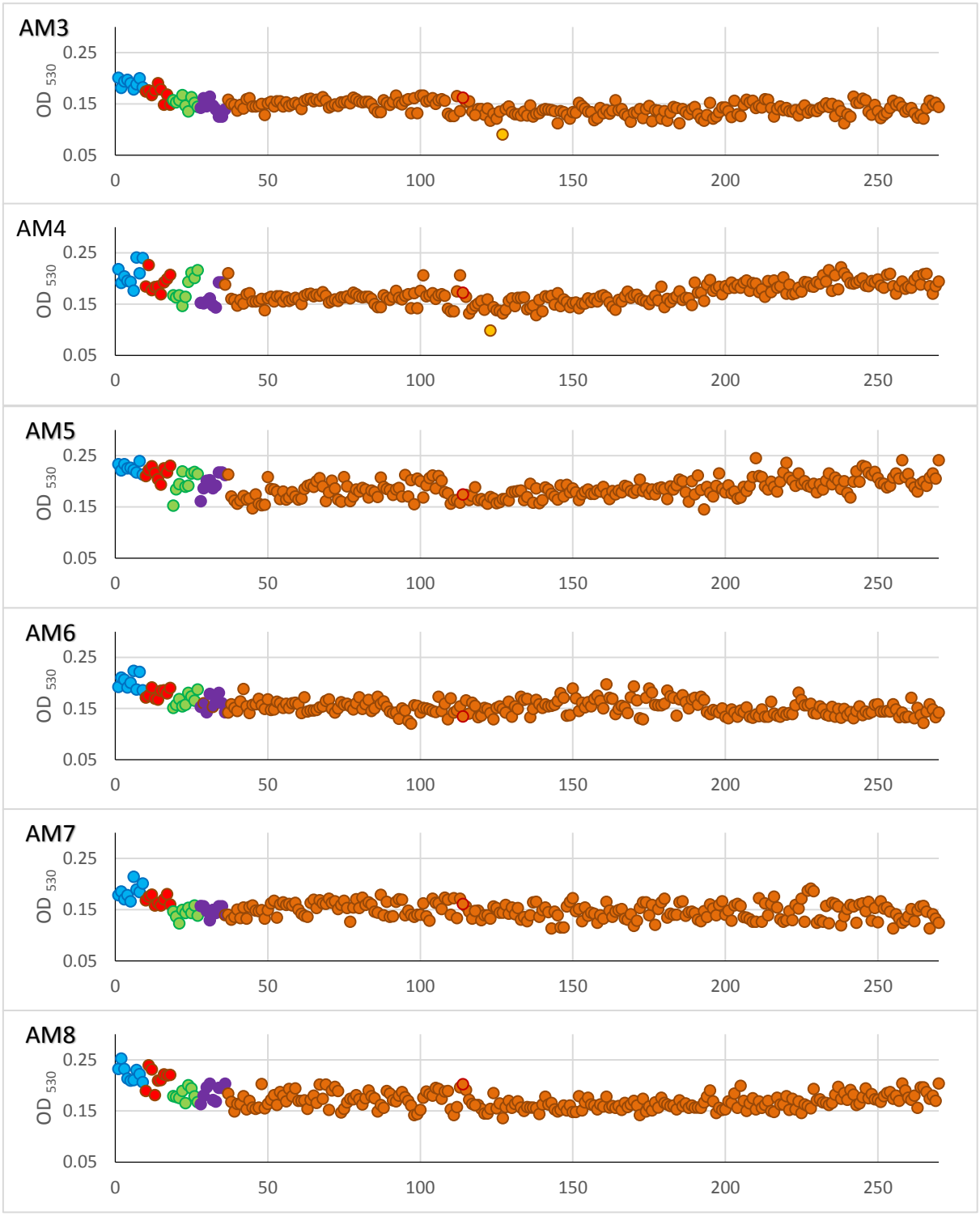

Appendix 2 figure 1. Effect of 25% yeast extracts of the different producers transformed with mix of decorative enzymes on S. mutans. Water control (blue), SC media control (red), control strain AM1 (green), AM3-AM8 (purple), and AM3-AM8 with combinatorial library (orange). Producers: (AM3) kaempferol, (AM4) dihydrokaempferol, (AM5) apigenin, (AM6) afzelechin, (AM7) resveratrol, (AM8) phloretin. The samples where inhibition was confirmed in a second experiment are marked in light orange.

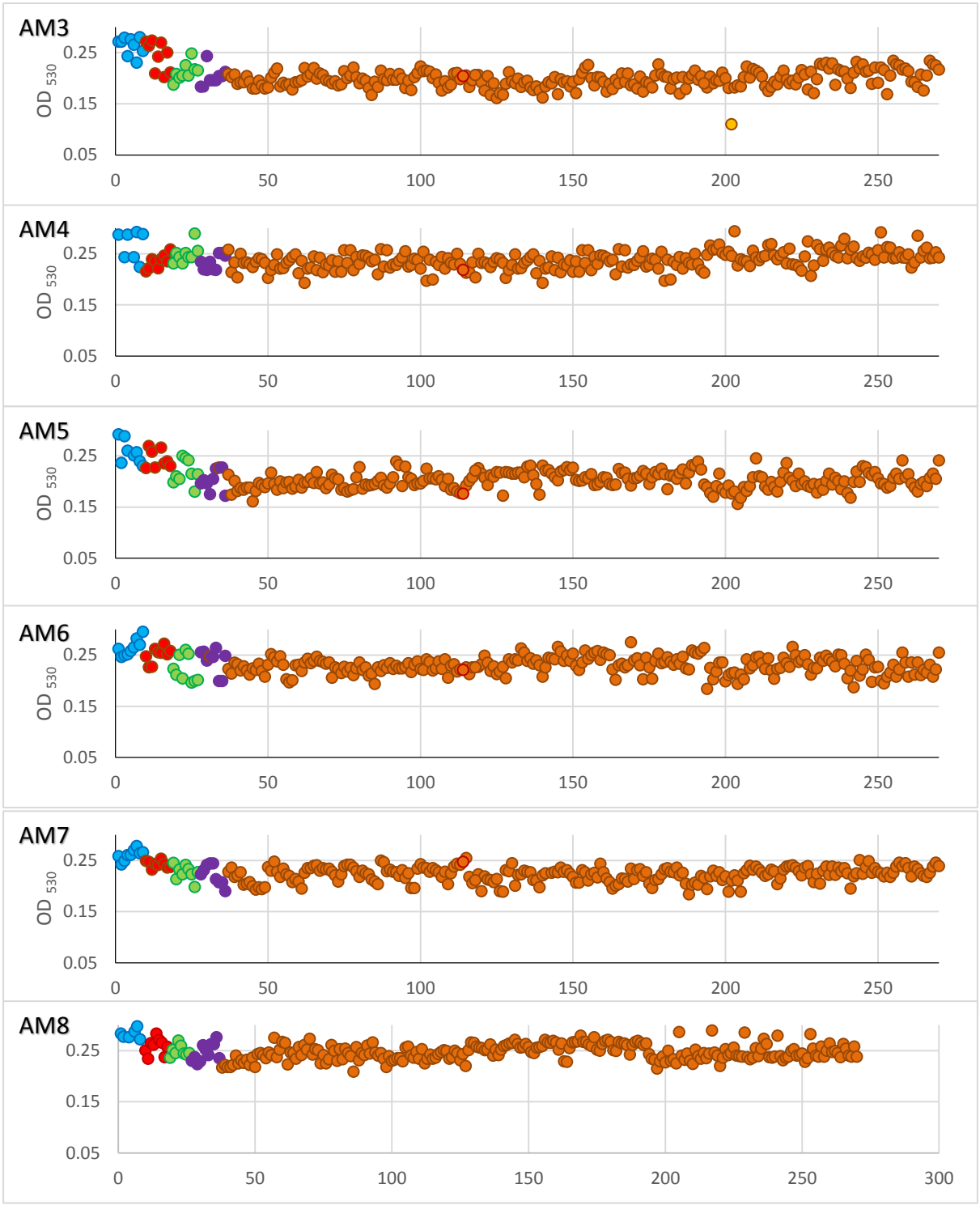

Appendix 2 figure 2. Effect of 25% yeast extracts of the different producers transformed with mix of decorative enzymes on S. sobrinus. Water control (blue), SC media control (red), control strain AM1 (green), AM3-AM8 (purple), and AM3-AM8 with combinatorial library (orange). Producers: (AM3) kaempferol, (AM4) dihydrokaempferol, (AM5) apigenin, (AM6) afzelechin, (AM7) resveratrol, (AM8) phloretin. The samples where inhibition was confirmed in a second experiment are marked in light orange.

References

Abbott DA, Zelle RM, Pronk JT *et al.* Metabolic engineering of *Saccharomyces cerevisiae* for production of carboxylic acids: Current status and challenges. *FEMS Yeast Res* 2009;**9**:1123–36.

Agati G, Azzarello E, Pollastri S *et al.* Flavonoids as antioxidants in plants: Location and functional significance. *Plant Sci* 2012;**196**:67–76.

Ahuja I, Kissen R, Bones AM. Phytoalexins in defense against pathogens. *Trends Plant Sci* 2012;**17**:73–90.

Alberstein M, Eisenstein M, Abeliovich H. Removing allosteric feedback inhibition of tomato 4-coumarate:CoA ligase by directed evolution. *Plant J* 2012;**69**:57–69.

Alcaráz LE, Blanco SE, Puig ON *et al.* Antibacterial activity of flavonoids against methicillin-resistant *Staphylococcus aureus* strains. *J Theor Biol* 2000;**205**:231–40.

Alissa EM, Ferns GA. Functional foods and nutraceuticals in the primary prevention of cardiovascular diseases. *J Nutr Metab* 2012;**2012**, DOI: 10.1155/2012/569486.

Alper H, Fischer C, Nevoigt E *et al.* Tuning genetic control through promoter engineering. *PNAS* 2005;**103**:12678–83.

Alvarez MA, Debattista NB, Pappano NB. Antimicrobial activity and synergism of some substituted flavonoids. *Folia Microbiol (Praha)* 2008;**53**:23–8.

Amalesh S, Das G, Das KS. Roles of flavonoids in Plants. *Int J Pharm Sci Tech* 2011;**6**:12–35.

Ammar N, Diwany E, Osman N *et al.* Flavonoids as a Possible Preventive of Dental Plaque. *Arch Pharm Res* 1990;**13**:211–3.

Anand K, Sarkar A, Kumar A *et al.* Combinatorial Antitumor Effect of Naringenin and Curcumin Elicit Angioinhibitory Activities *In Vivo*. *Nutr Cancer* 2012;**64**:714–24.

Annadurai T, Muralidharan AR, Joseph T *et al.* Antihyperglycemic and antioxidant effects of a flavanone, naringenin, in streptozotocin-nicotinamide-induced experimental diabetic rats. *J Physiol Biochem* 2012;**68**:307–18.

Arct J, Pytkowska K. Flavonoids as components of biologically active cosmeceuticals. *Clin Dermatol* 2008;**26**:347–57.

Aritua V, Achor D, Gmitter FG *et al.* Transcriptional and Microscopic Analyses of Citrus Stem and Root Responses to Candidatus Liberibacter asiaticus Infection. *PLoS One* 2013;**8**:4–8.

Arslan S, Silici S, Perçin D *et al.* Antimicrobial activity of poplar propolis on mutans streptococci and caries development in rats. *Turkish J Biol* 2012;**36**:65–73.

Assini JM, Mulvihill EE, Sutherland BG *et al.* Naringenin prevents cholesterol-induced systemic inflammation, metabolic dysregulation, and atherosclerosis in Ldlr$^{-/-}$ mice. *J Lipid Res* 2013;**54**:711–24.

Austin MB, Noel JP. The chalcone synthase superfamily of type III polyketide synthases. *Nat Prod Rep* 2003;**20**:79–110.

Avila H, Smânia EF, Monache F *et al.* Bioorganic & Medicinal Chemistry Structure – activity relationship of antibacterial chalcones. *Bioorg Med Chem* 2008;**16**:9790–4.

Badria FA, Zidan OA. Natural products for dental caries prevention. *J Med Food* 2004;**7**:381–4.

Baerends RJS, Simon E, Meyer JP *et al.* A method for producing modified resveratrol. 2015. WO 2015028324 A2. DOI: http://www.google.com/patents/WO2015028324A2?cl=tr

Bai X, Zhang X, Chen L *et al.* Protective effect of naringenin in experimental ischemic stroke: Down-regulated NOD2, RIP2, NF- κB, MMP-9 and Up-regulated claudin-5 expression. *Neurochem Res* 2014;**39**:1405–15.

Bailey DG, Dresser G, Arnold JMO *et al.* Grapefruit – medication interactions : Forbidden fruit or avoidable consequences ? *CMAJ* 2012;**185**:1–8.

Balasundram N, Sundram K, Samman S. Phenolic compounds in plants and agri-industrial by-products: Antioxidant activity, occurrence, and potential uses. *Food Chem* 2006;**99**:191–203.

Barreca D, Bellocco E, Laganà G *et al.* Biochemical and antimicrobial activity of phloretin and its glycosilated derivatives present in apple and kumquat. *Food Chem* 2014;**160**:292–7.

Basile A, Giordano S, López-Sáez JA *et al.* Antibacterial activity of pure flavonoids isolated from mosses. *Phytochemistry* 1999;**52**:1479–82.

Bassard J-E, Richert L, Geerinck J *et al.* Protein-protein and protein-membrane associations in the lignin pathway. *Plant Cell* 2012;**24**:4465–82.

Becker JVW, Armstrong GO, Van Der Merwe MJ *et al.* Metabolic engineering of *Saccharomyces cerevisiae* for the synthesis of the wine-related antioxidant resveratrol. *FEMS Yeast Res* 2003;**4**:79–85.

Beekwilder J, Wolswinkel R, Jonker H *et al.* Production of resveratrol in recombinant microorganisms. *Appl Environ Microbiol* 2006;**72**:5670–2.

Beighton D. The complex oral microflora of high-risk individuals and groups and its role in the caries process. *Community Dent Oral Epidemiol* 2005;**33**:248–55.

Benavente-García O, Castillo J. Update on uses and properties of citrus flavonoids: New findings in anticancer, cardiovascular, and anti-inflammatory activity. *J Agric Food Chem* 2008;**56**:6185–205.

Bergman LW. Growth and maintenance of yeast. *Methods Mol Biol* 2001;**177**:9–14.

Berner M, Krug D, Bihlmaier C *et al.* Genes and enzymes involved in caffeic acid biosynthesis in the actinomycete *Saccharothrix espanaensis*. *J Bacteriol* 2006;**188**:2666–73.

Bharati AJ, Bansal YK. in Vitro Production of Flavonoids : a Review. 2014;**3**:508–33.

Blount JW, Korth KL, Masoud SA *et al.* Altering Expression of Cinnamic Acid 4-Hydroxylase in Transgenic Plants Provides Evidence for a Feedback Loop at the Entry Point into the Phenylpropanoid Pathway. *Plant Physiol* 2000;**122**:107–16.

Boeke JD, Trueheart J, Natsoulis G *et al.* 5-Fluoroorotic Acid as a Selective Agent in Yeast Molecular Genetics. 1987;**154**:164–75.

Bowen WH. Do we need to be concerned about dental caries in the coming millennium? *Crit Rev Oral Biol Med* 2016;**13**:126–31.

Brandl MT, Huynh S. Effect of the surfactant Tween 80 on the detachment and dispersal of *Salmonella enterica* serovar Thompson single cells and aggregates from Cilantro leaves as revealed by image analysis. *Appl Environ Microbiol* 2014;**80**:5037–42.

Braus GH. Aromatic amino acid biosynthesis in the yeast *Saccharomyces cerevisiae*: a model system for the regulation of a eukaryotic biosynthetic pathway. *Microbiol Rev* 1991;**55**:349–70.

Buyuksirit T, Kuleasan H. Antimicrobial Agents Produced by Yeasts. 2014;**8**:1013–6.

Céliz G, Daz M, Audisio MC. Antibacterial activity of naringin derivatives against pathogenic strains. *J Appl Microbiol* 2011;**111**:731–8.

Chan MMY. Antimicrobial effect of resveratrol on dermatophytes and bacterial pathogens of the skin. *Biochem Pharmacol* 2002;**63**:99–104.

Chen H, Kim HU, Weng H *et al.* Malonyl-CoA synthetase, encoded by ACYL ACTIVATING ENZYME13, is essential for growth and development of *Arabidopsis*. *Plant Cell* 2011;**23**:2247–62.

Chen X, Nielsen KF, Borodina I *et al.* Increased isobutanol production in *Saccharomyces cerevisiae* by overexpression of genes in valine metabolism. *Biotechnol Biofuels* 2011;**4**:21.

Chen X, Yang X, Shen Y *et al.* Increasing Malonyl-CoA derived product through controlling the transcription regulators of phospholipid synthesis in *Saccharomyces cerevisiae*. *ACS Synth Biol* 2017. DOI: 10.1021/acssynbio.6b00346.

Chen Y, Zhang Y, Siewers V *et al.* Ach1 is involved in shuttling mitochondrial acetyl units for cytosolic C2 provision in *Saccharomyces cerevisiae* lacking pyruvate decarboxylase. *FEMS Yeast Res* 2015;**15**:1–8.

Cherry JM, Adler C, Ball C *et al.* SGD: Saccharomyces genome database. *Nucleic Acids Res* 1998;**26**:73–9.

Chiruvella KK, Mohammed A, Dampuri G *et al.* Phytochemical and Antimicrobial Studies of Methyl Angolensate and Luteolin-7-O-glucoside Isolated from Callus Cultures of *Soymida febrifuga*. *Int J Biomed Sci* 2007;**3**:269–78.

Chun OK, Chung SJ, Song WO. Estimated dietary flavonoid intake and major food sources of U.S. adults. *J Nutr* 2007;**137**:1244–52.

Clinical and Laboratory Standards Institute (CLSI). Methods for dilution antimicrobial susceptibility tests for bacteria that grow aerobically, approved standard. 2015. M07–A10 (10th ed.). Wayne, PA, USA: Clinical and Laboratory Standards Institute.

Cordova AC, Jackson LSM, Berke-Schlessel DW *et al.* The cardiovascular protective effect of red wine. *J Am Coll Surg* 2005;**200**:428–39.

Cragg G. Natural products in drug discovery and development. *J Nat Prod* 1997;**60**:52–60.

Cushnie TPT, Lamb AJ. Antimicrobial activity of flavonoids. *Int J Antimicrob Agents* 2005;**26**:343–56.

Cushnie TPT, Lamb AJ. Recent advances in understanding the antibacterial properties of flavonoids. *Int J Antimicrob Agents* 2011;**38**:99–107.

D`Almeida RE, Alberto R, Quispe C *et al.* Antimicrobial phenylpropanoids from the Argentinean highland plant *Parastrephia lucida* (Meyen) Cabrera. *J Ethnopharmacol* 2012;**142**:407–14.

Daglia M. Polyphenols as antimicrobial agents. *Curr Opin Biotechnol* 2012;**23**:174–81.

Dao TTH, Linthorst HJM, Verpoorte R. Chalcone synthase and its functions in plant resistance. *Phytochem Rev* 2011;**10**:397–412.

Davies J, Davies D. Origins and Evolution of Antibiotic Resistance. *Microbiol Mol Biol Rev* 2010;**74**:417–33.

Davison J, Maillard J, Pages J *et al.* Opinion on Triclosan - Antimicrobial Resistance. *J Ethnopharmacolv* 2010;142:407–14.

Del Rio D, Rodriguez-Mateos A, Spencer JPE *et al.* Dietary (Poly)phenolics in Human Health: Structures, Bioavailability, and Evidence of Protective Effects Against Chronic Diseases. *Antioxid Redox Signal* 2013;**18**:1818–92.

Dhamodhar P, Sreenivasa M, Channarayappa *et al.* Prevalence, characterization and heterogeneity studies on *Streptococcus mutans* isolated from Bangalore urban population. *Int J Pharm Bio Sci* 2014;**5**:122–8.

Dicarlo JE, Norville JE, Mali P *et al.* Genome engineering in *Saccharomyces cerevisiae* using CRISPR-Cas systems. *Nucleic Acids Res* 2013;**41**:4336–43.

Eichenberger M, Lehka B, Folly C *et al.* Metabolic engineering of *Saccharomyces cerevisiae* for *de novo* production of dihydrochalcones with known antioxidant, antidiabetic, and sweet tasting properties. *Metab Eng* 2016;**39**:80–89.

Engels B, Dahm P, Jennewein S. Metabolic engineering of taxadiene biosynthesis in yeast as a first step towards Taxol (Paclitaxel) production. *Metab Eng* 2008;**10**:201–6.

Epstein H. Cosmeceuticals and polyphenols. *Clin Dermatol* 2009;**27**:475–8.

Erdogan CS, Vang O. Challenges in analyzing the biological effects of resveratrol. *Nutrients* 2016;**8**, DOI: 10.3390/nu8060353.

Ferrer J-L, Austin MB, Stewart C *et al.* Structure and function of enzymes involved in the biosynthesis of phenylpropanoids. *Plant Physiol Biochem* 2008;**46**:356–70.

Flagfeldt DB, Siewers V, Huang L *et al.* Characterization of chromosomal integration sites for heterologous gene expression in *Saccharomyces cerevisiae*. *Yeast* 2009:545–51.

Flikweert MT, Van Dijken JP, Pronk JT. Metabolic responses of pyruvate decarboxylase-negative *Saccharomyces cerevisiae* to glucose excess. *Appl Environ Microbiol* 1997;**63**:3399–404.

Fowler ZL, Gikandi WW, Koffas MAG. Increased malonyl coenzyme A biosynthesis by tuning the *Escherichia coli* metabolic network and its application to flavanone production. *Appl Environ Microbiol* 2009;**75**:5831–9.

Fowler ZL, Koffas MAG. Biosynthesis and biotechnological production of flavanones: Current state and perspectives. *Appl Microbiol Biotechnol* 2009;**83**:799–808.

Fraser CM, Chapple C. The phenylpropanoid pathway in *Arabidopsis*. *Arabidopsis Book* 2011;**9**:e0152.

Fuhr U, Klittich K, Staib A. Inhibitory effect of grapefruit juice and its bitter principal, naringenin, on CYP1A2 dependent metabolism of caffeine in man. *Br J Clin Pharmacol* 1993;**35**:431–6.

Garcia Vanegas K, Lehka BJ, Mortensen UH. SWITCH: a dynamic CRISPR tool for genome engineering and metabolic pathway control for cell factory construction in *Saccharomyces cerevisiae*. *Microb Cell Fac* 2017;16(25).

Georgiev V, Ananga A, Tsolova V. Recent advances and uses of grape flavonoids as nutraceuticals. *Nutrients* 2014;**6**:391–415.

Gietz RD, Schiestl RH. High-efficiency yeast transformation using the LiAc/SS carrier DNA/PEG method. 2008;**2**, DOI: 10.1038/nprot.2007.13.

Goldblum S, Warren CB. Nootkatone as an insecticide and insect repellent. 2014. WO 2014031790 A1

Goodey AR, Tubb RS. Genetic and Biochemical Analysis of the Ability of *Saccharomyces cerevisiae* to Decarboxylate Cinnamic Acids. *Microbiology* 1982;**128**:2615–20.

Goršeta K. Fissure Sealing in Occlusal Caries Prevention. In: Virdi MS. *Emerging Trends in Oral Health Sciences and Dentistry*. CC BY 3.0 license, 2015. Kristina Goršeta (2015). Available from: https://www.intechopen.com/books/emerging-trends-in-oral-health-sciences-and-dentistry/fissure-sealing-in-occlusal-caries-prevention

Guengerich FP, Kim D. *In vitro* inhibition of dihydropyridine oxidation and aflatoxin B1 activation in human liver microsomes by naringenin and other flavonoids. *Carcinogenesis* 1990;**11**:2275–9.

Hansen EH, Møller BL, Kock GR *et al.* De novo biosynthesis of Vanillin in fission yeast (*Schizosaccharomyces pombe*) and baker's yeast (*Saccharomyces cerevisiae*). *Appl Environ Microbiol* 2009;**75**:2765–74.

Harborne JB, Williams CA. Anthocyanins and other flavonoids. *Nat Prod Rep* 2001;**18**:310–33.

Hartmann M, Schneider TR, Pfeil A *et al.* Evolution of feedback-inhibited beta /alpha barrel isoenzymes by gene duplication and a single mutation. *Proc Natl Acad Sci U S A* 2003;**100**:862–7.

Hatano T, Aga Y, Shintani Y *et al.* Minor favonoids from licorice. *Phytochemistry* 2000;**55**:9–13.

Hazelwood LH, Daran J-MG, van Maris AJA *et al.* The Ehrlich Pathway for Fusel Alcohol Production: a Century of Research on *Saccharomyces cerevisiae* Metabolism. *Appl Environ Microbiol* 2008;**74**:2259–66.

He J, Giusti MM. Anthocyanins: Natural Colorants with Health-Promoting Properties. *Annu Rev Food Sci Technol* 2010;**1**:163–87.

Heo HJ, Kim DO, Shin SC *et al.* Effect of Antioxidant Flavanone, Naringenin, from Citrus junos on Neuroprotection. *J Agric Food Chem* 2004;**52**:1520–5.

Hinderer W, Seitz H. Chalcone Synthase from Cell Suspension Cultures of *Daucus carota* L. *Arch Biochem Biophys* 1985;**240**:265–72.

Hirose H, Hirose K, Isogai E *et al.* Close association between *Streptococcus sobrinus* in the saliva of young children and smooth-surface caries increment. *Caries Res* 1993; **27**:292-297.

Hoffmann-Campo CB, Harborne JB, McCaffery AR. Pre-ingestive and post-ingestive effects of soya bean extracts and rutin on *Trichoplusia ni* growth. *Entomol Exp Appl* 2001;**98**:181–94.

Hong KK, Nielsen J. Metabolic engineering of *Saccharomyces cerevisiae*: A key cell factory platform for future biorefineries. *Cell Mol Life Sci* 2012;**69**:2671–90.

Hotze M, Schröder G, Schröder J. Cinnamate 4-hydroxylse from Catharanthus roseus, and a strategy for the functional expression of plant cytochrome P450 proteins as translational fusion with P450 reductase in *Escherichia coli*. *FEBS Lett* 1995;**374**:345–50.

Houghton-Larsen J, Hicks PM, Naesby M, *et al.* Recombinant production of steviol glycosides. 2013. WO2013022989 A2. DOI: http://www.google.com/patents/WO2013022989A2?cl=en

Hsieh LS, Ma GJ, Yang CC *et al.* Cloning, expression, site-directed mutagenesis and immunolocalization of phenylalanine ammonia-lyase in *Bambusa oldhamii*. *Phytochemistry* 2010;**71**:1999–2009.

Hwang E Il, Kaneko M, Ohnishi Y *et al.* Production of plantspecific flavanones by *Escherichia coli* containing an artificial gene cluster. *Appl Environ Microbiol* 2003;**69**:2699–706.

Iwaki K, Koya-Miyata S, Kohno K *et al.* Antimicrobial activity of *Polygonum tinctorium* Lour: Extract against oral pathogenic bacteria. *J Nat Med* 2006;**60**:121–5.

Jakubowska A, Korona R. Epistasis for growth rate and total metabolic flux in yeast. *PLoS One* 2012;**7**, DOI: 10.1371/journal.pone.0033132.

Jayaraman J, Jesudoss VAS, Menon VP *et al.* Anti-inflammatory role of naringenin in rats with ethanol induced liver injury. *Toxicol Mech Methods* 2012;**22**:568–76.

Jendresen CB, Stahlhut SG, Li M *et al.* Highly active and specific tyrosine ammonia-lyases from diverse origins enable enhanced production of aromatic compounds in bacteria and *Saccharomyces cerevisiae*. *Appl Environ Microbiol* 2015;**81**:4458–76.

Jensen NB, Strucko T, Kildegaard KR *et al.* EasyClone: method for iterative chromosomal integration of multiple genes in *Saccharomyces cerevisiae*. *FEMS Yeast Res* 2014;**14**:238–48.

Jiang H, Wood K V, Morgan JA. Metabolic Engineering of the Phenylpropanoid Pathway in *Saccharomyces cerevisiae*. *Appl Environ Microbiol* 2005;**71**:2962–9.

Jiang N, Doseff AI, Grotewold E. Flavones: From biosynthesis to health benefits. *Plants* 2016;**5**:1–25.

Julien BN, Wallace DM. Fragrance and methods for production of 5-epi-β-vetivone, 2-isopropyl-6, 10-dimethyl-spiro[4.5]deca-2,6-dien-8-one, and 2-isopropyl-6, 10-dimethyl-spiro[4.5]deca-1, 6-dien-8-one. 2014. US 8642815 B2

Jung UJ, Kim HJ, Lee JS *et al.* Naringin supplementation lowers plasma lipids and enhances erythrocyte antioxidant enzyme activities in hypercholesterolemic subjects. *Clin Nutr* 2003;**22**:561–8.

Kannappan S, Anuradha CV. Naringenin enhances insulin-stimulated tyrosine phosphorylation and improves the cellular actions of insulin in a dietary model of metabolic syndrome. *Eur J Nutr* 2010;**49**:101–9.

Katz M P, Durhuus T, Smits H P *et al.* Production of Metabolites. 2013. US 20130209613 A1, DOI: http://www.google.com/patents/US20130209613

Katz M P, Smits HP, Förster J, Nielsen JB. 2015. Metabolically engineered cells for the production of resveratrol or an oligomeric or glycosidically-bound derivative thereof. US 9040269 B2. DOI: http://www.google.com/patents/US9040269

Karhumaa K, Wiedemann B, Hahn-Hägerdal B *et al.* Co-utilization of L-arabinose and D-xylose by laboratory and industrial *Saccharomyces cerevisiae* strains. *Microb Cell Fact* 2006;**5**:18.

Keasling JD. Manufacturing Molecules Through Metabolic Engineering. *Science* 2010;**330**:1355–8.

Khosla C, Keasling JD. Metabolic Engineering For Drug Discovery and Development. *Nat Drug Discov* 2003;**2**:1019–25.

Kim BG, Kim JH, Kim J *et al.* Accumulation of flavonols in response to ultraviolet-B irradiation in soybean is related to induction of flavanone 3-β-hydroxylase and flavonol synthase. *Mol Cells* 2008;**25**:247–52.

Kim DH, Jung E a, Sohng IS *et al.* Intestinal bacterial metabolism of flavonoids and its relation to some biological activities. *Arch Pharm Res* 1998;**21**:17–23.

Klein J, Heal JR, Hamilton WDO *et al.* Yeast Synthetic Biology Platform Generates Novel Chemical Structures as Scaffolds for Drug Discovery. *ACS Synth Biol* 2014;**3**:314–23.

Koo H, Hayacibara MF, Schobel BD *et al.* Inhibition of *Streptococcus mutans* biofilm accumulation and polysaccharide production by apigenin and tt-farnesol. *J Antimicrob Chemother* 2003;**52**:782–9.

Koo H, Jeon JG. Naturally occurring molecules as alternative therapeutic agents against cariogenic biofilms. *Adv Dent Res* 2009;**21**:63–8.

Koo H, Rosalen PL, Cury J a *et al.* Effects of Compounds Found in Propolis on *Streptococcus mutans* Growth and on Glucosyltransferase Activity. *Antimicrob Agents Chemother* 2002;**46**:1302–9.

Koopman F, Beekwilder J, Crimi B *et al. De novo* production of the flavonoid naringenin in engineered *Saccharomyces cerevisiae*. *Microb Cell Fact* 2012;**11**, DOI: 10.1007/s13318-014-0193-x.

Kreuzaler F, Hahlbrock K. Enzymic synthesis of an aromatic ring from acetate units. Partial purification and some properties of flavanone synthase from cell-suspension cultures of *Petroselinum hortense*. *Eur J Biochem* 1975;**56**:205–13.

Kuijpers NGA, Solis-Escalante D, Bosman L *et al.* A versatile, efficient strategy for assembly of multi-fragment expression vectors in *Saccharomyces cerevisiae* using 60 bp synthetic recombination sequences. *Microb Cell Fact* 2013;**12**:47.

Kuramitsu HK, He X, Lux R *et al.* Interspecies interactions within oral microbial communities. *Microbiol Mol Biol Rev* 2007;**71**:653–70.

Kyndt JA, Meyer TE, Cusanovich MA *et al.* Characterization of a bacterial tyrosine ammonia lyase, a biosynthetic enzyme for the photoactive yellow protein. *FEBS Lett* 2002;**512**:240–4.

Jagetia GC, Venkatesha VA, Reddy TK. Naringin, a citrus flavonone, protects against radiation-induced chromosome damage in mouse bone marrow. *Mutagenesis* 2003;**18**:337–43.

Lan W, Lu F, Regner M *et al.* Tricin, a flavonoid monomer in monocot lignification. *Plant Physiol* 2015;**167**:1284–95.

Landry CR, Townsend JP, Hartl DL *et al.* Ecological and evolutionary genomics of *Saccharomyces cerevisiae*. *Mol Ecol* 2006;**15**:575–91.

Latunde-dada AO, Cabello-hurtado F, Czittrich N *et al.* Flavonoid 6-hydroxylase from soybean (*Glycine max L.*), a novel plant P-450 monooxygenase. *J Biol Chem* 2001;**276**:1688–95.

Lee FW, Da Silva NA. Sequential delta-integration for the regulated insertion of cloned genes in *Saccharomyces cerevisiae*. *Biotechnol Prog* 1997;**13**:368–73.

Lee KA, Moon SH, Lee JY *et al.* Antibacterial activity of a novel flavonoid, 7-O-butyl naringenin, against methicillin-resistant *Staphylococcus aureus* (MRSA). *Food Sci Biotechnol* 2013;**22**:1725–8.

Lehka BJ, Eichenberger M, Bjørn-Yoshimoto WE, Garcia Vanegas K, Buijs N, Jensen NB, Dannow Dyekjær J, Jenssen H, Simón E, Naesby M. Improving heterologous production of phenylpropanoids in *Saccharomyces cerevisiae* by tackling an unwanted side reaction of Tsc13, an endogenous double bond reductase. *FEMS Yeast Res* 2017;**17**:1–12.

Leonard E, Lim KH, Saw PN *et al.* Engineering central metabolic pathways for high-level flavonoid production in *Escherichia coli*. *Appl Environ Microbiol* 2007;**73**:3877–86.

Leonard E, Yan Y, Fowler ZL *et al.* Strain improvement of recombinant *Escherichia coli* for efficient production of plant flavonoids. *Mol Pharm* 2008;**5**:257–65.

Leonard E, Yan Y, Lim KH *et al.* Investigation of two distinct flavone synthases for plant-specific flavone biosynthesis in *Saccharomyces cerevisiae*. *Appl Environ Microbiol* 2005;**71**:8241–8.

Li H, Ban Z, Qin H *et al.* A Heteromeric Membrane-Bound Prenyltransferase Complex from Hop Catalyzes Three Sequential Aromatic Prenylations in the Bitter Acid Pathway. *Plant Physiol* 2015;**167**:650–9.

Li M, Borodina I. Application of synthetic biology for production of chemicals in yeast *Saccharomyces cerevisiae*. *FEMS Yeast Res* 2015;**15**:1–12.

Li M, Kildegaard KR, Chen Y *et al. De novo* production of resveratrol from glucose or ethanol by engineered *Saccharomyces cerevisiae*. *Metab Eng* 2015;**32**:1–11.

Lim CG, Fowler ZL, Hueller T *et al.* High-yield resveratrol production in engineered *Escherichia coli*. *Appl Environ Microbiol* 2011;**77**:3451–60.

Lim YH, Kim IH, Seo JJ. *In vitro* activity of kaempferol isolated from the Impatiens balsamina alone and in combination with erythromycin or clindamycin against *Propionibacterium acnes*. *J Microbiol* 2007;**45**:473–7.

Liu H, Orjala J, Sticher O *et al.* Acylated flavonol glycosides from leaves of *Stenochlaena palustris*. *J Nat Prod* 1999;**62**:70–5.

Lõoke M, Kristjuhan K, Kristjuhan A. Extraction of genomic DNA from yeasts for PCR-based applications. *Biotechniques* 2011;**50**:325–8.

Lopez D, Vlamakis H, Kolter R. Biofilms. *CSH Perspect Biol* 2010:1–12.

Louie GV, Bowman ME, Moffitt MC *et al.* Structural Determinants and Modulation of Substrate Specificity in Phenylalanine-Tyrosine Ammonia-Lyases. *Chem Biol* 2006;**13**:1327–38.

Lu MF, Xiao ZT, Zhang HY. Where do health benefits of flavonoids come from? Insights from flavonoid targets and their evolutionary history. *Biochem Biophys Res Commun* 2013;**434**:701–4.

Lucarini R, Tozatti MG, Silva MLA *et al.* Antibacterial and anti-in fl ammatory activities of an extract , fractions , and compounds isolated from *Gochnatia pulchra* aerial parts. *Brazicial J Med Biol Res* 2015;**48**:822–30.

Luque A, Sebai SC, Santiago-Schübel B *et al. In vivo* evolution of metabolic pathways by homeologous recombination in mitotic cells. *Metab Eng* 2014;**23**:123–35.

Luttik MAH, Vuralhan Z, Suir E *et al.* Alleviation of feedback inhibition in *Saccharomyces cerevisiae* aromatic amino acid biosynthesis: Quantification of metabolic impact. *Metab Eng* 2008;**10**:141–53.

Mandalari G, Bennett RN, Bisignano G *et al.* Antimicrobial activity of flavonoids extracted from bergamot (*Citrus bergamia* Risso) peel, a byproduct of the essential oil industry. *J Appl Microbiol* 2007;**103**:2056–64.

van Maris AJA, Geertman JA, Vermeulen A *et al.* Directed evolution of pyruvate decarboxylase-negative *Saccharomyces cerevisiae*, yielding a C_2-independent, glucose-tolerant, and pyruvate-hyperproducing yeast. *Appl Environ Microbiol* 2004;**70**:159–66.

Marston A and Hostettmann K. Separation and Quantification of Flavonoids. In: Andersen ØM, Markham KR. *Flavonoids, Chemistry, Biochemistry and applications*. Boca Raton: Taylor & Francis Group, 2006, 1–36.

Maury J, Germann SM, Baallal Jacobsen SA *et al.* EasyCloneMulti: A set of vectors for simultaneous and multiple genomic integrations in *Saccharomyces cerevisiae*. *PLoS One* 2016;**11**:1–22.

Mazi-Kotwal N, Madhavan S. Drug Interactions with Grapefruit Juice. *Br J Med Pract* 2002;**346**:1294–9.

Mckenna R, Thompson B, Pugh S *et al.* Rational and combinatorial approaches to engineering styrene production by *Saccharomyces cerevisiae*. 2014:1–12.

Meadows AL, Hawkins KM, Tsegaye Y *et al.* Rewriting yeast central carbon metabolism for industrial isoprenoid production. *Nat Publ Gr* 2016;**537**:694–7.

Medina VG, Almering MJH, Van Maris AJA *et al.* Elimination of glycerol production in anaerobic cultures of a *Saccharomyces cerevisiae* strain engineered to use acetic acid as an electron acceptor. *Appl Environ Microbiol* 2010;**76**:190–5.

Mikkelsen MD, Buron LD, Salomonsen B *et al.* Microbial production of indolylglucosinolate through engineering of a multi-gene pathway in a versatile yeast expression platform. *Metab Eng* 2012;**14**:104–11.

Miyahisa I, Kaneko M, Funa N *et al.* Efficient production of (2S)-flavanones by *Escherichia coli* containing an artificial biosynthetic gene cluster. *Appl Microbiol Biotechnol* 2005;**68**:498–504.

Mol JNM, Obbins MP, Dixon RA *et al.* Spontaneous and enzymic rearrangement of naringenin chalcone to flavanone. *Phytochemistry* 1985;**24**:2267–9.

Moon SH, Lee JH, Kim KT *et al.* Antimicrobial effect of 7-O-butylnaringenin, a novel flavonoid, and various natural flavonoids against *Helicobacter pylori* strains. *Int J Environ Res Public Health* 2013;**10**:5459–69.

Mukai N, Masaki K, Fujii T *et al.* PAD1 and FDC1 are essential for the decarboxilation of phenylacrylic acid in *Saccharomyces cerevisiae*. *J Biosci Bioeng* 2010; **109**:564–59

Munro AW, Girvan HM, McLean KJ. Cytochrome P450-redox partner fusion enzymes. *Biochim Biophys Acta* 2007;**1770**:345–59.

Naesby M, Nielsen SV, Nielsen CA *et al.* Yeast artificial chromosomes employed for random assembly of biosynthetic pathways and production of diverse compounds in *Saccharomyces cerevisiae*. *Microb Cell Fact* 2009;**8**:45.

Nevoigt E. Progress in metabolic engineering of *Saccharomyces cerevisiae*. *Microbiol Mol Biol Rev* 2008;**72**:379–412.

Nicolle E, Souard F, Faure P *et al.* Flavonoids as promising lead compounds in type 2 diabetes mellitus: molecules of interest and structure-activity relationship. *Curr Med Chem* 2011;**18**:2661–72.

Nielsen J, Larsson C, van Maris A *et al.* Metabolic engineering of yeast for production of fuels and chemicals. *Curr Opin Biotechnol* 2013;**24**:398–404.

Nour-Eldin HH, Hansen BG, Nørholm MHH *et al.* Advancing uracil-excision based cloning towards an ideal technique for cloning PCR fragments. *Nucleic Acids Res* 2006;**34**:e122.

Olsen KM, Hehn A, Jugdé H *et al.* Identification and characterisation of CYP75A31, a new flavonoid 3'5'-hydroxylase, isolated from *Solanum lycopersicum*. *BMC Plant Biol* 2010;**10**:21.

Ortiz-Andrade RR, Sánchez-Salgado JC, Navarrete-Vázquez G *et al.* Antidiabetic and toxicological evaluations of naringenin in normoglycaemic and NIDDM rat models and its implications on extra-pancreatic glucose regulation. *Diabetes, Obes Metab* 2008;**10**:1097–104.

Osawa K, Yasuda H, Maruyama T *et al.* Isoflavanones from the Heartwood of Swartzia polyphylla and Their Antibacterial Activity against Cariogenic Bacteria. *Chem Pharm Bull* 1992;**40**:2970–4.

Paddon CJ, Westfall PJ, Pitera DJ *et al.* High-level semi-synthetic production of the potent antimalarial artemisinin. *Nature* 2013;**496**:528–32.

Paes Leme AF, Koo H, Bellato CM *et al.* The role of sucrose in cariogenic dental biofilm formation-new insight. *J Dent Res* 2006;**85**:878–87.

Pandey KB, Rizvi SI. Plant polyphenols as dietary antioxidants in human health and disease. *Oxidative Med Cell Longev* 2009;**2**:270–8.

Partow S, Siewers V, Bjørn S *et al.* Characterization of chromosomal integration sites for heterologous gene expression in *Saccharomyces cerevisiae*. *Yeast* 2009;**26**:545–51.

Patra JK, Kim ES, Oh K *et al.* Antibacterial effect of crude extract and metabolites of *Phytolacca americana* on pathogens responsible for periodontal inflammatory diseases and dental caries. *BMC Complement Altern Med* 2014;**14**:343.

Paulo L, Ferreira S, Gallardo E *et al.* Antimicrobial activity and effects of resveratrol on human pathogenic bacteria. *World J Microbiol Biotechnol* 2010;**26**:1533–8.

Peralta-Yahya PP, Zhang F, del Cardayre SB *et al.* Microbial engineering for the production of advanced biofuels. *Nature* 2012;**488**:320–8.

Peters NK, Frost JW, Long SR. A Plant Flavone, Luteolin, Induces Expression of Rhizobium meliloti Nodulation Genes. *Sci New Ser* 2016;**233**:977–80.

Petrovska BB. Historical review of medicinal plants' usage. *Phcog Rev*. 2012;**6**(11):1-5. DOI:10.4103/0973-7847.95849.

Pietta PG. Flavonoids as antioxidants. *J Nat Prod* 2000;**63**:1035–42.

Prabhakar AR, Karuna YM, Yavagal C *et al.* Cavity disinfection in minimally invasive dentistry - comparative evaluation of *Aloe vera* and propolis: A randomized clinical trial. Contemp Clin Dent 2015;**6**(Suppl 1):S24-S31. doi:10.4103/0976-237X.152933.

Ralston L, Subramanian S, Matsuno M *et al.* The quantitative disposition of 3-O-methyl-(+)-catechin in man following oral administration. *Plant Physiol* 2005;**137**:1375–88.

Ranaud S, de Lorgeril M. Wine, alcohol, platelets, and the french paradox for coronary heart disease. *Lancet* 1992; **339**(8808):1523–26.

Redden H, Alper HS, Keaveney M *et al.* The development and characterization of synthetic minimal yeast promoters. *Nat Commun* 2015;**6**:7810.

Ríos-Hoyo A, Gutiérrez-Salmeán G. New Dietary Supplements for Obesity: What We Currently Know. *Curr Obes Rep* 2016;**5**:262–70.

Rivière C, Pawlus AD, Mérillon J-M. Natural stilbenoids: distribution in the plant kingdom and chemotaxonomic interest in Vitaceae. *Nat Prod Rep* 2012;**29**:1317.

Ro D, Paradise EM, Ouellet M *et al.* Production of the antimalarial drug precursor artemisinic acid in engineered yeast. *Nature* 2006;**440**:3–6.

Ro DK, Douglas CJ. Reconstitution of the entry point of plant phenylpropanoid metabolism in yeast (*Saccharomyces cerevisiae*): Implications for control of metabolic flux into the phenylpropanoid pathway. *J Biol Chem* 2004b;**279**:2600–7.

Rodriguez A, Kildegaard KR, Li M *et al.* Establishment of a yeast platform strain for production of *p*-coumaric acid through metabolic engineering of aromatic amino acid biosynthesis. *Metab Eng* 2015;**31**:181–188.

Romagnoli G, Luttik MAH, Kötter P *et al.* Substrate specificity of thiamine pyrophosphate-dependent 2-oxo-acid decarboxylases in *Saccharomyces cerevisiae*. *Appl Environ Microbiol* 2012;**78**:7538–48.

Romanos MA, Scorer CA, Clare JJ. Foreign Gene Expression in Yeast : a Review. 1992;**8**:423–88.

Roostita LB, Fleet GH, Wendry SP *et al.* Determination of yeasts antimicrobial activity in milk and meat products. *Adv J Food Sci Technol* 2011;**3**:442–5.

Sakai A, Shimizu Y, Hishinuma F. Integration of heterologous genes into the chromosome of *Saccharomyces cerevisiae* using a delta sequence of yeast retrotransposon Ty. *Appl Microbiol Biotechnol* 1990;**33**:302–6.

Salman HA, Senthikumar R. Identification and antibiogram profile of *Streptococcus mutans* and *Streptococcus sobrinus* from dental caries subjects. *J Appl Pharm Sci* 2015;**5**:054–7.

Santos CNS, Koffas M, Stephanopoulos G. Optimization of a heterologous pathway for the production of flavonoids from glucose. *Metab Eng* 2011;**13**:392–400.

Sato M, Fujiwara S, Tsuchiya H *et al.* Flavones with antibacterial activity against cariogenic bacteria. *J Ethnopharmacol* 1996;**54**:171–6.

Saunders CA, Wolf FR, Mukharji I. Method and composition for increasing the accumulation of squalene and specific sterols in yeast. 1995. US 5460949 A,

Savoia D. Plant-derived antimicrobial compounds: alternatives to antibiotics. *Future Microbiol* 2012;**7**:979–90.

Schalk M, Cabello-Hurtado F, Pierrel M-A *et al.* Piperonylic Acid, a Selective, Mechanism-Based Inactivator of the trans-Cinnamate 4-Hydroxylase: A New Tool to Control the Flux of Metabolites in the Phenylpropanoid Pathway1. *Plant Physiol* 1998;**118**:209–18.

Scheideler M, Schlaich NL, Fellenberg K *et al.* Monitoring the switch from housekeeping to pathogen defense metabolism in *Arabidopsis thaliana* using cDNA arrays. *J Biol Chem* 2002;**277**:10555–61.

Schenck CA, Chen S, Siehl DL *et al.* Non-plastidic, tyrosine-insensitive prephenate dehydrogenases from legumes. Nat Chem Biol 2015;**11**(1):52-7.

Schmidheini T, Sperisen P, Paravicini G *et al.* A Single Point Mutation Results in a Constitutively Activated and Feedback-Resistant Chorismate Mutase of *Saccharomyces cerevisiae*. *J Bacteriol* 1989;**171**:1245–53.

Schmitz-Hoerner R, Weissenböck G. Contribution of phenolic compounds to the UV-B screening capacity of developing barley primary leaves in relation to DNA damage and repair under elevated UV-B levels. *Phytochemistry* 2003;**64**:243–55.

Schnappauf G, Krappmann S, Braus GH. Tyrosine and tryptophan act through the same binding site at the dimer interface of yeast chorismate mutase. *J Biol Chem* 1998;**273**:17012–7.

Schnee S, Viret O, Gindro K. Role of stilbenes in the resistance of grapevine to powdery mildew. *Physiol Mol Plant Pathol* 2008;**72**:128–33.

Schwarz KJ, Boitz LI, Methner FJ. Enzymatic formation of styrene during wheat beer fermentation is dependent on pitching rate and cinnamic acid content. *J Inst Brew* 2012;**118**:280–4.

Seitz C, Ameres S, Forkmann G. Identification of the molecular basis for the functional difference between flavonoid 3'-hydroxylase and flavonoid 3'5'-hydroxylase. *FEBS Lett* 2007;**581**:3429–34.

Sham PC and Purcell SM. (2014). From Statistical power and significance testing in large-scale genetic studies, Box 3: Bonferroni methods and permutation procedures. *Nat Rev Genet* **15:**335–46. DOI:10.1038/nrg3706

Shao Z, Zhao H, Zhao H. DNA assembler, an *in vivo* genetic method for rapid construction of biochemical pathways. *Nucleic Acids Res* 2009;**37**:1–10.

Shi S, Chen Y, Siewers V *et al.* Improving production of malonyl coenzyme A-derived metabolites by abolishing Snf1-dependent regulation of Acc1. *MBio* 2014;**5**:1–8.

Shiba Y, Paradise EM, Kirby J *et al.* Engineering of the pyruvate dehydrogenase bypass in *Saccharomyces cerevisiae* for high-level production of isoprenoids. *Metab Eng* 2007;**9**:160–8.

Shin SY, Han NS, Park YC *et al.* Production of resveratrol from *p*-coumaric acid in recombinant *Saccharomyces cerevisiae* expressing 4-coumarate:coenzyme A ligase and stilbene synthase genes. *Enzyme Microb Technol* 2011;**48**:48–53.

Shin SY, Jung SM, Kim MD *et al.* Production of resveratrol from tyrosine in metabolically engineered *Saccharomyces cerevisiae*. *Enzyme Microb Technol* 2012;**51**:211–6.

Sicińska P, Pytel E, Maćczak A *et al.* The use of various diet supplements in metabolic syndrome. *Postepy Hig Med Dosw* 2015;**69**:25–33.

Siddiqui MS, Thodey K, Trenchard I *et al.* Advancing secondary metabolite biosynthesis in yeast with synthetic biology tools. *FEMS Yeast Res* 2012;**12**:144–70.

Simón E, Lehka BJ, Vazquez CC. Biosynthesis of phenylpropanoids and phenylpropanoid derivatives. 2016. WO 2016189121 A1.

Singh M, Kaur M, Silakari O. Flavones: An important scaffold for medicinal chemistry. *Eur J Med Chem* 2014;**84**:206–39.

Skjoedt ML, Snoek T, Kildegaard KR, Arsovska D *et al.* Engineering prokaryotic transcriptional activators as metabolite biosensors in yeast. *Nature Chemical Biology* 2016;**12**: 951–958.

Da Silva NA, Srikrishnan S. Introduction and expression of genes for metabolic engineering applications in *Saccharomyces cerevisiae*. *FEMS Yeast Res* 2012;**12**:197–214.

Sohn H. Antimicrobial and cytotoxic activity of 18 prenylated flavonoids isolated from medicinal plants: *Morus alba L., Morus mongolica Schneider, Broussnetia papyrifera (L.)*

Vent, *Sophora flavescens Ait* and *Echinosophora koreensis Nakai*. *Phytomedicine* 2004;**11**:666–72.

Sosa T, Chaves N, Alias JC *et al.* Inhibition of Mouth Skeletal Muscle Relaxation by Flavonoids of *Cistus ladanifer* L.: A Plant Defense Mechanism Against Herbivores. *J Chem Ecol* 2004;**30**:1087–101.

Stapleton PD, Shah S, Hamilton-Miller JMT *et al.* Anti-*Staphylococcus aureus* activity and oxacillin resistance modulating capacity of 3-O-acyl-catechins. *Int J Antimicrob Agents* 2004;**24**:374–80.

Stoclet JC, Chataigneau T, Ndiaye M *et al.* Vascular protection by dietary polyphenols. *Eur J Pharmacol* 2004;**500**:299–313.

Sydor T, Schaffer S, Boles E. Considerable Increase in Resveratrol Production by Recombinant Industrial Yeast Strains with Use of Rich Medium. *Appl Environ Microbiol* 2010;**76**:3361–3.

Tapas A, Sakarkar D, Kakde R. Flavonoids as Nutraceuticals: A Review. *Trop J Pharm Res* 2008;**7**:1089–99.

Tajuddeen N, Sallau MS, Musa AM *et al.* Flavonoids with antimicrobial activity from the stem bark of *Commiphora pedunculata* (Kotschy & Peyr.) Engl. *Nat Prod Res* 2014;**28**:1915–8.

Tehlivets O, Scheuringer K, Kohlwein SD. Fatty acid synthesis and elongation in yeast. *Biochim Biophys Acta - Mol Cell Biol Lipids* 2007;**1771**:255–70.

Teichner Warren, Leskoo Megan. Cashing in on the booming market for dietary supplements. *Consum Shopp Insights* 2013:1–5.

Trantas E, Koffas M a. G, Xu P *et al.* When plants produce not enough or at all: metabolic engineering of flavonoids in microbial hosts. *Front Plant Sci* 2015;**6**:1–16.

Trantas E, Panopoulos N, Ververidis F. Metabolic engineering of the complete pathway leading to heterologous biosynthesis of various flavonoids and stilbenoids in *Saccharomyces cerevisiae*. *Metab Eng* 2009;**11**:355–66.

Treutter D. Significance of flavonoids in plant resistance and enhancement of their biosynthesis. *Plant Biol* 2005;**7**:581–91.

Tsuchiya H, Iinuma M. Reduction of membrane fluidity by antibacterial sophoraflavanone G isolated from *Sophora exigua*. *Phytomedicine* 2000;**7**:161–5.

Tsuchiya H, Sato M, Iinuma M *et al.* Inhibition of the growth of cariogenic bacteria *in vitro* by plant falvanones. *Experientia* 1994;**50**:846–9.

Tsuchiya H, Sato M, Miyazaki T *et al.* Comparative study on the antibacterial activity of phytochemical flavanones against methicillin-resistant *Staphylococcus aureus*. *J Ethnopharmacol* 1996;**50**:27–34.

Ubersax J, Platt D. Genetically modified microbes producing isoprenoids. 2010. US 20100311065 A1, DOI: http://www.google.com/patents/US20100311065.

Uzel A, Sorkun K, Önçag Ö *et al.* Chemical compositions and antimicrobial activities of four different Anatolian propolis samples. *Microbiol Res* 2005;**160**:189–95.

Vannelli T, Wei Qi W, Sweigard J *et al.* Production of *p*-hydroxycinnamic acid from glucose in Saccharomyces cerevisiae and *Escherichia coli* by expression of heterologous genes from plants and fungi. *Metab Eng* 2007a;**9**:142–51.

Vannelli T, Xue Z, Breinig S *et al.* Functional expression in *Escherichia coli* of the tyrosine-inducible tyrosine ammonia-lyase enzyme from yeast *Trichosporon cutaneum* for production of *p*-hydroxycinnamic acid. *Enzyme Microb Technol* 2007b;**41**:413–22.

Verwaal R, Wu L, Damveld RA, *et al.* Succinic acid production in a eukaryotic cell. **2012**. US 20120165569 A1, DOI: http://www.google.com/patents/US20120165569.

Vidak M, Rozman D, Komel R. Effects of flavonoids from food and dietary supplements on glial and glioblastoma multiforme cells. *Molecules* 2015;**20**:19406–32.

Vogt T. Phenylpropanoid biosynthesis. *Mol Plant* 2010;**3**:2–20.

Vos T, de la Torre Cortés P, van Gulik WM *et al.* Growth-rate dependency of *de novo* resveratrol production in chemostat cultures of an engineered *Saccharomyces cerevisiae* strain. *Microb Cell Fact* 2015;**14**:133.

Wang Y, Chen H, Yu O. A plant malonyl-CoA synthetase enhances lipid content and polyketide yield in yeast cells. *Appl Microbiol Biotechnol* 2014;**98**:5435–47.

Wang J, Guleria S, Koffas MAG *et al.* Microbial production of value-added nutraceuticals. *Curr Opin Biotechnol* 2016;**37**:97–104.

Wang Y, Halls C, Zhang J *et al.* Stepwise increase of resveratrol biosynthesis in yeast *Saccharomyces cerevisiae* by metabolic engineering. *Metab Eng* 2011a;**13**:455–63.

Wang Y, Yi H, Wang M *et al.* Structural and Kinetic Analysis of the Unnatural Fusion Protein. *J Am Chem Soc* 2011b;**133**:20684–7.

Wang Y, Yu O. Synthetic scaffolds increased resveratrol biosynthesis in engineered yeast cells. *J Biotechnol* 2012;**157**:258–60.

Watts KT, Lee PC, Schmidt-Dannert C. Biosynthesis of plant-specific stilbene polyketides in metabolically engineered *Escherichia coli*. *BMC Biotechnol* 2006a;**6**:22.

Watts KT, Lee PC, Schmidt-Dannert C. Exploring recombinant flavonoid biosynthesis in metabolically engineered *Escherichia coli*. *ChemBioChem* 2004;**5**:500–7.

Watts KT, Mijts BN, Lee PC *et al.* Discovery of a Substrate Selectivity Switch in Tyrosine Ammonia-Lyase, a Member of the Aromatic Amino Acid Lyase Family. *Chem Biol* 2006b;**13**:1317–26.

Weinhandl K, Winkler M, Glieder A *et al.* Carbon source dependent promoters in yeasts. *Microb Cell Fact* 2014;**13**:1–17.

Weisshaar B, Jenkins G. Phenylpropanoid biosynthesis and its regulation. *Curr Opin Plant Biol* 1998;**1**:251–7.

Wilcox LJ, Borradaile NM, Huff MW. Antiatherogenic Properties of Naringenin, a Citrus Flavonoid. *Cardiovasc Drug Rev* 2006;**17**:160–78.

Wood N. The effects of selected dietary bioflavonoid supplementation on dental caries in young rats fed a high-sucrose diet. *J Med Food* 2007;**10**:694–701.

Wu CH, Lin JA, Hsieh WC *et al.* Low-Density-Lipoprotein (LDL)-bound flavonoids increase the resistance of LDL to oxidation and glycation under pathophysiological concentrations of glucose *in vitro*. *J Agric Food Chem* 2009;**57**:5058–64.

Wu J, Du G, Chen J *et al.* Enhancing flavonoid production by systematically tuning the central metabolic pathways based on a CRISPR interference system in *Escherichia coli*. *Sci Rep* 2015;**5**:13477.

Wu J, Liu P, Fan Y *et al.* Multivariate modular metabolic engineering of *Escherichia coli* to produce resveratrol from l-tyrosine. *J Biotechnol* 2013;**167**:404–11.

Wu J, Yu O, Du G *et al.* Fine-tuning of the fatty acid pathway by synthetic antisense RNA for enhanced (2S)-naringenin production from L-tyrosine in *Escherichia coli*. *Appl Environ Microbiol* 2014a;**80**:7283–92.

Wu J, Zhou T, Du G *et al.* Modular optimization of heterologous pathways for *de novo* synthesis of (2S)-Naringenin in *Escherichia coli*. *PLoS One* 2014b;**9**:1–9.

Wu T, He M, Zang X *et al.* A structure-activity relationship study of flavonoids as inhibitors of *E. coli* by membrane interaction effect. *Biochim Biophys Acta* 2013;**1828**:2751–6.

Xu P, Ranganathan S, Fowler ZL *et al.* Genome-scale metabolic network modeling results in minimal interventions that cooperatively force carbon flux towards malonyl-CoA. *Metab Eng* 2011;**13**:578–87.

Xue Z, McCluskey M, Cantera K *et al.* Identification, characterization and functional expression of a tyrosine ammonia-lyase and its mutants from the photosynthetic bacterium *Rhodobacter sphaeroides*. *J Ind Microbiol Biotechnol* 2007a;**34**:599–604.

Xue Z, McCluskey M, Cantera K *et al.* Improved production of *p*-hydroxycinnamic acid from tyrosine using a novel thermostable phenylalanine/tyrosine ammonia lyase enzyme. *Enzyme Microb Technol* 2007b;**42**:58–64.

Yamamoto H, Yatou A, Inoue K. 8-Dimethylallylnaringenin 2'-hydroxylase, the crucial cytochrome P450 mono-oxygenase for lavandulylated flavanone formation in *Sophora flavescens* cultured cells. *Phytochemistry* 2001;**58**:671–6.

Yan Y, Kohli A, Koffas MAG. Biosynthesis of natural flavanones in *Saccharomyces cerevisiae*. *Appl Environ Microbiol* 2005;**71**:5610–3.

Yao LH, Jiang YM, Shi J *et al.* Flavonoids in food and their health benefits. *Plant Foods Hum Nutr* 2004;**59**:113–22.

Yoo H, Widhalm JR, Qian Y *et al.* An alternative pathway contributes to phenylalanine biosynthesis in plants via a cytosolic tyrosine: phenylpyruvate aminotransferase. *Nat Commun* 2013;**4**:2833.

Yoshida K, Mori M, Kondo T. Blue flower color development by anthocyanins: from chemical structure to cell physiology. *Nat Prod Rep* 2009;**26**:884–915.

Yu JS, Moon E, Choi SU *et al.* Asarotonide, a new phenylpropanoid with a rare natural acetonide group from the rhizomes of *Acorus gramineus*. *Tetrahedron Lett* 2016;**57**:1699–701.

Zabala G, Zou J, Tuteja J *et al.* Transcriptome changes in the phenylpropanoid pathway of *Glycine max* in response to *Pseudomonas* syringae infection. *BMC Plant Biol* 2006;**6**:26.

Zhang Y, Li SZ, Li J *et al.* Using unnatural protein fusions to engineer resveratrol biosynthesis in yeast and mammalian cells. *J Am Chem Soc* 2006;**128**:13030–1.